

# **Immunological evaluation of biodegradable particle based nanoparticles encapsulating OMP antigen as potential vaccine candidate**

*Dissertation submitted in partial fulfillment  
of the requirements of the degree of  
**Doctor of Philosophy***

*in*

***Life Science***

*by*

***Pradipta Ranjan Rauta***  
**(Roll No. 510LS103)**

*Based on research carried out  
under the supervision of  
**Prof. Bismita Nayak***



**December, 2016**

**Department of Life Science  
National Institute Of Technology Rourkela**



Department of Life Science  
National Institute of Technology Rourkela

---

December 05, 2016

## Certificate of Examination

Roll no: 510LS103

Name: *Pradipta Ranjan Rauta*

Title of the dissertation: *Immunological evaluation of biodegradable particle based nanoparticles encapsulating OMP antigen as potential vaccine candidate*

We the below signed, after checking the dissertation mentioned above and the official record book (s) of the student, hereby state our approval of the dissertation submitted in partial fulfillment of the requirements of the degree of *Doctor of Philosophy* in *Department of Life Science* at *National Institute of Technology Rourkela*. We are satisfied with the volume, quality, correctness, and originality of the work.

**Bismita Nayak**  
Principal Supervisor

**Sujit Kumar Bhutia**  
Member, DSC

**R K Patel**  
Member, DSC

**Kunal Pal**  
Member, DSC

**Triveni Krishnan**  
External Examiner

**Rasu Jayabalan**  
Chairperson, DSC

**Sujit Kumar Bhutia**  
Head of Department



Department of Life Science  
National Institute of Technology Rourkela

---

**Dr. Bismita Nayak**  
Assistant Professor  
Department of Life Science  
National Institute Of Technology Rourkela  
Rourkela-769008, Odisha, India

December 05, 2016

### **Supervisor's Certificate**

This is to certify that the work presented in this dissertation entitled **Immunological evaluation of biodegradable particle based nanoparticles encapsulating OMP antigen as potential vaccine candidate**" by "Pradipta Ranjan Rauta", Roll Number 510LS103, is a record of original research carried out by him under my supervision and guidance in partial fulfillment of the requirements of the degree of Doctor of Philosophy in Life Science. Neither this dissertation nor any part of it has been submitted earlier for any degree or diploma to any institute or university in India or abroad.

**Bismita Nayak**

#### **Contact**

Phone: [+91 661 2462682](tel:+916612462682) (Office)

E-mail: [nayakb@nitrrkl.ac.in](mailto:nayakb@nitrrkl.ac.in), [bismita.nayak@gmail.com](mailto:bismita.nayak@gmail.com)

*Dedicated To*

**My Parents**

**Pradipta Ranjan Rauta**

# Declaration of Originality

I, Pradipta Ranjan Rauta, Roll Number, 510LS103 hereby declare that this dissertation entitled **"Immunological evaluation of biodegradable particle based nanoparticles encapsulating OMP antigen as potential vaccine candidate"** presents my original work carried out as a doctoral student of NIT Rourkela and, to the best of my knowledge, contains no material previously published or written by another person, nor any material presented by me for the award of any other degree or diploma of NIT Rourkela or any other institution. Any contribution made to this research by others, with whom I have worked at NIT Rourkela or elsewhere, is explicitly acknowledged in the dissertation. Works of other authors cited in this dissertation have been duly acknowledged under the section "References". I have also submitted my original research records to the scrutiny committee for evaluation of my dissertation.

I am fully aware that in case of any non-compliance detected in future, the Senate of NIT Rourkela may withdraw the degree awarded to me on the basis of the present dissertation.

December 05, 2016  
NIT Rourkela

**Pradipta Ranjan Rauta**

# ACKNOWLEDGEMENT

I avail this opportunity to express my indebtedness, deep gratitude and sincere thanks to my supervisor Prof. (Miss.) Bismita Nayak, Assistant Professor, Department of Life Science, National Institute of Technology, Rourkela for her in depth supervision and guidance, constant encouragement and co-operative attitude for bringing out this thesis work successfully. I enjoyed the freedom she gave me throughout this work that was instrumental in discovering a scientific “self” within me. I feel proud that I am one of her doctoral students and I consider myself extremely lucky to get the opportunity to work under the guidance of such a dynamic personality.

My special thanks to the Director, National Institute of Technology, Rourkela for his encouragement, valuable suggestion and providing all the facilities to complete this dissertation work successfully. I am also very thankful to all the members of my doctoral scrutiny committee – Prof. Rasu Jayabalan (Chairman) and Prof. Sujit Kumar Bhutia of the Department of Life Science, Prof. R. K. Patel of the Department of Chemistry and Prof. Kunal Pal of the Department of Biomedical and biotechnology engineering for their thoughtful advice, inspiration and encouragement throughout the research work. I take this opportunity to thank all other faculty members and the supporting staff members of the Life Science department for their timely co-operation and support at various phases of experimental work. I would like to extend sincere thanks to Prof Marília Mateus and Prof. Gabriel Monteiro for their constant guidance and support to successfully complete the part of my work at Institute for Biotechnology and Bioengineering, Instituto Superior Técnico, Lisboa, Portugal. I would like to extend special thanks to my lab members Debasis, Sarbani, Manisha, Sanjiv for their valuable suggestions and encouragement. I would also like to extend special thanks to all my elders, friend and well wishers for their constant help, motivations and encouragement.

I would like to acknowledge Ministry of Human Resource Development (MHRD), Govt. of India for providing financial assistance throughout my research. I would also like to acknowledge European Commission for providing me the opportunity to work as PhD mobility fellow (Erasmus Mundus heritage fellow) at f Institute for Biotechnology and Bioengineering, Instituto Superior Técnico, Lisboa, Portugal as well as financial assistance for 10 months.

And it goes without saying, that I am indebted to my parents Mr. Bijaya Kumar Rauta and Mrs. Pravati Rauta, brother Mr. Prem Ranjan Rauta, and sister Mrs. Sasmita Rauta whose patience, support and endurance made completion of my thesis. I greatly indebted to my wife, Mrs Dipti Mohanta who had always been very supportive, caring and everlasting support she has given me.

Above all, I would like to thank the almighty for his enormous blessings.

December 5, 2016  
NIT Rourkela

Pradipta Ranjan Rauta

## ABSTRACT

Advanced vaccine research approaches need to explore on biodegradable nanoparticles (NPs) based vaccine carrier that can serve as antigen delivery systems as well as immuno-stimulatory action to induce both innate and adaptive immune response. The biodegradable polymeric particles like polylactide-co-glycolide (PLGA) or polylactide (PLA), not only work as a delivery system but also, provide adjuvant activity and marks in the development of long -lasting immunity. In this PhD dissertation work, the immunogenicity of PLA and PLGA NPs encapsulating outer membrane protein (Omp) antigen (*Aeromonas hydrophila* and *Vibrio cholerae*) were evaluated. Initially, Various NPs formulations of PLA and PLGA loaded with model protein (Bovine Serum Albumin) or drug (Clindamycin hydrochloride) were prepared by solvent evaporation method varying drug/protein: polymer concentration and optimized for size, encapsulation efficiency, drug loading, morphology etc. *A. hydrophila* Omp antigen loaded PLA-Omp ( $223.5 \pm 13.19$  nm) and PLGA-Omp ( $166.4 \pm 21.23$  nm) NPs were prepared using double emulsion method by efficiently encapsulating the antigen reaching the encapsulation efficiency  $44 \pm 4.58$  % and  $59.33 \pm 5.13$  % respectively. Despite low antigen loading in PLA-Omp, it exhibited considerably slower antigen release *in vitro* than PLGA-Omp NPs. Upon intraperitoneal immunization in fish, *Labeo rohita* with all antigenic formulations (PLA-Omp NP, PLGA-Omp NP, FIA-Omp, PLA NP, PLGA NP, PBS as control), significantly higher bacterial agglutination titre and haemolytic activity were observed in the case of PLA-Omp and PLGA-Omp immunized groups compared to rest of the groups at both 21 days and 42 days. The antigen specific antibody response was significantly increased and persisted up to 42 days of post immunization by PLA-Omp, PLGA-Omp, FIA-Omp. PLA-Omp NPs showed a better immune response (higher bacterial agglutination titre, haemolytic activity, specific antibody titre, higher percent survival upon *A. hydrophila* challenge) than PLGA-Omp in *L. rohita* confirming its better efficacy. Comparable antibody response of PLA-Omp and PLGA-Omp with FIA-Omp treated groups suggested that PLA and PLGA could be a replacement for Freund's adjuvant (for stimulating antibody response) to overcome many side effects offering long lasting immunity. Similarly, *V. cholerae* Omp antigen loaded PLA-Omp ( $196.24 \pm 34.25$  nm) and PLGA-Omp ( $165.34 \pm 3.5$  nm) NPs were prepared using double emulsion method by efficiently encapsulating the antigen reaching the encapsulation efficiency  $57.85 \pm 4.15$  % and  $69.18 \pm 1.68$  respectively. After intraperitoneal immunization in BALB/c mice, the type and strength of immune responses elicited (cellular and humoral) by formulated NPs were evaluated. The antibody titre (IgG1, IgG2a) were significantly higher ( $P < 0.05$ ; Kruskal-Wallis test and post hoc Dunn multiple comparisons) in PLA-Omp NPs, PLGA-Omp NPs treated groups than respective PLA and PLGA NPs treated groups from 7 days to 56 days as confirmed by ELISA tests. Also, PLA-Omp NPs and PLGA-Omp NPs induced significantly higher ( $P < 0.05$ ; Kruskal-Wallis test and post hoc Dunn multiple comparisons) antigen specific IgG titers than Omp antigen treated groups at all-time intervals except 0 day. From the spleen cell analysis (Cell surface phenotype through FACs study), a

significantly higher cellular activation was observed in the case of PLA-Omp and PLGA-Omp NPs in comparison to Omp antigen alone. Enhanced immune responses elicited by PLA-Omp and PLGA-Omp NPs might be attributed to strong memory T cell response (higher effector memory T cell), efficient induction of dendritic cell (DC) activation (higher MHC I, MHC II, CD 86 expression) and follicular helper T cell differentiation in spleen favoring the generation of antibody responses. Another study aimed at developing a DNA vaccine as well as a delivery system to boost antigenic outer membrane protein (Omp) that would act as potential vaccine candidate was conducted. NPs based delivery systems for plasmid DNA (pDNA) (which encode conserved Omp) administration might be keys to improve the transfection efficiency *in vivo* even at a lower dose. The conserved antigenic protein sequences [*omp*(211-382), *omp*(211-382)opt, *omp*(703-999) and *omp*(703-999)opt] of outer membrane protein were identified using bioinformatics tools. The sequences were cloned into a pVAX-GFP expression vector and successfully transformed into *E. coli* (DH5 $\alpha$ ). The large scale pDNA production was achieved with shake flask cultures and the pDNA was purified by hydrophobic interaction chromatography (HIC). The formulated PLGA-chitosan NP/plasmid DNA nano complex of ~200 nm ( $199.25 \pm 22.29$  nm and  $205.25 \pm 33.59$ ) was transfected into CHO cells that confirmed improved transfection efficiency (fluorescence intensity measurement corresponding to GFP expression level from the FACs study) at a lower dose. The DNA entrapment assay demonstrated the possible protection of pDNA inside the pDNA-NP complex. The protection from enzymatic digestion that NP complex confers to pDNA was evaluated and confirmed by gel electrophoresis after treatment with DNase. Further, physio-chemical characterizations of formulated nano complex and extensive transfection studies have proved the functionality of the system *in vitro*. Overall, the successful formulations of NP based antigen delivery system with all desirable physiochemical characteristics were obtained under highly controlled conditions and reproducibility. The immunological evaluation studies suggest that PLA/PLGA NPs based delivery system could be a novel antigen carrier for fish and mice ensuring its application for commercial value and product development. Further work based on present optimized results can be taken forward for next level vaccine design and approval.

**Keywords:** *PLA; PLGA; Omp; nanoparticles; adjuvant; antigen carrier; immune response.*



# List of Figures

Sl No.	Title of figure	Page No
2.1	The size ranges of nanoparticles used in nanovaccinology.....	13
2.2	Schematic representation of different nanoparticle delivery systems (Polymeric nanoparticle, Inorganic Nanoparticle, Oil-in-water emulsion, Liposome, Virus-like particle, ISCOM).....	14
2.3	Preparation of antigen-encapsulating nanoparticles by w/o/w emulsion method.....	19
2.4	Interaction of nanoparticle with antigen. Formulation of nanoparticle and antigen of interest can be through attachment (e.g. conjugation, encapsulation, or adsorption) or simple mixing.....	27
3.1	Size (a) and charge (b) distribution pattern of CLH loaded PLA NPs (PLA-CLH 2). The drug: polymer ratio is 1:10. The average size and zeta potential were $323.5 \pm 16.39$ nm and $-30.5 \pm 4.95$ mv respectively.....	45
3.2	Size (a) and charge (b) distribution pattern of CLH loaded PLGA NPs (PLGA-CLH 2). The drug: polymer ratio is 1:10. The average size and zeta potential were $258.3 \pm 11.23$ nm and $-33.5 \pm 3.0$ mv respectively.....	45
3.3	In vitro CLH release from CLH-PLA 2 and CLH-PLGA 2 NPs.....	47
3.4	SEM photograph of (a) CLH-PLA2 (Drug: polymer- 1:10) and (b) CLH-PLGA2 (Drug: polymer- 1:10).....	47
3.5	DSC data: a. Thermal analysis graph of Clindamycin hydrochloride (CLH), blank PLA, CLH conjugated with PLA (CLH-PLA2); (b) Thermal analysis graph of Clindamycin hydrochloride (CLH), blank PLGA, and CLH conjugated with PLGA (CLH-PLGA 2).....	48
3.6	FTIR data analysis of CLH -PLA 2(a) and CLH -PLGA-3 (b).....	49
4.1	Size and charge (zeta potential) distribution pattern of Omp loaded PLA nanoparticles (PLA-Omp) determined by dynamic light scattering (DLS) method. The average size and zeta potential were $223.5 \pm 13.19$ nm and $-26.5 \pm 4.75$ mv respectively.....	61
4.2	Size and charge (zeta potential) distribution pattern of Omp loaded PLGA nanoparticles (PLGA-Omp) determined by dynamic light scattering (DLS) method. The average size and zeta potential were $166.4 \pm 21.23$ nm and $-31.3 \pm 6.5$ mv respectively.....	61
4.3	In Vitro comparison of Omp antigen release from PLA and PLGA nanoparticles.....	62
4.4	SEM photograph of (a) PLA-Omp nanoparticles (b) PLGA-Omp nanoparticles.....	62
4.5	Variation in the bacterial agglutination activity of sera derived from different treated groups of <i>L. rohita</i> at 21 and 42 days post-immunization. Bars represent mean $\pm$ S.E. Mean value bearing same superscript are not statistically significant ( $p > 0.05$ ) at 21 and 42 days post-immunization.....	64

4.6	Variation in hemolysis activity of sera from different treated groups of <i>L. rohita</i> at 21 and 42 days post-immunization. Bars represent mean log <sub>2</sub> titre values $\pm$ S.E. Mean value bearing same superscript are not statistically significant ( $p > 0.05$ ) at 21 and 42 days post-immunization.....	65
4.7	Variation in the specific antibody level of sera collected from different treated groups of <i>L. rohita</i> at 21 and 42 days post-immunization. Bars represent mean OD values $\pm$ S.E. Mean value bearing same superscript are not statistically significant ( $p > 0.05$ ) at 21 and 42 days post-immunization..	66
4.8	Challenge study: variation of % survival in different treated groups of <i>L. rohita</i> after 42 days post-immunization. Bars represent mean $\pm$ S.E. Mean value bearing same superscript are not statistically significant ( $p > 0.05$ ) at 42 days post-immunization.....	67
5.1	Physico-chemical properties of antigen loaded NPs. Size and charge (zeta potential) distribution pattern of (A) PLA-OmpNp(size: $196.24 \pm 34.25$ nm; zeta potential: $-25.2 \pm 5.45$ mv) and(B) PLGA-OmpNp(size: $165.34 \pm 3.5$ nm; zeta potential: $-32.5 \pm 6.15$ mv)determined by dynamic light scattering (DLS) method. The morphology of PLA-Omp NPs (C) and PLGA-Omp NPs (D) were investigated by field emission-scanning electron microscopy. (E)Comparison of Omp release (in vitro) from PLA and PLGA nanoparticles. (F) Fluorescence microscopy images of HEK cells after 4 h of incubation with the coumarin 6-loaded PLA/PLGA-Omp nanoparticles..	80
5.2	ATR-FTIR spectrum of formulated NPs. Similar spectral bands were observed at 2337 cm <sup>-1</sup> (C $\equiv$ N stretching- presence of nitriles), 1712 cm <sup>-1</sup> (C=O stretching- presence of carboxylic acid), 1529 cm <sup>-1</sup> (N-H bending- presence of Amide-II), 1068 cm <sup>-1</sup> (C-H stretching- presence of aliphatic amines), 891 cm <sup>-1</sup> (C-H bending) for OMP, blank PLA and PLGA NPs. Apart from common bands observed in OMP and blank NPs some additional peaks were also observed in the case of encapsulated PLA-OMP and PLGA-OMP nanoparticles at 2936 cm <sup>-1</sup> (C-H stretching, the presence of alkanes), 1680 cm <sup>-1</sup> (C=O stretching, the presence of amide -I). The characteristic peaks of PLA and PLGA were observed at 1710 cm <sup>-1</sup> and 1060 cm <sup>-1</sup> that correspond to the presence of the $\alpha$ , $\beta$ unsaturated esters and carboxylic acids and ethers. The common peak at 1064 cm <sup>-1</sup> resulted from the overlapping of several bands including the absorption due to vibration modes of CH <sub>2</sub> OH and C-O stretching vibrations coupled to C-O bending. It was also observed that upon encapsulation of OMP to PLA and PLGA the characteristic peaks associated with OMP, PLA and PLGA remained intact with no loss of any functional peaks between the absorbance spectra of OMP and OMP encapsulated PLA/PLGA NPs.....	81
5.3	Antibody immune response induced after vaccination of BALB/c mice with different antigenic formulations (PLA-Omp, PLGA-Omp, Pmp, PLA, PLGA, PBS) at a different time. A and B represents serum IgG1 levels in vaccinated mice (n=5/group). C and D represent Serum IgG2a levels in vaccinated mice (n=5/group). Data are the mean value (* $p < 0.05$ ) for immunized mice vs control groups.....	82
5.4	Mice were injected intraperitoneally with PBS (control), PLA NPs, PLGA	

	NPs, PLA-Omp NPs, PLGA-Omp NPs, Omp. Splenocytes were isolated after 0 and 7 day post immunization. Splenocytes were stained with various surface markers, as indicated, and analyzed by flow cytometry. The gating logic was as follows: plasmacytoid dendritic cells (CD11c+, B220+), myeloid dendritic cells (CD11c+, B220-), B cells (CD11c-, B220+), granulocytes (GR-1+, F4/80-), macrophages (GR-1-, F4/80+). Cell numbers were normalized to day 0 values. Data are expressed as the mean $\pm$ SEM (n =3). *p < 0.05.....	84
5.5	Frequency of central (CD44hiCD62Lhi)/effector (CD44hiCD62Llow) memory CD4+ and CD8+ T cells. Mice (n = 6) were immunized three times as described in the methods section. Splenocytes were harvested 10 days after the third immunization and restimulated ex vivo with antigen for 60 h. The frequency of CD44hiCD62Lhi CD4+ T cells, CD44hiCD62Llow CD4+ T cells, CD44hiCD62Lhi CD8+ T cells, and CD44hiCD62Llow CD8+ T cells (A) were measured by flow cytometry. FACS plots in B and C are representative of the mean percentages of 6 mice in each group. Data in (A) are expressed as the mean $\pm$ SEM (n =6). *p < 0.05.....	85
5.6	The frequency of follicular helper CD4+ T cells in the splenocytes of immunized mice. Balb/c mice (n = 3) were intraperitoneally vaccinated with different vaccine formulations. Mice were euthanized 9 days later, and splenocytes were isolated. The frequency of follicular helper CD4+ T cells (CD4+CXCR5hiPD-1hi) was determined by flow cytometry. (A) Percentage of follicular helper CD4+ T cells (CD4+CXCR5hiPD-1hi) in CD4+ T cells and (B). Representative flow cytometry plots. Data are expressed as the mean $\pm$ SEM (n $\frac{1}{4}$ 3). *p < 0.05.....	86
6.1	Alignment of designed pVAX-GFP-omp(211-382) and pVAX-GFP-omp(703-999) sequence with their respective optimized sequences [pVAX-GFP-omp(211-382)opt and pVAX-GFP-omp(703-999)opt showing the nucleotide differences.....	98
6.2	Screening of positive clones based on pVAX-GFP for pVAX-GFP-omp(211-382) (a), pVAX-GFP-omp(211-382)opt (b), pVAX-GFP-omp(703-999) (c), pVAX-GFP-omp(703-999)opt (d). Lanes 1: DNA ladder (200 bp-10,000bp) and other lanes; 2-5 (a), 2-7 (b), 2-7 (c), 2-7 (d): RE digestion (Eco R1 and Kpn 1) of corresponding cloned plasmids.....	100
6.3	Chromatogram and Gel photograph of sample pulls at the different peak in the chromatogram (a. pVAX-GFP-omp(211-382), b. pVAX-GFP-omp(211-382)opt, c. pVAX-GFP-omp(703-999), d. pVAX-GFP-omp(703-999)opt. M-Molecular weight marker, F- feed, FT- (A3-A4), PS1- (A9-A12), PP- (B3-B7), PS2- (B12-C6), PI- (C7-C10).....	101
6.4	Transfection efficiency (%T $\times$ MI) of positive control (pVAX-GFP), pVAX-GFP-omp(211-382), pVAX-GFP-omp(211-382)opt, pVAX-GFP-omp(703-999) and pVAX-GFP-omp(703-999)opt transfected CHO cells after 24 hr and 48 hr of incubation.....	103
6.5	Size and charge (zeta potential) distribution pattern of pDNA loaded Chi/PLGA NPs by dynamic light scattering (DLS) method. The average	

	size of pVAX-GFP-omp(211-382)-NP complex was $199.25 \pm 22.29$ nm (a) and zeta potential was $23.25 \pm 2.25$ mV. Similarly, The average size of pVAX-GFP-omp(211-382)-NP complex was $205.25 \pm 33.59$ nm (c) and zeta potential was $26.35 \pm 2.38$ mV.....	105
6.6	DNA entrapment assay: The relative fluorescence of pDNA and pDNA-NP complex ( $n = 5$ ; mean $\pm$ standard error). Maximum fluorescence is exhibited by free pDNA [pVAX-GFP-omp(211-382) and pVAX-GFP-omp(211-382)opt]. Decreasing pDNA/NP ratios yield decreasing fluorescence intensities. The value corresponding to fluorescence of water (negative control) indicates complete complexation of all free pDNA with NPs.....	105
6.7	Plasmid and pDNA/NP complexes after nuclease digestion using DNase I: lane A: 1 kb Molecular weight marker; lane B: 100 ng plasmid [pVAX-GFP-omp(211-382)]; lane C: pVAX-GFP-omp(211-382)-NP complex; lane D: 100 ng pVAX-GFP-omp(211-382) with DNase I; lane E: pVAX-GFP-omp(211-382)-NP complex with DNase I.....	107
6.8	SEM photograph of (a) pVAX-GFP-omp(211-382)-NP complex (b) pVAX-GFP-omp(211-382)opt-NP complex.....	107
6.9	Transfection efficiency (%T $\times$ MI) patterns of control (pVAX-GFP), pVAX-GFP-omp(211-382)+ Lipofectamine 2000, pVAX-GFP-omp(211-382)-NP complex and pVAX-GFP-omp(211-382)opt-NP complex after 24 hr incubation.....	108
7.1	TMHMM 2.0 based exo-membrane localization and topology of OMP.....	116
7.2	The 3D model of <i>V. cholerae</i> OMP from various angles.....	119
7.3	Validation of the 3-D model of <i>V. cholerae</i> OMP with ProSa-web. The upper panel is template (PDB id: 2HUE) and lower is OMP. (a) Overall model quality of 2HUE ( $Z=-5.77$ ). (b) Local model quality of 2HUE. (c) Overall model quality of OMP ( $Z=-5.28$ ). (d) Local model quality of OMP.	120
7.4	The Ramachandran plot for <i>V. cholerae</i> OMP. The plot shows the acceptability of the model.....	121
7.5	3-D structures of 9 mers (YKSISPQDA) epitopes created by DISTILL.....	122

# List of Tables

Sl. No	Title of the table	Page No
2.1	Polymeric materials currently being investigated at nanoscale for drug delivery application; advantages and disadvantages.....	15
2.2	Summary of the various types of NPs currently being studied for their use as vaccine carriers.....	24
3.1	Physical properties of BSA loaded PLA and PLGA NPs.....	44
3.2	Physical properties of CLH loaded PLA and PLGA NPs.....	46
3.3	Antibacterial activity of Clindamycin hydrochloride conjugated with PLA (CLH-PLA 2), Clindamycin hydrochloride conjugated with PLGA (CLH-PLGA 2) and Clindamycin hydrochloride, in vitro MIC in µg/mL.	50
4.1	Physical properties of Omp loaded PLA and PLGA nanoparticles. The results were expressed as mean ± standard deviation.....	60
5.1	Physical properties of Omp loaded PLA and PLGA nanoparticles. The results were expressed as mean ± standard deviation.....	79
6.1	Transfection study results (% Transfection, Mean Intensity and %T × MI values of positive control (pVAX-GFP), pVAX-GFP-omp(211-382), pVAX-GFP-omp(211-382)opt, pVAX-GFP-omp(703-999) and pVAX-GFP-omp(703-999)opt transfected CHO cells) after 24 h and 48 h incubation.....	102
6.2	Transfection study results (% Transfection, Mean Intensity & %T × MI values of pVAX-GFP-omp(211-382), pVAX-GFP-omp(211-382)opt transfected CHO cells) after 1day, 2day, 3 day, 6 day, 8 day incubation...	104
7.1	Antigenic B-cell epitopes of <i>V. cholerae</i> OMP Epitopes are identified by B-cell epitope prediction with BCPreds (BCPred algorithm and AAP Prediction algorithm).....	116
7.2	T-cell epitopes of OMP ( <i>V. cholerae</i> ). The common antigenic B-cell epitope “FFAGGDNNLRGYGYKSISPQDASGALTGAKY” was analyzed for its ability to bind MHC I and MHC II molecules using Propred I and Propred. A common epitope “YKSISPQDA” (9 mers) that generates both TCL and HCL mediated immune response was selected.....	118
7.3	MHCPred Result of sequence YKSISPQDA.....	118

## List of Abbreviations

<b>Abbreviations</b>	<b>Full Form</b>
AGE	Agarose Gel Electrophoresis
APCs	Antigen-presenting Cells
ANOVA	Analysis of Variance
BCA	Bicinchoninic Acid
BSA	Bovine Serum Albumin
CHF	Chloroform
CFA	Complete Freund's Adjuvant
CLH	Clindamycin Hydrochloride
CT	Cholera Toxin
CTL	Cytotoxic T lymphocyte
DCs	Dendritic Cells
DCM	Dichloromethane
Chi	Chitosan
CHO	Chinese Hamster Ovary
DLS	Dynamic Light Scattering
DMEM	Dulbecco's Modified Eagle Medium
DMRT	Duncan's Multiple Range Tests
DSC	Differential Scanning Calorimetric Thermogram
DMSO	Dimethyl Sulfoxide
EAP	External Aqueous Phase
EB	Elution Buffer
ELISA	Enzyme-Linked Immunosorbent Assays
FDA	Food and Drug Administration
FIA	Freund's Incomplete Adjuvant
FITC	Fluorescein Iso Thiocyanate
FTIR	Fourier Transformed Infrared
gDNA	Genomic DNA
GFP	Green Fluorescent Protein
ID	Intradermal

IM	Intramuscular
HA	Hyaluronic Acid
HIC	Hydrophobic Interaction Chromatography
HIV	Human Immunodeficiency Virus
IAP	Internal Aqueous Phase
ISCOMs	Immunostimulating Complexes
LPS	Lipopolysaccharide
LN	Lymph Node
MHC	Major Histocompatibility Complex
MIC	Minimum Inhibitory Concentration
mV	millivolt
NPs	Nano particles
Omp	Outer membrane protein
OMVs	Outer Membrane Vesicles
OP	Organic Phase
OVA	Ovalbumin
PBS	Phosphate Buffered Saline
PCL	Poly( $\epsilon$ -caprolactone)
PFA	Paraformaldehyde
PDI	Polydispersity Index
pDNA	Plasmid DNA
PEG	Poly Ethylene Glycol
PEI	Polyethylenimine
PGA	Poly(Glycolic Acid)
PHB	Poly(Hydroxybutyrate)
PLA	Poly(Lactic Acid)
PLGA	Poly(Lactide-co-Glycolide)
PVA	Poly(Vinyl Alcohol)
SC	Subcutaneous
SD	Standard Deviation
SE	Standard Error
SEM	Scanning electron microscopy

FE-SEM	Field Emission Scanning Electron Microscopy
TBST	TBS with 0.05% Tween 20
TCP	Toxin-coregulated Pilus
TEM	Transmission Electron Microscopy
Th	T helper
TLR	Toll-Like Receptor
w/o/w	Water-in-oil-in-water
VLPs	Virus-Like Particles



# Contents

<b>Certificate of Examination</b>	<b>ii</b>
<b>Supervisor's Certificate</b>	<b>iii</b>
<b>Dedication</b>	<b>iv</b>
<b>Declaration of Originality</b>	<b>v</b>
<b>Acknowledgement</b>	<b>vi</b>
<b>Abstract</b>	<b>vii-viii</b>
<b>List of Figures</b>	<b>ix-xii</b>
<b>List of Tables</b>	<b>xiii</b>
<b>List of Abbreviations</b>	<b>xiv-xvi</b>
<b>1 Chapter 1: Introduction.....</b>	<b>1-10</b>
<b>1.1 Background.....</b>	<b>1</b>
<b>1.2 Vaccines and vaccination.....</b>	<b>2</b>
<b>1.3 Adjuvants and vaccine delivery systems.....</b>	<b>2</b>
<b>1.4 Nano-Particle Vaccine.....</b>	<b>3</b>
<b>1.5 Nanoparticle – delivery system.....</b>	<b>4</b>
<b>1.6 Nanoparticle carrier system.....</b>	<b>4</b>
<b>1.6.1 Poly (lactic acid) (PLA).....</b>	<b>4</b>
<b>1.6.2 Poly lactic-co-glycolic acid (PLGA).....</b>	<b>5</b>
<b>1.7 Protein Vaccine and delivery strategy.....</b>	<b>5</b>
<b>1.8 DNA Vaccination and delivery strategy.....</b>	<b>6</b>
<b>1.8.1 <i>Aeromonas hydrophila</i>.....</b>	<b>7</b>
<b>1.8.2 <i>Vibrio cholerae</i>.....</b>	<b>7</b>
<b>1.9 Outer membrane protein as vaccine target.....</b>	<b>7</b>
<b>1.10 Motivation.....</b>	<b>8</b>
<b>1.11 Objectives.....</b>	<b>8</b>
<b>1.12 Thesis outline.....</b>	<b>9</b>
<b>2 Chapter 2: Review of Literature.....</b>	<b>11-36</b>
<b>2.1 Nanotechnology: A therapeutic approach.....</b>	<b>12</b>
<b>2.2 Nanoparticles.....</b>	<b>12</b>
<b>2.3 Types of nanoparticles.....</b>	<b>14</b>

2.3.1	Polymeric nanoparticles (PNPs).....	14
2.3.2	Inorganic nanoparticles.....	15
2.3.3	Liposomes.....	16
2.3.4	Immunostimulating complex (ISCOM).....	16
2.3.5	Virus-like particles.....	17
2.3.6	Self-assembled proteins.....	17
2.3.7	Emulsions.....	17
2.4	Nanoparticles Preparation Methods.....	17
2.4.1	Preparation antigen/drug loaded polymeric nanoparticles.....	18
2.5	Characterization of Drug loaded nanoparticles.....	19
2.5.1	Particle size.....	19
2.5.2	Surface properties of NPs.....	20
2.5.3	Drug loading.....	21
2.5.4	Drug release.....	21
2.6	Vaccine induced immunity.....	22
2.7	Antigens Delivery Using Nanoparticles.....	22
2.8	Nanoparticles mediated dendritic cell activation.....	23
2.9	Gene delivery by polyion complex NPs.....	25
2.10	Nanoparticle-Antigen Interaction.....	26
2.11	Nanoparticle-Antigen presenting cell (APC) Interaction.....	27
2.12	Nanoparticle-Biosystem Interaction.....	28
2.13	Routes of administration.....	28
2.13.1	Mucosal Vaccination.....	28
2.13.2	Parenteral vaccination.....	29
2.13.3	Intradermal route.....	30
2.14	The bacterial pathogen: <i>Aeromonas hydrophila</i> .....	30
2.14.1	Systematic position.....	30
2.14.2	Pathogenesis.....	31
2.14.3	Prevention and control.....	32
2.14.4	Outer membrane protein: <i>A. hydrophila</i> .....	32
2.15	The bacterial pathogen: <i>Vibrio cholerae</i> .....	32
2.15.1	Systematic position.....	32
2.15.2	Pathogenesis.....	33

2.15.3	Prevention and control.....	34
2.15.4	Outer membrane protein: <i>V. cholerae</i> .....	35
2.16	Challenges and future prospective.....	36
3	Chapter 3: Enhanced efficacy of Clindamycin hydrochloride encapsulated in PLA/PLGA based nanoparticle system for oral delivery.....	37-53
3.1	Introduction.....	37
3.2	Materials and Methods.....	39
3.2.1	Materials.....	39
3.2.2	Preparation of PLA-BSA and PLGA-BSA NPs.....	39
3.2.3	Preparation of CLH-PLA and CLH-PLGA NPs.....	39
3.2.4	Characterization.....	40
3.2.5	Determination of drug loading efficiency.....	40
3.2.6	In vitro drug release study.....	41
3.2.7	SEM Study.....	41
3.2.8	DSC analysis.....	41
3.2.9	Fourier transformed infrared spectra.....	42
3.2.10	Antibacterial activity.....	42
3.3	Results .....	43
3.3.1	Physical properties.....	43
3.3.2	Loading Efficiency.....	46
3.3.3	<i>In Vitro</i> Drug Release.....	46
3.3.4	SEM Study.....	47
3.3.5	DSC studies.....	48
3.3.6	FTIR Analysis.....	48
3.3.7	Antimicrobial activity.....	49
3.4	Discussion.....	50
3.5	Conclusion.....	53
4	Chapter 4: Parenteral immunization of PLA/PLGA nanoparticle encapsulating outer membrane protein (Omp) from <i>Aeromonas hydrophila</i> ; Evaluation of immunostimulatory action in <i>Labeo rohita</i> (rohu)	54-70
4.1	Introduction.....	54
4.2	Materials and methods.....	56
4.2.1	Materials.....	56
4.2.2	Preparation of OM proteins.....	56
4.2.3	Preparation of biodegradable and biocompatible based	

	nanoparticles.....	56
4.2.4	Characterization of nanoparticles.....	57
4.2.5	Immunization protocol.....	58
4.2.6	Preparation of anti-rohu-globulin rabbit serum.....	58
4.2.7	Immune responses study.....	58
4.2.8	Challenge study.....	59
4.2.9	Statistical analysis.....	59
4.3	Results.....	60
4.3.1	Physico-chemical properties of antigen loaded nano particles.....	60
4.3.2	Loading efficiency.....	61
4.3.3	In vitro drug release.....	61
4.3.4	SEM Study.....	62
4.3.5	Immune responses study.....	63
4.3.6	Challenge study.....	66
4.4	Discussion.....	67
4.5	Conclusion.....	70
5	<b>Chapter 5: Evaluation of the immune responses (specific) in higher vertebrate model (mice) after intraperitoneal immunization of Omp antigen (<i>V. cholerae</i>) encapsulated PLA/PLGA nano-particles</b>	<b>71-89</b>
5.1	Introduction.....	71
5.2	Materials and methods.....	73
5.2.1	Materials.....	73
5.2.2	Preparation of OM proteins Preparation of major outer membrane proteins (Omp).....	74
5.2.3	Preparation and characterization of PLA-Omp and PLGA-Omp nanoparticles.....	74
5.2.4	Characterization of PLA-Omp and PLGA-Omp nanoparticles.....	75
5.2.5	Immunization studies.....	76
5.2.6	Determination of Omp specific IgG1 and IgG2a antibodies by ELISA.....	76
5.2.7	Spleen cell analysis.....	77
5.2.8	Determination of memory T cell responses by flow cytometry.....	77
5.2.9	Expression of MHC and Co-stimulatory molecules on dendritic cells in spleen.....	77

5.2.10	Determination of follicular helper CD4+ T cells in spleen	78
5.2.11	Statistical Analysis.....	78
5.3	Results.....	78
5.3.1	Formulation and Physico-chemical properties of antigen loaded NPs.....	78
5.3.2	Antigen specific antibody response in vaccinated mice....	81
5.3.3	Splenocyte proliferation Assay.....	83
5.3.4	Spleen cell analysis.....	83
5.3.5	Memory T cell responses.....	84
5.3.6	Expression of MHC and the co stimulatory molecule CD86 on DCs.....	87
5.3.7	Frequency of follicular CD4+ T cells in spleen.....	87
5.4	Discussion.....	87
6	Chapter 6: Development of DNA vaccines to boost antigenic outer membrane protein antigenicity	90-111
6.1	Introduction.....	90
6.2	Materials & Methods.....	92
6.2.1	Design of gene constructs for pVAX-GFP expression vector.....	92
6.2.2	Plasmid DNA production in E. coli DH5α transformants	93
6.2.3	Plasmid DNA recovery and purification.....	94
6.2.4	In vitro culture and transfection of CHO cells.....	95
6.2.5	Flow cytometry analysis.....	96
6.2.6	Chi/PLGA-pDNA Complex.....	96
6.2.7	Particle Size, Size Distribution, and Zeta Potential.....	97
6.2.8	DNA Entrapment.....	97
6.2.9	Enzymatic Digestion Assays.....	97
6.2.10	SEM Study.....	97
6.2.11	Data analysis.....	98
6.3	Results.....	98
6.3.1	Design of omp gene construct in pVAX-GFP expression vector.....	98
6.3.2	Cloning.....	99
6.3.3	Sequence analysis.....	99
6.3.4	Plasmid DNA production and its up-scaled purification by hydrophobic interaction chromatography (HIC).....	100

6.3.5	Transfection Efficiency.....	101
6.3.6	Physico-chemical properties of pDNA-NP complex.....	104
6.3.7	DNA entrapment assay.....	106
6.3.8	Enzymatic Degradation of pDNA and Complexes.....	106
6.3.9	SEM studies.....	107
6.3.10	<i>In vitro</i> transfection study with pDNA-NPs complex.....	108
6.4	Discussion.....	108
6.5	Conclusion.....	111
7	<b>Chapter 7: In Silico identification of outer membrane protein (Omp) and subunit vaccine design against pathogenic <i>Vibrio cholerae</i></b>	<b>112-123</b>
7.1	Introduction.....	112
7.2	Materials and Methods.....	114
7.2.1	In silico Epitope vaccine design.....	114
7.2.2	Sequence Retrieval and B–Cell Antigenic site prediction....	114
7.2.3	B-Cell epitope prediction.....	114
7.2.4	T-Cell epitope prediction.....	114
7.2.5	Selection of epitopes.....	114
7.2.6	Homology modelling and model validation.....	115
7.2.7	Characterization of epitopes.....	115
7.3	Results.....	115
7.3.1	Antigen Selection.....	115
7.3.2	Identified Antigenic B-cell Epitopes.....	116
7.3.3	Identified candidate peptide vaccines.....	117
7.3.4	3-D modeling of <i>V. cholerae</i> OMP.....	119
7.3.5	Validation of the model.....	119
7.3.6	Characterization of the epitope .....	121
7.4	Discussion.....	122
7.5	Conclusion.....	123
8	<b>Chapter 8: Summary and Conclusion</b>	<b>124-129</b>
8.1	Summary.....	124
8.2	Conclusion and future investigation.....	128
	<b>References</b>	<b>130-164</b>
	<b>Publications</b>	<b>165-166</b>
	<b>Curriculum Vitae</b>	<b>167</b>

# Chapter I

## Introduction

### 1.1. Background

Today's leading research on vaccine approaches mostly focuses on the development of naturally acquiring immunity by inoculation of non-pathogenic but still immunogenic components of the pathogen or closely related organisms. Generally, these conventional approaches have been most successful in developing vaccines that can elicit an immune response based on antigen-specific antibody and cytotoxic T-lymphocyte (CTL) responses [1], [2]. The growing issues of vaccine safety are in alarming rate owing to their weak immunogenicity, imperfect immunization procedures, and failure to acquire booster doses to potentiate prime doses. So, these issues have paved the way towards research for developing new generation preventive and therapeutic vaccine. Adjuvants are the immunological agents that act to accelerate, enhance and prolong antigen-specific immune responses when used along with specific antigens. Adjuvants are used for multiple purposes; to accelerate a robust immune response by enhancing immunogenicity, provide antigen dose sparing, reduce booster immunization requirements, offers prolonged and improved protection [3], [4]. There is a crucial requirement for enhanced and effective vaccine formulations (with or without adjuvant) having minimal compositions like purified proteins, recombinant proteins and synthetic peptides, etc. for specific disease antigen in question. Adjuvants in vaccine formulations vary to a greater extent due to many issues; e.g. the chemical nature, mode of action, the safety and efficacy of adjuvants. The adverse effects concerned with the prolonged use of adjuvants use are the hyperactivation of the immune system, neurotoxicity, and many detrimental effects. There is also an urgent requirement for the development of novel carriers which could be target specific to achieve therapeutic drug concentration. Therefore, a relatively new system which is stable with antigen combination and can provide comparable immunity to that of adjuvants eventually can be treated as a complete replacement for the existing adjuvants in use should take the lead for development of advanced vaccine formulations.

Therefore, a better delivery system which could mimic the natural infection, reduce the need for booster immunization and also could address the other complications hopes to improve the vaccine efficacy. Controlled delivery systems comprising biodegradable nano-encapsulated peptide or protein antigens are of immense interest because they can potentially deliver the

antigens to the preferred locations at predetermined rates and durations to produce an optimal immune response. Various biodegradable polymeric particles like polylactide-co-glycolide (PLGA) or polylactide (PLA), not only work as an antigen delivery system but also afford adjuvant activity and marks in the development of long-lasting immunity after a single dose of injection. The polymeric NPs can be surface altered and functionalized either by adsorbing amphiphilic excipients onto pre-formed particles or by covalently linking excipients to the core-forming polymer prior to NP preparation to improve their biodistribution. The NPs can also be conjugated to targeting ligands which direct particles to specific cells/tissues. Among possible delivery systems, nanoparticles (NP) based delivery of DNA vaccines to APCs, is a very promising approach used for optimizing DNA vaccine formulation for immunotherapy [5], [6].

## **1.2. Vaccines and vaccination**

A vaccine may be defined as “biological preparation of microorganisms or their antigenic components which can provide acquired immunity against the appropriate pathogens, but it does not itself cause disease” [7] or simply as “a dead or attenuated (non-pathogenic) form of the pathogen”[8]. In addition to the immunogenic components, vaccines consist of an adjuvant/delivery system that aid in the induction of innate and adaptive responses, and stabilizers/surfactants that contribute to the immunogens staying intact during storage and administration. In general, vaccines are further sorted into a number of sub-categories mainly based on the condition of the antigen. These include heat or formalin inactivated whole microorganisms, antigen subunits (peptides, proteins, toxoids and its conjugates) and live/attenuated microorganisms, as well as plasmid DNA (pDNA) vaccines encoding immune inducing peptides/proteins of pathogenic origin.

## **1.3. Adjuvants and vaccine delivery systems**

Adjuvants (from Latin word, *adjuvare*: to aid) are essential components of most clinically used vaccines. In a broad sense, adjuvants are pharmacological agents that can accelerate, reinforce, improve or modify the effect of antigen. Adjuvants can be used for various purposes: to enhance immunogenicity, to accelerate the immune response, provide antigen dose sparing, reduce the need for booster immunizations, increase the period of protection, or improve efficacy in immune compromised individuals [9]. Vaccine delivery systems are commonly particulate adjuvants and comprise constructs such as emulsions (oil-in-water and water-in-oil), mineral salts ( $Al(OH)_3$ ), virus-like particles (VLPs), liposomes, immune stimulating complexes (ISCOMs) and nano/microparticles of chitosan, alginate and poly (lactide-co-glycolide) (PLGA)[9]–[15]. Despite the long history, the exact mechanism of adjuvant action is poorly understood. The general understanding is that adjuvants improve the immune response by; (1)



increasing the immunogenicity of highly purified or recombinant antigens (reduce the dose of antigen); (2) enhancing the magnitude, speed and duration of the immune response; (3) modulating antibody specificity, avidity, subclass or isotype distribution; (4) stimulating CTL responses; and/or (5) generating antigen depots and/or pulsed antigen release [2], [16], [17].

## **1.4. Nanoparticle vaccine**

Nanovaccines that comprise of nanoparticles are emerging as novel approach to the methodology of vaccination. The motivation for nanoparticles as vaccine systems develops from the idea that several components essential for vaccine efficacy can be rationally assembled, optimized independently, and incorporated into a single vehicle to induce an effective immune response. Various advantages have been shown by the researchers working and investigating the different aspects related to nano vaccine. Nanoparticle-based vaccination strategy offers significant distinct advantages over conventional vaccines e.g. (1) nanoparticles can efficiently protect their cargo from degradation in physiological conditions, (2) Size and shape of NPs can be specifically adjusted to mimic characteristics of pathogens, allowing effective draining through the lymphatic system and subsequent internalization in APCs, (3) Furthermore, size and charge strongly affect biodistribution and retention of particles in lymph nodes and spleens thus promoting effector and memory immune responses, (4) Surface modification of NPs also provides additional opportunities for enhancing target specific delivery by conjugation of receptor ligands or antibodies, (5) nanoparticle based co-delivery of antigens and adjuvants targeted to the specific APCs, that leads to optimal antigen presentation and immune activation, (6) Again, the cytosolic delivery of antigens within APCs can be achieved by NP systems intended to promote endosomal escape, thus allowing for effective antigen cross-presentation and induction of cytotoxic CD8<sup>+</sup> T lymphocyte (CTL) response.

Biodegradable NPs can be made from a range of materials such as polysaccharides, amino acids and synthetic biodegradable polymers. The selection of the ideal polymer is based on diverse designs and application criteria. It depends on various factors such as 1) size of the preferred nanoparticles, 2) nature of the drug (stability, aqueous solubility, etc.) to be enclosed in the polymer, 3) extent of biocompatibility and biodegradability, 4) surface functionality and 5) drug release profile. The procedures for the preparation of nanoparticles, based upon selection of preferred criteria, can be categorized as following 1) dispersion of preformed polymers, 2) ionic gelation method for hydrophilic polymers and 3) polymerization of monomers. Despite the availability of a large number of vaccines in the market, their cost per dose and delivery of multiple doses are the limiting factors of these vaccines. Furthermore, the requirement for cold storage is another drawback of conventional vaccines. So, the efforts have been taken to develop

biodegradable polymeric NPs as vaccine delivery systems to induce both humoral and cellular immune responses. Entrapment efficiency, release kinetics and additional physical features like construction, size assortment and porosity, which determine the potency of the formulation, can be controlled by using a suitable aggregation of different polymers.

## **1.5. Nanoparticle – delivery system**

In recent years, significant research has been done using nanoparticles as drug delivery vehicles for immunization. The benefit of using polymeric nanoparticles is to allow encapsulation of bioactive molecules and protect them against hydrolytic and enzymatic degradation. Nanoparticles loaded with plasmid DNA offer sustained release due to their quick escape from the degradative endo-lysosomal. Because of their endolysosomal escape and intracellular uptake, nanoparticles could discharge DNA at a constant rate resulting in continuous gene expression. Nanoparticulate vaccine delivery system can also be helpful to enhance the weaker immune response generated by synthetic peptide vaccines [18].

## **1.6. Nanoparticle carrier system**

The alternative drug delivery approach (nanoscale) typically incorporates one or more of the following materials: biologics, polymers, carbon-based materials, silicon-based materials, or metals. Biodegradable polymer nanoparticles, characteristically comprising of polylactic acid (PLA), polyglycolic acid (PGA), or Poly lactic-co-glycolic acid (PLGA), are being studied for the delivery of proteins and genes, anticancer drugs, etc. Other polymers being studied for nanoscale drug carriers consist of poly(3-hydroxybutanoic acid) (PHB), poly alkyl cyanoacrylate, poly(organophosphazene), poly(caprolactone) (PCL), poly(ethylene glycol) (PEG), poly(ethylene oxide) (PEO), and copolymers such as PLA-PEG. There have been a diversity of materials used to engineer solid nanoparticles, both with and without surface functionality. Possibly, the majority of polymers are the aliphatic polyesters, specifically the hydrophobic PLA [poly(lactic acid)], the hydrophilic PGA [poly(glycolic acid)] and their copolymer PLGA [poly(lactide- co-glycolide)].

### **1.6.1. Poly (lactic acid) (PLA)**

PLA (polylactic acid) polymer has been extensively studied in medical implants, suture, and drug delivery systems since 1980s. PLA is a biocompatible and biodegradable polymer which is metabolized into monomeric units of lactic acid in the body. Lactic acid is a natural intermediate by-product of anaerobic respiration, which is converted into glucose by the liver during the Cori

cycle. Glucose then is utilized as an energy source in the body. The use of PLA nanoparticles is, therefore, safe and devoid of any major toxicity.

### **1.6.2. Poly lactic-co-glycolic acid (PLGA)**

Poly (lactic-co-glycolic acid) (PLGA) NPs have unbelievable perspective in the applications connecting diagnostics, targeting and therapy. It is the most widely used biodegradable synthetic polymer nanocarrier with a relatively long history of biomedical usage. PLGA based vaccines delivery is a promising approach for boosting immune responses against a range of antigens such as recombinant proteins, peptide and DNA [5]. The poly (lactic-co-glycolic acid) (PLGA) copolymer can act as an attractive delivery system because of its superb biocompatibility, high safety profile[19], [20].It undergoes non-enzymatic hydrolysis in the body to produce biodegradable metabolite monomers such as lactic acid and glycolic acid that are natural metabolites (Figure 1.1). The lactic acid and glycolic acids are generally found in the body and participate in a number of biochemical and physiological pathways. So, there is very minimal systemic toxicity associated with the use of PLGA for the biomedical applications. In addition, the release kinetics of this system can be easily manipulated by varying the ratio of PLA: PGA. The PLGA particle size has been varied and surface modifications have been introduced into vaccine formulations for use in oral, mucosal, and systemic delivery. The sizes, surface modification, and release profiles of PLGA particles were shown to influence the immunogenicity of entrapped antigens.

## **1.7. Protein Vaccine and delivery strategy**

Recent advances in vaccinology demonstrate that proteins and peptides are the basis of a new generation vaccine. Protein vaccines are composed of purified or recombinant proteinaceous antigens from a pathogen, such as a bacterium or virus. When administered, it can elicit a protective immune response against the pathogen. High molecular weight, structural fragility, hydrophilicity, and complexity are the main hurdles to the use of protein drugs [21]. Indeed, these macromolecules can easily undergo denaturation, degradation and eventually inactivation (physical, chemical, and enzymatic machinery) during formulation, storage, and delivery [22], [23].The use of a properly designed carrier for the sustained and targeted delivery of protein antigen offers several advantages compared with traditional administration: it can enhance the amount of drug that reaches the targeted site, improve the transportation mechanism and protect the drug against degradation, inactivation, and metabolization phenomena. Nanoparticles, such

as polymeric micelles, liposomes, lipoplexes and polyplexes have been extensively investigated as targeted drug carrier systems over the past three decades.

## **1.8. DNA Vaccination and delivery strategy**

DNA vaccination or genetic immunization represents a novel strategy, which can serve as a viable alternative to conventional vaccine approaches. During the past two decades, the DNA vaccines have been investigated and tried to induce immune responses against a range of infectious pathogens and tumor antigens [24]. The novelty and usefulness of DNA vaccines stem from the several unique features, namely, they are conceptually safe, non-replicating and non-infectious, thereby overcome safety concern associated with live-attenuated vaccines. The DNA vaccine can be manufactured on large-scale with high purity and stability in a cost-effective manner and can be preserved without the need for a cold chain. More importantly, DNA vaccine can induce antigen-specific mucosal (IgA), humoral (protective neutralizing antibodies) and cellular (cytotoxic T lymphocytes) immune responses [25]. The mechanism of a DNA vaccine can in many ways be compared to that of a virus, as it requires the similar cellular machinery in order to replicate and also triggers immune responses normally seen with viral infections. Unlike conventional viral vaccines based on subunits or killed the virus, a DNA vaccine may conserve the structure and hence also antigenicity of a transgenic antigen/protein. A significant obstacle to the successful development of DNA vaccine is their low immunogenicity in humans and in large animals. Numerous factors may contribute to their poor immunogenicity including low transfection efficiency of naked DNA, insufficient antigen expression, and intra and extracellular barriers in the host[26]. The viral and nonviral vectors are used to enhance DNA delivery and transfection efficiency. Viral vectors are very efficient, but they are associated with several safety concerns such as immune response to vector itself, difficulty in manufacturing, limited DNA carrying capacity and oncogenicity of transduced cells. On the other hand, non-viral vectors are gaining increased interest because of their improved safety profile, ease of preparation and adjuvant properties [27]. The non-viral carriers that are currently investigated for DNA vaccine delivery include biodegradable PLGA NPs, cationic liposomes, cationic block copolymers, polycationic dendrimers, and cationic polymers (poly-L-lysine, polyethyleneimine and chitosan). In the case of synthetic polymers like PLGA, besides DNA protection, the encapsulation permits a controlled DNA delivery system to be designed with controllable degradation times and release kinetics of DNA for sustained gene expression over a required time.

### **1.8.1. *Aeromonas hydrophila***

*A. hydrophila* is a pathogenic gram-negative bacterium associated with lower vertebrates like fish, amphibians [28]. Aeromoniasis, an important fish disease is caused by this bacterium [29]. *A. hydrophila* infections in fishes have been reported from time to time in many Asian countries including China, Thailand, Philippines and India [30].

### **1.8.2. *Vibrio cholerae***

*Vibrio cholerae* is a "comma" shaped Gram-negative bacteria [31] with a single, polar flagellum for movement. *V. cholerae* can cause syndromes ranging from asymptomatic to cholera gravis. Symptoms include abrupt onset of watery diarrhea (a grey and cloudy liquid), occasional vomiting, and abdominal cramps [32]. Dehydration can lead to death in a few hours to days in untreated children. Cholera affects an estimated 3-5 million people worldwide and causes 100,000-130,000 deaths a year as of 2010 [33]. Cholera remains both epidemic and endemic in many areas of the world. This occurs mainly in the developing world [34] due to poor sanitary and socioeconomic conditions.

## **1.9. Outer membrane protein as vaccine target**

The OM of pathogenic gram-negative bacteria is mainly responsible for establishing initial adherence, modulate host-pathogen interaction, overall survival of the organism and propagation of virulence factor [35]. It also has protective antigenicity, because OM components are easily recognized as a foreign antigen by immunological defense systems of the hosts. Outer membrane proteins (Omps) are located at host–bacterial interface in pathogenic gram-negative bacteria and are important for host immune responses and as targets for drug therapy. The Outer Membrane (OM) of *A. hydrophila* is a complex structure which mainly consists of lipopolysaccharide (LPS), phospholipids and a group of outer membrane proteins (Omps). Omps are located at host–bacterial interface in *A. hydrophila* and can be targeted for drug therapy [36]. Similarly, the Outer Membrane (OM) of *V. cholerae* is a complex structure that mainly consists of lipopolysaccharide (LPS), phospholipids and a group of outer membrane proteins (Omps). High levels of transcripts for OmpU and multiple OM structures (OmpS, OmpV, OmpK, OmpC, OmpW, and OmpA) were present along with a number of conserved hypothetical proteins [37]. Virulence-related outer membrane proteins (Omps) are essential to bacterial survival within macrophages and for eukaryotic cell invasion that could be an alternative candidate for development of subunit vaccine against *V. cholerae*.

## 1.10. Motivation

A better delivery system which could mimic the natural infection, reduce the need for booster immunization and also could address the other complications hopes to improve the vaccine efficacy. Various biodegradable polymeric particles like polylactide-co-glycolide (PLGA) or polylactide (PLA), not only work as a delivery system but also provide adjuvant activity and marks the development of long-lasting immunity after a single injected dose. So, a relatively new system which is stable with antigen combination and can provide comparable immunity to that of adjuvants, eventually, can be treated as a complete replacement for the existing adjuvants in use and should take the lead for development of advanced vaccine formulations. The strategy here is to develop such a system. Omcs are highly immunogenic due to their exposed epitopes on the cell surface. There are safety concerns with the use of oil adjuvant (Freund's incomplete adjuvant; FIA) in multivalent vaccine formulations for fish due to the generation of adverse side effects (e.g., adhesions). Therefore, alternative molecules or certain combinations of them (targeting specific cellular responses) as adjuvants are desirable in order to enhance overall immunogenicity and efficacy without reducing protection levels. There are only a few reports available on PLA/PLGA NP based vaccine formulations with adjuvant like effects and sustained target specific release to generate an optimal immune response for which more elaborate and conclusive studies are needed to define the protective roles of PLA/PLGA nanoparticulate system. PLA/PLGA NPs encapsulating Omp antigen from *A. hydrophila* and *V. cholerae* would be a better antigenic carrier model in fish and mice respectively. These NP delivery systems would increase the antigen persistence *in vivo*, improve the initial antigen exposure to immune system after immunization. The combined action of PLA/PLGA NPs and OMP would result in the generation of enhanced and prolonged adjuvant-induced antigen-specific immune responses. Among possible delivery systems, nanoparticles (NP) based delivery of DNA vaccines to APCs, is an emerging and promising approach used for optimizing DNA vaccine formulation for immunotherapy. Nanoparticles based delivery systems for plasmid DNA (pDNA) (which encode Omp gene of interest) administration may be the key to improve transfection efficiency *in vivo* even at lower doses.

## 1.11. Objectives

In the present study, various NPs formulations of PLA and PLGA loaded with model protein (BSA) or drug (clindamycin hydrochloride) were prepared by solvent evaporation method varying drug/protein: polymer concentration and optimized for size, encapsulation efficiency, drug loading, morphology, etc. Then, PLA/PLGA NPs encapsulating Omp antigen from *A. hydrophila* were formulated and their efficacy were compared with adjuvant formulations to

develop a better antigenic carrier model in fish. Similarly, the efficacy is also compared between PLA encapsulated and PLGA encapsulated Omp NP-immunized groups and a correlation is established evaluating the results of innate and adaptive immune response studies in *L. rohita*. In another attempt, PLA/PLGA-Omp (Omp from *V. cholerae*) nanoparticles were formulated with desired physicochemical properties and evaluation of type and strength of immune responses (Humoral and cellular) elicited by formulated NPs was elucidated by comparing all possible combinations in mice.

Thus, the specific objectives of the current study are

1. Preparation and characterization of PLA and PLGA loaded with model protein (BSA) or drug (Clindamycin hydrochloride) NPs varying drug/protein:polymer concentration
2. Preparation, Characterization and In vitro study of biodegradable and biocompatible based PLA and PLGA nanoparticles with encapsulation of OMP antigens.
3. Parenteral immunization of PLA/PLGA nanoparticle encapsulating outer membrane protein (Omp) from *A. hydrophila*; Evaluation of immunostimulatory action in lower vertebrate (fish).
4. Evaluation of the immune responses (specific) in mice model after intraperitoneal immunization of Omp antigen (*V. cholerae*) encapsulated PLA/PLGA nanoparticles
5. Development of DNA vaccines to boost antigenic OMP (outer membrane protein) antigenicity.
6. In Silico identification of outer membrane protein (Omp) and subunit vaccine design against pathogenic *V. cholerae*.

## 1.12. Thesis outline

This thesis has been organized into 7 chapters and each chapter contains self-describing illustrations, necessary tables and figures. Chapter 1 includes a general introduction about vaccine and vaccination, nanoparticle-based vaccine delivery, biodegradable nanoparticles and their use in nanomedicine. Chapter 2 covers relevant literature to the current work. Chapter 3 includes the preparation of PLA and PLGA NPs loaded with BSA (model protein) or drug (Clindamycin hydrochloride) and optimization studies for size, charge, encapsulation efficiency, drug loading, etc. Chapter 4 contains objective 3 that describe the immunological evaluation of PLA/PLGA nanoparticle encapsulating outer membrane protein (*Aeromonas hydrophila*) in fish (*L. rohita*). Chapter 5 includes objective 4 which describe the formulation of PLA/PLGA-Omp (Omp of *V. cholerae*) nanoparticles with desired physicochemical properties and evaluation of type and strength of immune responses elicited by formulated NPs was elucidated

by evaluating antigen-specific antibody response and cellular response studies in *mice*. Chapter 6 includes objective 5 that describe the development of pDNA vaccine as well as a delivery system to boost antigenic outer membrane protein (Omp) that would act as a potential vaccine candidate. Chapter 7 summarizes major findings of all objectives.



# Chapter 2

## Review of Literature

The major goals of today's vaccine research mostly aimed at the development of acquired immunity naturally by inoculation of immunogenic components (non-pathogenic) of the pathogen or closely related organisms. In general, these conventional approaches have been most successful for developing vaccines that can induce an immune response based on antigen-specific antibody and cytotoxic T-lymphocyte (CTL) responses [1], [2]. The growing issues of vaccine safety are in alarming rate owing to their weak immunogenicity, imperfect immunization procedures and failure to acquire booster doses to potentiate prime doses. So, these issues have paved the way towards research for developing new generation preventive and therapeutic vaccine. Adjuvants are the immunological agents that act to accelerate, enhance and prolong antigen-specific immune responses when used in combination with specific antigens. Adjuvants are used for multiple purposes; to accelerate a robust immune response by enhancing immunogenicity, provide antigen dose sparing, reduce booster immunization requirements, offers prolonged and improved protection [3], [4]. There is a crucial requirement for enhanced and effective vaccine formulations (with or without adjuvant) having minimal compositions like purified proteins, recombinant proteins and synthetic peptides, etc. for specific disease antigen in question. There is also an urgent requirement for the development of novel carriers that could be target specific to achieve therapeutic drug concentration.

Adjuvants in vaccine formulations vary to a greater extent due to many issues; e.g. the chemical nature, mode of action, the safety and efficacy of adjuvants. The adverse effects concerned with the prolonged use of adjuvants use are the hyperactivation of the immune system, neurotoxicity and many detrimental effects. Therefore, a relatively new formulation that is stable with antigen combination and can provide comparable immunity to that of adjuvants eventually can be treated as a complete replacement for the existing adjuvants in use should take the lead for development of advanced vaccine formulations. Currently, controlled delivery systems consisting of biodegradable microspheres/nanosphere act as a promising vaccine carrier because it can potentially deliver the antigens to the specific locations at predetermined rates and durations to generate an optimal immune response.

## 2.1. Nanotechnology: A therapeutic approach

Nanotechnology can be defined as the manipulation, modeling, exact placement and manufacture of material at the nanometer scale. The impact of nanotechnology in different fields, including medicine, is immense [38] due to its wide application in the treatment of the major health threats including infectious diseases, cancer, metabolic diseases, inflammations and autoimmune diseases. The explosive growth of nanotechnology not only offer perfections to existing techniques but also helpful in discovering new tools with versatile applications [39]. The practice of nanotechnology in vaccinology, in particular, has been increasing exponentially in the past decade that has evolved the term, “nanovaccinology” [40]. In both therapeutic and prophylactic approaches, nanoparticles are used as either a delivery system for sustained and target specific antigen delivery and/or as adjuvant (immunostimulant) to enhance the antigenicity. A number of approved nano-sized vaccine and drug delivery systems ascertain the revolution in disease treatment and prevention [41]–[44]. The manipulation of drug/antigen at nanoscale level mostly relies upon the bioactive characteristics such as solubility, controlled release, retention time [45]. The surface area of the increased functionality of nanoparticles lends itself to further biomedical applications [46] and gene therapy [47].

Therapeutic nanovaccinology is mostly focused on cancer treatment [48]–[50] and other diseases, such as Alzheimer's [51], hypertension [52] and nicotine addiction [42], etc. On the other hand, prophylactic nanovaccinology has been applied for the prevention of different infectious diseases. There are many prophylactic nano-vaccines that have been approved for human use and more are in pre-clinical or clinical trials [53], [54].

## 2.2. Nanoparticles

A nanoparticle is regarded as a small object that behaves as a whole unit in terms of its properties and transport. With the advances in the types of nanoparticles, any particulate materials in size range 1–1000 nm are considered as nanoparticles (FDA, 2011), that act as excellent drug carriers by enhancing aqueous solubility, targeting drug to specific location and increasing resistance time in the body (increasing half-life for clearance/increasing specificity for its associated receptors). However, nanomedicine concept is based upon the use of nanoparticles at the level of 1-100 nm [47], [55], [56]. Although nanoparticles are considered to be in nano dimensions below 100 nm size, but relative increase in size (size >100 nm) is generally observed and accepted in the area of drug delivery systems when there is efficient drug loading and especially where sufficient amount of drug may be needed to load onto the particles [57]. Nanoparticles are becoming key components in a wide range of applications because of their potential applications in biomedical, optical, and electronic fields [58].

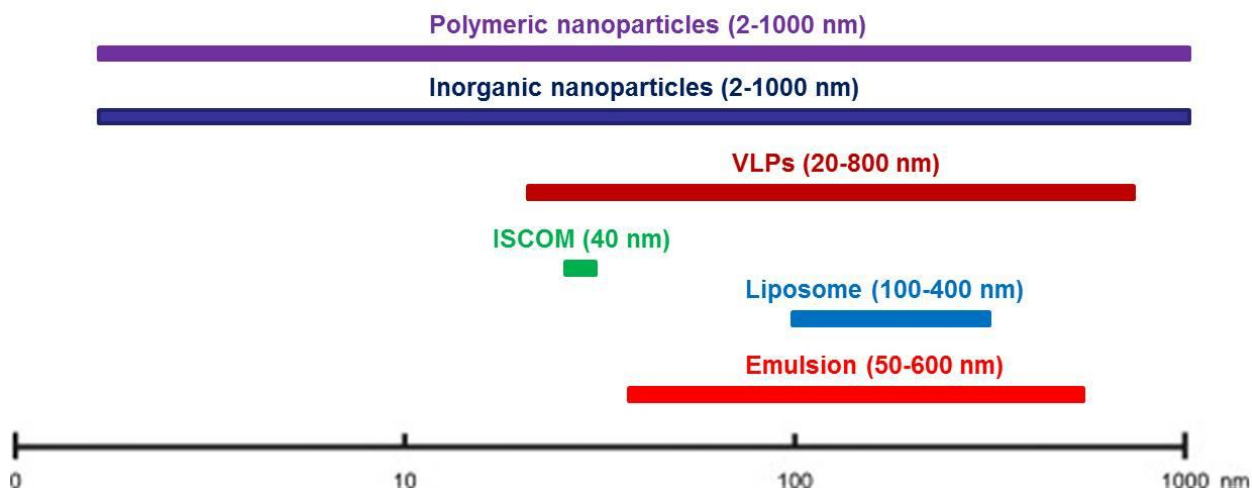


**Figure 2.1: The size range of nanoparticles used in nanovaccinology**

Nanotechnology offers the opportunity to design nanoparticles varying in size, shape, composition, and surface properties, for application in the field of medicine [41], [59]. Nanoparticles have size similarity with cellular components, due to which they can enter living cells using the cellular endocytosis mechanism, in particular, pinocytosis [60]. As a revolutionary new 21<sup>st</sup> century technology, nanotechnology is starting to impact by developing theranostic nanoparticles for diagnosis of diseases as well as the drug delivery for disease prevention and treatment. The emergence of virus-like particles (VLPs), quantum dots and magnetic nanoparticles, marks a conjunction of protein biotechnology with inorganic nanotechnology that has achieved a significant progress for Nanomedicine.

The vaccine antigen is either encapsulated within or coupled onto the surface of the nanoparticles. The encapsulated antigen undergoes controlled delivery (pre-determined rate and duration) avoiding rapid degradation and short-lived immune response.

Nanoparticles in conjugation with antigen allow target specific presentation of the antigen to the immune system mimicking pathogen infection, thereby provoking a similar response. Nanoparticles are also responsible for the prolonged release of antigens to maximize exposure to the immune system. The potential of nanoparticles is more explored to deliver vaccines through nontraditional approaches such as topical, inhalation or optical delivery as well combining multiple antigens in a single particulate system so as to protect against more than one disease [61].

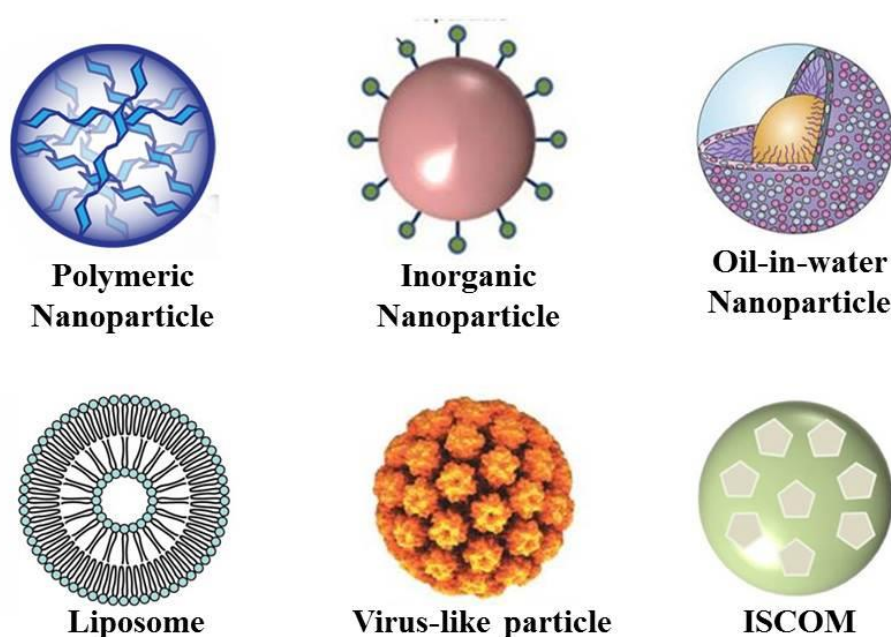


Figure 2.2: Schematic representation of different nanoparticle delivery systems (Polymeric nanoparticle, Inorganic nanoparticle, Oil-in-water emulsion, Liposome, Virus-like particle, ISCOM)

## 2.3. Types of nanoparticles

### 2.3.1. Polymeric nanoparticles (PNPs)

Polymeric nanoparticles (PNPs) consist of a polymer that has gained much deliberation due to advancement in polymer science and technology. Two types of polymers can be used in nano delivery that is natural and synthetic. Biocompatibility and biodegradability are essential features for potential application as tissue engineering, drug and gene delivery and new vaccination strategies. Most polymers used to prepare nanoparticles consists of synthetic polymers are, such as poly(d,l-lactide-co-glycolide) (PLG) [62]–[64], poly(d,l-lactic-co glycolic acid)(PLGA) [64]–[69], poly(g-glutamic acid) (g-PGA) [5], [66], poly(ethylene glycol) (PEG) [63], and polystyrene [70], [71]. Poly (D, L- lactide-co-glycolide) (PLGA), polylactic acid (PLA), are considered to be highly beneficial because of their biodegradable and biocompatible nature [65], [72]. They are widely used for human research due to their FDA approval (The Food and Drug Administration, U.S.A.). These polymeric nanoparticle- based antigen/drug delivery offers several advantages over traditional delivery methods, including the ability for drug delivery to a specific site such as an intracellular infection [73], [74], reducing systemic toxicity [75] and also to facilitate sustained release of a drug, minimizing dosing regimens [76].

**Table 2.1: Polymeric materials currently being investigated at the nanoscale for drug delivery application; advantages and disadvantages.**

Type	Polymer	Advantages	Disadvantages
Natural	cellulose, starch, chitosan, carrageenan, alginates, xanthan gum, gellan gum, pectins	Less toxic Biocompatibility Biodegradable Easily available	High degree of variability in natural materials derived from animal sources  Structurally more complex  Extraction process very complicated and high cost
Synthetic	poly(lactic acid) (PLA), poly(cyanoacrylates) (PACA), poly(acrylic acid), poly(anhydrides), poly(amides), poly (ortho esters), poly(ethylene glycol), and poly(vinyl alcohol) (PVA) and other like poly(isobutyl cyanoacrylate) (PIBCA), poly(ethylene oxide) (PEO), poly( $\alpha$ - caprolactone) (PCL)	Biocompatibility	Toxic  Non degradable  Synthetic process is very complicated and high cost

Natural polymers based on polysaccharide have also been used to prepare nanoparticle adjuvants, such as chitosan [77]–[79], alginate [80], pullulan [81], [82] and inulin [83], [84] etc. Chitosan-based nanoparticles have been widely investigated due to their biodegradability, biocompatibility, nontoxic nature and available in desired shapes and sizes [5], [85], [86]. The choice of polymer and the ability to control drug release have made them ideal candidates for delivery of vaccines, cancer therapy and delivery of targeted antibiotics, etc. Moreover, polymeric nanoparticles based drug delivery can also be applied in tissue engineering as well as drug delivery for other animals [87].

### 2.3.2. Inorganic nanoparticles

Inorganic nanoparticles have measure impact on modern materials science research due to their possible technological importance, particularly in the field of bio-nanotechnology, having unique physical properties including size-dependent magnetic, optical, electronic and catalytic properties [88]. Inorganic nanoparticles are able to interact with light and/or magnetic fields, thus spreading their possible applications in the areas of fluorescence labeling, magnetic resonance imaging (MRI) and stimulus-responsive drug delivery that are crucial to the diagnosis and treatment of disease [89]. Inorganic nanoparticles, as a viable alternative to organic forms, could be used for vaccine delivery. Many inorganic nanoparticles have been explored for their application in vaccine delivery. Despite non-biodegradable nature, the inorganic nanoparticles have advantages like unique rigid structure controllable synthesis [70]. The four most common inorganic NPs are 1) noble metal, 2) magnetic 3) fluorescence, and 4) multifunctional, e.g., luminescent magnetic [90]. Among noble metals, gold nanoparticles (AuNPs) are mostly used in vaccine delivery [91], as they can be easily manipulated into different shapes (spherical, rod, cubic, etc.) and size [92], and can be surface-engineered by conjugating carbohydrates [93].

Gold nanoparticles have also been used as antigen carrier to target viruses such as influenza [94] and foot-and-mouth disease [95], or as a DNA vaccine adjuvant for human immunodeficiency virus (HIV) [96]. Carbon nanoparticles are another commonly-studied composition for drug and vaccine delivery [61]. Multiple copies of protein or peptide antigens can be conjugated onto carbon nanotube (CNTs) for delivery and have enhanced the level of antibody response [97]–[100]. Silica-based inorganic nanoparticles (SiNPs) are biocompatible in nature and have excellent properties as nanocarriers for various biomedical applications, such as tumor targeting, real-time multimodal imaging, and vaccine delivery [101], [102]. Calcium phosphate nanoparticles can be formulated by using calcium chloride, dibasic sodium phosphate and sodium citrate under specific conditions. The biocompatible and nontoxic nature with variable size (50–100 nm) [103] of calcium phosphate nanoparticles made them as useful adjuvants for DNA vaccines offering mucosal immunity [103], [104].

### **2.3.3. Liposomes**

A liposome is an artificially-prepared spherical vesicle composed of a lamellar phase lipid bilayer. Liposomes have been known as potential drug delivery vehicles for nearly four decades [105]. Liposomal and polymeric drug conjugates are the two prevailing classes of commercially available nanoparticle-based therapeutic products [106]. Liposomes are generally formulated from biologically inert lipids that are non-toxic and biodegradable. Liposomes are generally formulated from biologically inert lipids that are non-toxic and biodegradable in nature. Loading of both hydrophobic and hydrophilic molecules is facilitated by the lipid bi-layered structure of liposomes. The beneficial properties of liposomal-mediated delivery in in-vitro studies are substantiated by the literature [107]. Liposomes, which are formed by biodegradable and nontoxic phospholipids can encapsulate antigen within the core for delivery [108]. There are, also, several liposomal therapeutic vaccine formulations against diseases like, hepatitis A malaria, tuberculosis, influenza, prostate cancer and colorectal cancer that are at different clinical stages [91]. A number of liposome systems have been established and approved for human use, such as Inflexal® V and Epaxal® [108], [109].

### **2.3.4. Immunostimulating complex (ISCOM)**

Immune stimulating complexes (ISCOMs) are generally open cage-like spherical structures (40 nm in diameter) that are spontaneously formed when mixing cholesterol, phospholipids and Quillaia saponins together under a specific stoichiometry. These complexes have immune stimulating properties and are thus mostly used as a vaccine adjuvant to induce a stronger immune response and longer protection [17], [110], [111]. ISCOMs display high adjuvant activity against a broad range of bacterial and viral antigens [112]–[114].

### **2.3.5. Virus-like particles**

Virus-like particles (VLPs), comprised of capsid proteins that can induce an immune response without having genetic material required for replication, promote immunogenicity. These have been established and approved as vaccines in some cases [115], [116]. In addition, many of these VLPs can be used as molecular platforms for genetic fusion or chemical attachment of heterologous antigenic epitopes [54]. VLPs take the good aspects of viruses and avoid the bad. The naturally-optimized nanoparticle size and repetitive structural order of VLPs are responsible for inducing potent immune responses, even in the absence of adjuvant [117]. A variety of VLPs and virus-based nanoparticles are being explored for use as vaccines and epitope platforms [54]. However, VLPs can also act as a delivery platform where a target antigen from a virus unrelated to the VLP used is modularized on the surface of a VLP [118].

### **2.3.6. Self-assembled proteins**

Self-assembling systems that attempt to drive higher levels of quaternary protein structuring have emerged for the formulation of nanoparticle-based vaccines. The protein like Ferritin can self-assemble into nearly-spherical 10 nm structure. By genetically fusing influenza virus haemagglutinin (HA) to ferritin, the recombined protein spontaneously assembled into an octahedrally-symmetric particle and then reformed eight trimeric HA spikes [119] to induce an enhanced immune response, which typically is processed to destroy rather than build a viral structure.

### **2.3.7. Emulsions**

Another type of nanoparticles used as adjuvants in vaccines delivery is nano-sized emulsions [120], [121]. These nanoparticles can exist as oil-in-water or water-in-oil forms, where the droplet size can vary from 50 nm to 600 nm [121]. Emulsions can carry antigens inside their core for efficient vaccine delivery [121] or can also be simply mixed with the antigen. One commonly used emulsion is MF59<sup>TM</sup>, an oil-in-water emulsion which has been licensed as a safe and potent vaccine adjuvant in over 20 countries [122]. Recently, a tailorable nano-sized emulsion (TNE) platform technology has been developed using non-covalent click self-assembly for antigen and drug delivery [123], [124]. Targeted delivery of protein antigen to dendritic cells was achieved [124].

## **2.4. Nanoparticles Preparation Methods**

Synthesis of nanoparticles has emerged in the last decade as an interaction between nanotechnology and biotechnology. Due to the possible wide application of nanoparticles, this emerging science put modern material science research at the tip. These nanoparticles are designed to exhibit new and/or novel characteristics associated with size, morphology,

functionality and distribution pattern [125]. There are several possible means of nanoparticle synthesis ranging from totally chemical methods to fully biological processes [125] such as reduction in solutions, chemical and photochemical reactions, thermal decomposition, radiation-assisted [126], electrochemical and finally most recently green synthesis [127]–[129].

#### **2.4.1. Preparation antigen/drug-loaded polymeric nanoparticles**

Polymeric NPs have attracted much attention due to their ability to deliver drugs/antigens as well as being biodegradable in nature. The release kinetics of encapsulated drugs from polymeric NPs can be regulated by compositional variation [130]. These types of NPs can be formulated from a wide range of polymers e.g. poly( $\alpha$ -hydroxy acids), polysaccharides, or poly(amino acids) to create a vesicle which can either accommodate or display antigens/drug. The most commonly used poly ( $\alpha$ -hydroxy acids) based polymeric NPs are either poly (lactic acid) (PLA) or poly (lactic-*co*-glycolic acid) (PLGA) which are often synthesized using a double emulsion-solvent evaporation technique [131], [132]. Firstly the polymer (PLA or PLGA) is dissolved in an organic solvent followed by the addition of the drug which is then emulsified to get a primary emulsion. Then, a water-in-oil-in-water emulsion is formed with the addition of an emulsifying agent (e.g., polyvinyl alcohol or polyvinyl pyrrolidone). This results in the encapsulation of the antigen in polymeric NPs. The solution is then allowed to solvent evaporation and then freeze-dried to prevent degradation of the polymer due to water-catalyzed ester hydrolysis [133]–[135]. But, the limitations with this method are lower antigen entrapment efficiency and possibility of protein denaturation at the oil-water interface [136]. This limitation can be avoided by the addition of stabilizers such as surfactants or sugars, (trehalose or sucrose) which provide stability against denaturation by maintaining the protein in its native form. For preserving encapsulated protein/antigen stability, the alternative method uses poly(amino acids) such as poly ( $\gamma$ -glutamic acid) ( $\gamma$ -PGA), poly(L-arginine), poly( $\epsilon$ -lysine) or poly(L-histidine) that avoid emulsion step for NP synthesis [137]–[139]. These amphiphilic copolymers self-assemble through hydrophobic interactions to form structures comprising a hydrophobic core and a hydrophilic outer shell [132], [140]. Furthermore,  $\gamma$ -PGA based polymeric NPs offer more stability due to the presence of  $\gamma$ -linked glutamic acids that are not easily recognized by common proteases [141]. The poly (amino acid) based nanoparticles are formulated by dissolving the polymer in dimethyl sulfoxide (DMSO). The size of NPs is controlled by varying the salt concentration resulting in monodispersed forms [142]. The protein-encapsulated  $\gamma$ -PGANPs can be prepared by emulsifying the protein (in saline) to  $\gamma$ -PGA (in DMSO) followed by centrifugation [143]. The resulting encapsulation is stable over an acidic pH range [143].



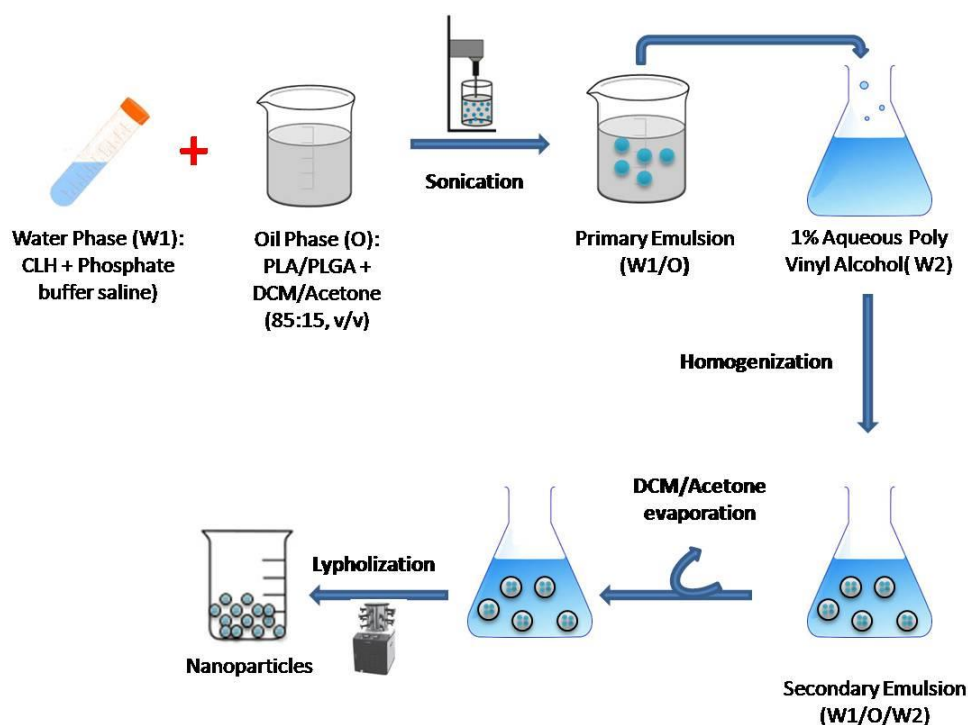


**Figure 2.3: Preparation of antigen-encapsulating nanoparticles by w/o/w emulsion method**

Hydrophilic polysaccharide polymeric NPs such as dextran and chitosan are also good candidates for vaccine delivery. Chitosan NPs often used because of its favorable characteristics e.g. biocompatibility, biodegradability into non-toxic products in vivo [144]. Chitosan NPs can be prepared by a self-assembly procedure through chemical modification [145]. Similarly, a complex coacervation process is used where particles would spontaneously form due to mixing of two hydrophilic colloids together; with chitosan precipitating around plasmid DNA [146]. Again, an ionic gelation method has also been used to prepare chitosan NPs which is based on the presence of positively charged amino groups in chitosan and the negative charge of tripolyphosphate[147]. Sometimes these colloids are further modified by the addition of other components like polyethylene glycol in order to aid properties absorption or to slow down release.

## 2.5. Characterization of Drug-loaded nanoparticles

Various parameters; size, physical, chemical, morphological properties, drug encapsulation efficiency and release profile of antigens are known to play a key role in the designing efficient polymeric nanoparticle-based delivery [148].

### 2.5.1. Particle size

Particle size and its distribution patterns are the most important characteristics of nanoparticle-based drug delivery systems. They determine the targeting ability, in vivo distribution, biological fate and toxicity of nanoparticle systems. In addition, the size can also influence the drug

encapsulation, release and stability. The nanoparticles of sub-micron size have numerous advantages over microparticles as a potential drug delivery system [149]. Usually, nanoparticles have relatively higher intracellular uptake as compared to microparticles and available for a wide range of biological targets because of their small size and relative mobility. Although nanoparticles are considered to be in nano dimensions below 100 nm size, but relative increase in size (size >100 nm) is generally observed and accepted in the area of drug delivery systems when there is efficient drug loading and especially where sufficient amount of drug may be needed to load onto the particles [57]. It was also reported that nanoparticles can cross the blood-brain barrier following the opening of tight junctions by hyperosmotic mannitol that can provide sustained delivery of therapeutic agents for diseases like brain tumors. Drug release is also influenced by particle size. Smaller NPs have larger surface area. Therefore, most of the drug associated would be at or near the particle surface, leading to fast drug release. However, larger particles have large cores that permit more amounts of drug to be encapsulated and their slow release profile [150]. The small sized NPs have a greater chance of aggregation of particles during storage and transportation. The formulation of nanoparticles with smaller size with enhanced stability is a really a challenge. Polymer degradation can also be controlled by the particle size. The rate of polymer (PLGA) degradation was found to increase with increasing particle size in vitro that might be due to autocatalytic degradation of the polymer [151]. Presently, the fastest and most routine method of determining particle size is by dynamic light scattering or photon-correlation spectroscopy. Photon-correlation spectroscopy determines the diameter of the particle due to Brownian motion and light scattering properties. The results obtained are usually verified by scanning or transmission electron microscopy (SEM or TEM).

### **2.5.2. Surface properties of NPs**

The surface hydrophobicity of formulated NPs also determines the amount of adsorbed blood components, mostly proteins (Opsonins) that in turn influence the *in-vivo* outcome of nanoparticles [152], [153]. The conventional nanoparticles are rapidly opsonized and cleared by the macrophages [154]. It is essential to minimize the opsonization and to prolong the circulation of nanoparticles in vivo, which can be accomplished by (a) surface modification by coating of nanoparticles with hydrophilic polymers/surfactants; (b) formulation of nanoparticles with biodegradable copolymers with hydrophilic components such as polyethylene oxide, polyethylene glycol (PEG), poloxamine, poloxamer, and polysorbate 80 (Tween 80). The zeta potential of a nanoparticle is commonly used to characterize the surface charge property of nanoparticles [155]. Zeta potential otherwise known as the electrokinetic potential at the surface of the colloidal particles has a great significance in comparing the stability of colloidal

dispersions [156]. The zeta potential indicates the degree of repulsion between adjacent particles and similarly charged particles in the dispersion. For molecules and particles that are small enough, a high zeta potential confers stability (dispersion will resist aggregation). Nanoparticles with a zeta potential (surface charge) above (+/-) 30 mV have been shown to be stable in suspension, as the surface charge prevents aggregation of the particles [157]. The zeta potential can also be used to determine whether a charged active material is encapsulated within the core of the nanocapsule or adsorbed onto the surface.

### **2.5.3. Drug loading**

The ideal nanoparticulate system should have a high drug-loading capacity thereby reducing the drug quantity for the administration. Generally, drug loading can be achieved by two methods: a. incorporation method (adding at the time of nanoparticles formulation), b. adsorption/absorption technique (Absorbing the drug after formation of nanoparticles) [158]. Encapsulation of protein antigens depends on series of factors like polymer nature, method of formulations and molecular interaction between polymers, etc. The amount of drug bound to NP depends on the chemical structure of the drug/polymer ratio and the conditions of drug loading [159]. Hydrophilic polymers show higher encapsulation than hydrophobic polymer due to enhanced molecular interactions between the polymer and the drug [160]. Entrapment efficiency is very much dependent on the solid-state drug solubility in the matrix material or polymer (solid dispersion or dissolution), which is related to the molecular weight, polymer composition, drug polymer interaction and the presence of functional end groups [161]–[163]. In the case of macromolecules or protein, the higher loading efficiency is achieved when it is loaded at or near its isoelectric point (with minimum solubility and maximum adsorption) [164]. For smaller molecules, the use of ionic interaction between the drug and matrix materials can be a very effective approach to increase the drug encapsulation [165].

### **2.5.4. Drug release**

Drug release and polymer degradation are important factors to develop an ideal nanoparticulate system. Generally, drug release from nanoparticles rate depends on many factors: (1) solubility of the drug; (2) drug diffusion through the nanoparticle matrix; (3) desorption of the surface attached/adsorbed drug; (4) nanoparticle matrix erosion/degradation. Thus, the properties like solubility, diffusion and biodegradation of the matrix materials govern the release process [158]. The rapid initial burst release is particularly attributed to weakly bound or adsorbed drug to the surface of nanoparticles [166]. The solubility and diffusivity of the drug in polymer matrix also plays measure role in controlling drug release. When the drug is encapsulated by incorporation

method, the system offers a relatively small burst effect and better-sustained release characteristics [167].

The in vitro drug release can be studied by various methods e.g.: (1) dialysis bag diffusion technique; (2) side-by-side diffusion cells with artificial/biological membranes; (3) reverse dialysis bag technique; (4) agitation followed by centrifugation; (5) Ultrafiltration or centrifugal ultrafiltration techniques [158]. Usually, the release study is performed by controlled agitation followed by centrifugation.

## **2.6. Vaccine-induced immunity**

The objective of vaccination with any formulation is to express the innate and adaptive immune responses to infection [168], [169]. The antigen-presenting cells such as dendritic cells play an important role in both innate and adaptive immune responses [170]. On recognition of microbial surface determinants, antigen-presenting cells (APC) undergo maturation leading to a redistribution of MHC (MHC I and MHC II) molecules from intracellular compartments to the cell surface, secretion of cytokines, morphological changes of dendritic cells and cytoskeleton reorganization [61].

The antigens are internalized either through the endocytic pathway or non-endocytic pathways [171]. The non-endocytic pathways involve the engulfment of antigen by the APCs (phagocytosis) and its degradation by proteolytic enzymes and reactive oxygen species. The resulted degraded products (peptides) are then displayed on MHC class II molecules and are recognized by CD4<sup>+</sup> T cells to stimulate the antibody production and the formation of memory T-cells [61]. However, in the case of non-endocytic pathways, antigens derived from the pathogen are processed via proteasome which then display peptides on MHC class I molecules [172]. The displayed antigen is recognized by CD8<sup>+</sup> T cells that have cytotoxic activity toward infected host cells. In practice, the response against pathogen infection may encompass a mix of all these (MHC I and MHC II response), further complicated by the stimulation of pro-inflammatory Th17 cells and controlled by regulatory T-cells, but a predominant responses (Th1 or Th2) may be necessary to resolve the infection [173].

## **2.7. Antigens delivery using nanoparticles**

Antigen-loaded polymeric nanoparticles represent a novel approach for the enhancement of antigen-specific humoral and cellular immune responses via selective targeting [5], [170]. Dendritic cells (DCs) are known to be initiators and modulators of immune responses by processing antigens through both MHC I and MHC II pathways. Immature DCs encounters pathogens, specific antigens, or particulate antigens at the introduction site. After phagocytosis, the foreign antigen has been taken up into the DCs that present the antigens on MHC class II or

MHC class I molecules by cross-priming [172]. Therefore, the antigen delivery to DCs is of key importance in the development of effective vaccines.

OVA encapsulated within  $\gamma$ -PGA-Phe nanoparticles (OVA-NPs) were efficiently taken up into DCs, whereas the uptake of OVA alone was hardly detectable [5]. Similarly, other types of nanoparticles like PLGA or liposomes are efficiently phagocytosed by the DCs, ensuing in their intracellular localization [174], [175].

## **2.8. Nanoparticles mediated dendritic cell activation**

The current research has been focused largely on determining the degree of DC maturation induced by exposure to polymeric nanoparticles [176]–[178]. After successful antigen delivery to DCs, the control over DC maturation is deeply involved in the development of effective vaccines. The maturation of DCs is associated with increased expression of many cell surface markers, including some co-stimulatory molecules CD40, CD80, CD83, CD86, MHC class I, and MHC class II [179].

Upon exposure of these DCs to the nanoparticles, the expression of co-stimulatory molecules (maturation markers) was increased in a dose-dependent manner [180]. However, both the uptake of nanoparticles and characteristics of the polymers forming the nanoparticles are important for the induction of DC maturation. Previous research observed higher effects of DC activation by the nanoparticles despite the smaller size. Thus, the DC maturation is affected by the surface interactions between the nanoparticles and DCs [143], [181]. DC maturation by PLGA nanoparticles was observed by a modest increase in the expression of MHC class II and CD86 compared to controls [175].

**Table 2.2: Summary of the various types of NPs currently being studied for their use as vaccine carriers.**

Type	Matrix/expression system	Size	Antigen (pathogen)	Route of immunization	References
<b>Polymeric</b>	Poly(lactic-co-glycolic acid) (PLGA); Poly(lactic acid) (PLA); Poly(glycolic acid) (PGA); Poly(hydroxybutyrate) (PHB); Chitosan;	100–200nm 800nm 1–5µm 248 nm	Docetaxel; TetHc (Tetanus); Hepatitis B; SBm7462 ( <i>Boophilus microplus</i> ); Rv1733c ( <i>M. tuberculosis</i> ); SPf66 ( <i>P. falciparum</i> malaria) Dtxd (Diphtheria) Ovalbumin gp120 (HIV-1)	Intramuscular, Intravenous	[5], [61], [67], [182]–[184]
<b>Non-degradable</b>	Gold; Silica; Carbon; Iron	2–150nm 5–470nm 20–300 nm	Plasmid DNA expressing hemagglutinin 1 (Influenza); Hepatitis B; MSP1 ( <i>Plasmodium falciparum</i> ) BSA	Intradermal, Intramuscular, Subcutaneous, Intravenous	[95], [98], [184]–[187]
<b>Liposomes (non-viral lipids)</b>	MPLA; Phospholipid S100 and cholesterol; Phosphatidylcholine and cholesterol;	50–500nm 200 nm	R32NS1 (malaria); Cholera toxin; Circumsporozoite (malaria); Lipid A; CtUBE fusion peptide ( <i>H. pylori</i> ); KWC <i>Y. pestis</i> ; Polysaccharides ( <i>Streptococcus pneumoniae</i> serotype 14) VMP001 ( <i>Plasmodium vivax</i> ) RTS,S/AS01B ( <i>Plasmodium falciparum</i> CSP + hepatitis B protein hybrid)	Intramuscular, Intravenous, Subcutaneous, Oral, Intranasal	[61], [67], [184], [188]–[190]
<b>Virus-like particles</b>	Baculovirus <i>E. coli</i> Mammalian cells Yeast	55–60 nm (HPV) 100–200 nm (HIV) 80–120 nm (H1N1) 27–60 nm	Major capsid protein, L1 (HPV); FMS-like tyrosine kinase receptor-ligand, FL (HIV); gag precursor protein, pr45 (HIV); HIV env cDNA (HIV); Haemagglutinin (H1N1); Nicotinamide (H1N1) Matrix protein M1 (H1N1)	Intramuscular, Subcutaneous, Intraperitoneal, Oral, Intranasal	[61], [184], [191]–[194]
<b>ISCOMs</b>	Saponin (Quil A) Phospholipid (phosphatidylethanolamine, phosphatidylcholine) Cholesterol Viral proteins	40 nm	HIV-1(gp120/160) FIV(p130) <i>E. falciformis</i> (p27)	Intramuscular, Subcutaneous, Oral	[61], [184], [195]–[197]

## 2.9. Gene delivery by polyion complex NPs

Over the past decades, the interest in the possibility of using gene-based therapy and DNA vaccination for treatment of both genetic and acquired diseases such as infections, degenerative disorders and cancer, has grown exponentially, mostly due to the development of several methods for delivering genes to mammalian cells (viral and non-viral vectors) [198], [199]. Genetic or DNA vaccination is the common name for vaccination methods that induce immunity by transfecting eukaryotic host cells with DNA that encodes a therapeutic protein, instead of injecting antigens in the form of proteins or peptides. This approach (the third vaccine revolution) provides a number of potential advantages over other traditional approaches, like generation of both humoral and cell-mediated immune responses, improved vaccine stability, the absence of any infectious agent and the relative ease of large-scale manufacture with high purity [6], [200], [201]. The safety, simplicity, versatility, stability, ease of production, nontoxicity, and broad of immunity and long-lasting cytotoxic T lymphocyte responses make DNA vaccines very attractive for antiviral/antibacterial/anticancer immunization strategies [25], [202]–[204].

The use of plasmids as vectors is an active area of investigation due to their great potential for a safe use in prophylactic and therapeutic vaccination. Once administered, DNA vaccines activate both humoral and cellular immune responses against targeted illnesses. Novel delivery systems for administration of pDNA vaccines are central to address the above-discussed necessities [5], [6], [205]. This delivery system should be a modern and sophisticated form of an adjuvant with engineered immunological properties. Among possible delivery systems, nanoparticles (NP) based delivery of DNA vaccines to APCs, is an emerging and promising approach used for optimizing DNA vaccine formulation for immunotherapy [5], [6].

DNA delivery is, however, a difficult procedure and an appropriate vector is required for efficient protection as well as DNA release. Non-viral gene delivery mainly relies on DNA condensation induced by cationic agents. Cationic polymers have been widely preferred to condense DNA through electrostatic interactions between negatively charged DNA and the positively charged cation [206]. The biocompatible nanopolymers such as poly-(D, L-lactide-co-glycolide) (PLGA) and chitosan are attractive for DNA delivery applications [5], [61], [207], [208]. Chitosan NPs hold promise because of their ability to protect encapsulated nucleic acid-based antigens from nuclease degradation and promote delivery of adsorbed DNA to APCs [209], [210]. In the case of synthetic polymers like PLGA, besides DNA protection, the encapsulation permits a controlled DNA delivery system to be designed with controllable degradation times and release kinetics of DNA for prolonged gene expression over a required time. For example, PLGA undergoes ester hydrolysis in the physiological environment with the

formation of biocompatible monomers [211]. Nanoparticles based delivery systems for plasmid DNA (pDNA) (which encode target gene of interest) administration may be keys to improve the transfection efficiency *in-vivo* even at a lower dose. To improve the transfection efficiency of Chitosan/DNA complexes,  $\gamma$ -PGA/Chitosan/DNA-conjugated nanoparticles were formulated by an ionic-gelation method for transdermal gene delivery using a low-pressure gene gun [105]. Moreover, the pDNA/PEI/ $\gamma$ -PGA complex was highly taken up by the cells via a  $\gamma$ -PGA-specific receptor-mediated pathway and showed extremely high transfection efficiencies [212].

## 2.10. Nanoparticle-Antigen interaction

Vaccine formulations comprising nanoparticles and antigens can be classified by nanoparticle action into those based on delivery system or immune potentiator approaches. As a delivery system, nanoparticles can deliver antigen to the immune cell in 2 ways, (a) co-ingestion of the antigen and nanoparticle by the immune cell, or (b) transient delivery, i.e. protect the antigen and its control release at the target location. For immune potentiator approaches, nanoparticles activate certain immune pathways that might then augment antigen processing and improve immunogenicity [208], [213]. The attachment of antigen has been achieved through simple physical adsorption or more complex methods, such as encapsulation or chemical conjugation. The physical adsorption of antigen onto a nanoparticle is performed on the basis of charge or hydrophobic interaction [213], [214], where the interaction between nanoparticle and antigen is relatively weak that lead to rapid disassociation *in vivo*. The stronger interaction is observed in the case of encapsulation and chemical conjugation of antigen to nanoparticles. The antigens are mixed with nanoparticle precursors during formulation, resulting in encapsulation of antigen into nanoparticles [208]. On the other hand, the antigen is chemically cross-linked to the surface of a nanoparticle which is released inside the cell after taken up together with the nanoparticle [215]. The attachment or interaction of antigen with nanoparticles are not essential for immune potentiator approaches and sometimes, it may be undesirable in cases modified antigenic structure that occurs at the nanoparticle interface.



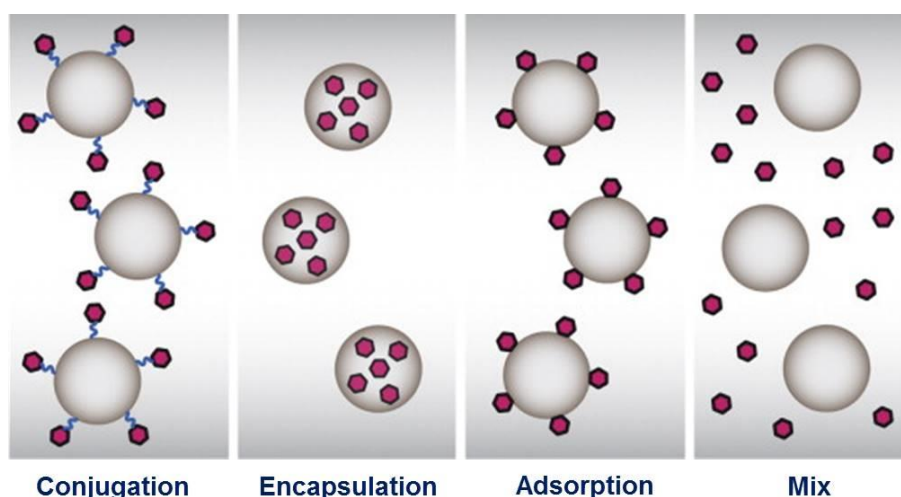


**Figure 2.4: Interaction of nanoparticle with antigen.** Formulation of nanoparticle and antigen of interest can be through attachment (e.g. conjugation, encapsulation, or adsorption) or simple mixing.

## 2.11. Nanoparticle-Antigen presenting cell (APC) interaction

The incorporation antigenic component into nanoparticles has attracted extensive attention towards the mechanism for efficient antigen delivery to antigen presenting cells (APCs) and subsequently induce their maturation followed by cross-presentation of antigen to induce a potent immune response [176], [177], [216].

The APCs like dendritic cells (DCs) and macrophages are measure role in antigen processing as they efficiently uptake and process antigen. So, the better understanding of the mechanism behind nanoparticle and APCs interaction is very important for developing efficacious nanoparticle vaccines [217], [218].

DCs preferentially uptake virus-sized particles (20–200 nm) while macrophages preferentially uptake larger sized particles (0.5–5  $\mu\text{m}$ ) [219]. In the smaller the particle size, a higher percentage of the DCs interacted with the polystyrene spheres [220]. Similarly, PLA nanoparticles of size 200–600 nm were efficiently taken up by macrophages in comparison to microparticles [221].

Particle shape and surface charge are equally important particulate physicochemical factors and play crucial roles in the interaction between particles and APCs. In general, cationic particles induced high phagocytosis activity of APCs, because of the anionic nature of cell membranes [220]. Recently, particle shape has been identified as having a significant effect on the ability of macrophages to internalize particles via actin-driven movement of the macrophage membrane [222]. For larger particles ( $>1 \mu\text{m}$ ), particle shape plays a central role in phagocytosis by macrophages as the uptake of particles is strongly dependent on the shape at the interface between particles and APCs [222]. The hydrophobic particles are reported to induce a higher immune response in comparison to hydrophilic ones [223], [224]. A number of other factors

such as surface modification (e.g. PEGylation, targeting ligands) and vaccine cargo have been shown to influence the interaction between nanoparticles and APCs as well [225].

## **2.12. Nanoparticle-Biosystems interaction**

The knowledge of the interaction of nanoparticles with biological systems is very much essential in designing safe and efficacious nanoparticle vaccines as it determines the fate of nanoparticles *in vivo*. The physicochemical properties of nanoparticles including size, shape, surface charge density, and nature (hydrophobicity) affect the interaction of nanoparticles with immune cells [224] and plasma proteins [226], [227]. These interactions with nanoparticles, as well as the morphology of vascular endothelium, play a significant role in the distribution of nanoparticles in various tissues and organs of the body [208].

The lymph node targeted nanoparticle-based vaccine delivers the antigen at LN by direct drainage [228], [229] or by migration of activated peripheral APCs [230] for optimum induction of immune response. The delivery of nanoparticles to the LN is mainly influenced by size. Nanoparticles with a lower size range of 10–100 nm can easily pass through the extracellular matrix and move to the LNs where they are taken up by resident DCs for activation of the immune response [208]. However, the larger nanoparticle (>100 nm) linger at the administration point and are subsequently encountered by local APCs [208]. The biological environment and route of administration can also affect the draining of nanoparticles to the LN [208], [231]. After successful antigen delivery, the nanoparticles should undergo degradation and make it cleared from the body. If the nanoparticles are not degraded or excreted from the body, it accumulates in different tissues and organ causing adverse effects. Clearance of nanoparticles could be achieved through degradation by the immune system or by renal or biliary clearance [232].

## **2.13. Routes of administration**

The applications of the nanoparticle-based vaccine in oral and parenteral routes have been very well explored and applications in pulmonary and ocular delivery have been discovered. However, their applications in nasal, buccal and topical delivery are still awaiting exploration [233].

### **2.13.1. Mucosal Vaccination**

#### **Oral delivery**

Oral delivery of drugs/antigen using nanoparticles has been shown to be far superior to the delivery of free drugs in terms of bioavailability, biodistribution and residence time [234]. The advantage of using polymeric nanoparticles is to allow encapsulation of bioactive molecules and protect them against enzymatic and hydrolytic degradation time [234]. The use of submicron-

size particular systems in oral drug delivery, especially peptide drugs, has attracted considerable pharmaceutical interest. The efficacy of the orally administered drug mainly depends on its solubility and absorption through the gastrointestinal tract. So, a drug candidate that represents poor aqueous solubility and/or decomposition rate limited absorption is believed to possess low and/or highly variable oral bioavailability [226].

### **Pulmonary delivery**

The main problems with the nasal delivery of antigens are; a. the free antigen is readily cleared from the nasal cavity, b. poor absorption by the nasal epithelial cells, c. generate a low immune response. To overcome these problems, encapsulation of antigen into bioactive nanoparticles is a promising approach to nasal vaccine delivery[235]. Pulmonary drug delivery has many advantages, offering a large surface area for solute transport, rapid drug uptake, and improved drug bioavailability compared to other drug delivery strategies [236], [237]. Nanosuspensions may demonstrate to be an ideal approach for delivering drugs that display poor solubility in pulmonary secretions [226]. Furthermore, because of the nanoparticulate nature and uniform molecular distribution of nano-suspensions, it is very likely that in each aerosol containing the drug, leads to even distribution of the drug in the lungs as compared to the microparticulate form of the drug. Nanosuspensions could be exploited in all available types of the nebulizer[238].

### **2.13.2. Parenteral vaccination**

Parenteral routes commonly employed for vaccination purposes include the intramuscular (IM), subcutaneous (SC), and intradermal (ID) routes.

#### **Intramuscular route**

The IM route is a very popular route for routine vaccination to induce both cellular and humoral immune response. Myoblasts are antigen-presenting cells (APCs) found in the muscle tissue responsible for immune response generation after IM administration. However, due to the inadequate number of dendritic cells in the muscle in comparison to the skin, it is necessary to administer higher doses of antigen by the IM route in order to elicit an effective immune response [239]. Myocytes are incapable of activating T cells directly as they do not express major histocompatibility complex (MHC) class II molecules and are devoid of co-stimulatory compounds. Myocytes do not express major histocompatibility complex (MHC) class II molecules and are devoid of co-stimulatory compounds, rendering them incapable of directly activating T cells [240]. IM immunization results in a predominant Th2 response unless boosters are given subsequently [239]. Examples of vaccines which are currently administered via the IM route include hepatitis A, hepatitis B, diphtheria toxoid, inactivated polio vaccine, pertussis,

human papillomavirus (HPV), rabies vaccine, Streptococcus pneumonia, and tetanus toxoid [241].

### **Subcutaneous route**

The SC route is very valuable for antigen delivery due to the drainage of antigen from the injection site to lymph nodes that contain the immunocompetent cells. Nanoparticles have been explored extensively by the subcutaneous route for adjuvant vaccine purposes [242], [243]. Particles less than 100 nm in size are able to enter the lymphatic capillaries via the gaps between lymphatic endothelial cells. Particles between 100-1000 nm undergo phagocytosis by APCs, such as dendritic cells, followed by passage into lymphatic capillaries [241]. The antigen immunization through this route offers many advantages that include lower clearance and longer persistence at the site of administration resulting in prolonged antigen presentation to the immune system [244]. Examples of vaccines which are currently administered via the SC route include the anthrax vaccine.

### **2.13.3. Intradermal route**

Intradermal route of vaccination is the most common method for the delivery of drugs and genes. It involves the injection in the outer layer of the skin to reach immunologically sensitive epidermis. Generally, the drug is emulsified with an adjuvant to form a depot so as to allow prolonged release of drugs in a controlled manner. The nanoparticle-based intradermal delivery is able to induce DC maturation and enhance immune responses after intradermal injection [245]. The intradermal injection of hen egg lysozyme (HEL)/CpG (cytosine-guanine tandems) nanoparticles induced a more pronounced Th1 immune response compared with the HEL and HEL/CpG topical formulations [246]. Similarly, the intradermal delivery of OVA-loaded stabilized thiolated N-Trimethyl Chitosan (TMC)- Hyaluronic acid (HA) particles have elicited superior immunogenicity compared to non-stabilized particles indicated by higher IgG titers [247].

## **2.14. The bacterial pathogen: *Aeromonas hydrophila***

### **2.14.1. Systematic position**

Phylum: Proteobacteria

Class: Gammaproteobacteria

Order: Aeromonadales

Family: Aeromonadaceae

Genus: *Aeromonas*

Species: *hydrophila*

The genus *Aeromonas* is one of the several medically significant genera that have increasingly become a troublesome group for physicians and microbiologists alike by virtue of their changing phylogenetic relationships, evolving taxonomy and controversial role in certain diseases [248]. *Aeromonads* are ubiquitous, oxidase positive, facultatively anaerobic, glucose-fermenting, Gram-negative bacteria that are native to aquatic environments [249]. They have been found in brackish, fresh, estuarine, marine, chlorinated and unchlorinated water supplies worldwide, with highest numbers obtained in the warmer months [28], [249]. *Aeromonads* have been isolated from diseased cold- and warm-blooded animals for over 100 years and from humans since the early 1950s [250]. The ubiquitous nature of *Aeromonas* species in aquatic environments provides ample opportunity for animals, particularly fish and amphibians, to come into contact with, and to ingest organisms. Such contact may lead to infection, which depends on the species and the virulence of the strains encountered, may have life-threatening consequences.

### 2.14.2. Pathogenesis

Aeromoniasis, an important fish disease is caused by this bacterium [29]. *A. hydrophila* has been associated with several disease conditions in fish, including tail rot, fin rot, dropsy, ulcers and haemorrhagic septicaemia. Haemorrhagic septicaemia is characterized by the presence of small surface lesions, often leading to sloughing off of the scales, haemorrhaging in the gills and anus, ulcers, abscesses, exophthalmia (bulging eyes), and abdominal swelling (dropsy) often seen in European carp culture. Internally, there may be the presence of ascitic fluid in the peritoneal cavity, anaemia, and swelling of the kidney and liver [29], [251].

The bacteria multiply in the intestine, causing a haemorrhagic mucous-desquamative catarrh (excessive mucous secretion). Toxic metabolites of *A. hydrophila* are absorbed from the intestine and induced poisoning. Capillary haemorrhage occurs in the dermis of fins and trunk and in the submucosa of the stomach. Hepatic cells and epithelia of renal tubules show degeneration. Glomeruli are destroyed and the tissue becomes haemorrhagic, with exudates of serum and fibrin [251].

*Aeromonas* species produce many products that may be toxic to other cells. Some are released from viable cells in soluble form. Others may remain associated with the cell surface, and still others may be released upon cell death. Three of the extracellular proteins of *Aeromonas* species that have been implicated in pathogenicity have been cloned, sequenced, and characterized biochemically. These are aerolysin, GCAT (glycerophospholipid: cholesterol acyltransferase), and a serine protease [252], [253].

*A. hydrophila* produces other toxins such as  $\alpha\beta$  hemolysins and enterotoxins in host organisms as well as enzymes such as phospholipases, proteases and acetylcholinesterase [254], [255]

which are very important for the development of resistant strains and pathogenicity for the host organisms while acetylcholinesterase is extremely lethal to fish.

### 2.14.3. Prevention and control

Chemotherapeutic agents are used for the treatment of *A. hydrophila* in fish farms. Isolates of *A. hydrophila* in fish have been found to be sensitive to chloramphenicol, florfenicol, tetracycline, sulphonamide, nitrofurantoin derivatives, and pyridine carboxylic acids [256], [257]. However, antibacterial therapy provides only short-term relief if adverse environmental conditions such as high water temperature, low water flows, low oxygen levels, or crowding are not promptly corrected. Prevalence of many serotypes in a locality complicates the process of developing vaccines to this pathogen. To-date no such commercial vaccine is available in the world to prevent aeromoniasis in fish. However, recent reports on the use of immunostimulatory substances in fish have shown promising results to protect from aeromoniasis in fish [258].

### 2.14.4. Outer membrane protein: *A. hydrophila*

The Outer Membrane (OM) of *A. hydrophila* is a complex structure which mainly consists of lipopolysaccharide (LPS), phospholipids and a group of outer membrane proteins (Omps). The OM of pathogenic gram-negative bacteria is mainly responsible for establishing initial adherence, modulate host-pathogen interaction, overall survival of the organism and propagation of virulence factor [35]. It also has protective antigenicity, because OM components are easily recognized as foreign substances by immunological defense systems of the hosts. Omps are reported to be conserved among different serovars. Some of them serve as adhesins and play an important role in virulence [36]. Omps are located at host-bacterial interface in *A. hydrophila* and can be targeted for drug therapy [36].

## 2.15. The bacterial pathogen: *Vibrio cholerae*

### 2.15.1. Systematic position

Phylum: Proteobacteria

Class: Gammaproteobacteria

Order: Vibrionales

Family: Vibrionaceae

Genus: *Vibrio*

Species: *cholerae*

*Vibrio cholerae* is a "comma" shaped Gram-negative bacteria [31] with a single, polar flagellum for movement. It is a facultative anaerobic organism. It has two circular chromosomes, together

overall 4 million base pairs of DNA sequence and 3,885 predicted genes [31]. The genes for cholera toxin are carried by CTXphi (CTX $\phi$ ), a temperate bacteriophage inserted into the *V. cholerae* genome. CTX $\phi$  can transmit cholera toxin genes from one *V. cholerae* strain to another through horizontal gene transfer. The genes for toxin coregulated pilus are coded by the VPI pathogenicity island (VPI). The main reservoirs of *V. cholerae* are human and aquatic sources such as brackish water and estuaries, often in association with copepods or other zooplankton, shellfish, and aquatic plants [259]. The primary association between humans and pathogenic strains is through water, predominantly in economically reduced areas that do not have good water sanitization systems [260]. There are two serogroups of *V. cholerae*; O1 and O139 can cause the occurrence of cholera. O1 causes the majority of outbreaks while O139 (first identified in Bangladesh in 1992) is restricted to Southeast Asia. There are some other serogroups of *V. cholerae*, with or without the cholera toxin gene (including the non-toxigenic strains of the O1 and O139 serogroups), can also cause a cholera-like illness. Only toxigenic strains of serogroups O1 and O139 have been reported to cause widespread epidemics. *V. cholerae* O1 has two biotypes, classical and El Tor, and each biotype has two distinct serotypes, Inaba and Ogawa. The symptoms of infection are indistinguishable, although more people infected with the El Tor biotype remain asymptomatic or have only a mild illness. In recent years, infections with the classical biotype of *V. cholerae* O1 have become very rare and are limited to parts of Bangladesh and India [261]. Recently, new variant strains have been detected in several parts of Asia and Africa. Observations suggest these strains cause more severe cholera with higher case fatality rates.

### 2.15.2. Pathogenesis

*V. cholerae* enters the human body through ingestion of contaminated water or food. The bacteria enter the intestines; embed itself in the villi of intestinal absorptive cells, and releases cholera toxin. Cholera toxin (CT) is an enterotoxin made up of five B-subunits that form a pore to fits one A-subunit [262]. CT is made from filamentous phage gene, CTX $\phi$  [263]. A phage gene is also responsible for another virulence factor of *V. cholerae*, which is toxin co-regulated pilus (TCP) (a receptor for CTX $\phi$ ) [264]. *V. cholerae* can cause syndromes ranging from asymptomatic to cholera gravis. Symptoms include abrupt onset of watery diarrhea (a grey and cloudy liquid), occasional vomiting, and abdominal cramps [32]. Dehydration ensues, with symptoms and signs such as thirst, decreased skin turgor, dry mucous membranes, hypotension, sunken eyes, weak or absent radial pulse, tachypnea, tachycardia, hoarse voice, cramps, oliguria, renal failure, somnolence, seizures, coma, and death. Dehydration can lead to death in a few hours to days in untreated children. The disease is also particularly dangerous for pregnant

women and their fetuses during late pregnancy, as it may cause premature labor and fetal [32], [263], [264]. In cases of cholera gravis involving severe dehydration, up to 60% of patients can die; however, less than 1% of cases treated with rehydration therapy are fatal. The disease typically lasts 4–6 days [32], [265]. Worldwide, diarrhoeal disease, caused by cholera and many other pathogens, is the second-leading cause of death for children under the age of 5 and at least 120,000 deaths are estimated to be caused by cholera each year [260], [266]. Cholera affects an estimated 3-5 million people worldwide and causes 100,000-130,000 deaths a year as of 2010 [33].

### 2.15.3. Prevention and control

Treatment includes rehydration and replacement of lost electrolytes, which are important ions, such as sodium and potassium, used in biochemical processes to keep the body alive. Because of the low quality of water treatment in many poverty ridden countries, rehydration with clean water can be impossible without medical aid and supplies. Oral cholera vaccines are increasingly used as an additional tool to control cholera outbreaks in combination with the traditional interventions to improve safe water supply, sanitation, hand washing and other means to improve hygiene. Cholera vaccines are vaccines that are effective in preventing cholera. However, since it does not provide 100% immunity from the disease, food hygiene precautions should also be taken into consideration when visiting an area where there is a high risk of becoming infected with cholera. Oral vaccines provide protection in 52% of cases the first year following vaccination and in 62% of cases the second year [267]. There are two variants of the oral vaccine currently in use: WC-rBS and BivWC. WC-rBS (marketed as "Dukoral") is a monovalent inactivated vaccine containing killed whole cells of *V. cholerae* O1 plus additional recombinant cholera toxin B subunit. BivWC (marketed as "Shanchol" and "mORCVAX") is a bivalent inactivated vaccine containing killed whole cells of *V. cholerae* O1 and *V. cholerae* O139. mORCVAX is only available in Vietnam. Bacterial strains of both Inaba and Ogawa serotypes and of El Tor and Classical biotypes are included in the vaccine. The vaccine acts by inducing 2 types of antibodies; the antibacterial intestinal antibodies that prevent the bacteria from attaching to the intestinal wall and the anti-toxin intestinal antibodies that prevent the cholera toxin from binding to the intestinal mucosal surface [268]. But still there exist problems for which new strategy and research is needed in this area. Currently, cholera research more focused for identification of Vc virulence factors and their regulation should lead to a universal and hopefully one dose cholera vaccine with high efficiency [269]. It has been appreciated for some time that Vc cells express protective antigens associated with their outer membrane (OM), yet new subunit or kW-C vaccines featuring OM structures have not been developed as



alternatives to the oral cholera vaccines that do not (or do not optimally) express Vc protective antigens [37].

#### **2.15.4. Outer membrane protein: *V. cholerae***

Virulence-related outer membrane proteins (Omps) are expressed in Gram-negative bacteria and are essential to bacterial survival within macrophages and for eukaryotic cell invasion. The outer membrane proteins of enteric pathogens are one of the several factors that are involved in the interaction between the bacterium and the epithelial cell surface and confers resistance to the bacterium to bile salts and to host defense factors such as lysozyme and leukocyte proteins

The Outer Membrane (OM) of *V. cholerae* is a complex structure that mainly consists of lipopolysaccharide (LPS), phospholipids and a group of outer membrane proteins (Omps). . High levels of transcripts for OmpU and multiple OM structures (OmpS, OmpV, OmpK, OmpC, OmpW, and OmpA) were present along with a number of conserved hypothetical proteins [37]. Apart from major virulent factors (toxin-coregulated pilus; TCP and cholera toxin; CT), large number other factors associated with the outer membrane (OM), including lipopolysaccharide (LPS), OM porins (OMPs) and flagella are mainly responsible for establishing initial adherence, modulate host-pathogen interaction, overall survival of the organism and propagation of virulence factor [270]. The ToxR and ToxS regulatory proteins have long been considered to be at the root of the *V. cholera* virulence regulon, called the ToxR regulon. ToxR activates the transcription of OmpU and represses the transcription of OmpT, outer membrane porins important for *V. cholerae* virulence [271], [272]. OmpU is more protective (compared to OmpT) against the bactericidal effects of bile salts and other anionic detergents [273]. An OmpU (a general porin) prologue, vca1008, identified by IVET is required for mouse colonization [274]. OMVs are also promising immunogenic platforms and may play important roles in bacterial survival and pathogenesis [275]. OMVs, Outer membrane vesicles function in transport of virulence factors, adherence to and entry into host cells, or modulation of the host response. OMVs largely reflect the composition of the outer membrane and periplasm of their donor gram-negative bacteria. Immunization with *Vibrio cholerae* outer membrane vesicles induces protective immunity in mice by inducing specific, high-titer immune responses of similar levels against a variety of antigens present in the OMVs [270], [276]. Omps are highly immunogenic due to their exposed epitopes on the cell surface. Virulence-related outer membrane proteins (Omps) are essential to bacterial survival within macrophages and for eukaryotic cell invasion that could be an alternative candidate for development of subunit vaccine against *V. cholerae*.

## 2.16. Challenges and future perspective

The rapid advancement in the field of nanomedicine might be due to more focus on developing a whole new range of nanovaccines with novel delivery mechanisms. However, the application of nanoparticles in vaccine delivery is still at an early stage of development. The challenges with nanoparticle-based vaccine include many factors, e.g. difficulty in reproducibly synthesizing stable and non-aggregated nanoparticles having consistent and desirable properties, a lack of fundamental understanding about the role of physical properties of nanoparticles affecting biodistribution, targeting and nanoparticle- biosystem interactions at all levels from the cell through tissue and to the whole body. Again, the limitations of NPs for the delivery of vaccines range from concerns over the toxicity of the particles to difficulties in producing the materials and presenting antigens in their native form. Therefore, rational design in combination with the reproducible synthesis of nanoparticles with desirable properties, functionalities and efficacy become increasingly important, and it is anticipated that the adoption of new technologies will speed up the development of suitable nanoparticles for pharmaceutical applications. Furthermore, there is a need for developing novel vaccine systems by integrating some other essential properties, such as specific targeting, slow release, alternative administration methods and delivery pathways to fulfil the demand of the single-dose and needle-free delivery will become practical near future.

# Chapter 3

## Preparation and characterization of PLA and PLGA loaded with model protein (BSA) or drug (Clindamycin hydrochloride) nanoparticles

### 3.1. Introduction

Biodegradable nanoparticles (NPs) are gaining increased attention for their ability to serve as a viable carrier for site specific delivery of drugs and vaccine. Recently nanoparticles (NPs) (diameter: 10 to 1000 nm) delivery system has been proposed as colloidal drug carriers [277], which serve as excellent carriers by enhancing aqueous solubility, increasing resistance time in the body (increasing half-life for clearance/increasing specificity for its associated receptors) and targeting drug to specific location in the body. Moreover, polymeric NPs have been proved to enhance the oral bioavailability of orally inactive antibiotics [278]. Various polymers have been employed in the formulation of NPs for drug delivery research to increase therapeutic benefits. Among them, poly (D, L- lactide-co-glycolide) (PLGA), polylactic acid (PLA), are considered to be highly beneficial because of their biodegradable and biocompatible nature [65]. They are widely used for human research due to their FDA approval (The Food and Drug Administration, U.S.A.) [279].

Clindamycin hydrochloride (7-chloro-7-deoxylincomycin hydrochloride) is a semi-synthetic analogue of a natural antibiotic lincomycin. It is available as a white crystalline powder and administered orally. It is commonly used in topical treatment for acne and infections of the skin, soft tissue and infections and peritonitis [280]. In patients with hypersensitivity to penicillin, clindamycin is used to treat infections caused by susceptible pathogenic aerobic bacteria. It is widely used for the treatment of anaerobic infections caused by susceptible anaerobic bacteria, including dental infections [281] and infections of the respiratory tract, skin and soft tissue infections and peritonitis [282]. Clindamycin is also known to be useful in treating toxic shock syndrome in combination with vancomycin [283] and reducing the risk of premature births in women diagnosed with bacterial vaginosis [284]. Antimicrobial actions of clindamycin include a breakdown of bacterial cell membrane and inhibition of toxin synthesis [285]. The bacteriostatic effect of clindamycin is

due to inhibition of bacterial protein synthesis by binding to the 50S rRNA of the large bacterial ribosome subunit that inhibits the ribosomal translocation [285].

Clindamycin is a time-dependent antibiotic; exerts its best bactericidal effect when the drug is maintained above the MIC value in the formulation or alone. Hence, the time at which the therapeutic drug concentration is above the MIC ( $T > MIC$ ) value is considered as the primary parameter and should be kept as a minimum standard to achieve the desired clinical outcomes [76]. Therefore, sustained-release preparation has an important primary role in the clindamycin delivery. There are several problems associated with conventional methods of Clindamycin use. The drug could not reach the appropriate amount to the site of infection due to low bioavailability and drug loss. There are also incidences of low efficacy due to degradability. We hypothesize that if the drug can be encapsulated within a biodegradable system, it would enhance the drug efficiency to a greater extent by conserving its natural therapeutic property. It will not only protect the drug in its native structure but also be helpful in delivering the required amount of drug at the target site in an efficient manner. This can be monitored and compared by analyzing the changes in structural and physiochemical properties of the free drug and the encapsulated drug. In the current study, an attempt has been made to formulate CLH-PLA and CLH-PLGA NPs by a double emulsion solvent evaporation method with an aim to overcome the above mentioned demerits. Here, we propose a better delivery model to offer several advantages over conventional administration and delivery methods, including the ability for drug delivery to a specific site such as an intracellular infection [73], [74], reducing systemic toxicity [75] and also to facilitate sustained release of an antibiotic, minimizing dosing regimens [76]. The characterization and comparison study of the above formulated NPs were performed in order to foresee possibilities to design further an endocytosable controlled drug release system which would provide less alteration to the general structure of the drug and can be available in intact form at the molecular level. It might be useful in the treatment of various bacterial infections as well as it will reduce other related side effects.

Bovine serum albumin (BSA) was used as model protein since it is one of the most stable and extensively used proteins for evaluating novel sustained release drug delivery system [286]. There are many types of research on the development of biodegradable nanoparticles encapsulating protein or peptide drugs. However, effects of critical parameters influencing the size and surface charge, protein encapsulation, preferred protein release pattern, extending the duration of release, the stability of proteins in the formulation, narrowing polydispersity of nanoparticles etc. are under investigation to formulate them commercially.

So, in an another attempt, formulation of PLA and PLGA NPs loaded with BSA was carried out by of double emulsion solvent evaporation and characterization studies were performed to optimize the physical parameters such as size, charge, PDI, drug loading etc.

## 3.2. Materials and Methods

### 3.2.1. Materials

The drug, Clindamycin hydrochloride (CLH), polymer; polylactic acid (PLA; molecular weight: 85,000- 160,000 Da), poly (D,L-lactic-co-glycolic) acid (PLGA50: 50; molecular weight: 40,000-75,000 Da) and polyvinyl alcohol (PVA) were procured from Sigma-Aldrich, USA. Dichloromethane (DCM) and Acetone (analytical grade) were purchased from Merck India Pvt Ltd. Ultrapure water from Milli-Q water system (Millipore, USA) was used throughout the study.

### 3.2.2. Preparation of PLA-BSA and PLGA-BSA NPs

PLA and PLGA nanoparticles were formulated by water-in-oil-in-water (W/O/W) multiple emulsion method. In brief, the polymer was dissolved in dichloromethane (DCM), which constituted the organic phase (OP) at a concentration of 50 mg/mL. Primary emulsion was made using sonication (40W, 80% duty cycle, 20 cycles) (Brason, sonifier 450, USA) between antigen solution in internal aqueous phase (IAP) with that of the polymer solution as OP. The ratio was optimized at 1:5, 1:8 and 1: 10 for bovine serum albumin (BSA). Bovine serum albumin (2.5% W/V), Sucrose (10% W/V) and Sodium bicarbonate (2% W/V) were added to internal aqueous phases during primary emulsion step. The resulting primary emulsion was added dropwise to external aqueous phase (EAP) containing (1% W/V) PVA and (10% W/V) Sucrose solution. The secondary emulsion was prepared by homogenization technique carried out at 10,000 rpm for 10 min (Virtis, Cyclone I. Q. USA) for nanoparticle preparation process. The ratio of primary aqueous phase (IAP) to external aqueous phase (EAP) during secondary emulsion step was maintained at 1: 4. After secondary emulsification process, the solution was stirred overnight at room temperature for the complete evaporation of DCM. The particles thus formed were washed three times with ice-cold MQ water and lyophilized to get free flowing powder of BSA-encapsulated particles.

### 3.2.3. Preparation of CLH-PLA and CLH-PLGA NPs

The CLH-PLA and CLH-PLGA NPs were prepared by following double emulsion solvent evaporation method according to Machado and Evangelista with little modifications [287]. For organic phase (OP), 0.4 gm of PLGA/PLA polymers were dissolved in 8ml organic mixture (dichloromethane: acetone; 85:15, v/v). For internal aqueous phase (IAP), CLH at varied concentration i.e. 20 mg (drug: polymer; 1:20), 40 mg (drug: polymer; 1:10). 80 mg (drug:

polymer; 1:5) were dissolved in phosphate buffered saline (PBS) (67mM, pH 6.0). The two solutions (OP and IAP) were mixed by ultrasonication (LABSONIC ® M, B. Braun Biotech) for 30 sec under cooling (output 4, 40% duty cycle) to form W<sub>1</sub>/O emulsion. The W<sub>1</sub>/O emulsion mixture was slowly added to 100 ml of 1% (w/v) aqueous PVA solution with a high-speed homogenization at 8500 rpm for 8 min. The resulting w<sub>1</sub>/o/w<sub>2</sub> emulsion was stirred at 300 rpm overnight for the maximum evaporation of the organic solvent. Then the precipitated NPs were washed three times with ultrapure water at 12000 rpm for 15 min and the supernatants were stored for estimation of free drug. Finally, the pellet samples (NPs) were lyophilized and then used for further characterization. The prepared CLH- PLA NPs were named as CLH- PLA 1 (drug: polymer; 1:20), CLH- PLA 2 (drug: polymer; 1:10), CLH- PLA 3 (drug: polymer; 1:5). Similarly CLH-PLGA NPs were named as CLH- PLGA 1 (drug: polymer; 1:20), CLH- PLGA 2 (drug: polymer; 1: 10), CLH- PLGA 3 (drug: polymer; 1:5).

### 3.2.4. Characterization of NPs

#### Particle size, zeta potential and polydispersity index measurements

The size (Hydrodynamic diameter), size distribution (Poly Dispersity Index) and zeta potential (Surface charge) of the NPs were analyzed by Zeta sizer (ZS 90, Malvern Instruments Ltd, Malvern, UK). The lyophilized samples were made an appropriate dilution with PBS (67 mm, pH 6.0). Aliquots from each preparation batch were sampled in dynamic light scattering (DLS) cuvettes and NPs were then examined for equivalent diameters, size distribution, zeta potential and polydispersity index. Particles diameters were assessed at a scattering angle of 90° and at a temperature of 25°C. Then determinations for diameter, zeta potential and polydispersity index were measured for each preparation (in triplicate) and the standard deviations were calculated.

### 3.2.5. Determination of drug loading efficiency

The loading efficiencies of CLH-PLA and CLH-PLGA NPs were calculated spectrophotometrically using standard curve method prepared by varying concentration of CLH [288]. For standard curve, different dilutions of the drug in PBS (3 ml) were taken and heated with 3 ml of 1% KIO<sub>4</sub> solution, 2 ml of 30% H<sub>2</sub>SO<sub>4</sub> and 10 ml of cyclohexane on a water bath at 60° for 45 min then cooled and the cyclohexane layer was removed. The extraction was repeated (× 2) with 5 ml of cyclohexane and the combined extracts were diluted to 25 ml before the absorbance was measured at 520 nm. A similar procedure was followed for supernatants (containing free drugs) reserved for determination of drug. The OD value was put in the standard curve equation to find out the total drug content.

The amount of drug loaded in the NPs was calculated by subtracting the free drug present in the supernatant from the total drug added during the preparation of the NPs using the following formula

$$\text{Loading Efficiency (\%)} = \frac{\text{Total amount of Drug} - \text{Free Drug}}{\text{Total amount of Drug}} \times 100$$

Similarly, the antigen loading in NPs (PLA-BSA and PLGA-BSA) was determined from the total amount of antigen added in the formulation and the antigen amount that was not encapsulated. For this, the concentration of antigen (BSA) in the supernatant was analyzed by Pierce™ BCA (Bicinchoninic acid) Protein Assay Kit (Thermo Scientific) to determine free antigen concentration [289]. The amount of BSA protein encapsulated in the NPs was calculated by subtracting the free protein present in the supernatant from the total protein added during the preparation of the nanoparticles using the following formula

$$\text{Encapsulation Efficiency (\%)} = \frac{\text{Total amount of protein} - \text{Free protein}}{\text{Total amount of protein}} \times 100$$

### 3.2.6. In vitro drug release study

The rate of CLH released from NPs was measured as a function of time during incubation in 1X PBS. Triplicate samples of 5 mg NPs were suspended in 1 ml PBS in a microcentrifuge tube and sonicated briefly in an ultrasonic water bath. The samples were then incubated on an orbital shaker (200 rpm) at 37°C. At defined time points the samples were centrifuged. The supernatant was collected and reconstituted by adding fresh PBS. The supernatant was collected and the pellet (NPs) was reconstituted by adding fresh PBS. The drug content in the supernatant was estimated [288] as discussed above. The percentage of drug release was plotted against time and the cumulative release was calculated.

### 3.2.7. SEM Study

The morphology of the NPs was investigated by scanning electron microscopy (Jeol 6480LV JSM microscope). The NPs were fixed on adequate support and coated with platinum using platinum sputter module in a higher vacuum evaporator. Observations under different magnifications were performed at 20kv.

### 3.2.8. DSC analysis

The physical states of CLH-PLA 2, CLH-PLGA 2 NPs and blank polymeric NPs were characterized by differential scanning calorimetric thermogram analysis (Netzch DSC 200 F<sup>s</sup>). The samples (~12 mg) were sealed in aluminum pans and heated under nitrogen by heating rate of 10<sup>0</sup>C/min, the heat flow being recorded from 30<sup>0</sup>C to 200<sup>0</sup>C. Indium was used as standard reference material to calibrate the temperature and energy scales of the DSC instruments. The data were analyzed and DSC thermographs were plotted with the help of Microsoft excel.

### 3.2.9. Fourier transformed infrared spectra

FT-IR spectra (Shimadzu FTIR spectrophotometer: Model 8400 S) of CLH, CLH-PLA 2 and CLH-PLGA 2NPs were recorded in potassium bromide pellets. The spectrum was recorded between 4000 and 400cm<sup>-1</sup> using a high energy ceramic source and DLATGS detectors. Characterization by Fourier Transform Infrared (FTIR) was specifically carried out to determine the adsorption of the drug in the prepared NPs by studying the chemical properties of CLH conjugated NPs. After knowing the functional groups, its bonding nature with NP was also characterized.

### 3.2.10. Antibacterial activity

The antibacterial activities of the CLH-PLA 2, CLH-PLGA 2 NPs and CLH were studied against *Streptococcus faecalis* and *Bacillus cereus*. The minimum inhibitory concentration (MIC) values were determined by following CLSI guidelines for the broth microdilution method [290]. Briefly, bacterial strains were cultured onto Luria-Bertani Agar medium (containing 0.5% peptone, 0.5% yeast extract, 1% NaCl and 1.5% Agar, at pH 7.5 ± 0.2). The stock solution was prepared by suspending the NPs in 4 ml of aqueous solution (phosphate buffer 67 mM, pH 7.4, 0.05% Tween 20 and 0.02% sodium azide) contained in borosilicate vials. The NPs were incubated at 37°C with shaking for 24 h. Supernatant samples of 500µl were collected by centrifugation and stored at 4°C until checked for antimicrobial activities. . Chloramphenicol (a common antibiotic) was used as the positive control and PBS was used as the negative control. Bacterial cultures were added to the sterilized Mueller-Hinton Broth (MHB) (containing 30% beef extract, 1.75% casein acid hydrolysate and 0.15% starch, pH 7.4 ± 0.2). The MIC was determined by using 2-fold serial dilutions in the medium (MHB) containing 1.95–1000 µg/ml of the test compounds. To each well of 96 well microtitre plate, 150 µl of medium (MHB) was taken in duplicate, to which 10 µl of 0.5 McFarland standard (1.5 × 10<sup>8</sup> CFU/ml) culture pathogens from MHB was added. The inoculated plates were incubated at 37<sup>0</sup>C for 24 h. After incubation, the bacterial growth was monitored by measuring the turbidity of the culture by a microtitre plate optical colorimeter (OD600). The MIC was determined as the lowest



concentration of compound at which the visible growth of the organisms was completely inhibited.

The results of experimental assays were expressed as mean value  $\pm$  standard error (SE). Student t'test or One-way ANOVA (analysis of variance) followed by Duncan's multiple range tests (DMRT) was performed using SPSS18 software to compare the variations in various parameters at a significance level of difference ( $p < 0.05$ ).

### 3.3. Results

#### 3.3.1. Physical properties

##### PLA-BSA and PLGA-BSA NPs

PLA and PLGA micro and nanoparticles were prepared by a double solvent evaporation method. Then BSA (2.5%) (PI of 4.8) was used as a model protein. The BSA encapsulated PLA nanoparticles size was varied from  $162.7 \pm 13.26$  nm to  $258.3 \pm 35.12$  nm. The particle size of PLA NPs (blank) was recorded as  $43.73 \pm 4.77$  nm. When OP: IAP (2.5% BSA) is maintained at 1:5, 1:8, 1:10, the size of the formulated PLA NPs were  $258.3 \pm 35.12$  nm (PLA-BSA1),  $196.8 \pm 23.22$  nm (PLA-BSA2) and  $162.7 \pm 13.26$  nm (PLA-BSA3) respectively. However, the loading efficiency (%) of PLA-BSA1, PLA-BSA2 and PLA-BSA3 were  $61.6 \pm 5.25$ ,  $69.6 \pm 10.12$  and  $82.4 \pm 6.21$  respectively. Similarly, The BSA encapsulated PLGA nanoparticles size was varied from  $113.5 \pm 11.76$  nm to  $335.6 \pm 30.21$  nm. The particle size of PLGA NPs (blank) was recorded as  $178.6 \pm 17.34$  nm. When OP: IAP (2.5% BSA) is maintained at 1:5, 1:8, 1:10, the size of the formulated PLGA NPs were  $335.6 \pm 30.21$  nm (PLGA-BSA1),  $138.5 \pm 21.27$  nm (PLGA-BSA2) and  $138.5 \pm 21.27$  nm (PLGA-BSA3) respectively. The zeta potential values of PLA-BSA NPs were ranged from  $-24.7 \pm 3.21$  mV to  $-32.7 \pm 5.32$  mV, while for PLGA-BSA NPs; it varied from  $-19.1 \pm 3.45$  mV to  $-30.1 \pm 2.14$  mV. The negative charge confirmed the surface charge of both PLA and PLGA NPs. The PDI values for all NPs were within good range. In the case of PLA-BSA NPs, the PDI value was lowest for PLA-BSA3 ( $0.337 \pm 0.03$ ). Similar results were also found for PLGA-BSA NPs, where PDI value was found lowest for PLGA-BSA3 ( $0.356 \pm 0.04$ ). The physical properties of all the formulations are mentioned in Table 3.1.

**Table 3.1. Physical properties of BSA loaded PLA and PLGA NPs**

Polymer	Sample code	Formulation code	Ratio of Organic Phase: Internal Aqueous Phase (OP: IAP)	Mean Particle Size	PDI	Zeta Potential	Loading Efficiency (%)
PLA	1	PLA blank		43.73±5.77	0.303±0.07	-24.8±6.75	-
	2	PLA-BSA1	1:5	258.3±35.12	0.465±0.08	-32.7±5.32	61.6±5.25
	3	PLA-BSA2	1:8	196.8±23.22	0.403±0.06	-20.5±4.31	69.6±10.12
	4	PLA-BSA3	1:10	162.7±13.26	0.337±0.03	-24.7±3.21	82.4±6.21
PLGA	5	PLGA Blank		178.6±17.34	0.324±0.06	-19.9±4.32	-
	6	PLGA-BSA1	1:5	335.6±30.21	0.537±0.05	-19.1±3.45	65.28±5.25
	7	PLGA-BSA2	1:8	138.5±21.27	0.518±0.04	-30.1±2.14	81.28±7.23
	8	PLGA-BSA3	1:10	138.5±21.27	0.356±0.04	-20.3±4.56	91.22±9.45

**CLH-PLA and CLH-PLGA NPs**

Various formulation factors were reported to play a key role on the physiochemical properties of polymeric nano/ microparticles formed [291]. In this study, CLH loaded in PLA and PLGA NPs were prepared by w/o/w double emulsion evaporation technique varying the drug to polymer ratio. The effect of the drug concentrations (1: 20, 1: 10, 1: 5) on the size of the obtained NPs was analyzed. The physical properties of all the formulations are mentioned in Table 3.2. The particle size of PLA NPs (blank) was recorded as  $42.93 \pm 1.77$  nm. The particle size increased with the drug encapsulation into the NPs. The sizes of NPs were  $203.35 \pm 12.04$ ,  $323.5 \pm 16.39$ ,  $827.4 \pm 10.20$  nm at a different drug to polymer concentration i.e. 1:20, 1:10 and 1: 5 respectively. In case of PLGA NPs (blank), the particle size was  $178.6 \pm 12.11$  nm, while for CLH- PLGA 1( 1:20), CLH- PLGA 2 (1: 10), CLH- PLGA 3 (1:5), the particle sizes were  $196.45 \pm 8.78$  ,  $258.3 \pm 11.23$  and  $456.5 \pm 12.36$  nm respectively. The zeta potential values of CLH-PLA NPs were ranged from  $-17.6 \pm 6.55$  mV to  $-30.5 \pm 4.95$  mV, while for CLH-PLGA NPs; it varied from  $-21.7 \pm 5.34$  mV to  $-33.5 \pm 3.0$  mV. The negative charge confirmed the surface charge of both PLA and PLGA NPs. But very interestingly, the zeta potential were highest when the drug: polymer concentration was 1:10 ( $-30.5 \pm 4.95$  mV for CLH- PLA2 and  $-33.5 \pm 3.0$  mV for CLH-PLGA2). The size and charge distribution patterns of CLH-PLA2, CLH-PLGA 2 are shown in Figure 3.1 and 3.2 respectively. The PDI values for all NPs were within good range. In the case of CLH-PLA NPs, the PDI value was lowest for CLH-PLA 2 ( $0.219 \pm 0.01$ ). Similar results were also found for CLH-PLGA NPs, where PDI value was found lowest for CLH-PLGA 2 ( $0.176 \pm 0.01$ ).

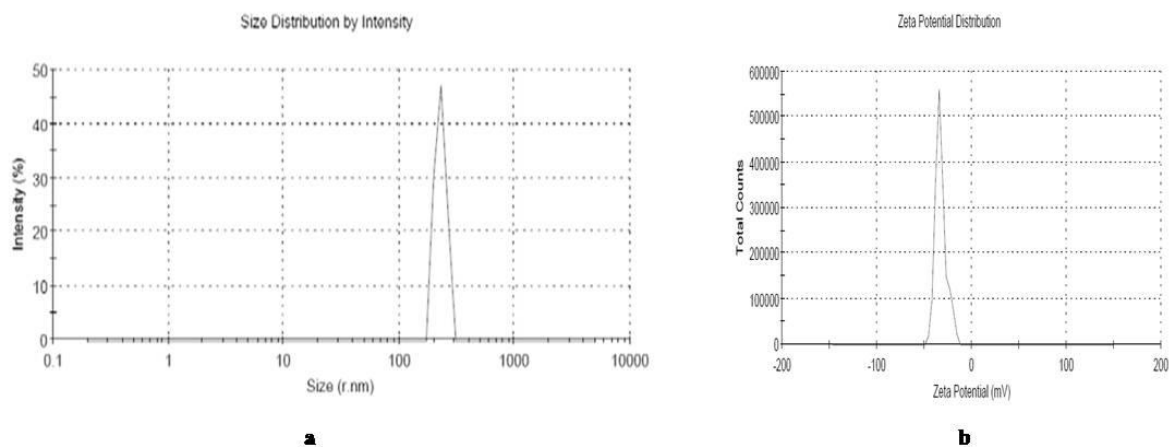


**Figure 3.1** Size (a) and charge (b) distribution pattern of CLH loaded PLA NPs (PLA-CLH 2). The drug: polymer ratio is 1:10. The average size and zeta potential were  $323.5 \pm 16.39$  nm and  $-30.5 \pm 4.95$  mV respectively.

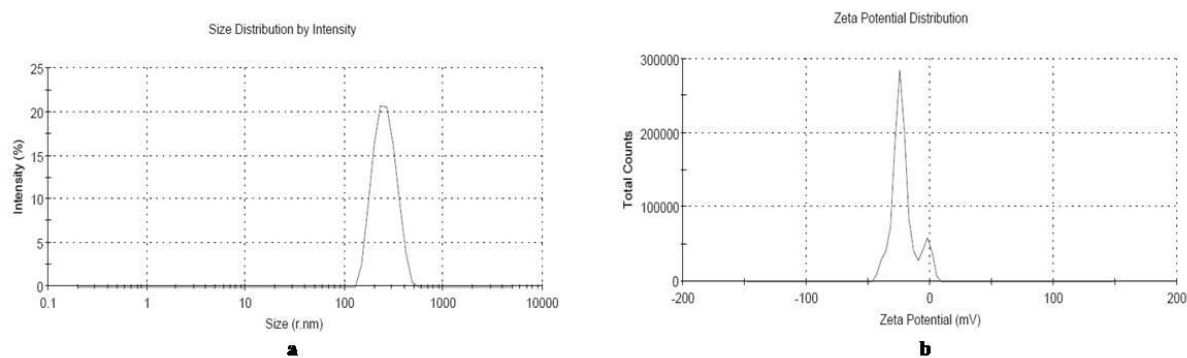


**Figure 3.2** Size (a) and charge (b) distribution pattern of CLH loaded PLGA NPs (PLGA-CLH 2). The drug: polymer ratio is 1:10. The average size and zeta potential were  $258.3 \pm 11.23$  nm and  $-33.5 \pm 3.0$  mV respectively.

**Table 3.2. Physical properties of CLH loaded PLA and PLGA NPs**

Polymer	Sample (Code)	Conc. of Drug (mg)	Conc. of Polymer (mg)	Ratio of drug: Polymer	Mean Particle size (Diameter in nm $\pm$ SD)	Zeta potential (mV) $\pm$ SD	Poly Dispersity Index (PDI) $\pm$ SD	Encapsulation efficiency (%)
PLA	Blank (PLA)	-	400	-	42.93 $\pm$ 1.77	-24.8 $\pm$ 7.67	0.454 $\pm$ 0.05	-
	CLH-PLA 1	20	400	1:20	203.35 $\pm$ 12.04	-19.8 $\pm$ 3.88	0.332 $\pm$ 0.03	7.2 $\pm$ 2.08
	CLH-PLA 2	40	400	1:10	323.5 $\pm$ 16.39	-30.5 $\pm$ 4.95	0.219 $\pm$ 0.01	21.35 $\pm$ 3.17
	CLH-PLA 3	80	400	1:5	827.4 $\pm$ 10.20	-17.6 $\pm$ 6.55	0.423 $\pm$ 0.04	24.5 $\pm$ 4.29
PLGA	Blank (PLGA)	-	400	-	178.6 $\pm$ 12.11	-32.7 $\pm$ 5.01	0.524 $\pm$ 0.03	-
	CLH-PLGA 1	20	400	1:20	196.45 $\pm$ 8.78	-25.5 $\pm$ 2.88	0.650 $\pm$ 0.05	45 $\pm$ 3.45
	CLH-PLGA 2	40	400	1:10	258.3 $\pm$ 11.23	-33.5 $\pm$ 3.0	0.176 $\pm$ 0.01	65.69 $\pm$ 2.28
	CLH-PLGA 3	80	400	1:5	456.5 $\pm$ 12.36	-21.7 $\pm$ 5.34	0.353 $\pm$ 0.03	72.35 $\pm$ 2.31

(CLH-PLA1-3, CLH-PLGA 1-3 were named according to the drug: polymer ratio. The drug: polymer ratio of CLH-PLA 1, CLH-PLA 2, CLH-PLA 3 were 1:20, 1:10, and 1:5 respectively. Similarly The drug: polymer ratio of CLH-PLGA 1, CLH-PLGA 2, CLH-PLGA 3 were 1:20, 1:10, and 1:5 respectively). The results were expressed as a mean  $\pm$  standard deviation.

### 3.3.2. Loading efficiency

The loading efficiencies increased with the increase in drug concentration. In the case of CLH-PLA NPs, the loading efficiency (%) increased from 7.2 $\pm$  2.08 to 24.5  $\pm$  4.29, when the drug: polymer concentration increased from 1:20 to 1:5. Similarly in case of CLH-PLGA NPs, the loading efficiencies (%) increased from 45  $\pm$  3.45 to 72.35  $\pm$  2.31, when the drug: polymer concentration increased from 1:20 to 1:5. This study showed the loading efficiency of CLH to PLGA was higher than CLH to PLA. CLH loading efficiency depended on the polymer type and the physical state of the drug (solid form or in solution form) during processing.

### 3.3.3. In vitro drug release

*In vitro* release of CLH was assessed from PLA and PLGA NPs into PBS (pH 7.4). The release profile of CLH from PLA and PLGA NPs is illustrated in Figure 3.3. It is observed that CLH release profile from CLH-PLGA is considerably slower than from CLH-PLA. In the case of CLH-PLA, 50 % of the drug was released within 4 hr. 75 % release of CLH was realized within a period of up more than 48 hr. But in the case of CLH-PLGA, 50% drug was released within 8 h and 75% release of CLH was realized within a period of up more than 72 h.

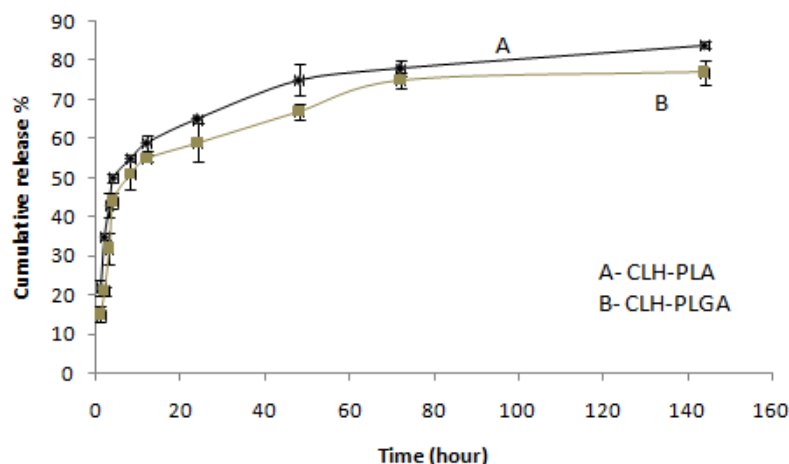


Figure 3.3. *In-vitro* CLH release from CLH-PLA 2 and CLH-PLGA 2 NPs.

### 3.3.4. SEM Study

The morphology of CLH loaded PLA and PLGA NPs were analyzed by SEM study. The NPs were spherical structures as confirmed by scanning electron microscope (SEM) (Figure 3.4). The surface morphologies of the particles were rough and rounded. Particles were found to be regular and isolated in nature.

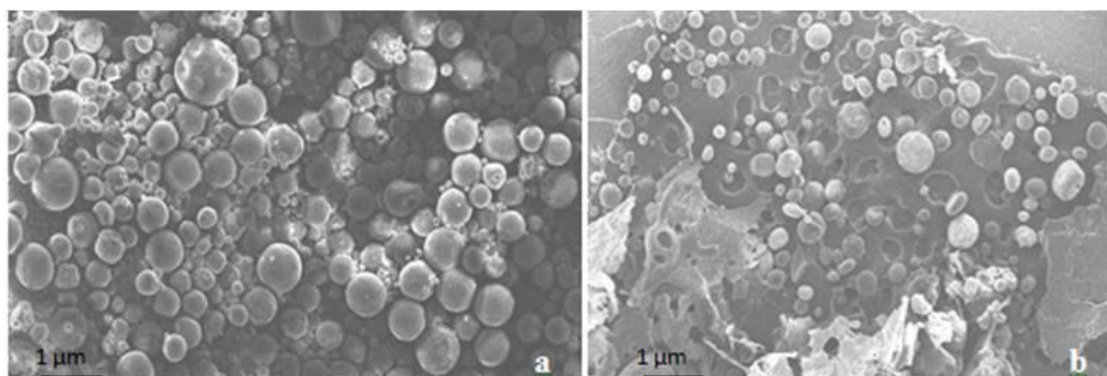
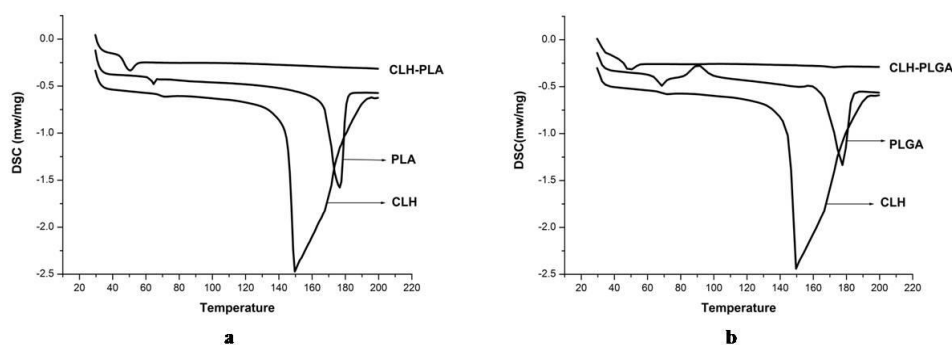


Figure 3.4 SEM photograph of (a) CLH-PLA2 (Drug: polymer- 1:10) and (b) CLH-PLGA2 (Drug: polymer- 1:10).

### 3.3.5. DSC studies

Thermal analytical studies of polymeric drug delivery systems are vital since the processes used for their preparation are able to modify the organization of the polymer chains [292]. Figure 3.5 shows DSC data of CLH, PLA NPs, PLGA NPs, CLH-PLA 2 and CLH-PLGA 2. In the current study, the blank PLA and PLGA polymer showed glass transition temperature ( $T_g$ ) at  $64.24^\circ\text{C}$  and  $67.5^\circ\text{C}$  respectively. Thermal analysis data (figure 3.5) showed that pure CLH possesses an endothermic peak at  $150^\circ\text{C}$  related to the melting point. CLH melting peak was depleted in the thermogram for the loaded PLA and PLGA NPs, indicating the presence of amorphous CLH in the NPs. The results also showed a decrease in glass transition temperature of PLA and PLGA polymer with respect to nano encapsulation of the drug.



**Figure 3.5 DSC data: a. Thermal analysis graph of Clindamycin hydrochloride (CLH), blank PLA, CLH conjugated with PLA (CLH-PLA2); (b) Thermal analysis graph of Clindamycin hydrochloride (CLH), blank PLGA, and CLH conjugated with PLGA (CLH-PLGA 2).**

### 3.3.6. FTIR analysis

FTIR analysis measures the selective absorption of light by the vibration modes of specific chemical bonds in the sample. The observation of vibration spectrum of encapsulated drug permits evaluation of the type of interaction occurring between the drug and polymer. This interaction is due to the vibrations of the atoms involved (in this interaction) can suffer alterations in intensity and frequency [293]. FTIR studies of CLH-PLA and CLH-PLGA NPs were performed to characterize the chemical structure of drug conjugated NPs. Figure 3.6 shows the FTIR spectra of CLH-PLA 2 and CLH-PLGA 2 NPs. Nearly similar peaks were observed in both the prepared NPs some of which occurred at  $3648\text{ cm}^{-1}$  (O-H stretching),  $3505\text{ cm}^{-1}$  (O-H stretching),  $2946\text{ cm}^{-1}$  (C-H stretching),  $2996\text{ cm}^{-1}$  (C-H stretching),  $1761\text{ cm}^{-1}$  (C=O stretching),  $1458\text{ cm}^{-1}$  (C-H bending),  $1386\text{ cm}^{-1}$  (N=O bending),  $1184\text{ cm}^{-1}$  (C-N stretching),  $1080\text{ cm}^{-1}$  (C-O stretching),  $870\text{ cm}^{-1}$  and  $756\text{ cm}^{-1}$  (N-H wags) for the CLH-PLA 2 NPs whereas  $3644\text{ cm}^{-1}$  (O-

H stretching),  $2999\text{ cm}^{-1}$  (C-H stretching),  $2955\text{ cm}^{-1}$  (C-H stretching),  $1761\text{ cm}^{-1}$  (C=O stretching),  $1458\text{ cm}^{-1}$  (C-H bending),  $1398\text{ cm}^{-1}$  (N=O bending),  $1183\text{ cm}^{-1}$ ,  $1086\text{ cm}^{-1}$  (C-N stretching),  $866\text{ cm}^{-1}$  and  $749\text{ cm}^{-1}$  (N-H wags) for the CLH-PLGA 2 NPs.

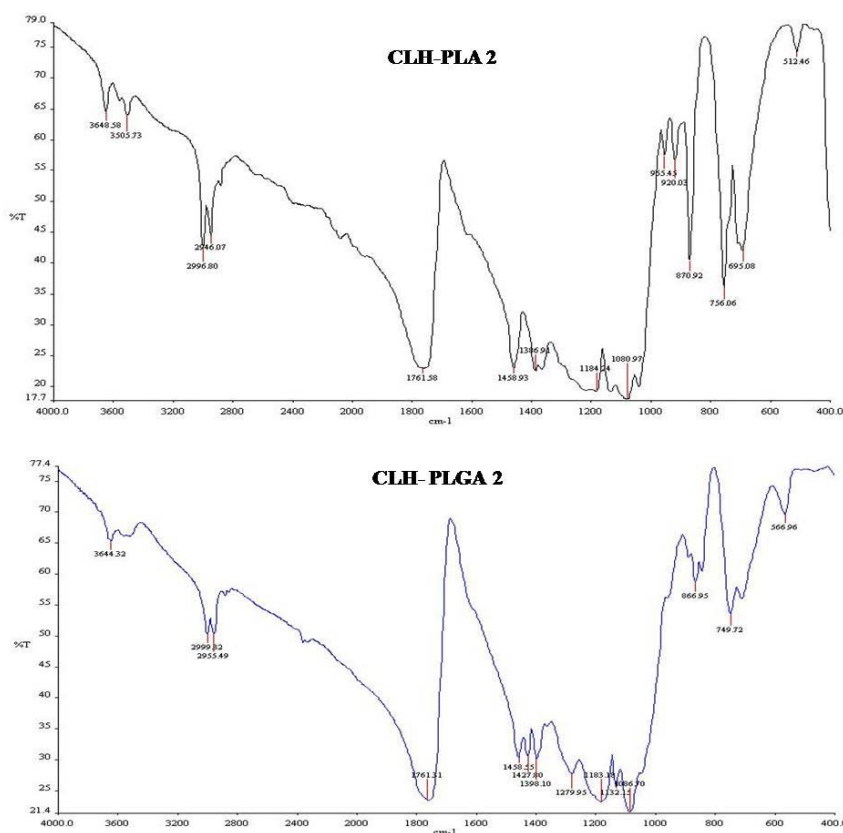


**Figure 3.6.** FTIR data analysis of CLH -PLA 2(a) and CLH -PLGA-3 (b).

As drug has a secondary amine group on its general structure whose peak is also detected by FTIR studies. The analysis shows no alteration of secondary amine structure after conjugation with PLA/PLGA NPs. But changes have been found after conjugation with PLA/PLGA for some functional groups like C=O, OH those which are abundant in PLGA/PLA NPs. These functional groups were found very less in number in case of CLH drug alone.

### 3.3.7. Antimicrobial activity

The antibacterial activities were evaluated for the selected nano formulations (CLH-PLA 2, CLH-PLGA 2) and CLH drug alone by determining their minimum inhibitory concentration (MIC) values against pathogenic microorganisms. The MIC values are mentioned in Table 3.3. In this study, MIC values of CLH were found to be  $0.48 \pm 0.01\text{ }\mu\text{g/mL}$  for *Streptococcus faecalis* and  $1.95 \pm 0.04\text{ }\mu\text{g/mL}$  for *Bacillus cereus*. However, these MIC values were decreased when the drug was encapsulated into PLA and PLGA NPs. CLH-PLA 2 showed MIC values of  $0.12 \pm 0.05\text{ }\mu\text{g/mL}$  and  $0.97 \pm 0.08\text{ }\mu\text{g/mL}$ , while CLH-PLGA 2 showed MIC values  $0.24 \pm 0.05\text{ }\mu\text{g/mL}$

and  $0.48 \pm 0.06$   $\mu\text{g/mL}$  against *Streptococcus faecalis* and *Bacillus cereus* respectively. MIC values of CLH were found to be increased when the drug was loaded into PLA and PLGA NPs as proved against *Streptococcus faecalis* and *Bacillus cereus*.

**Table 3.3 Antibacterial activity of Clindamycin hydrochloride conjugated with PLA (CLH-PLA 2), Clindamycin hydrochloride conjugated with PLGA (CLH-PLGA 2) and Clindamycin hydrochloride, in vitro MIC in  $\mu\text{g/mL}$**

Formulations	MIC ( $\mu\text{g/mL}$ ) $\pm$ Standard deviation	
	<i>Streptococcus faecalis</i>	<i>Bacillus cereus</i>
Clindamycin hydrochloride	$0.48 \pm 0.01$	$1.95 \pm 0.04$
PLA-CLH 2	$0.12 \pm 0.05$	$0.97 \pm 0.08$
PLGA-CLH 2	$0.24 \pm 0.05$	$0.48 \pm 0.06$

### 3.4. Discussion

NPs based drug delivery system is now becoming a useful tool for controlling various acute infectious stages, preventing complications and their relapse. Therefore, it is helpful in overcoming the sensible disadvantages with long-term therapies [294]. In addition, drugs delivered through nanospheres that target particularly to the infected cells should have reduced cytotoxicity associated with undesired biodistribution of the free drug. Depending upon the mode of action, NPs based drug delivery systems could perform better than microparticle based delivery system due to their size and better presentation of antigen [295], [296].

The particle size increased with the increase in drug concentration in the NPs. The sizes of NPs were  $203.35 \pm 12.04$ ,  $323.5 \pm 16.39$ ,  $827.4 \pm 10.20$  nm at a different drug to polymer concentration i.e. 1:20, 1:10 and 1: 5 respectively. Similarly, for CLH- PLGA 1(1:20), CLH- PLGA 2 (1: 10), CLH- PLGA 3 (1:5), the particle sizes were  $196.45 \pm 8.78$  ,  $258.3 \pm 11.23$  and  $456.5 \pm 12.36$  nm respectively. From the particle size analysis report, it can be concluded that the particle sizes were dependent on the initial concentration of the drug used during the preparation process. Similar results were also documented earlier [291], [297]. Zeta potential is a scientific term for the measurement of electro-kinetic potential at the surface of the colloidal particles, which has a great significance in comparing the stability of colloidal dispersions [156]. The zeta potential indicates the degree of repulsion between adjacent particles and similarly charged particles in the dispersion. For molecules and particles that are small enough, a high zeta potential confers stability (dispersion will resist aggregation). When the zeta potential is low, the attraction between the particles exceeds repulsive force for which leads to flocculate. When the drug: polymer concentration was 1:10, the zeta potential were highest for both CLH- PLA ( $-30.5 \pm 4.95$  mV) and CLH-PLGA ( $-33.5 \pm 3.0$  mV) confirming highest stability. The zeta potential values of CLH-PLA NPs and CLH-PLGA NPs confirmed that the drug: polymer



concentration is important for the stability of drug loaded NPs. Hence, the current study confirmed that the drug: polymer concentration is important for the stability of drug loaded NPs. The polydispersity index (PDI) is a measurement of the distribution of NPs and it gives the distribution range from 0.000 to 0.500. Polydispersity index greater than 0.5 values indicates the aggregation of particles [298]. The PDI values for all NPs were within good range. CLH-PLA2 and CLH-PLGA-2 NPs have lowest PDI values confirmed the monodispersed nature of the formulated NPs. CLH loading efficiency depended on the polymer type and the physical state of the drug (solid form or in solution form) during processing. The loading efficiency of CLH to PLGA was higher than CLH to PLA. The enhanced microencapsulation in the case of more hydrophilic polymers might be ascribed to enhanced molecular interactions between the drug and the polymer [160], [299]. This study showed the loading efficiency of CLH to PLGA was higher than CLH to PLA. This might be due to the reason that PLGA is more hydrophilic nature than PLA.

It is observed that CLH release profile from CLH-PLGA is considerably slower than from CLH-PLA. The rapid burst effect is very much delayed in case of CLH-PLGA. That conferred that binding of the drug to PLGA was stronger than to PLA. *In vitro* release data indicated proper drug (CLH) encapsulation that avoided the burst effect and offered an extended release profile. A similar type of drug release studies was observed in etodolac loaded PLGA NPs [300] and minocycline-loaded PLGA NPs [301]. Thus, PLGA-drug can be a better oral delivery system as it could withstand the drug even after 4 hr which is the standard required time for retaining food in the stomach. The surface morphologies of the particles were rough and rounded. Particles were found to be regular and isolated in nature. These regular and isolated forms of spherical structures were also observed earlier by Machado and Evangelista in case of cefoxitin loaded D, L-PLA NPs [287]. The smooth surface can also be correlated to lactide content that adds hydrophobicity to the polymer. So, that could prevent the retention of water and the shrinkage could be avoided while drying. Also, particle-particle contact formation was become less due to the presence of lactide (which causes hydrophobic) and ultimately prevents agglomeration [302].

T<sub>g</sub> (glass transition temperature) represents the measurement of polymer chain flexibility for the lactic acid polymers that indicates the hydrolysis pattern of the ester bonds [303]. The usual T<sub>g</sub> values reported for PLA and PLGA systems are more than 37 °C (so, they are glassy in nature) but can be clearly attributed to the presence of crystallites within the samples [304]. CLH melting peak (at 150 °C) was depleted in the thermogram for the loaded PLA and PLGA NPs, indicating the presence of amorphous CLH in the NPs. Similar results were also observed in

minocycline encapsulated PLGA NPs [301] and in cefoxitin loaded DL-PLA NPs [287]. With this, it can be suggested that the drug was more uniformly dispersed throughout the system in case of PLA and PLGA. The disappearance of the peak referred to the crystalline melting of the drug which indicates that the drug clindamycin is uniformly dispersed throughout the polymer matrix at a molecular level [287], [305]. The decrease in glass transition temperature of PLA and PLGA polymer was observed with respect to nano encapsulation of the drug. This may be due to increase in the size of the particles whereas the glass transition temperature is inversely related to the size of particles in case of the amorphous polymer [306].

From FTIR studies, it can be concluded that there is not much alteration in the general structure of CLH drug because of the presence of OH group and the drug is present in its native structure without forming any hydrogen bond with any other functional group. As CH group is also present in CLH drug, there is no alteration of CH group in the conjugated drug. C-O bond is common to both polymers and CLH drug. Therefore, it has no effect on to the CLH drug's general structure. These observations confirmed that the intact form of CLH drug and it was not involved in any chemical interactions with the polymers which were also observed for nimesulide-loaded ethylcellulose and methylcellulose NPs and microparticles [291]. The antibacterial activities of selected nano formulations (CLH-PLA 2, CLH-PLGA 2) and CLH drug alone were evaluated by determining their minimum inhibitory concentration (MIC) values against pathogenic microorganisms. MIC values of CLH were found to be increased when the drug was loaded into PLA and PLGA NPs as proved against *Streptococcus faecalis* and *Bacillus cereus*. Therefore, this study confirmed the enhanced antibacterial activity of drug loaded NPs than the standard free drug. Similar enhanced antimicrobial activities of drug loaded NPs were also observed by many researchers [74], [301], [307].

Hence, proving our hypothesis successful formulations of CLH loaded in PLA and PLGA NPs were carried out. From the DLS analysis, 1:10 dilution (Drug: polymer concentration) was proved to be the optimal ratio for the formulation of NPs. From CLH loading efficiency and release profile studies, more hydrophilic PLGA offers better encapsulation as well as extended CLH release profile confirming enhanced molecular interactions. Thermal analysis studies suggested that CLH was more uniformly dispersed throughout PLA and PLGA matrix at a molecular level. FTIR analysis confirmed the unaltered nature of drug CLH (no chemical interaction with polymer matrix), which was a very important parameter for better efficacy of CLH-PLA/PLGA nano complex. Enhanced antimicrobial activities of CLH-PLA/ CLH-PLGA NPs were proved against *Streptococcus faecalis* and *Bacillus cereus* measured through MIC

studies. Hence, the CLH drug was uniformly entrapped in PLA/PLGA NPs and the formulations were proven to exhibit more effective roles used at a lower concentration.

### 3.5. Conclusion

The therapeutic efficacy of the drug Clindamycin Hydrochloride was significantly enhanced by encapsulating into biodegradable polymer PLA/PLGA based nanoparticulate system when compared with the free drug. The hypothesis with which we initiated the work has been rightfully anticipated and we could successfully overcome the limitations of the drug when used alone. During the current investigation, CLH-PLA and CLH-PLGANPs of various sized particles were formulated by varying the drug to polymer ratio from 1:5 to 1:20. The size, zeta potential and polydispersity index values of CLH-PLA NPs and CLH-PLGA NPs confirmed that the drug: polymer concentration is important for the stability of drug loaded NPs. The drug to polymer ratio 1: 10 were found to be optimal ratio for the formulation to be stable and monodispersed CLH loaded PLA and PLGA NPs. NPs formulation (both CLH-PLA 2 and CLH-PLGA 2) showed a significantly higher drug loading efficiency and a controlled release profile extended up to 144 h. Higher drug loading and an extended CLH release profile were observed in the case of CLH-PLGA NPs which might be due to higher hydrophilic nature of PLGA that causes enhanced molecular interaction. The spherical and isolated structures of both CLH-PLA<sub>2</sub> and CLH-PLGA<sub>2</sub> NPs were confirmed by scanning electron microscope (SEM) study. The smooth surface and isolated nature of NPs can also be correlated to the presence of lactide that adds hydrophobicity to the polymer ultimately prevents agglomeration. The thermal behavior (DSC) studies of CLH-PLGANPs confirmed the disappearance of CLH endothermic peak (150<sup>0</sup>C) that indicated the uniform dispersion of drug at a molecular level within the system. From FTIR studies, it was found that there was not much alteration in the general structure of CLH drug (due to conserved OH, CH and C-O group etc.) after loading in PLA and PLGA NPs. The antimicrobial activities were enhanced in CLH-PLA NPs and CLH-PLGA NPs than the standard free drug evidenced from a decrease in MIC values tested against *Streptococcus faecalis* and *Bacillus cereus*. Our formulations are shown to be useful and effective To maintain a sustained release and drug concentration throughout medication process. Hence, we can conclude that by encapsulation of CLH into PLA and PLGA NPs, the various physiochemical properties of the drug increased to a satisfactory extent. The drug was more effective at lower concentration against pathogenic microorganisms which can be widely applied in a number of therapies by further designing successful endocytatable controlled drug release system.

# Chapter 4

## **Parenteral immunization of PLA/PLGA nanoparticle encapsulating outer membrane protein (Omp) from *Aeromonas hydrophila*; Evaluation of immunostimulatory action in *Labeo rohita* (rohu)**

### **4.1. Introduction**

Today's leading research on vaccine approaches mostly focuses on the development of naturally acquiring immunity by inoculation of non-pathogenic but still immunogenic components of the pathogen or closely related organisms. The growing issues of vaccine safety are in alarming rate owing to their weak immunogenicity, poor immunization procedures and failure to acquire booster doses to potentiate prime doses. These are some of the strong reasons which have paved the way towards research for the development of new generation therapeutic vaccine. Adjuvants are used for development of new generation vaccine formulations to serve in multiple ways; to enhance immunogenicity, provide antigen dosesparing, to accelerate a robust immune response, reduce the need for booster immunizations, increase the duration of protection, or improve efficacy in immunocompromised individuals in human and other live stocks. Hence, there is an urgent need for improved and effective, with or without adjuvant based novel vaccine formulations with minimal compositions like purified proteins, peptides, etc. for particular disease antigen in question. Because of the chemical nature and mode of action, the safety and efficacy of adjuvants in vaccine formulations vary to a greater extent. There are reports on adverse effects and hyperactivation of the immune system, neurotoxicity and detrimental effects when adjuvants are used for a prolonged period. Therefore, a relatively new system which is stable with antigen combination and can provide comparable immunity to that of adjuvants eventually can be treated as a complete replacement for the existing adjuvants in use should take the lead for development of advanced vaccine formulations. The strategy here is to develop such a system.

Currently, controlled delivery systems consisting of biodegradable microspheres/nanospheres act as a promising vaccine carrier because it can potentially deliver the antigens to the desired locations at predetermined rates and durations to generate an optimal immune response. The strategies that have been tested include the use of polymeric carriers such as chitosan, poly-(D,

L-lactide-co-glycolide) (PLGA), and poly(lactic acid) (PLA) as adjuvant or delivery carrier [5]. Indeed, polymeric micro- and nanoparticles have been used to develop vaccines against many infectious diseases [133], [297]. In fact, the immune response elicited by polymeric particles might be influenced by a number of factors, such as the inner structure of particulate carriers, use of an adjuvant, surface charge, particle size, and surface hydrophobicity. These parameters can also affect differential uptake by macrophages and dendritic cells, which play an important role in generating the immune response [308]. PLGA/PLA polymers have the advantage of being well characterized and commercially available for drug delivery systems [309]. Among the biodegradable microparticles, PLGA microparticles have been proved as a vaccine carrier in fish [310].

The growing bacterial infections in various aquaculture systems are gaining much more concern nowadays because of increased disease modalities affecting food market, human health and ultimately economic value including the added cost of controlling these diseases, recovery and wellbeing. *A. hydrophila* is a pathogenic gram-negative bacterium associated with lower vertebrates like fish, amphibians [28]. Aeromoniasis, an important fish disease is caused by this bacterium [29]. *A. hydrophila* infections in fishes have been reported from time to time in many Asian countries including China, Philippines, Thailand, and India [30]. Fish are free-living organisms mainly dependent on their innate immune system for survival. Nonspecific immunity act as a primary defence mechanism in fish and also, it plays a key role in the development of acquired immune response [311]. Like mammals, humoral immunity in fish involves the secretion of specific immunoglobulin directed to neutralize antigens and to activate complement cascade in response to pathogens [312].

The Outer Membrane (OM) of *A. hydrophila* is a complex structure which mainly consists of lipopolysaccharide (LPS), phospholipids and a group of outer membrane proteins (Omps). The OM of pathogenic gram-negative bacteria is mainly responsible for establishing initial adherence, modulate host-pathogen interaction, overall survival of the organism and propagation of virulence factor [35]. It also has protective antigenicity, because OM components are easily recognized as foreign substances by immunological defense systems of the hosts. Omps are reported to be conserved among different serovars. Some of them serve as adhesins and play an important role in virulence [36]. Omps are located at host-bacterial interface in *A. hydrophila* and can be targeted for drug therapy [36].

Omps are highly immunogenic due to their exposed epitopes on the cell surface. There are safety concerns with the use of oil adjuvant (Freund's incomplete adjuvant; FIA) in multivalent vaccine formulations for fish due to the generation of adverse side effects (e.g., adhesions). Therefore,

alternative molecules or certain combinations of them (targeting specific cellular responses) as adjuvants are desirable in order to enhance overall immunogenicity and efficacy without reducing protection levels [313]. There are only a few reports available on PLA/PLGA NP based vaccine formulations with adjuvant like effects and sustained target specific release to generate an optimal immune response for which more elaborate and conclusive studies are needed to define the protective roles of PLA/PLGA nanoparticulate system. In the present study, PLA/PLGA NPs encapsulating Omp antigen from *A. hydrophila* are compared with adjuvant formulations to develop a better antigenic carrier model in fish. The efficacy is also compared between PLA encapsulated and PLGA encapsulated OmpNP-immunized groups and a correlation is established evaluating the results of innate and adaptive immune response studies in *L. rohita*.

## 4.2. Materials and methods

### 4.2.1. Materials

The polymer; polylactic acid (PLA; molecular weight: 85,000- 160,000 Da), poly (D, L-lactic-co-glycolic) acid (PLGA 50: 50; molecular weight: 40,000-75,000 Da), N-Lauroylsarcosine sodium salt, trehalose dihydrate and polyvinyl alcohol (PVA) were procured from Sigma-Aldrich, USA. Chloroform was purchased from Merck India Pvt. Ltd. Ultrapure water from Milli-Q water system (Millipore, USA) was used throughout the study.

### 4.2.2. Preparation of OM proteins

In order to isolate the proteins of the OM of *A. hydrophila*, the respective strain was grown to late exponential phase. Cells were harvested from I L culture (4,500 ×g, 15 min, 4°C), washed twice in 10 mM HEPES, pH 7.5, and resuspended in 10 mM HEPES, pH 7.5, with one Sigma FAST™ protease inhibitor cocktail tablet (EDTA free) per 20 gm cell mass. Cells were disrupted by ultrasonication for 30 min at 10 watts at an interval of 30 s. Unbroken cells were removed by centrifugation (4,000×g, 15 min). The supernatant containing the OM proteins was transferred to a new tube and centrifuged again (13,000 ×g, 30 min, 4°C). The pellet was resuspended in 0.8 ml 10 mM HEPES, pH 7.5, plus 1% N-Lauroylsarcosine sodium salt and incubated for 30 min. After centrifugation (13,000 ×g, 30 min, 4°C), the pellet was washed once with 1 ml of 10 mM HEPES, pH 7.5, and resuspended in 50 µl of 10 mM HEPES, pH 7.5. The protein concentration was determined by Pierce™ BCA (Bicinchoninic acid) Protein Assay Kit (Thermo Scientific). Purified OM proteins were lyophilized stored at -80°C for further use.

### 4.2.3. Preparation of biodegradable and biocompatible based nanoparticles

NPs containing different antigens were formulated using a double emulsion-solvent evaporation technique with little modification [314]. In this method, an aqueous solution of antigen dissolved

in 500 µl of citrate buffer (pH=8) was emulsified with 100 mg of PLGA/PLA in chloroform solution (3 ml) to get a primary emulsion. Emulsification was carried out by ultrasonicator (Sartorius LABSONIC® M) at an amplitude of 5 for 20 seconds in an ice-cooled bath. The primary emulsion (w/o) was further emulsified in an aqueous PVA solution (10 ml, 2% w/v) in a drop-wise manner and then emulsified with a high-speed homogenizer for 2 min at 10000 rpm. The w/o/w double emulsion was added to 80 ml double distilled water and was stirred at 500 rpm for 2 hours at room temperature to allow the organic solvent evaporation. The NPs were recovered by centrifuge at 37,500 g for 45 min and washed thrice with sterile deionized water. Then the particles were lyophilized using 2.5% trehalose dihydrate as a cryoprotectant.

#### 4.2.4. Characterization of nanoparticles

##### Particle size, zeta potential and polydispersity index measurements

The size (Hydrodynamic diameter), size distribution (Poly Dispersity Index) and zeta potential (Surface charge) of the NPs were analyzed by Zeta sizer (ZS 90, Malvern Instruments Ltd, Malvern, UK). The lyophilized samples were made an appropriate dilution with deionized nano-pure water and sonicated at an amplitude of 40 and 0.5-sec pulse cycle for 5 min. Aliquots from each preparation batch were sampled in dynamic light scattering (DLS) cuvettes and nanoparticles were then examined for equivalent diameters, zeta potential and polydispersity index. Particles diameters were assessed at a scattering angle of 90° and at a temperature of 25°C. Then determinations for average mean diameter, zeta potential and polydispersity index were measured for each preparation and the standard deviations were calculated.

##### Encapsulation efficiency measurement

The antigen loading in NPs (PLA-Omp and PLGA-Omp) was determined from the total amount of antigen added in the formulation and the antigen amount that was not encapsulated. For this, the concentration of antigen (Omp protein) in the supernatant was analyzed by Pierce™ BCA (Bicinchoninic acid) Protein Assay Kit (Thermo Scientific) to determine free antigen concentration (Janes and Alonso, 2003).

The amount of Omp protein encapsulated in the NPs was calculated by subtracting the free protein present in the supernatant from the total protein added during the preparation of the nanoparticles using the following formula

$$\text{Encapsulation Efficiency (\%)} = \frac{\text{Total amount of protein} - \text{Free protein}}{\text{Total amount of protein}} \times 100$$

##### In vitro antigen release study

The rate of antigen released from NPs was measured as a function of time during incubation in 1X PBS. Triplicate samples of 50 mg of NPs were suspended in 3 mL PBS in a microcentrifuge

tube and sonicated at an amplitude of 40 and 0.5-sec pulse cycle for 2 min. The samples were then incubated on an orbital shaker (100 rpm) at 37°C. At defined time points, the samples were centrifuged. After centrifugation, the supernatant was collected and NPs were reconstituted by adding the same volume of fresh PBS. The protein concentration in the supernatant was estimated by BCA method as described earlier. The percentage of protein release was plotted against time and the cumulative release was calculated.

### SEM Study

The surface morphology of the NPs was investigated by scanning electron microscopy (Jeol 6480LV JSM microscope). The NPs were fixed on adequate support and coated with platinum using platinum sputter module in a higher vacuum evaporator. Observations under different magnifications were performed at 20kv.

### 4.2.5. Immunization protocol

Indian major carp, *L. rohita* (rohu), juveniles of average weight of  $50 \pm 10$  g were acclimatized in the wet laboratory 15 days prior to the start of the experiment. They were fed with a standard diet in two divided doses daily with constant aeration and daily one-third water exchange (to remove the waste feed and faecal matter) with water temperature 27-30°C. Fishes were separated into 7 groups (20 fishes in each group) and they were intraperitoneally immunized separately with 0.1 ml of different preparations @ 50 µg of Omp in PLA NPs (Group 1), 50 µg of Omp in PLGA NPs (Group 2), 50 µg of Omp in FIA-Omp (Group 3), 50 µg free native Omp (group 4), PLA NP (group 5), PLGA NP (group 6) and only PBS (group 7 as control). All the treated group fish (10 fish in each group) were bled at an interval of 3-weeks (at 21 and 42 days post-immunization) to study various immune parameters.

### 4.2.6. Preparation of anti-rohu-globulin rabbit serum

The rohu immunoglobulin serum was obtained by ammonium sulphate precipitation method. Polyclonal antiserum (anti-rohu globulin) to purified rohu immunoglobulin was prepared in a one-year-old New Zealand white rabbit using standard immunization protocols [315]. *L. rohita* purified Ig (~200 µg) was emulsified with an equal volume of Freund's complete adjuvant (FCA) and injected into the rabbit intramuscularly, followed by 2 booster doses (with Freund's incomplete adjuvant) at day 14 and 28. After 14 days of the last injection, the rabbit was bled. The separated serum was aliquoted and preserved at -20 °C for future use.

### 4.2.7. Immune responses study

#### Bacterial agglutination titre

Bacterial agglutination titre in the serum of individual fish was determined by plate agglutination technique [316]. Briefly, the heat-inactivated sera were diluted two-fold serially in PBS (pH 7.2) (with  $\text{Ca}^{++}$  and  $\text{Mg}^{++}$ ) in a 96 well 'U'-shaped microtitre plates. Then 50 µL of formalin-killed *A.*



*hydrophila* (adjusted to OD 2) was added to each well. The plate was incubated overnight at 25 °C. The bacterial agglutination titre was defined as the last dilution of serum showing maximal positive agglutinin.

#### **Haemolysin titre**

Haemolytic activity of unheated serum was determined by two-fold serially diluting with PBS in 'U'-shaped microtitre plates (pH 7.2) and using 1% freshly prepared rabbit RBC suspension [317]. Haemolysin titre was defined as the last dilution of serum showing maximum positive haemolysis.

#### **ELISA (enzyme-linked immunosorbent assays)**

An indirect ELISA assay was performed using 96 well microtitre polystyrene plates (Nunc, Denmark). The wells were separately coated with 50 µl of purified Omp (1 µg/well) diluted in carbonate-bicarbonate buffer (pH 9.6) overnight at 4 °C. The wells were washed thrice with TBST (TBS with 0.05% Tween 20) and blocked with 5% skim milk powder for 2 hr at room temperature. After blocking, the wells were further washed in TBST. The fish sera raised against various antigenic treatments were two-fold diluted from an initial dilution of 1:10 with TBS (pH 7.2) and added to antigen-coated wells in duplicate (per each dilution). The plates were incubated at 37 °C for 1 hr and washed thrice in TBST. Then the adsorbed rabbit antiserum to rohu immunoglobulin (1:40,000) was added (1 hr incubation) followed by HRP conjugated anti-rabbit immunoglobulin antibody (Genei) (1 hr incubation). The wells were then thoroughly washed with TBST and the reaction was visualized after adding 100 µL/well of TMB/H<sub>2</sub>O<sub>2</sub> (Genei). The reaction was allowed to proceed for 10 min, stopped with 100 µL 1N sulphuric acid, and absorbance was read at 450 nm with an automatic plate reader (Imax Microplate Reader, Biorad). The antibody activity was expressed in terms of O.D value after subtracting the values obtained by unimmunized healthy sera.

#### **4.2.8. Challenge study**

For challenge study, the virulent strain of *A. hydrophila* isolate was grown in tryptone soya broth at 30 °C for 24 h. Two days after the last bleeding, all the fishes (20 fish) from each group were injected intraperitoneally with a dose of  $7.5 \times 10^6$  CFU of *A. hydrophila* per gram body weight of fish. A control fish group was injected with 0.1 ml PBS. Mortality in any group was observed until 20 days and percent survival was calculated after 20 days post challenge. The cause of death and pathological signs were verified by re-isolation of bacteria from samples of from the kidney of 10% dead/infected fish as described by Sahoo et al. [318].

#### **4.2.9. Statistical analysis**

The results of experimental assays (for each group) were expressed as mean value  $\pm$  standard error (SE). One-way ANOVA (analysis of variance) followed by Duncan's multiple range tests

(DMRT) was performed using SPSS18 software to compare the variations in various immune parameters at a significance level of difference ( $p < 0.05$ ) in different injected groups.

## 4.3. Results

### 4.3.1. Physico-chemical properties of antigen-loaded nanoparticles

In this study, Omp loaded in PLA and PLGA NPs were prepared by w/o/w double emulsion evaporation technique. The Omp antigen was successfully encapsulated in PLA and PLGA NPs. All the physical properties like the size (Hydrodynamic diameter), size distribution (Poly Dispersity Index) and zeta potential (Surface charge) have been characterized by DLS analysis (Table 4.1).

**Table 4.1. Physical properties of Omp loaded PLA and PLGA nanoparticles. The results were expressed as mean  $\pm$  standard deviation.**

Polymer	Sample(Code)	Mean Particle size (Diameter in nm $\pm$ SD)	Zeta potential (mV) $\pm$ SD	Poly Dispersity Index (PDI) $\pm$ SD	Encapsulation efficiency (%)
PLA	Blank (PLA)	125.23 $\pm$ 23.77	-23.8 $\pm$ 5.67	0.350 $\pm$ 0.05	-
	PLA-Omp	223.5 $\pm$ 13.19	-26.5 $\pm$ 4.75	0.147 $\pm$ 0.06	44 $\pm$ 4.58
PLGA	Blank (PLGA)	98.6 $\pm$ 12.11	-25.7 $\pm$ 5.01	0.424 $\pm$ 0.03	-
	PLGA-Omp	166.4 $\pm$ 21.23	-31.3 $\pm$ 6.5	0.308 $\pm$ 0.05	59.33 $\pm$ 5.13

The particle size of blank PLA NPs were recorded as 125.23 $\pm$  23.77nm, whereas PLA encapsulated Omp NPs (PLA-Omp) possessed the average size of 223.5 $\pm$  13.19 nm (Figure 4.1). Similarly, the particle size of blank PLGA NPs and PLGA encapsulated Omp NPs (PLGA-Omp) were 98.6  $\pm$  12.11 nm and 166.4 $\pm$  21.23 nm respectively (Figure 4.2).

Zeta potential otherwise known as the electrokinetic potential at the surface of the colloidal particles has a great significance in comparing the stability of colloidal dispersions. The zeta potential values of blank PLA NPs and PLA-Omp NPs were -23.8  $\pm$  5.67mV and -26.5  $\pm$  4.75 mV respectively (Figure 4.1). Similarly, the zeta potential values of blank PLGA NPs and PLGA-Omp NPs were -25.7  $\pm$  5.01mV and -31.3  $\pm$  6.5mV respectively (Figure 4.2).

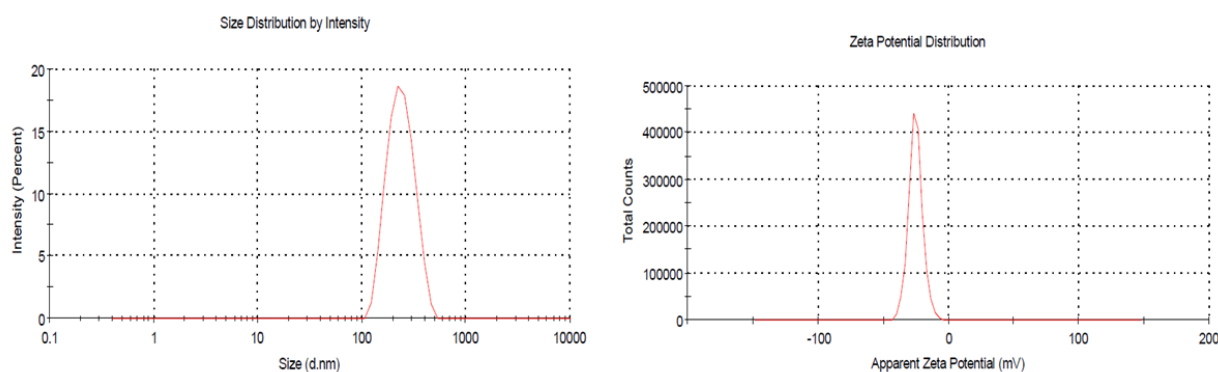


**Figure 4.1.** Size and charge (zeta potential) distribution pattern of Omp loaded PLA nanoparticles (PLA-Omp) determined by dynamic light scattering (DLS) method. The average size and zeta potential were  $223.5 \pm 13.19$  nm and  $-26.5 \pm 4.75$  mV respectively.

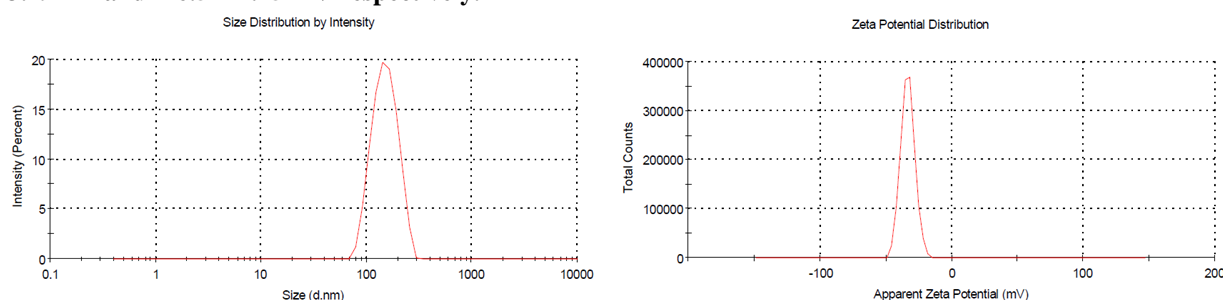


**Figure 4.2.** Size and charge (zeta potential) distribution pattern of Omp loaded PLGA nanoparticles (PLGA-Omp) determined by dynamic light scattering (DLS) method. The average size and zeta potential were  $166.4 \pm 21.23$  nm and  $-31.3 \pm 6.5$  mV respectively.

The PDI values of blank PLA NPs and PLA-Omp NPs were  $0.350 \pm 0.05$  and  $0.147 \pm 0.06$  respectively. Similarly, The PDI values of blank PLGA NPs and PLGA-Omp NPs were  $0.424 \pm 0.03$  and  $0.308 \pm 0.05$  respectively. Hence, the PDI values are within the good range confirming the monodispersity nature of the formulated nanoparticles.

#### 4.3.2. Loading efficiency

The drug/antigen loading efficiency depends upon the polymer nature, the physical state of the antigen/drug and the molecular interactions between the drug and the polymer. Omp encapsulation efficiency (%) in PLA NPs was  $44 \pm 4.58$  (Mean  $\pm$  SD), whereas in PLGA NPs it was  $59.33 \pm 5.13$  (Mean  $\pm$  SD) (Table 1). The encapsulation of Omp in PLGA is significantly higher ( $p < 0.05$ ) than the PLA.

#### 4.3.3. In vitro drug release

*In-vitro* release of Omp was assessed from PLA-Omp and PLGA-Omp NPs into PBS (pH 7.4). The release profile of Omp from PLA-Omp and PLGA-Omp NPs is illustrated in Figure 4.3. It could be seen that NPs release the Omp protein from PLA considerably slower than from PLGA. In the case of PLGA-Omp NPs, 50 % of the antigen was released within 4 hr of incubation whereas in the case of PLA-Omp NPs, it took almost 24 hr to release 50% of the total antigen. The initial burst release was rapid in PLGA-Omp NPs than that of PLA-Omp NPs. The burst release rates were; in PLA-Omp NPs 23% at 1hr, 25% at 2 hr, 28.17% in 3 hr, 35% at 4 hr, 42%

in 8 hr, 48% in 12 hr, 52% in 24 hr, 55.67% in 48 hr; in PLGA-Omp NPs 40.67% at 1hr, 43% at 2 hr, 46 % in 3 hr, 49% at 4 hr, 51% in 8 hr, 55.33% in 12 hr, 59% in 24 hr, 66.33% in 48 hr. The rapid burst effect is very much delayed with PLA-Omp NPs.

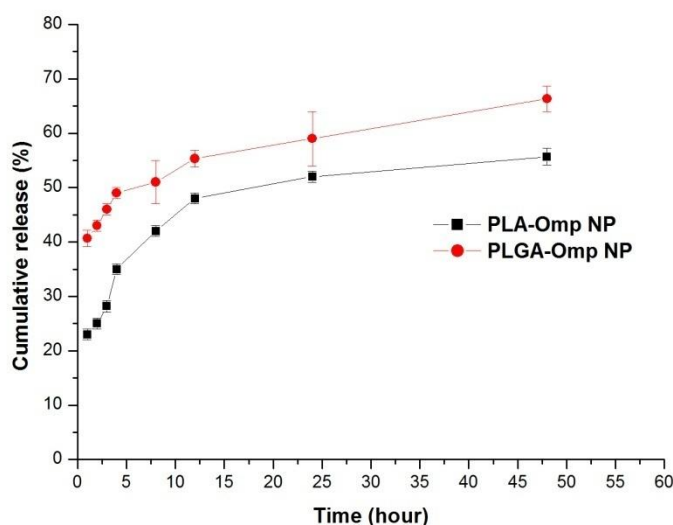


Figure 4.3. *In vitro* comparison of Omp antigen release from PLA and PLGA nanoparticles

#### 4.3.4. SEM study

The morphology of PLA-Omp NPs and PLGA-Omp NPs were analyzed by SEM analysis (Figure 4.4). The NPs were spherical in structures as confirmed by scanning electron microscope (SEM). The particles were found to be round, uniform and isolated in nature.

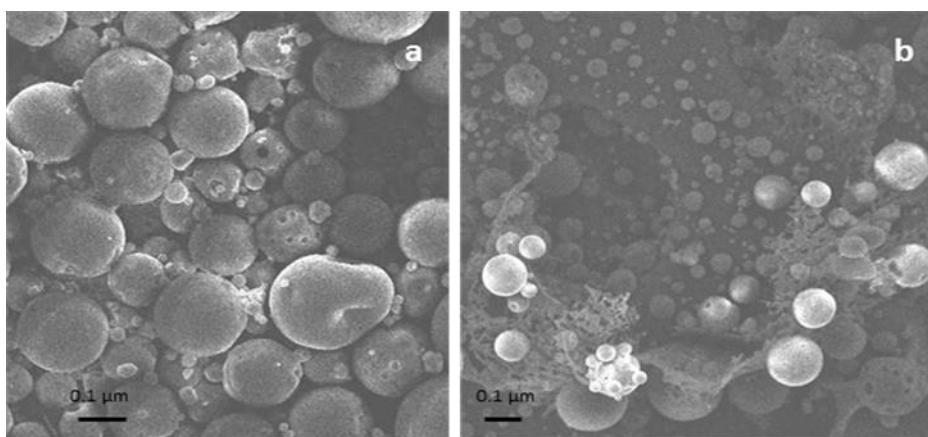


Figure 4.4. SEM photograph of (a) PLA-Omp nanoparticles (b) PLGA-Omp nanoparticles

#### 4.3.5. Immune responses study

The non-specific immune parameters of fish following the injection with different antigen preparations (PLA-Omp NPs, PLGA-Omp NPs, FIA-Omp, Omp, PLA NPs and PLGA NPs, control), at 21 and 42 days post-immunization are evaluated. A clear variation in few of the non-specific immune parameters was observed. For each parameter, the mean value and standard error (Mean  $\pm$  SE) was calculated separately.

##### **Bacterial agglutination titre**

The effect of different antigenic formulations for generation of specific immune response was measured through bacterial agglutination titre on day 21 and 42 of post immunization. The results revealed that the titre was significantly higher ( $p < 0.05$ ) in all treated groups than control, PLA blank NPs and PLGA blank NPs (Figure 4.5). The bacterial agglutination titre was highest in the case of PLA-Omp NPs treated groups, which is significantly higher than all other treatments (FIA-Omp, Omp, PLA NPs and PLGA NPs, control), but the value was not significantly different from PLGA-Omp NPs treatment. Also, PLGA-Omp NPs treated groups showed significantly higher bacterial agglutination activity than FIA-Omp, Omp, PLA NPs, PLGA NPs and PBS treated groups. These parameters did not vary much in all treated groups at 21 and 42 days post-immunization.

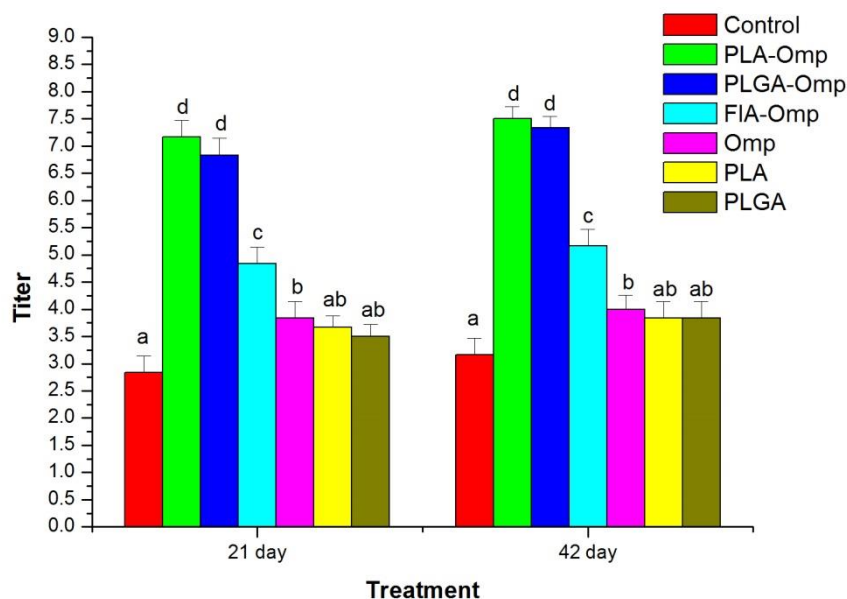


Figure 4.5. Variation in the bacterial agglutination activity of sera derived from different treated groups of *L. rohita* at 21 and 42 days post-immunization. Bars represent mean  $\pm$  S.E. Mean value bearing same superscript are not statistically significant ( $p > 0.05$ ) at 21 and 42 days post-immunization.

### Haemolysin titre

The haemolysin activity showed similar trend like that of bacterial agglutination titre. The mean haemolysin titre was highest in case of PLA-Omp NPs treated groups followed by PLGA-Omp NPs, FIA-Omp, Omp, PLGA NPs, PLA NPs, PBS (control) treated groups both at 21 and 42 days post-immunization (Figure 4.6). The titre were significantly higher ( $p < 0.05$ ) in all treated groups than the control. PLA-Omp NPs and PLGA-Omp NPs treated groups showed significant higher haemolytic activity than all other treated groups and were comparable to each other. This haemolysin titre did not deviate much in all treated groups at 21 and 42 days post-immunization.

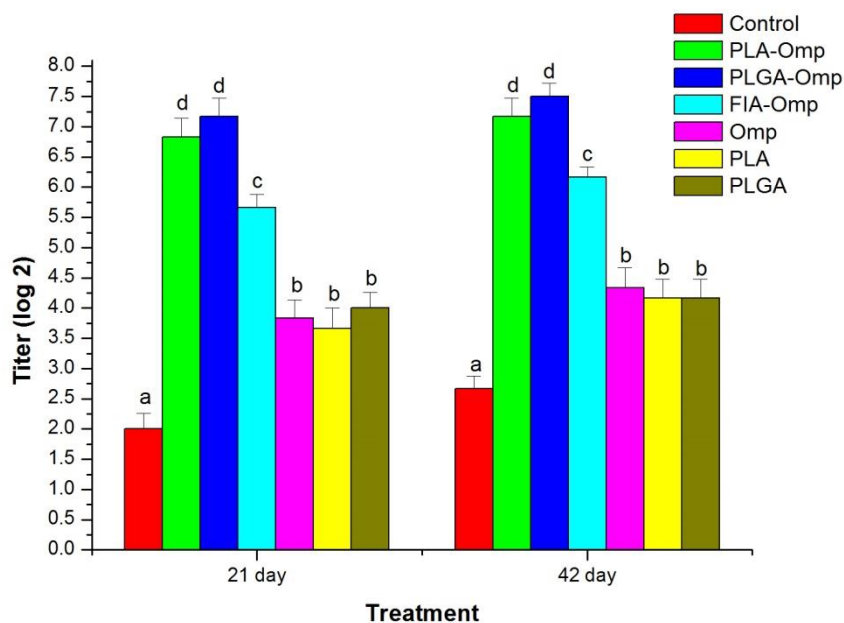


Figure 4.6. Variation in haemolysin activity of sera from different treated groups of *L. rohita* at 21 and 42 days post-immunization. Bars represent mean log<sub>2</sub> titre values  $\pm$  S.E. Mean value bearing same superscript are not statistically significant ( $p > 0.05$ ) at 21 and 42 days post-immunization.

#### Specific immune responses (Specific antibody titre)

The serum antibody level in different antigen treated sera was measured by indirect ELISA. The antibody level were expressed as mean OD (after subtraction the OD value obtained by unimmunized healthy sera)  $\pm$  SE (Figure 4.7). The antibody level were significantly higher ( $p < 0.05$ ) in PLA-Omp NPs, PLGA-Omp NPs, FIA-Omp treated groups than Omp, PLA NPs and PLGA NPs treated groups at 21 and 42 days post-immunization. The antibody level was higher in PLA-OMP NPs treated groups than PLGA-OmpNPs, FIA-Omp treated groups, although it was not significant. However, no significant difference ( $p > 0.05$ ) in the antibody level at 21 and 42 days post-immunization was recorded between these two groups.

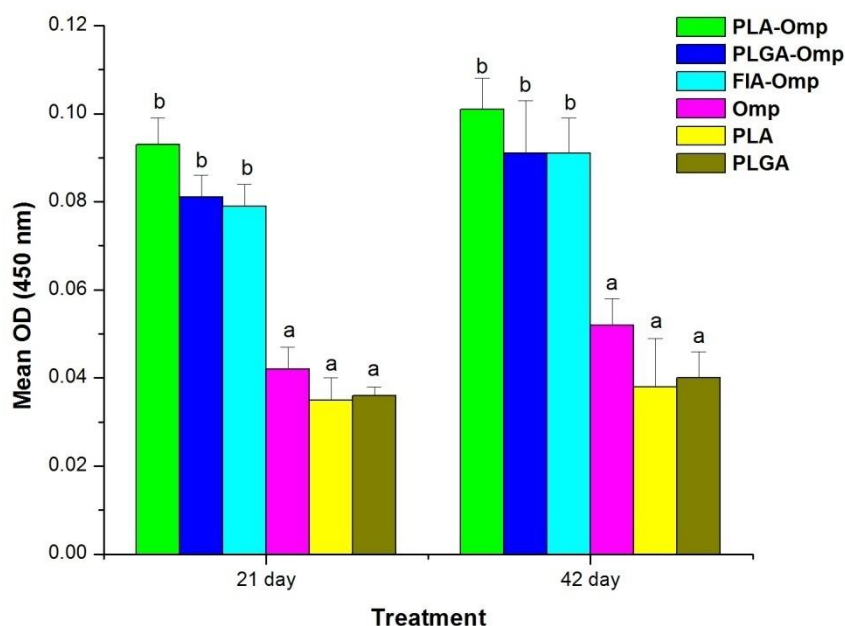


Figure 4.7. Variation in the specific antibody level of sera collected from different treated groups of *L. rohita* at 21 and 42 days post-immunization. Bars represent mean OD values  $\pm$  S.E. Mean value bearing same superscript are not statistically significant ( $p > 0.05$ ) at 21 and 42 days post-immunization.

#### 4.3.6. Challenge study

The infected fish injected with *A. hydrophila* showed typical signs of haemorrhagic septicaemia. The mortality reached its plateau after 48 hr of exposure to the bacterium. After 20 days post challenge, the percent survival values were calculated and expressed as Mean  $\pm$  SE (Figure 4.8). In challenge study, the % survivals were higher in the case of PLA-Omp NPs, PLGA-Omp NPs, FIA-Omp treated groups with 80, 75 and 75 respectively. But in case of PLA NPs, PLGA NPs, Omp and PBS (control) treated groups, the % survivals were 60, 55, 65 and 45 respectively. However, % survival value was significantly higher in case PLGA-Omp NPs, PLA-Omp NPs, FIA-Omp treated groups in comparison to control (PBS treated) and Omp treated groups.



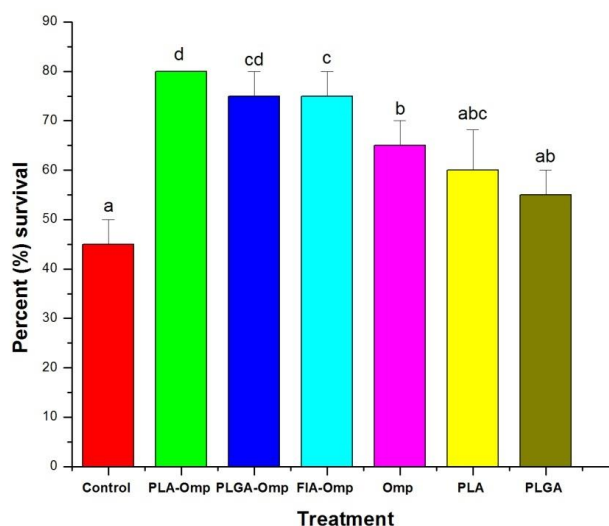


Figure 4.8. Challenge study: variation of % survival in different treated groups of *L. rohita* after 42 days post-immunization. Bars represent mean  $\pm$  S.E. Mean value bearing same superscript are not statistically significant ( $p > 0.05$ ) a 42 days post-immunization.

## 4.4. Discussion

Biodegradable NPs are gaining increased attention for their ability to serve as an excellent carrier for site specific delivery of small molecular weight drugs as well as macromolecules such as proteins, peptides or genes in the body using various routes of administration [319]. They can be easily taken up by the antigen presenting cells (APC) and can modulate body's immunity to generate a protective response [5]. Among various NPs, PLA and PLGA based NPs have been used to develop protein and peptide-based nanomedicines, nano-vaccines, and genes for in-vivo delivery systems [320]. In the current study, the immunological effects of PLA and PLGA NPs as antigen carrier encapsulating Omp of *A. hydrophila* were investigated.

The isolated Omp of *A. hydrophila* was encapsulated in PLA/PLGA NPs and the formulated nanospheres were characterized for evaluation of various physiochemical properties and comparative analysis of immune response generated to that of other antigenic preparations such as FIA-Omp, Omp, PLA NPs, PLGA NPs and PBS (as control). Various parameters; size, physical chemical morphological properties, encapsulation efficiency and the release profile of antigens are known to play a key function in the designing efficient polymeric nano/ micro particle based delivery system through molecular interaction [148]. There was an increase in size observed for PLA-Omp NPs (from  $125.23 \pm 23.77$  nm to  $223.5 \pm 13.19$  nm) and PLGA-Omp NPs (from  $98.6 \pm 12.11$  nm to  $166.4 \pm 21.23$  nm). Although nanoparticles are considered to be in nano dimensions below 100 nm size, but relative increase in size (size  $>100$  nm) is generally observed and accepted in the area of drug delivery systems when there is efficient drug loading and especially where sufficient amount of drug may be needed to load onto the particles [57]. As the

formulated PLA Omp NPs and PLGA-Omp NPs were < 500 nm size range, these particles could be successfully endocytosed in the body [321]. Zeta potential (electro-kinetic potential), is an essential property of colloidal particles and plays a major role in the NPs stability [156]. The stable nature was confirmed by the zeta potential values of PLA-Omp NPs ( $-26.5 \pm 4.75$  mv) and PLGA-OmpNPs ( $-31.3 \pm 6.5$ mv).The polydispersity index (PDI) is a measurement of the distribution of NPs and gave a distribution range from 0.000 to 0.500. Polydispersity index more than 0.5 values indicates the aggregation of particles (poly disperses) [298]. The PDI value of PLA-Omp NPs ( $0.147 \pm 0.06$ ) and PLGA-Omp NPs ( $0.308 \pm 0.05$ ) confirmed the monodispersity nature. The spherical, regular and isolated nature of PLA-Omp NPs and PLGA-OmpNPs were revealed by SEM analysis. Similar morphology patterns were also observed earlier by Behera et al. in the case of PLGA-omp microparticles [322].

Encapsulation of protein antigens depends on series of factors like polymer nature, molecular interaction between polymers, method of formulations, etc. The amount of drug bound to NP depends on the chemical structure of the drug/polymer ratio and the conditions of drug loading [159]. Hydrophilic polymers show higher encapsulation than hydrophobic polymer due to enhanced molecular interactions between the polymer and the drug [160]. Significantly higher encapsulation of Omp protein ( $p < 0.05$ ) was achieved in the case of PLGA-Omp NPs ( $59.33 \pm 5.13$  %) than PLA-Omp NPs ( $44 \pm 4.58$  %).

The design of PLA/PLGA based NP delivery system was mainly focused on overcoming some limitations like high initial burst, incomplete release and instability of the encapsulated proteins [294], [323]. In the current study, the Omp protein release profile in PLA NPs is comparatively slower than PLGA, which could be attributed to more hydrophilic nature of PLGA [324]. Also, high initial burst release was observed in the case of PLGA-Omp NPs that might be due to the diffusion of the protein through water-filled pores (facilitated water uptake from the release medium) in the PLGA matrix [324]. Higher protein loading may be another reason for high initial burst release by creating a protein concentration gradient between the polymeric particles and the release medium [325]. The rapid burst effect is very much delayed (almost took 24 hr to release 50% of total antigen) in the case of PLA-Omp NPs, which may be due to higher lactide content [324].

Both specific and non-specific immune parameters were evaluated in sera of *L. rohita* immunized with seven antigenic formulations (PLGA-Omp NPs, PLA-Omp NPs, FIA-Omp, Omp, PLA NPs, PLGA NPs and PBS as control) that elicited immune responses at varying levels at both 21 and 42 days post-immunization. PLA/PLGA particles can also act as adjuvant [297] and their use in humans and in veterinary medicine has been accepted by the FDA.

Antigen-loaded polymeric NPs represent an exciting approach to the enhancement of antigen-specific humoral and cellular immune responses via selective targeting of the antigen to APCs like dendritic cells as well as macrophages [5].

The non-specific immune response offers more importance than the specific immune response to produce first line defense against all pathogens in fish. Nevertheless, specific immunity requires a longer time for antibody to build up and specific cellular activation. Different innate parameters such as bacterial agglutination titre, haemolysin titre showed a similar pattern of response at 21 days and 42 days post immunization. A significant higher immune response was observed in the case of PLA-Omp NPs and PLGA-Omp NPs than all other treatments. There is a significant difference in immune response of PLA-Omp NPS and PLGA-Omp NPs when compared to control. These results also confirmed that PLA-Omp NPs are better delivery systems as compared to all other treated groups, as the immune responses generated by PLA-Omp NPs were higher despite its lower antigen loading. Many research have already been carried out for the evaluation of PLA/PLGA vaccine carrier system and its role in innate immune parameters [322], [326]. However, significantly enhanced ( $p < 0.05$ ) immune response generated in case of PLA-Omp NPs and PLGA-Omp NPs confirmed the activation of the innate immune system. This might be due to the adjuvant property of PLA/PLGA polymer itself as well as combined cellular action with NPs. Significantly higher titres in the case of PLGA-Omp NPs and PLA-Omp NPs were observed than FIA-Omp treated groups which again confirmed better immunogenicity of our formulated NPs. Similar higher immune response (bacterial agglutination titre and haemolysin activity) was observed in the case of PLGA-Omp microparticles over FIA-Omp treated fish [310].

The specific antibody response was significantly increased and persisted up to 42 days of post-immunization by either PLA-Omp/PLGA-Omp NPs or FIA-Omp. But no significant difference in antibody titre was observed between PLA-Omp/PLGA-Omp NPs treated groups and FIA-Omp treated groups. However, comparable antibody response of PLA-Omp NPs and PLGA-Omp NPs with that of FIA-Omp treated groups suggests that both PLA and PLGA could be a complete replacement for Freund's adjuvants (for stimulating antibody response) to overcome many side effects [327] simultaneously offering a long-lasting immunity [310]. Again, enhanced antibody level in case of PLA-Omp NPs, PLGA-Omp NPs over respective PLA and PLGA blank NPs was achieved confirming the combined immune action PLA/PLGA with Omp protein antigen. Similar results were observed by using PLGA as protein/peptide vaccine carrier in fish, mice [322], [328].

From the challenge experiments, the survival rates calculated (as % survival) in the case of PLA-Omp NPs treated groups was 80%, which was significantly higher than all other treated groups. PLGA-Omp NPs and FIA-Omp immunized groups have shown same % survival ( $75 \pm 5$ ) which was significantly higher than the control group. Hence, the better efficacy of PLA/PLGA-Omp NPs as increased protection system against *A. hydrophila* by activating immune responses was confirmed. A similar increase in protection was also observed by Behera and Swain, in the case of PLGA-Omp microparticles [322]. Here we have shown that among the nanoparticulate system, PLA-omp NPs shows better results than PLGA-Omp NPs.

## 4.5. Conclusion

PLA/PLGA NPs were evaluated for their ability to serve as an excellent carrier for site specific delivery of macromolecules such as Omp through parenteral immunization in *L. rohita*. PLA-Omp NPs (size:  $223.5 \pm 13.19$  nm) and PLGA-Omp NPs (size:  $166.4 \pm 21.23$  nm) were prepared using double emulsion method in which antigen was efficiently encapsulated reaching encapsulation efficiency  $44 \pm 4.58$  % and  $59.33 \pm 5.13$  % respectively. The physical properties like zeta potential values and polydispersity index (PDI) values confirmed the stability as well as monodisperse nature of the formulated NPs. The spherical and isolated nature of Omp loaded PLA and PLGA NPs were revealed by SEM analysis. Upon immunization in *L. rohita*, PLA/PLGA-Omp NPs showed encouraging results by activating both innate and specific immune response against *A. hydrophila* in fish without any side effects. Significant higher bacterial agglutination titre, haemolytic activity and specific antibody titre confirmed the combined immune activation. Considering the adverse side effects of oil adjuvant (FIA), the current study also proved the comparable antibody response of PLA-Omp NPs and PLGA-Omp NPs with that of FIA-Omp treated groups. Therefore, PLA and PLGA may be a replacement for Freund's adjuvants (for stimulating antibody response) to overcome many side effects offering long lasting immunity. Again, the better efficacy of PLA/PLGA-Omp NPs system was confirmed by increased protection against *A. hydrophila* by activating immune responses by challenge study. In comparison to PLGA-Omp NPs, PLA-Omp NPs offered a better immune response in terms of higher bacterial agglutination titre, haemolytic activity, specific antibody titre, higher percent survival upon *A. hydrophila* challenge in *L. rohita*. It can be concluded that PLA/PLGA NPs based delivery system would be a novel antigen carrier for parenteral immunization in fish. This is probably the first report on the delivery of PLA-Omp and PLGA-Omp NPs against *A. hydrophila* in *L. rohita*. Hence, more focused research on designing and formulation would be attributed to PLA/PLGA NPs based on vaccine delivery system in fish model.

# Chapter 5

## **Evaluation of the immune responses (specific) in mice after intraperitoneal immunization of Omp antigen (*Vibrio cholerae*) encapsulated PLA/PLGA nano-particles**

### **5.1. Introduction**

The advanced therapeutic approach involves vaccines as effective interventions to control infectious diseases that were the leading cause of death in the worldwide [329]. The current vaccine research is mostly focused on the development of acquired immunity based on antigen specific antibody and cytotoxic T lymphocytes (CTL) response by the inoculation of immunogenic (non-pathogenic) components of the pathogen or closely related organisms [1], [2].

However, the existing issues of vaccine safety such as inadequate immunogenicity, poor immunization procedures and failure to acquire booster doses to potentiate prime doses necessitate the development of new generation therapeutic vaccine. A safer and attractive alternative to live attenuated vaccine, subunit vaccine have several desirable qualities, e.g. they (1) can be produced in a highly characterized state, (2) target immune responses towards specific microbial epitopes, (3) enable incorporation of unnatural components and (4) can be freeze dried, allowing non-refrigerated transport and storage. But, the inadequate ability of subunit vaccine to stimulate potent immune responses requires the addition of immunostimulatory agents (adjuvants) to ensure long-term protective immunity by serving in many ways; to enhance immunogenicity, provide antigen dose sparing, to accelerate a robust immune response, reduce the need for booster immunizations, increase the duration of protection, or improve efficacy in immunocompromised individuals in human and other live stocks [3], [4]. The recent advancement of novel vaccine adjuvant formulations, particulate based adjuvants system offers several advantages including: ability to form multimolecular aggregates that target antigen-presenting cells (APCs), protection against degradation, sustained release of antigen [330]–[332]. Polymer-based delivery systems (natural or synthetic) consisting of biodegradable microspheres/nanosphere act as a promising vaccine carrier for their controlled

target specific delivery [330]. The polymeric carriers such as poly-(D, L-lactide-co-glycolide) (PLGA), and poly(lactic acid) (PLA) have been extensively investigated as adjuvants or delivery carrier for subunit-based vaccines [5], [333]. The efficacy of the immune response elicited by particle-based vaccines might be significantly influenced by a number of physicochemical characteristics such as structures of particulate carriers [5], [334], particle size [169], [331], surface charge [220], hydrophobicity [335], route of administration [336], [337], antigen release kinetics [169], [338] etc. By regulating the antigen exposure to the immune system (slow and continuous antigen release kinetics), polymer based particles remarkably influence in eliciting optimal immune responses [297], [338].

Targeted and prolonged antigen delivery to effective antigen presenting cell (APCs) like dendritic cells (DCs) is one of the recent vaccine strategies, that have a crucial role in initiating adaptive immune response by internalizing antigens through major histocompatibility complex (MHC) class I to CD8<sup>+</sup> T lymphocytes and MHC II to CD4<sup>+</sup> T lymphocytes [5], [339]. These types of DCs mediated immune response have been successfully achieved by the use of combined association of the antigens with polymeric nanoparticles [340]. The immunization of antigen with poly(lactic-co-glycolic acid) (PLGA) nanoparticles displayed enhanced induction of antibody mediated immune response as well as the improved memory T cell response that could be attributed to targeted antigen delivery, controlled antigen release and efficient induction of dendritic cell (DC) activation and follicular helper T cell differentiation [340].

Cholera, a life-threatening secretory diarrheal disease is caused by *Vibrio cholerae* transmitted via the oral fecal routes [341]. It has the ability to cause major outbreaks, particularly in African and Asian developing countries with poor sanitation. The Outer Membrane (OM) of *V. cholerae* is a complex structure that consists of mainly lipopolysaccharide (LPS), phospholipids and a group of outer membrane proteins (Omps). Apart from major virulent factors (toxin-coregulated pilus; TCP and cholera toxin; CT), large number other factors associated with the outer membrane (OM), including lipopolysaccharide (LPS), OM porins (OMPs) and flagella are mainly responsible for establishing initial adherence, modulate host-pathogen interaction, overall survival of the organism and propagation of virulence factor [270]. Immunization with *Vibrio cholerae* outer membrane vesicles induces protective immunity in mice by inducing specific, high-titer immune responses of similar levels against a variety of antigens present in the OMVs [270]. Omps are highly immunogenic due to their exposed epitopes on the cell surface. Virulence-related outer membrane proteins (Omps) are essential to bacterial survival within macrophages and for eukaryotic cell invasion that could be an alternative candidate for development of subunit vaccine against *V. cholerae*.

Considering the advantages of polymeric nanoparticles as adjuvant and novel delivery systems, the current study was carried out to explore the type and strength of immune responses elicited by PLA/PLGA nanoparticles encapsulated with OMP of *V. cholerae*. The formulation of antigen-polymeric particles needed to be focused on the generation of optimal immune response for which more elaborate and conclusive studies are needed to define the protective roles of the nanoparticulate system. Although there are some interesting positive reports available on PLA/PLGA NP based vaccine formulations, they still need more extensive investigation in terms of formulation, antigen encapsulation, molecular interaction, antigen exposure kinetics and resultant antigen-specific immune responses.

So, we hypothesized that encapsulating OMP antigen in PLA/PLGA nanoparticles would increase the antigen persistence in vivo, improve the initial antigen exposure to immune system after immunization. The combined action of PLA/PLGA NPs and OMP would result in the generation of enhanced and prolonged adjuvant-induced, antigen-specific immune responses.

Here, an attempt was made to formulate PLA/PLGA-Omp nanoparticles with desired physicochemical properties and evaluation of type and strength of immune responses elicited by formulated NPs was elucidated by comparing all possible combinations. The efficacy is also compared between PLA encapsulated and PLGA encapsulated OmpNP-immunized groups and a correlation is established evaluating the results of antigen-specific immune response studies in mice. The efficacy is also compared between PLA encapsulated and PLGA encapsulated OmpNP immunized groups and a correlation was established evaluating the results of antigen-specific antibody response and cellular response studies in *mice*.

## 5.2. Materials and Methods

### 5.2.1. Materials

The polymer; polylactic acid (PLA; molecular weight: 85,000- 160,000 Da), poly (D, L-lactic-co-glycolic) acid (PLGA 50: 50; molecular weight: 40,000-75,000 Da), N-Lauroylsarcosine sodium salt, trehalose dihydrate and polyvinyl alcohol (PVA) were procured from Sigma-Aldrich, USA. Ethyl acetate was purchased from Merck India Pvt Ltd. Ultrapure water from Milli-Q water system (Millipore, USA) was used throughout the study. The medium for splenocytes culture was RPMI 1640 (Himedia) with 10% fetal bovine serum (Himedia). All ELISA antibodies were obtained from Santa Cruz biotechnology. Fluorochrome conjugated anti-mouse antibodies were obtained from Miltenyi Biotec Asia Pacific Pvt Ltd.

### 5.2.2.Preparation of OM proteins

#### Preparation of major outer membrane proteins (Omp)

In order to isolate the proteins in the OM of *V. cholerae*, the respective strain was grown to late exponential phase. Cells were harvested from I L culture ( $4,500 \times g$ , 15 min,  $4^{\circ}C$ ), washed twice in 10 mM HEPES, pH 7.5, and resuspended in 10 mM HEPES, pH 7.5, with one Sigma FAST<sup>TM</sup> protease inhibitor cocktail tablet (EDTA-free) per 20 gm cell mass. Cells were suspended in a 10 ml lysis buffer (0.1 M Tris, 10 mM EDTA) and disrupted by ultrasonication for 30 min at 10 watts an interval of 30s ( $4^{\circ}C$ ). The cell lysate was treated with DNase (100  $\mu g/ml$ ) and RNase (100  $\mu g/ml$ ) for 30 min at  $37^{\circ}C$ . The debris were removed by centrifugation ( $4,500 \times g$ , 15 min). The supernatant containing the OM proteins were centrifuged again ( $100,000 \times g$ , 1 h,  $4^{\circ}C$ ) (Sorvall Combi, USA). The crude cell pellet was resuspended in 0.8 ml 10 mM HEPES, pH 7.5, plus 1% N-Lauroylsarcosine sodium salt for 30 min at  $37^{\circ}C$ . After centrifugation ( $100,000 \times g$ , 1 h,  $4^{\circ}C$ ), the pellet was washed once with 1 ml of 10 mM HEPES, pH 7.5, and resuspended in 50  $\mu l$  of 10 mM HEPES, pH 7.5. The protein concentration was determined by Pierce<sup>TM</sup> BCA (Bicinchoninic acid) Protein Assay Kit (Thermo Scientific). For determination of the LPS contamination, total carbohydrates in the purified protein were measured (Westphal and Jann, 1965). Purified OM proteins were lyophilized stored at  $-80^{\circ}C$  for further use.

### 5.2.3. Preparation and characterization of PLA-Omp and PLGA-Omp nanoparticles

#### Preparation of PLA-Omp and PLGA-Omp nanoparticles

NPs containing different antigens were formulated using a double emulsion-solvent evaporation technique with little modification [314]. In this method, 50 mg of antigen dissolved in 500  $\mu l$  of citrate buffer (pH=8) was emulsified with 600 mg of PLGA/PLA in ethyl acetate solution (12 ml) to get a primary emulsion. Emulsification was carried out by sonication (Sartorius LABSONIC<sup>®</sup> M) at an amplitude of 5 for 20 seconds in an ice bath. The resulting primary emulsion (w/o) was further emulsified in an aqueous PVA solution (30 ml, 2% w/v) in a drop-wise manner and then emulsified with a high-speed homogenizer for 2 min at 10000 rpm. The w/o/w double emulsion was added to 80 ml deionized water and was stirred at 500 rpm for 2 hours at room temperature to allow the organic solvent evaporation. The NPs were recovered by centrifuge at  $37,500 g$  for 45 min and washed thrice with sterile deionized water to remove residual PVA. Then the particles were lyophilized using 2.5% trehalose dihydrate as a cryoprotectant. Blank polymeric (PLA/PLGA) NPs were prepared by using only 500  $\mu l$  deionized water as an internal aqueous phase.



### 5.2.4. Characterization of PLA-Omp and PLGA-Omp nanoparticles

#### Particle size, zeta potential and polydispersity index measurements

The size (Hydrodynamic diameter), size distribution (Poly Dispersity Index) and zeta potential (Surface charge) of the NPs were analyzed by Zeta sizer (ZS 90, Malvern Instruments Ltd, Malvern, UK). Then determinations for average mean diameter, zeta potential and polydispersity index were measured for each preparation and the standard deviations were calculated.

#### Morphology

The morphology of the nanoparticles was investigated by field emission scanning electron microscopy (FE-SEM; Nova Nano SEM 450/FEI). Observations were taken at different magnifications performed at 15 kV.

#### Cellular uptake studies

Cellular uptake of PLA-Omp and PLGA-Omp nanoparticles was observed by fluorescence microscopy using a hydrophobic dye; Coumarin 6 preloaded at the time of particle formulation step.

#### Encapsulation efficiency measurement

The antigen encapsulation in NPs (PLA-Omp and PLGA-Omp) was determined from the total amount of antigen added in the formulation and the antigen amount that was not encapsulated. For this, the concentration of Omp antigen in the supernatant was analyzed by Pierce™ BCA (Bicinchoninic acid) Protein Assay Kit (Thermo Scientific) to determine free antigen concentration.

$$\text{Encapsulation Efficiency (\%)} = \frac{\text{Total amount of protein} - \text{Free protein}}{\text{Total amount of protein}} \times 100$$

#### *In vitro* antigen release study

The rate of antigen released from NPs was measured as a function of time during incubation in 1X phosphate buffered saline (PBS). The samples (50 mg of NPs) were suspended in PBS (3 ml) and carried out for sonication at an amplitude of 40 and 0.5-sec pulse cycle for 2 min. The samples were then incubated on an orbital shaker (100 rpm) at 37°C. At defined time intervals, the samples were centrifuged and the supernatant was processed for the estimation of protein (BCA method). The pelleted NPs were reconstituted by adding an equal volume of fresh PBS. The percentage of protein release was plotted against time and the cumulative release was calculated.

**FTIR study**

Fourier transformation infrared (FTIR) spectroscopy analysis was conducted to corroborate the possibility of interaction between the antigen and the polymer. The attenuated total reflectance (ATR)-FTIR spectrum was performed using a Bruker ALPHA spectrophotometer (Ettlinger, Germany) with a resolution of  $4\text{ cm}^{-1}$  and scan between  $4000$  and  $500\text{ cm}^{-1}$  by taking an average of 25 scans per sample. The results were analyzed through OPUS software.

**5.2.5. Immunization studies****Animals**

BALB/c mice were used in all experiments. Mice were housed with food and water ad libitum and monitored under full care and in accordance with the standard rules. All animals were acclimated for at least 1 week before use.

**Immunization protocol**

Seven-week-old mice were randomly divided into 12 groups ( $n=6$ ) and intraperitoneally immunized at days 0, 14, and 28 with different formulations at the rate of  $25\text{ }\mu\text{g}$  antigens in  $50\text{ }\mu\text{l}$  PBS for the initial immunization at day 0 and  $0.25\text{ }\mu\text{g}$  antigen in  $50\text{ }\mu\text{l}$  PBS at days 14 and 28. The formulations are PLA-Omp, PLGA-Omp, PLA, PLGA, Omp, PBS (as control). Another same set of combinations are used with alum (Aluminium hydroxide) to compare the adjuvanticity of PLA and PLGA nanoparticles. Mice were anesthetized by inhalation of 2.5% isoflurane gas prior to all immunizations. All treated groups were bled at 0, 7, 14, 21, 28, 42 and 56 days after 1st immunization. Sera was separated and stored at  $-80^{\circ}\text{C}$  for further analysis. Splenocytes were collected at a particular time for flow cytometric assays.

**5.2.6. Determination of Omp specific IgG1 and IgG2a antibodies by ELISA**

Levels of immunoglobulin IgG1, IgG2 isotype antibodies to OMPs were determined by an enzyme-linked immunosorbent assay (ELISA) using 96 well microtitre polystyrene plates (Nunc, Denmark). The wells were separately coated with  $50\text{ }\mu\text{l}$  of purified Omp ( $1\text{ }\mu\text{g}/\text{well}$ ) diluted in carbonate-bicarbonate buffer (pH 9.6) overnight at  $4^{\circ}\text{C}$ . The wells were washed thrice with TBST (TBS with 0.05% Tween 20) and blocked with 5% skim milk powder for 2 hr at room temperature. After blocking, the wells were further washed thrice in TBST. After washing, appropriate sera were two-fold diluted from an initial dilution of 1:10 with TBS (pH 7.2) and added to antigen-coated wells in duplicate (per each dilution) and incubated at  $37^{\circ}\text{C}$  for 1 hr followed by washing thrice in TBST. Plates were then incubated with  $100\text{ }\mu\text{l}$  HRP conjugated goat immunoglobulin antibody against mouse IgG (IgG1 or IgG2a) (Santa Cruz, CA, USA) with standardized dilutions for 1 hr. The wells were then thoroughly washed with TBST and the reaction was visualized after adding  $100\text{ }\mu\text{L}/\text{well}$  of TMB/ $\text{H}_2\text{O}_2$  (Sigma-Aldrich).

The reaction was allowed to proceed for 10 min, stopped with 100  $\mu$ L 1N sulphuric acid, and absorbance was read at 450 nm with an automatic plate reader (Imax Microplate Reader, Biorad). The antibody activity was expressed in terms of O.D value after subtracting the values obtained by unimmunized healthy sera.

### **5.2.7. Spleen cell analysis**

Spleen cell analysis was performed in splenocytes collected from immunized mice after 4 weeks of 3<sup>rd</sup> immunization. Cells were harvested according to standard protocol. Single-cell suspensions of spleen, liver, and lung lymphocytes were generated for in vitro culture and flow cytometry by standard techniques, as previously described [342]. Cell viability was assessed by exclusion of trypan blue and flow cytometry using a commercially available kit (Live/Dead Staining Kit; Invitrogen). Cell surface phenotype was determined using a panel of murine cell surface markers,: APC-antiCD11C, FITC- anti CD45RA, PerCP- anti Gr1, PE-anti F4/80, Biotin- anti CD49b, Biotin-anti CD3 (Miltenyi Biotec). After washing, multiparameter analyzes were performed using a Becton, Dickinson LSR II flow cytometer (San Jose, CA) and analyzed using FCS Express software (DeNovo.).

### **5.2.8. Determination of memory T-cell responses by flow cytometry**

Flow cytometry was performed to measure the percentage of memory T cells in splenocytes collected from immunized mice 10 days after the third immunization. Cells were cultured in RPMI 1640 supplemented with 10% fetal bovine serum and restimulated with Omp(50  $\mu$ g/mL) for 60 h. Cells were then stained with the following set of fluorochrome-conjugated anti-mouse antibodies: FITC-anti-CD4, PerCP-anti-CD8a, PE-anti-CD44, and APC-anti-CD62L (Miltenyi Biotec). After washing, cell samples were examined by Becton, Dickinson LSR II flow cytometer (San Jose, CA) and analyzed using FCS Express software (DeNovo.).

### **5.2.9. Expression of MHC and Co-stimulatory molecules on dendritic cells in spleen**

Balb/c mice (n ¼ 3) were intraperitoneally vaccinated with different vaccine formulations (25  $\mu$ g antigens in 100  $\mu$ L buffer/mouse), and mice were euthanized at 1, 2, and 7 days post-immunization. Spleen cells were harvested and processed into single cell suspension. Cells were stained with a mixture of anti-mouse antibodies (APC-anti-CD11c, FITC-anti-MHC I, PE-anti-MHC II, and Biotin-anti-CD86; all from Miltenyi Biotec). Expression of MHC I, MHC II, and CD86 on CD11c<sup>+</sup> DCs was determined by Becton, Dickinson LSR II flow cytometer (San Jose, CA) and analyzed using FCS Express software (DeNovo.).

### 5.2.10. Determination of follicular helper CD4<sup>+</sup> T cells in spleen

Balb/c mice (n ¼ 3) were intramuscularly vaccinated with different vaccine formulations (25 µg antigen/100 µL buffer/ mouse, half dose at each site), and mice were euthanized 9 days after immunization. Spleen cells were harvested and processed into single cell suspension. Cells were stained with a mixture of anti-mouse antibodies (FITC-anti-CD4, APC-anti-CXCR5, and PE-anti-PD-1; all from Miltenyi Biotec). The percentage of follicular helper CD4<sup>+</sup> T cells (CD4<sup>+</sup>CXCR5<sup>hi</sup>PD-1<sup>hi</sup>) was determined by Becton, Dickinson LSR II flow cytometer (San Jose, CA) and analyzed using FCS Express software (DeNovo.).

### 5.2.11. Statistical Analysis

All values obtained in the current study were expressed as the mean ± standard error (SE)/ Standard deviation (SD). The values were tested for normality (Kolmogorov–Smirnov test). If data showed a normal distribution, either student's t-test or a one-way analysis of variance (ANOVA) was used to assess for statistical significance defined as P <0.05. If the data were not normally distributed, they were analyzed using a Kruskal–Wallis test with the same significance limit either the Kruskal–Wallis test with Dunn's multiple comparison post hoc tests or by the Mann–Whitney test using SPSS version 20(SPSS, Surrey UK).

## 5.3.Results

### 5.3.1. Formulation and Physico-chemical properties of antigen-loaded NPs

In this study, PLA-Omp, PLGA-Omp, PLA and PLGA NPs were prepared by w/o/w double emulsion evaporation technique with successful encapsulation of Omp antigen. All the physical properties like the size (Hydrodynamic diameter), size distribution (Poly Dispersity Index) and zeta potential (Surface charge) have been characterized by DLS analysis (Table 5.1). The particle size of blank PLA NPs were recorded as 116.34± 15.23 nm, whereas PLA encapsulated Omp NPs (PLA-Omp) possessed the average size of 196.24± 34.25 nm (Figure 5.1). Similarly, the particle size of blank PLGA NPs and PLGA encapsulated Omp NPs (PLGA-Omp) were 107.36± 23.15 nm and 165.34± 3.5 nm respectively (Fig. 2). The zeta potential values of blank PLA NPs and PLA-Omp NPs were -21.3 ± 6.75 mV and -25.2 ± 5.45 mV respectively (Figure 5.1). Similarly, the zeta potential values of blank PLGA NPs and PLGA-Omp NPs were -25.3 ± 5.15 mV and -32.5 ± 6.15 mV respectively (Figure 5.2). The polydispersity index (PDI) values of formulated NPs were within the good range confirming the monodispersity nature of the formulated NPs. Scanning electron micrographs (SEM) revealed the spherical in structures of formulated NPs. The particles were very much isolated and uniformly distributed.

**Table 5.1. Physical properties of Omp loaded PLA and PLGA nanoparticles. The results were expressed as mean $\pm$  standard deviation.**

Polymer	Sample(Code)	Mean Particle size (Diameter in nm $\pm$ SD)	Zeta potential (MV) $\pm$ SD	Poly Dispersity Index (PDI) $\pm$ SD	Encapsulation efficiency (%)
PLA	Blank (PLA)	116.34 $\pm$ 15.23	-21.3 $\pm$ 6.75	0.350 $\pm$ 0.05	-
	PLA-Omp	196.24 $\pm$ 34.25	-25.2 $\pm$ 5.45	0.147 $\pm$ 0.06	57.85 $\pm$ 4.15
PLGA	Blank (PLGA)	107.36 $\pm$ 23.15	-25.3 $\pm$ 5.15	0.424 $\pm$ 0.03	-
	PLGA-Omp	165.34 $\pm$ 3.5	-32.5 $\pm$ 6.15	0.308 $\pm$ 0.05	69.18 $\pm$ 1.68

The antigen content in PLA-Omp and PLGA-Omp nanoparticles varied as antigen loading dependent upon the polymer nature, the physical state of the antigen/drug and the molecular interactions between the antigen and the polymer. Omp encapsulation efficiency (%) in PLA NPs was 57.85  $\pm$  4.15 (Mean  $\pm$ SD), whereas in PLGA NPs it was 69.18 $\pm$  1.68 (Mean  $\pm$ SD) (Table 5.1). The antigen encapsulation in PLGA NPs is significantly higher ( $p < 0.05$ ) than the PLA NPs.

*In vitro* release profile of Omp from PLA-Omp and PLGA-OmpNPs is illustrated in Figure3 that revealed the sustained release of Omp antigen from both PLA and PLGA. It could be confirmed that the antigen release from PLA–Omp was in a considerably slower than from PLGA. In case of PLGA–Omp NPs, 50 % of the antigen was released within 8 hrs of incubation whereas in case of PLA-Omp NPs, it took almost 24 hrs to release 50% of the total antigen. The initial burst release was rapid in PLGA-Omp NPs in comparison to of PLA-Omp NPs.

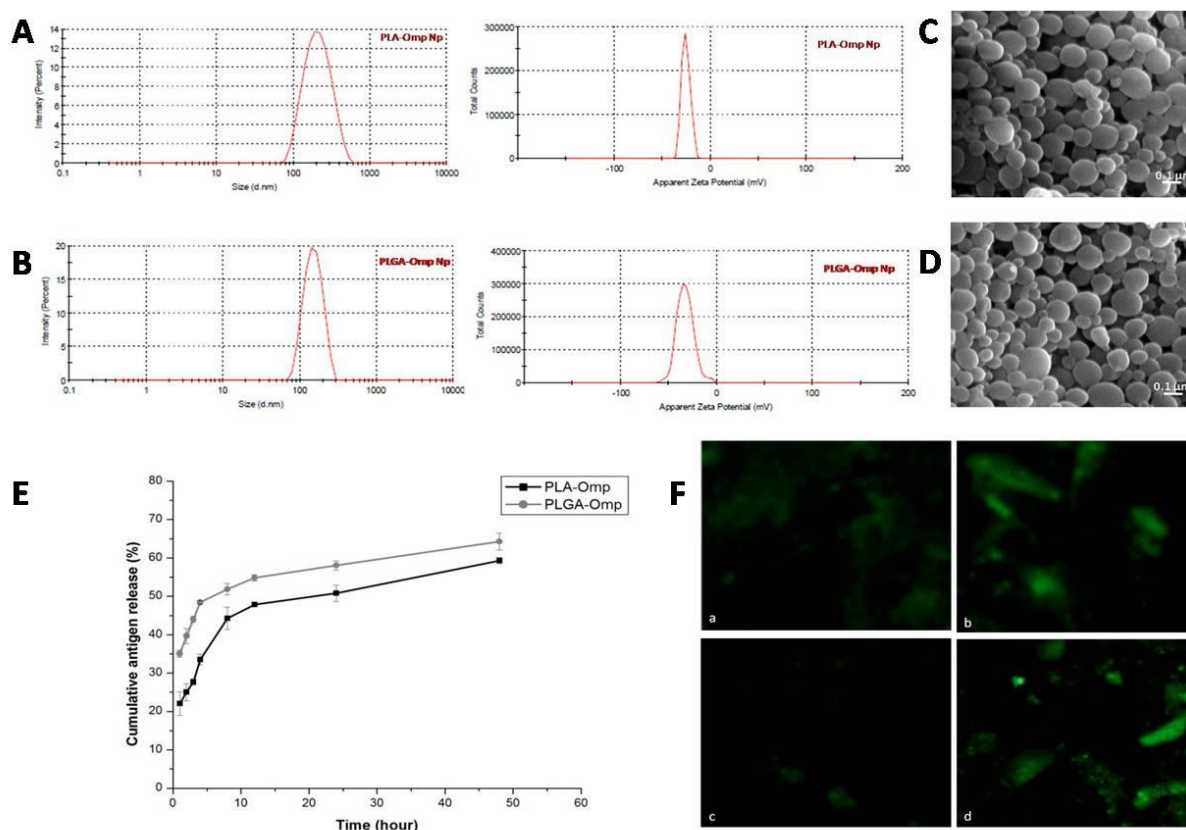


**Figure 5.1. Physico-chemical properties of antigen-loaded NPs.** Size and charge (zeta potential) distribution pattern of (A)PLA-OmpNp(size:  $196.24 \pm 34.25$  nm; zeta potential:  $-25.2 \pm 5.45$  mV) and(B) PLGA-OmpNp(size:  $165.34 \pm 3.5$  nm; zeta potential:  $-32.5 \pm 6.15$  mV)determined by dynamic light scattering (DLS) method.The morphology of PLA-Omp NPs (C) and PGA-Omp NPs (D) were investigated by field emission scanning electron microscopy. (E)Comparison of Omp release (in vitro) from PLA and PLGA nanoparticles.The burst release rates were; in PLA-Omp NPs 22.07% at 1hr, 25% at 2 hr, 27.67% in 3 hr, 33.53% at 4 hr, 44.23% in 8 hr, 47.84% in 12 hr, 50.84% in 24 hr, 59.28 % in 48 hr; in PLGA-Omp NPs 35.06% at 1hr, 39.67 % at 2 hr, 44.01% in 3 hr, 48.02 % at 4 hr, 51.87 % in 8 hr, 54.83% in 12 hr, 58.04% in 24 hr, 64.25% in 48 hr. The rapid burst effect is very much delayed with PLA-Omp NPs. (F) Fluorescence microscopy images of HEK cells after 4 h of incubation with the coumarin 6-loaded PLA/PLGA-Omp nanoparticles. The coumarin 6-loaded nanoparticles were green ( $\times 100$ ). a. HEK cells incubated with coumarin 6- PLA-Omp NPs for 12 hours; b. HEK cells incubated with coumarin 6- PLA-Omp NPs for 24 hours; c. HEK cells incubated with coumarin 6- PLGA-Omp NPs for 12 hours; d. HEK cells incubated with coumarin 6- PLGA-Omp NPs for 24 hours.

From the FTIR spectrum; it was also observed that upon encapsulation of OMP to PLA and PLGA, the characteristic peaks associated with OMP, PLA and PLGA remained intact so there was no loss of any functional peaks between the absorbance spectra of OMP and OMP encapsulated NPs. Thus, it can be stated that there is no occurrence of molecular interactions that could alter the chemical structure of the OMP at the time of study (Figure 5.2).

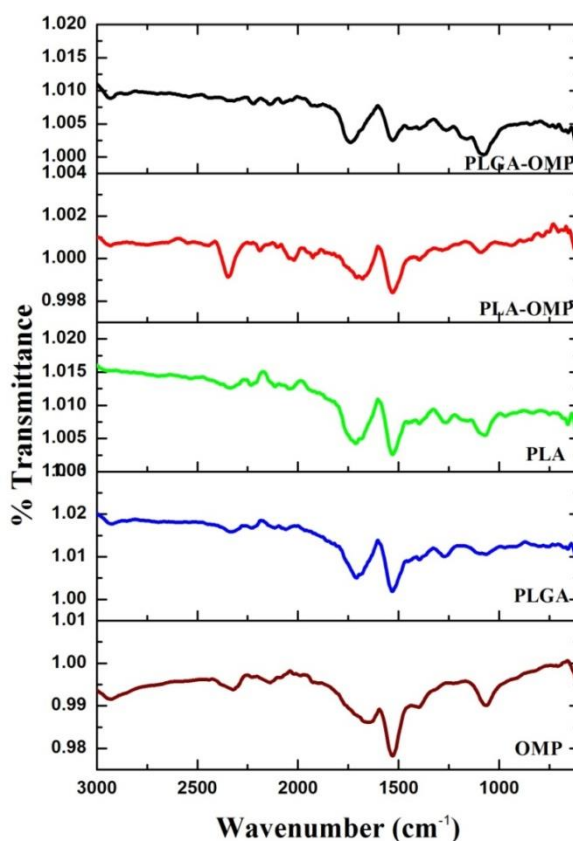


Figure 5.2. ATR-FTIR spectrum of formulated NPs. Similar spectral bands were observed at 2337  $\text{cm}^{-1}$  ( $\text{C}\equiv\text{N}$  stretching- presence of nitriles), 1712  $\text{cm}^{-1}$  ( $\text{C}=\text{O}$  stretching- presence of carboxylic acid), 1529  $\text{cm}^{-1}$  ( $\text{N}-\text{H}$  bending- presence of Amide-II), 1068  $\text{cm}^{-1}$  ( $\text{C}-\text{H}$  stretching- presence of aliphatic amines), 891  $\text{cm}^{-1}$  ( $\text{C}-\text{H}$  bending) for OMP, blank PLA and PLGA NPs. Apart from common bands observed in OMP and blank NPS some additional peaks were also observed in case of encapsulated PLA-OMP and PLGA-OMP nanoparticles at 2936  $\text{cm}^{-1}$  ( $\text{C}-\text{H}$  stretching, the presence of alkanes), 1680  $\text{cm}^{-1}$  ( $\text{C}=\text{O}$  stretching, presence of amide -I). The characteristic peaks of PLA and PLGA were observed at 1710  $\text{cm}^{-1}$  and 1060  $\text{cm}^{-1}$  that correspond to the presence of the  $\alpha$ ,  $\beta$  unsaturated esters and carboxylic acids and ethers. The common peak at 1064  $\text{cm}^{-1}$  resulted from the overlapping of several bands including the absorption due to vibration modes of  $\text{CH}_2\text{OH}$  and  $\text{C}-\text{O}$  stretching vibrations coupled to  $\text{C}-\text{O}$  bending. It was also observed that upon encapsulation of OMP to PLA and PLGA the characteristic peaks associated with OMP, PLA and PLGA remained intact with no loss of any functional peaks between the absorbance spectra of OMP and OMP encapsulated PLA/PLGA NPs.

### 5.3.2. Immune response study

#### Antigen-specific antibody response in vaccinated mice

The serum antibody level (IgG1, IgG2a) in different antigen-NP treated sera was measured by ELISA. The antibody level were expressed as mean OD (after subtraction the OD value obtained by unimmunized healthy sera)  $\pm$  SE (Figure 5.3). The overall antibody titers (IgG1, IgG2a) increased during the vaccination period (from 7 days to 56 days). Antigen-specific IgG1, IgG2a titers were above control levels for intraperitoneally immunized mice for all groups (7-56 days). Both IgG1 and IgG2 titers in vaccinated mice followed the similar pattern, but the IgG1 response is higher than IgG2 response.



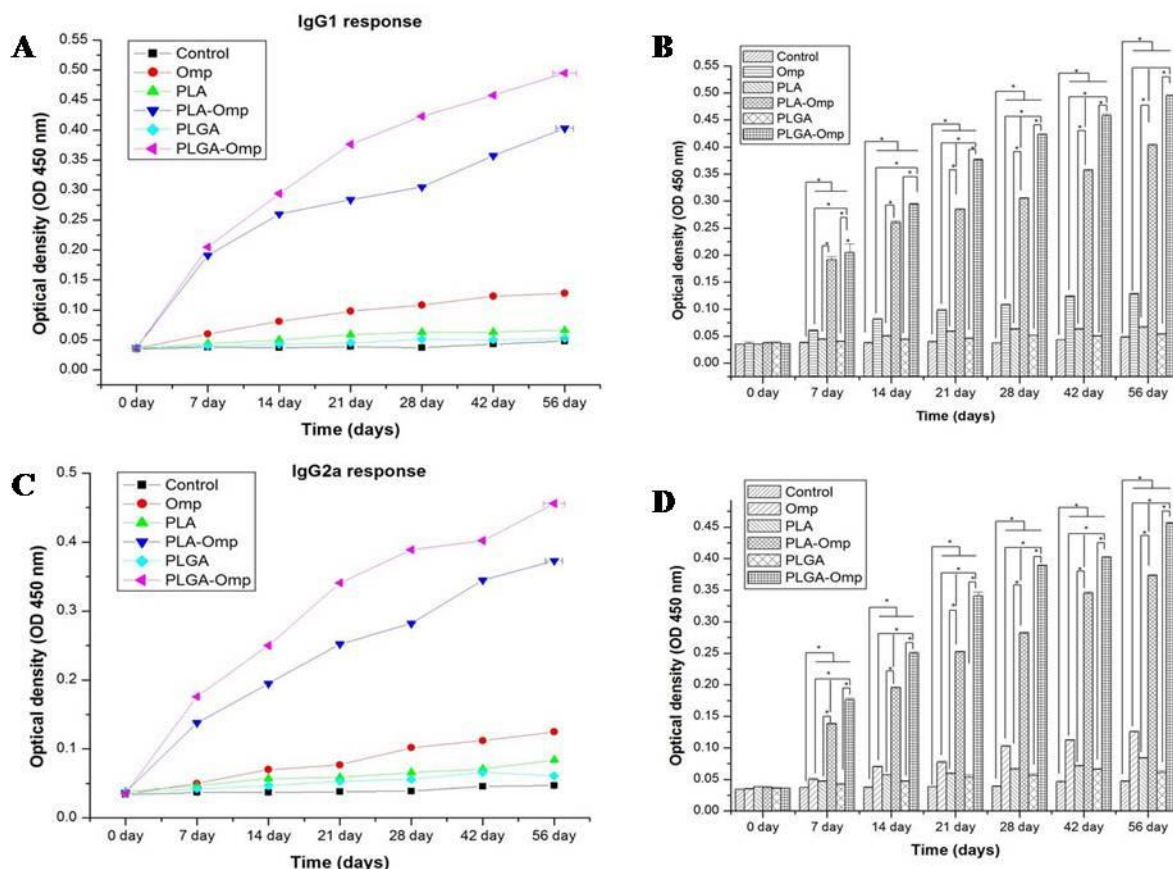


**Figure 5.3.** Antibody immune response induced after vaccination of BALB/c mice with different antigenic formulations (PLA-Omp, PLGA-Omp, Pmp, PLA, PLGA, PBS) at different time. A and B represents serum IgG1 levels in vaccinated mice (n=5/group). C and D represents Serum IgG2a levels in vaccinated mice (n=5/group). Data are the mean value (\* $p < 0.05$ ) for immunized mice vs control groups.

All vaccinated mice had comparable Ig titers at all points except 0 days, which were significantly higher than those for the control (PBS group) mice ( $P < 0.05$ ; Kruskal-Wallis test and post hoc Dunn multiple comparisons). The antibody level were significantly higher ( $p < 0.05$ ) in PLA-Omp NPs, PLGA-Omp NPs treated groups than respective PLA and PLGA NPs treated groups from 7 days to 56 days. PLA-Omp NPs and PLGA-Omp NPs induced significantly higher ( $p < 0.05$ ) antigen-specific IgG titers than Omp antigen treated groups at all-time intervals except 0 days. In comparison between PLA-omp and PLGA-Omp NPs, the later one showed higher antigen-specific IgG immune response although it is not significantly different ( $p > 0.05$ ). Another set of experiment that deals with immune response of all selected antigenic groups (PLA-omp, PLGA-Omp, PLA, PLGA, Omp, PBS as control) was performed in presence of alum (adjuvant) to compare the advancity of PLA and PLGA with Alum-treated groups showed similar pattern of antigen-specific IgG titer like alum untreated groups. Again PLA-Omp NPs-alum and PLGA-Omp NPs-alum showed slight higher antibody titer, but not significantly different ( $p > 0.05$ ).



IgG2a antibody level reveals a Th1 polarized immune response, and the ratio of IgG2a/IgG1 is indicative of Th1 biased immune response. Both PLA-Omp and PLGA-Omp NPs induced stronger IgG1 and IgG2a responses than Omp antigen ( $p < 0.05$ ). However, IgG2a responses are less robust than IgG1 response. Taken together, PLGA-Omp NPs developed more potent antigen-specific antibody with high titers among all antigenic formulations.

### **5.3.3. Splenocyte proliferation Assay**

In vitro proliferation of splenocytes was carried out to observe the influence of different antigenic formulations on splenocyte proliferation. Both PLA-Omp and PLGA-Omp NPs causes more efficient splenocyte proliferation in comparison to Omp antigen alone ( $p < 0.05$ ), which confirmed more potent induction of antigen-specific immune responses.

### **5.3.4.Spleen cell analysis**

A detailed analysis of spleen cell population after immunization showed an increase in the number of innate immune cells, such as myeloid DC and granulocytes (Figure 5.4). There was also an elevation in macrophage cell numbers, B cell, plasmacytoid DC. Interestingly, among the cell populations analyzed, the effector cells of the adaptive immune response (B cell) showed the highest expansion. Also PLA-Omp, PLGA-Omp NPs induced significantly higher cellular expansion than respective PLA and PLGA NPs. Again, a significant higher cellular activation was observed in the case of PLA-Omp and PLGA-Omp NPs in comparison to Omp antigen alone. However, no such significant difference was observed between PLA-Omp NPS and PLGA-Omp NPs except in the granulocyte cell subtypes.

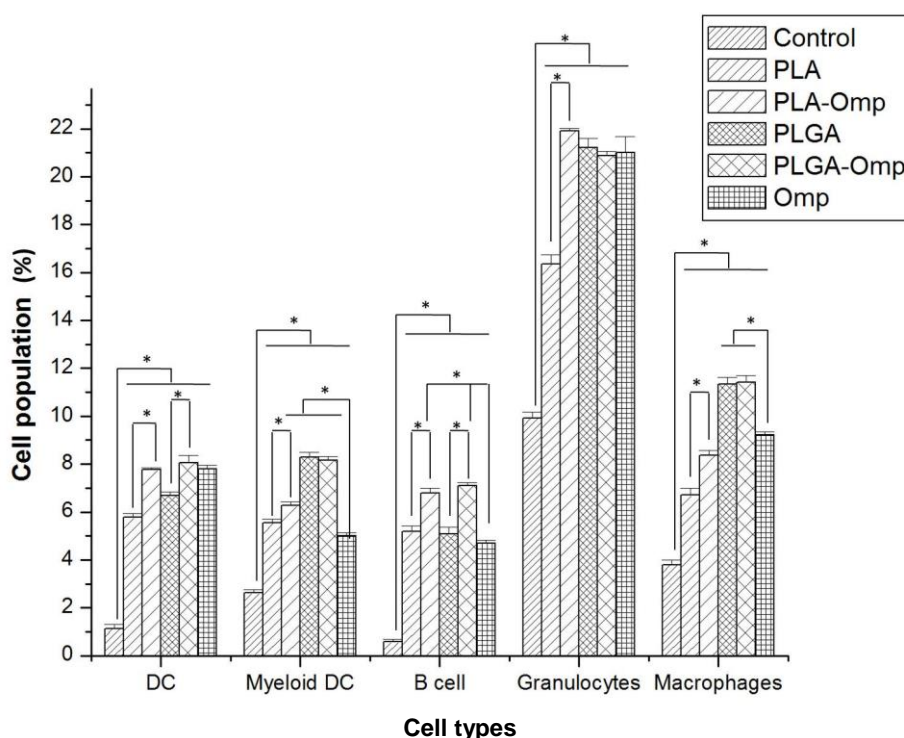


**Figure 5.4.** Mice were injected intraperitoneally with PBS (control), PLA NPs, PLGA NPs, PLA-Omp NPs, PLGA-Omp NPs, Omp. Splenocytes were isolated after 0 and 7-day post immunization. Splenocytes were stained with various surface markers, as indicated, and analyzed by flow cytometry. The gating logic was as follows: plasmacytoid dendritic cells (CD11c<sup>+</sup>, B220<sup>+</sup>), myeloid dendritic cells (CD11c<sup>+</sup>, B220<sup>-</sup>), B cells (CD11c<sup>-</sup>, B220<sup>+</sup>), granulocytes (GR-1<sup>+</sup>, F4/80<sup>-</sup>), macrophages (GR-1<sup>-</sup>, F4/80<sup>+</sup>). Cell numbers were normalized to day 0 values. Data are expressed as the mean  $\pm$  SEM (n =3). \*p < 0.05.

### 5.3.5.Memory T cell responses

Generation of Memory T cell response plays a crucial role in the case of successful vaccination to combat the reinfection. Memory T cells are major components of the memory immune responses. There are 2 important types of memory T cell: effector memory T cells (CD44<sup>hi</sup> CD62L<sup>low</sup>) and central memory T cells (CD44<sup>hi</sup> CD62L<sup>hi</sup>) [340]. For both CD4<sup>+</sup> and CD8<sup>+</sup> T cells, the frequency of effector memory T cells and central memory T cells were similar among splenocytes harvested from mice immunized with all different antigenic formulations (Figure 5.5). PLA-Omp and PLGA-Omp NPs induced higher ( $p < 0.05$ ) percentage of CD44<sup>hi</sup> CD62L<sup>low</sup> (effector memory T cells) cells in comparison to Omp as well as control (PBS). Also, PLA-OmpNPs and PLGA-Omp NPs induced significantly higher ( $p < 0.05$ ) response of CD44<sup>hi</sup> CD62L<sup>low</sup> (effector memory T cells) cells than respective PLA and PLGA NPs. Also, the percentage of effector memory cells (CD44<sup>hi</sup> CD62L<sup>low</sup>) was higher than central memory T cells (CD44<sup>hi</sup> CD62L<sup>hi</sup>) in case all immunized groups. The FACS plots of the mean percentages were shown in figure X. As a conclusion, both PLA-Omp and PLGA-Omp induced stronger effector memory T cell response among all formulation and PLGA-Omp NPs induced significantly higher response ( $p < 0.05$ ).

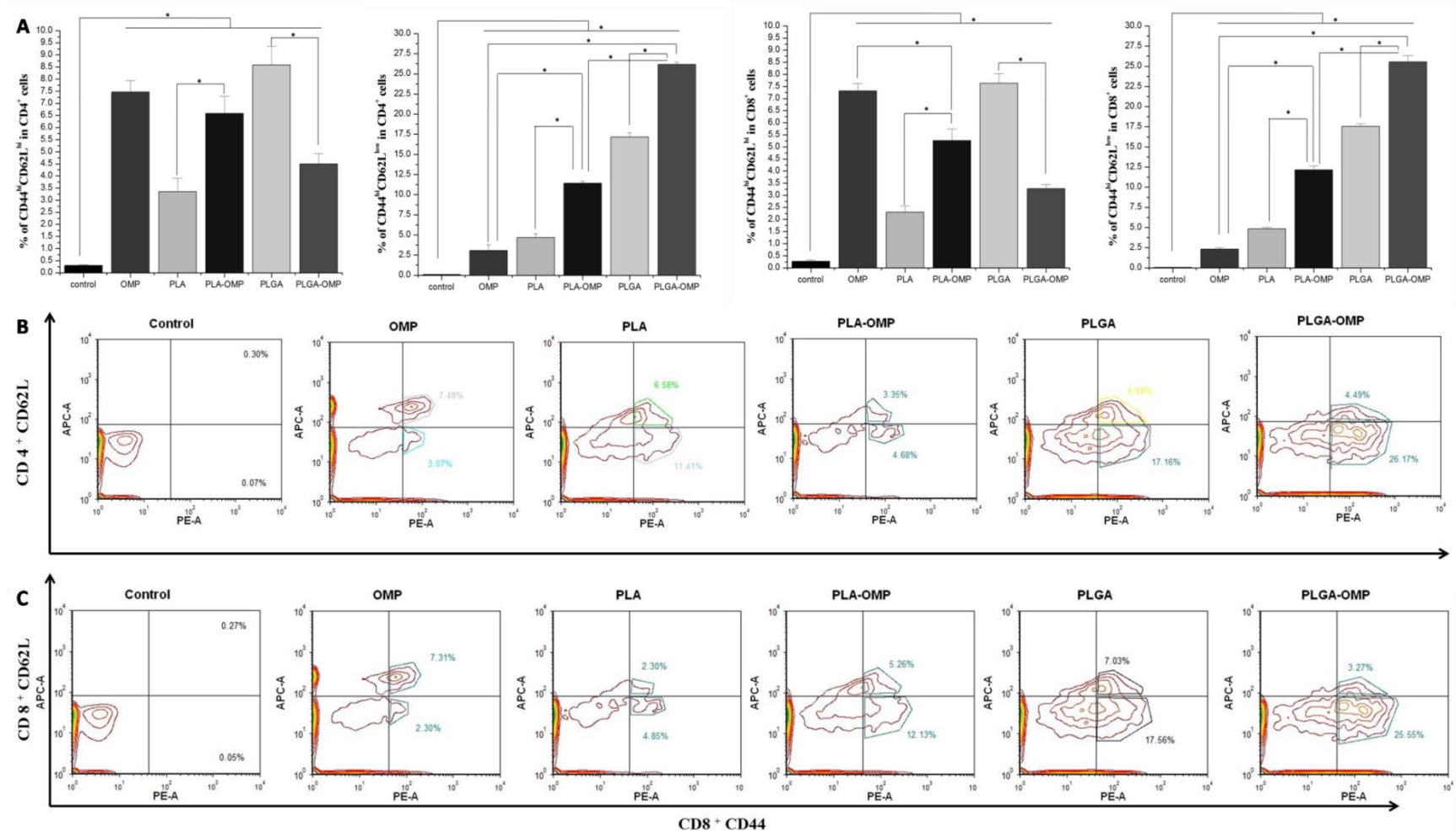


**Figure 5.5.** Frequency of central (CD44<sup>hi</sup>CD62L<sup>hi</sup>)/effector (CD44<sup>hi</sup>CD62L<sup>low</sup>) memory CD4<sup>+</sup> and CD8<sup>+</sup> T cells. Mice (n = 6) were immunized three times as described in the methods section. Splenocytes were harvested 10 days after the third immunization and restimulated ex vivo with antigen for 60 h. The frequency of CD44<sup>hi</sup>CD62L<sup>hi</sup> CD4<sup>+</sup> T cells, CD44<sup>hi</sup>CD62L<sup>low</sup> CD4<sup>+</sup> T cells, CD44<sup>hi</sup>CD62L<sup>hi</sup> CD8<sup>+</sup> T cells, and CD44<sup>hi</sup>CD62L<sup>low</sup> CD8<sup>+</sup> T cells (A) were measured by flow cytometry. FACS plots in B and C are representative of the mean percentages of 6 mice in each group. Data in (A) are expressed as the mean  $\pm$  SEM (n = 6). \*p < 0.05.

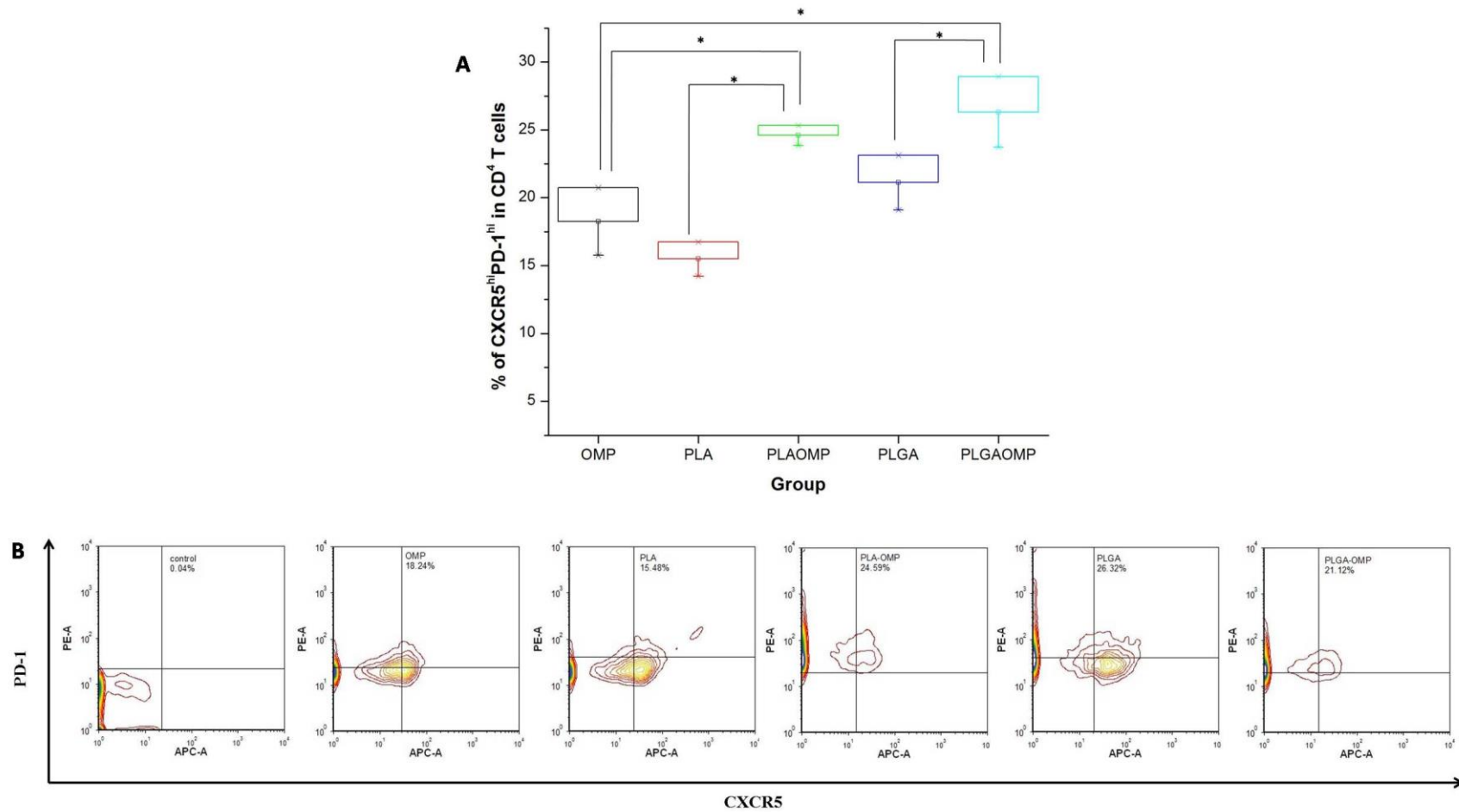


**Figure 5.6.** The frequency of follicular helper CD4<sup>+</sup> T cells in the splenocytes of immunized mice. Balb/c mice (n = 3) were intraperitoneally vaccinated with different vaccine formulations. Mice were euthanized 9 days later, and splenocytes were isolated. The frequency of follicular helper CD4<sup>+</sup> T cells (CD4<sup>+</sup>CXCR5<sup>hi</sup>PD-1<sup>hi</sup>) was determined by flow cytometry. (A) Percentage of follicular helper CD4<sup>+</sup> T cells (CD4<sup>+</sup>CXCR5<sup>hi</sup>PD-1<sup>hi</sup>) in CD4<sup>+</sup> T cells and (B). Representative flow cytometry plots. Data are expressed as the mean  $\pm$  SEM (n  $\frac{1}{3}$ ). \*p < 0.05.

### 5.3.6. Expression of MHC and the co-stimulatory molecule CD86 on DCs

Targeted and prolonged antigen delivery to effective antigen presenting cell (APCs) like dendritic cells (DCs) have a crucial role in initiating an adaptive immune response by internalizing and presenting antigens through MHC-I to CD8<sup>+</sup> T lymphocytes and MHC II to CD4<sup>+</sup> T lymphocytes. In this case, an attempt was made to find out the mechanism of DCs activation in the spleen. So, the expression of MHC I and MHC II costimulatory molecules (CD86) on DCs in spleen were measured by flow cytometry. PLA-Omp and PLGA-Omp NPs induced significantly higher MHC I, MHC II, CD 86 expression than Omp. However, no such significant difference found in the case of alum-NPs formulations. Again PLA-Omp and PLGA-Omp showed little bit different behavior towards MHC expressions. PLA-Omp NPs elicited significantly higher ( $p < 0.05$ ) MHC I, MHC II, CD86 expression than PLGA-Omp.

### 5.3.7. Frequency of follicular CD4<sup>+</sup> T cells in spleen

Follicular CD4<sup>+</sup> T cells are an important part of the generation of long-lived humoral immunity mediated by B cells. In this study, the activation of follicular CD4<sup>+</sup> T cells by different antigenic formulations to favor the antibody production was elucidated (Figure 5.6). The frequency of follicular CD4<sup>+</sup> T helper cells (CD4<sup>+</sup>CXCR5<sup>hi</sup>PD-1<sup>hi</sup>) was measured by flow cytometry. The frequency of CD4<sup>+</sup>CXCR5<sup>hi</sup>PD-1<sup>hi</sup> cells in the splenocytes of PLA-Omp and PLGA-OmpNP-immunized mice was significantly higher ( $p < 0.05$ ) than other antigenic formulation immunized mice. Also PLA-OmpNPs and PLGA-Omp NPs induced significantly higher ( $p < 0.05$ ) CD4<sup>+</sup>CXCR5<sup>hi</sup>PD-1<sup>hi</sup> cells than respective PLA and PLGA NPs. Also, the percentage of follicular CD4<sup>+</sup> T helper cells was significantly higher in case the of PLA-Omp and PLGA-OmpNps in comparison to Omp.

## 5.4. Discussion

Disease control or elimination requires the induction of protective immunity in a sufficient proportion of the population, which can be accomplished by efficient vaccination. Long-term immunity, a hallmark of adaptative immunity is conferred by the maintenance of antigen-specific immune effectors and/or by the induction of memory cells that may be capable of reactivating the immune effectors in the case of pathogen exposure. By playing a crucial role in vaccine development, NPs formulation allows improved not only antigen stability and adjuvanticity (leads to better immunogenicity) but also specifically targeted and sustained release [208]. Novel delivery system and adjuvants that boost immunogenicity are very much essential while designing advanced and sophisticated

vaccines [3]. Polymeric NPs have been increasingly investigated in current vaccine research as promising adjuvant and ideal delivery system that could activate both humoral and cellular immune response [5], [340], [343].

Fabrication procedure and several physicochemical properties such as the type of polymer, molecular interaction (polymer-antigen), antigen exposure kinetics significantly affect the combination of adjuvant activity of the polymer as well as immunogenicity of the antigen. The current study was focused with an aim to elucidate the formulation of polymeric (PLA/PLGA)-Omp NPs and to evaluate the immune response (humoral and cellular) in terms of antigen processing and generation of a response. The antigen was a conserved antigenic outer membrane protein (Omp) from *V. cholerae* keeping in mind to develop a novel subunit vaccine and its better efficacy through polymeric NPs mediated delivery to the specific immune system. Our proposed hypothesis was proved by observation of successfully enhanced antigen-specific antibody responses and increased generation of memory T cell in the PLA/PLGA-Omp NPs immunized mice.

Although particles of dimension below 100 nm are considered as nanoparticles, still relative increase in size (size~ 100-500 nm) can be essential in the area of drug delivery system for the efficient drug loading [57], [340]. Also, as the formulated PLA-Omp NPs and PLGA-Omp NPs were < 500 nm size range, these particles could be successfully endocytosed in the body. The lower size was observed in the case of fabricated PLGA-Omp NPs than PLA-Omp nanoparticles, which might be due to use of low molecular weight PLGA (50:50; 30-60 KDa). Surface charge density; zeta potential is essential to predict the fate of the NPs in vivo and to assess the stability of colloidal system through strong electrostatic repulsion of particles with each other [344]. PLA and PLGA being negatively charged polymers impacts anionic nature to formulated NPs (PLA, PLA-Omp, PLGA, and PLGA-Omp). Also zeta potential values more negative after successful encapsulation of Omp in both PLA and PLGA (PLA-Omp NPs:  $-25.2 \pm 5.45$  mV; PLGA-Omp NPs:  $-32.5 \pm 6.15$  mV), that proves more stability. Again the formulated NPs were confirmed their monodisperse nature as polydispersity index was maintained below 0.5 even after antigen encapsulation that prevents particle aggregation [298]. Higher antigen loading is one of the most desired qualities of successful design of NP-based vaccine delivery that reduces the amount of polymers and the loading of drug depends on the chemical structure (both polymer and drug) as well as the condition of loading [159]. Significantly higher encapsulation of Omp protein ( $p < 0.05$ ) was achieved in the case of PLGA-Omp NPs ( $69.18 \pm 1.68$  %) than PLA-Omp NPs ( $57.85 \pm 4.15$  %) like our previous studies [333] that

might be due to more hydrophilicity of PLGA causing enhanced intermolecular interaction. However, the Omp protein release profile in PLA-Omp NPs is comparatively slower than PLGA-Omp that could also be attributed to hydrophilic nature of PLGA (diffusion of the protein through water-filled pores) and higher antigen loading (create a concentration gradient with release medium). Higher lactide content in PLA might be an another cause in delaying the rapid burst effect as we observed in the case of PLA-Omp NPs (50% antigen release  $\approx$  24 hr). Surface morphology of the PLA and PLGA nanoparticles loaded with Omp were studied using a scanning electron microscope (SEM). The smooth surface can also be correlated to lactide content that adds hydrophobicity to the polymer. So, that could prevent the retention of water and the shrinkage could be avoided while drying. Also, particle-particle contact formation was become less due to the presence of lactide (which causes hydrophobic) and ultimately prevents agglomeration [302].

From the FTIR spectrum, it was also observed that upon encapsulation of Omp to PLA and PLGA the characteristic peaks associated with Omp, PLA and PLGA remained intact so there was no loss of any functional peaks between the absorbance spectra of Omp and Omp encapsulated nanoparticles. Thus, it can be stated that there is no occurrence of molecular interactions that could alter the chemical structure of antigen encapsulation to PLA and PLGA nanoparticles[345], [346].

# Chapter 6

## Development of DNA vaccines to boost antigenic outer membrane protein antigenicity

### 6.1. Introduction

Genetic/DNA immunization is a novel technique used to stimulate efficiently humoral and cellular immune responses to antigens [25], [202]–[204]. It involves the direct introduction into living host of a plasmid containing the DNA sequence encoding the antigen(s) against which an immune response is wanted, and relies on the *in situ* production of the target antigen. Ultimately, it results in the specific immune activation of the host against the delivered gene (antigen) [347]. This approach (the third vaccine revolution) provides a number of potential advantages over other traditional approaches, like generation of both humoral and cell-mediated immune responses, improved vaccine stability, the absence of any infectious agent and the relative ease of large-scale manufacture with high purity [6], [200], [201]. The safety, simplicity, versatility, stability, ease of production, nontoxicity, and broad of immunity and long-lasting cytotoxic T lymphocyte responses make DNA vaccines very attractive for antiviral/antibacterial/anticancer immunization strategies [25], [202]–[204].

DNA vaccines are composed of bacterial expression plasmids that normally contain two units: the antigen expression unit that includes the promoter, antigen-encoding and polyadenylation sequences and the production unit including the bacterial sequences necessary for plasmid amplification and selection [348]. After successful construction, the vaccine plasmid is transformed into *Escherichia coli* to produce multiple plasmid copies. The plasmid DNA is then purified in large scale from the bacteria, by separating the circular plasmid from genomic DNA, RNAs, proteins and other impurities. This purified DNA acts as the vaccine.

Regarding the clinical application of DNA vaccines, the difficulty for the vaccine to move through the cell membranes (after intramuscular administration) must be considered. Frequently, only small amounts of vaccine reach the antigen presenting cells (APC) to elicit immune responses [210], [349]. Hence, the current focus in molecular therapy has been to disclose the reasons for the lack of potential for DNA vaccines. There is a clear need to improve the transfection efficiency *in vivo* to reduce the vaccination dose of plasmid DNA.



Novel delivery systems for administration of pDNA vaccines are central to address the above discussed necessities [5], [205], [350]. This delivery system should be a modern and sophisticated form of an adjuvant with engineered immunological properties. Among possible delivery systems, nanoparticles (NP) based delivery of DNA vaccines to APCs, is an emerging and promising approach used for optimizing DNA vaccine formulation for immunotherapy [5], [350]. The biocompatible nanopolymers such as poly-(D,L-lactide-co-glycolide)(PLGA) and chitosan are attractive for DNA delivery applications [5], [61], [207], [208]. Chitosan NPs hold promise because of their ability to protect encapsulated nucleic acid-based antigens from nuclease degradation and promote delivery of adsorbed DNA to APCs [209], [210]. In the case of synthetic polymers like PLGA, besides DNA protection, the encapsulation permits a controlled DNA delivery system to be designed with controllable degradation times and release kinetics of DNA for prolonged gene expression over a required time. For example, PLGA undergoes ester hydrolysis in the physiological environment with the formation of biocompatible monomers [211]. Nanoparticles based delivery systems for plasmid DNA (pDNA) (which encode target gene of interest) administration may be keys to improve the transfection efficiency in vivo even at a lower dose.

*A. hydrophila* is a pathogenic gram-negative bacterium associated with lower vertebrates like fish, amphibians [28]. Aeromoniasis, an important fish disease is caused by this bacterium [29]. The Outer Membrane (OM) of *A. hydrophila* is a complex structure which consists of mainly lipopolysaccharide (LPS), phospholipids and a group of outer membrane proteins (Omps). The OM of pathogenic gram-negative bacteria is mainly responsible for establishing initial adherence, modulate host-pathogen interaction, overall survival of the organism and propagation of virulence factor [351]. It also has protective antigenicity, because OM components are easily recognized as foreign substances by immunological defense systems of the hosts. Omps are reported to be conserved among different serovars and are highly immunogenic due to their exposed epitopes on the cell surface. Some of them serve as adhesins and play an important role in virulence [351]. Omps are located at host–bacterial interface in *A. hydrophila* and can be targeted for drug therapy.

The research described herein was undertaken to develop a pDNA vaccine to boost antigenic outer membrane protein –(OMP) antigenicity and develop a vaccine candidate for *Aeromonas hydrophila*. The current investigation aimed at developing a DNA vaccine as well as a delivery system to boost antigenic outer membrane protein (Omp) that would act as a potential vaccine candidate. Nanoparticles based delivery systems for plasmid DNA (pDNA) (which encode target gene of interest) administration may be keyed to improve the

transfection efficiency in vivo even at a lower dose. Two conserved protein sequences and their codon optimized sequences of antigenic outer membrane protein were cloned into pVAX-GFP expression vector and successfully transformed into *E. coli* (DH5 $\alpha$ ). The large scale pDNA purification with high purity was achieved based on membrane hydrophobic interaction chromatography (HIC). The purified plasmid solutions were characterized in terms of final quality, physical properties (charge and size) of the pDNA molecule and its ability to transfect mammalian cells (CHO; Chinese hamster ovary) cultured in vitro. An attempt was made to formulate chitosan/PLGA-pDNA complex and the formulated polyplex were characterized in terms of size, size distribution and zeta potential by the dynamic light scattering (DLS) method. The effect of physicochemical properties of the polyplex nanoparticles on biologic stability, transfection efficiency and cytotoxicity was investigated.

## 6.2. Materials & Methods

### 6.2.1. Design of gene constructs for pVAX-GFP expression vector

#### Design of omp DNA vaccines

pVAX-GFP expression vector [352] was used for preparing the pVAX-GFP-based *omp* gene constructs. The vector consists of a pUC backbone, the CMV promoter, the BGH terminator, and a kanamycin resistance gene. The OMP sequences of all *A. hydrophila* serotypes were collected from NCBI database (GenBank; KF938895, JQ946882, JQ946885) and aligned to find out the conserved regions. These regions were analyzed for antigenicity by following bioinformatics tool VaxiJen v2.0 antigen prediction server. Among the conserved sequences, one was (KF938895<sub>211-382</sub>) selected on the basis of maximum VaxiJen score (higher predictable antigenicity). Another (KF938895<sub>703-999</sub>) was selected for comparison purposes. Two conserved outer membrane protein coding gene sequences [*omp*(211-382), *omp*(703-999)] were successfully designed in preparing the gene constructs in a pVAX-GFP expression vector. The pVax-GFP expression vector was used for preparing the pVAX-GFP-based *omp* gene constructs. Start (ATG) and stop codons were added to the two antigen gene sequences. A ribosomal binding site (ACC) was added upstream of the start codon. Two restriction sites (KpnI and EcoRI) in the pVAX1 multiple cloning sites were chosen that did not cut within the two antigen gene sequences. Those restriction sites were added respectively to the 5' and 3' end of the sequence and then checked for being in frame with GFP.

The designed sequences were further optimized for fish in the database using codon optimization software (Entelechon; <http://www.entelechon.com/bttool/bttool.html>) and another one optimized sequence was generated. The four designed sequences, *omp*(211-382),

*omp*(211-382)opt, *omp*(703-999) and *omp*703-999)opt, were synthesized (NZYTech, Portugal). All four synthesized sequences were cloned into a pVAX-GFP expression vector as specified below, leading to plasmids pVAX-GFP-*omp*(211-382), pVAX-GFP-*omp*(211-382)opt, pVAX-GFP-*omp*(703-999) and pVAX-GFP-*omp*(703-999)opt, respectively.

The vectors containing the synthesized *omp* gene fragments and the pVAX-GFP vector were double digested with EcoRI and KpnI (Promega). The purified linearized vector fragment (3662bp) and the *omp* gene sequences were recovered from agarose gel after electrophoresis and using the QIAquick Gel Extraction Kit (Qiagen). The ligation of the vector to each antigen fragment was set up at a molar ratio of 3:1. The ligations were performed by using T4 DNA ligase (Promega), following the manufacturer's procedure. Following the enzymatic reaction, each ligation mixture containing the ligated molecules was used to transform competent DH5 $\alpha$  cells previously prepared by the heat shock method. The transformed cells were thereafter plated onto kanamycin (30  $\mu$ g/mL) LB agar plates. The plates were incubated overnight at 37°C. Each well-isolated colony collected afterward from each Petri dish was inoculated into 5 mL LB broth with L-kanamycin (30  $\mu$ g/mL). The plasmids from every 5 mL overnight cultures were isolated using High Pure Plasmid isolation Kit (Roche) and screened for the positive clones by restriction digestion with EcoRI and KpnI (Promega). The selected positive clones from gel electrophoresis analysis were further confirmed by sequence analysis (STAB Vida, Portugal). Positive clones were further cultured in LB with kanamycin for cell banking at -80°C.

### 6.2.2. Plasmid DNA production in *E. coli* DH5 $\alpha$ transformants

Aliquots from positive *E. coli* clones harboring *omp*(211-382), *omp*(211-382)opt, *omp*(703-999) and *omp*(703-999)opt were withdrawn from the cell banks and inoculated in 5 mL LB broth for overnight culture. On the next day, these seed cultures were used for inoculation of 30 mL of LB medium with 30 mg/mL kanamycin in 100 mL shake flasks which grew overnight at 37°C and 250 rpm. Larger culture volumes (250 mL in 2 L shake flasks) were inoculated with the appropriate amount of overnight culture to an optical density at  $\lambda=600$  nm (OD<sub>600</sub>) of 0.2 and incubated under the same conditions for 8 h to harvest the cells in late exponential growth phase; an OD<sub>600</sub> of 3.2 was recorded at this stage. *E. coli* DH5 $\alpha$  with pVAX-GFP was also grown under the same conditions; Cells were harvested in a refrigerated centrifuge at 3500g, 4°C, for 15 min.

### 6.2.3. Plasmid DNA recovery and purification

Recovery and purification of plasmids were performed by alkaline lysis, followed by precipitation/solubilization, membrane hydrophobic interaction chromatography (HIC) and final polishing steps, as described elsewhere [353]. The harvested cells in the pellet were resuspended in 8 mL P1 solution (50 mM glucose, 25 mM Tris-HCl, pH 8.0, 10 mM EDTA). After complete resuspension, the total volume was transferred to smaller centrifuge tubes. Then, 8 mL P2 solutions (0.2N NaOH, 1% (w/v) SDS) were added to perform alkaline lysis followed by gentle homogenization. The tubes were incubated at room temperature for 10 min. After incubation, 8 mL P3 solution (5M potassium acetate, 6.8M glacial acetic acid) was added to stop lysis followed by gentle homogenization and the mixture was placed on ice for 10 min. The neutralized alkaline lysate was centrifuged at  $20,200\times g$  for 30 min at  $4^{\circ}\text{C}$  to remove cell debris and part of genomic DNA and proteins. The supernatant was placed in new tubes and again centrifuged to remove more debris. The resulting pDNA-containing lysate was stored at  $-20^{\circ}\text{C}$  until further processing.

To each defrosted pDNA-containing lysate ( $\approx 24$  mL with pH 5.0) 16.8 mL of isopropanol (100% v/v) were added and carefully mixed. The tubes were left at  $4^{\circ}\text{C}$  for at least 2 h to precipitate all nucleic acids (pDNA, RNA and traces of gDNA). The above mixture was centrifuged at  $20,200\times g$  and  $4^{\circ}\text{C}$  for 30 min and the supernatant was discharged. The pellet was washed with 2 mL of ethanol 70% (v/v) and centrifuged again with the same procedures as before. The supernatant was discharged and the tubes were inverted on top of the absorbent paper to remove traces of ethanol. The final pellet containing pDNA was resuspended in 6 mL of Tris-HCl (10 mM, pH 8.0) containing 1.52 g ammonium sulphate. The mixture was homogenized properly and left on ice for 2 h. Then the mixture was centrifuged at  $20,200\times g$  and  $4^{\circ}\text{C}$  for 30 min and the supernatant ( $\approx 6$  mL) was used for further purification.

A membrane adsorber Sartobind® Phenyl Nano unit (3 mL bed volume; Sartorius AG) was connected to a Äkta™ Purifier 10 FPLC system from GE Healthcare (Sweden), which continuously monitored the conductivity and UV absorbance at 260 nm. Previously to the chromatographic runs the membrane adsorber was washed with 20% ethanol, and then with MilliQ H<sub>2</sub>O and then equilibrated with a binding buffer (BB) –1.8 M ammonium sulphate in 10 mM Tris-HCl, pH 8.0. Runs were performed at a constant flow rate of 1 mL/min. A volume of 5 mL of a preliminarily purified pVax1-GFP solution ( $>200\text{ ng}/\mu\text{L}$ ), obtained as described above, was injected into the membrane adsorber at  $1\text{ mL}\cdot\text{min}^{-1}$  and allowed to flow through for 15 min, leading to the clearance of unbound solutes. Then a 20 mL long (20 min) gradient

from 0 to 40 % EB (elution buffer; 10 mM Tris-HCl, pH 8.0) was applied followed by a step change in conductivity from 40 % to 100 % EB that also runs through for 20 mL. Membrane chromatography was therefore used to elute the plasmid isoforms selectively. Fractions of 0.5 mL taken from the supercoiled-rich pDNA elution peak were collected and pooled (2 mL), analyzed by horizontal agarose gel electrophoresis (AGE) to confirm purity and then kept at  $-20^{\circ}\text{C}$  for further use. Electrophoreses were run in 15 cm 1% (w/v) agarose gels at 90 V for 2 h with TAE buffer (40mM Tris base, 20mM acetic acid and 1mM EDTA, pH 8.0), and stained with ethidium bromide (0.5  $\mu\text{g/mL}$ ).

Pooled HIC fractions were concentrated to a final volume of 0.3 mL and desalted during centrifugation in a swing bucket rotor for 5min at  $3,200\times g$  and  $4^{\circ}\text{C}$  in a 2 mL Amicon® Ultra centrifugal filters (Millipore, Ireland) bearing a 50 kDa Ultracel® cellulose membrane. The diafiltration was performed stepwise by adding 10mM Tris-HCl pH 8.0 in 5 diafiltration volumes ( $V \approx 1.5\text{mL}$ ) followed by centrifugation using the same settings as before [354]. Recovery of concentrated pVax1-GFP-derived plasmids was achieved by turning the respective Amicon upside down and centrifuging it again under the same conditions.

The final plasmid DNA concentration in purified solution was assessed from 3  $\mu\text{L}$  samples by spectrophotometry on a NanoVuePlus equipment (General Electric Healthcare, UK), after equilibration with 3  $\mu\text{L}$  of MiliQ  $\text{H}_2\text{O}$ . AGE was performed to confirm the quality of purified pDNA, although the overall purification and polishing have been demonstrated to permit efficient CHO cells transfection [354].

#### **6.2.4. In vitro culture and transfection of CHO cells**

In vitro expansion of CHO cells was performed by inoculating at a concentration of  $1.5 \times 10^6$  cells/mL in a T-75 culture flask with 10 mL of Dulbecco's Modified Eagle Medium (GIBCO) supplemented with 10% Fetal Bovine Serum (FBS from GIBCO, heat inactivated) and 1% penicillin and streptomycin (PenStrep from GIBCO) [355]. CHO cells were seeded 24 h prior to transfection into a 24-well tissue culture plate at a density of  $\approx 10^5$  cells/mL, to obtain a confluence of 70-80% on the day of transfection (within 24 h). At the time of transfection, the cells were washed with 500  $\mu\text{L}$  of PBS to remove dead cells and toxins. One microgram of pVAX-GFP, pVAX-GFP-omp(211-382), pVAX-GFP-omp(211-382)opt, pVAX-GFP-omp(703-999) and pVAX-GFP-omp(703-999)opt, was complexed with 1.5  $\mu\text{L}$  Lipofectamine 2000 (self-assembling) and added to each well. DMEM without FBS and antibiotics was added to a final volume of 500  $\mu\text{L}$  and incubated with the cells for a certain period of time (3 h and 6 h). After incubation, the medium was changed, the cells were washed with PBS, and

500  $\mu$ L of the complete medium (DMEM supplemented with 10% FBS and 1% PenStrep) were added to each well. The transfection experiments were performed in duplicate. Cells incubated without pDNA lipoplexes or pDNA biopolymer NP were used as negative control. Cells transfected with Lipofectamine 2000<sup>TM</sup>/pVAX-GFP DNA complexes were used as positive controls of the transfection. The transfection efficiency was evaluated using flow cytometry analysis after 24h or 48h of transgene expression.

### 6.2.5. Flow cytometry analysis

After 24 h or 48 h of transgene expression, the cells were washed with 500  $\mu$ L PBS and trypsinized for 5 min at 37°C. Afterward, complete medium was added to stop the action of trypsin, the cell suspension poured into Falcon tubes and the cells were centrifuged in a conventional bench top centrifuge (5 min, 1,500 $\times$ g, room temperature). Then, the supernatant was discarded and the cell pellet carefully washed with a small amount of PBS, to remove any traces of trypsin, and resuspended in 500  $\mu$ L 2% paraformaldehyde (PFA; freshly prepared). A FACScan Scalibur flow cytometer (Becton-Dickinson, NJ, USA) recorded the forward scatter (FSC), side scatter (SSC) and green fluorescence (FL1) while running each sample of transfected CHO cells. Green fluorescence intensity, corresponding to GFP expression level, FSC and SSC data were analyzed and histograms and dot plots were generated with CellQuest Pro Software © (Becton Dickinson, NJ, USA). The data were expressed as a mean  $\pm$  standard deviation.

### 6.2.6. Chi/PLGA-pDNA Complex

PLGA NPs were formulated using a double emulsion-solvent evaporation technique. The organic phase was prepared by dissolving 200 mg PLGA in 10 ml ethyl acetate (at 25 °C) with constant stirring at 400 rpm (2hr). An aqueous phase was made by dissolving PVA (100 mg) in 10 ml water (with 0.1 mM ethyl acetate water) at 75°C for 5 min, under stirring. After cooling 30 mg chitosan chloride was added to the PVA solution, and the mixture was stirred for 30 min at 1000 rpm. The solution was allowed to degas at room temperature until clear. 2.5 ml of the organic phase was emulsified with 10 ml aqueous phase under stirring at 14,000 rpm using high-speed homogenizer. Then, the emulsion sonicated for 10 min at 40% amplitude, 2 seconds on and 2 seconds off using ultrasonicator (Sartorius LABSONIC<sup>®</sup> M) in an ice bath. The emulsion was stirred at 500 rpm for 2 hours at room temperature to allow the organic solvent evaporation. The NPs were recovered by centrifuge at 37,500 g for 45 min and washed thrice with sterile deionized water. The sample was purified by dialysis, using 100,000 MWCO, 1.8 ml/cm dialysis membrane (HIMEDIA, India), against distilled water.

Dialysis was run for 8 hours, changing the water every 2 hours. The particle solution was recovered from inside the tube and place added with 2.5% trehalose dihydrate as cryoprotectant prior to freeze-drying. For Chi/PLGA-pDNA Complex Formation, 0.5 mg of dried NPs was 0.5 ml of deionized water. The solution was vortexed for 15 minutes at 1000 rpm. NPs and pDNA were combined in Millipore water, vortexed for 30 seconds, and allowed to complex at pDNA/NP ratios of 1:50 by weight at room temperature undisturbed for 1 hour.

#### **6.2.7. Particle Size, Size Distribution, and Zeta Potential**

The size (Hydrodynamic diameter), size distribution (Poly Dispersity Index) and zeta potential (Surface charge) of the pDNA-NP complexes were analyzed by Zeta sizer (ZS 90, Malvern Instruments Ltd, Malvern, UK). The lyophilized samples were made an appropriate dilution with deionized nano-pure water and sonicated at an amplitude of 40 and 0.5-sec pulse cycle for 5 min. Aliquots from each preparation batch were sampled in dynamic light scattering (DLS) cuvettes and nanoparticles were then examined for equivalent diameters, zeta potential and polydispersity index. Particles diameters were assessed at a scattering angle of 90° and at a temperature of 25°C. Then determinations for average mean diameter, zeta potential and polydispersity index were measured for each preparation and the standard deviations were calculated.

#### **6.2.8. DNA Entrapment**

To each sample, 25 µl of OliGreen (OG) fluorescent nucleic acid stain (1X) was added to complexes containing a total of 4 ng of pDNA and incubated at room temperature in a dark for 5 minutes. After incubation, the total volume was raised to 500 µl using Millipore water. The relative fluorescence was determined using 490 nm excitation and 520 nm emission wavelengths in a Luminescence Spectrophotometer.

#### **6.2.9. Enzymatic Digestion Assays**

DNase I (1U) (HIMEDIA) was added to free pDNA and pDNA-NP complexes (1: 50 pDNA/NP) in the supplied DNase buffer, followed by incubation for 10 minutes at 37°C. Plasmid digestion was analyzed via 1% agarose gel electrophoresis as described above.

#### **6.2.10. SEM Study**

The surface morphology of the pDNA-NP complexes was investigated by scanning electron microscopy (Jeol 6480LV JSM microscope). The NPs were fixed on adequate support and coated with platinum using platinum sputter module in a higher vacuum evaporator. Observations under different magnifications were performed at 20kv.

### 6.2.11. Data analysis

The results of experimental assays (for each group) were expressed as mean value  $\pm$  standard deviation (SD)/ standard error. One-way ANOVA (analysis of variance) followed by Duncan's multiple range tests (DMRT) was performed using SPSS18 software. For all tests,  $P < 0.05$  was considered statistically significant.

## 6.3. Results

### 6.3.1. Design of omp gene constructs in pVAX-GFP expression vector

The successful design of the selected constructs; *omp*(211-382), *omp*(703-999) was performed as mentioned in figure 1. The designed sequences were further optimized in the database using codon optimization software (<http://www.entelechon.com/bttool/bttool.html>) and another two sequences; *omp*(211-382)opt, and *omp*(703-999)opt were generated (and from now on designated "opt"). The designed optimized sequences were aligned with respective nonoptimized sequences (*omp*(211-382), *omp*(703-999)) to observe the nucleotide differences (Figure 6.1).

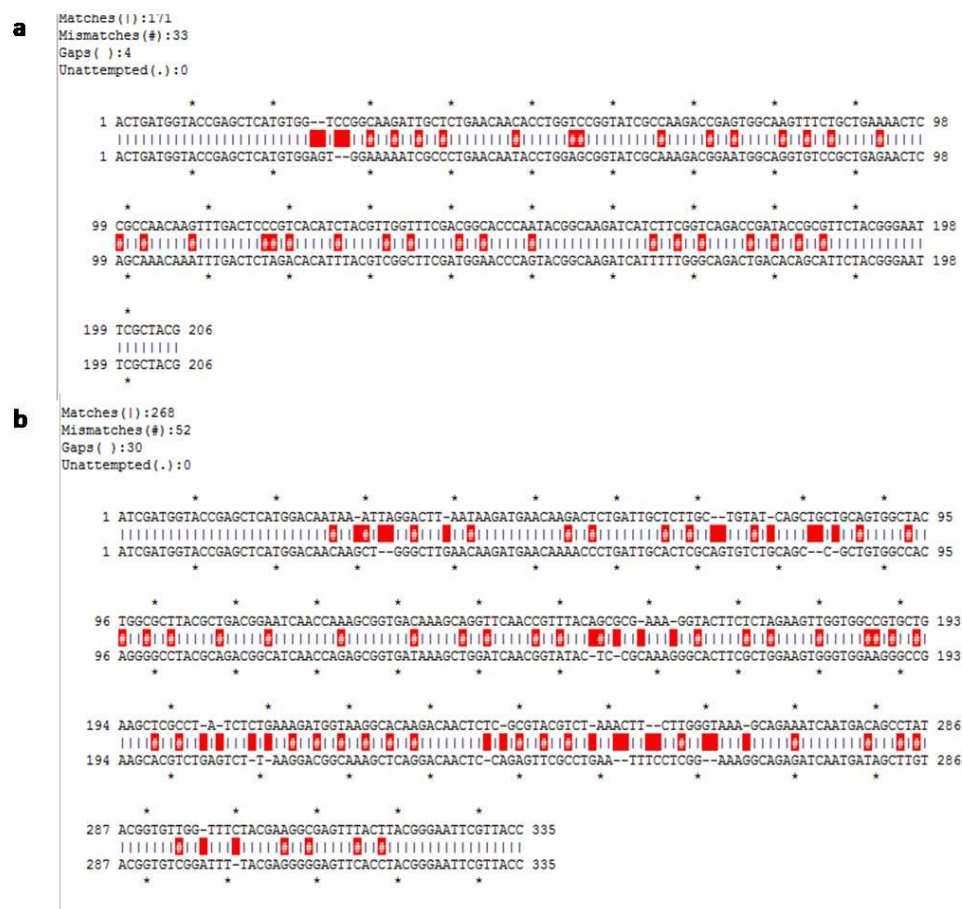


Figure 6.1. Alignment of designed pVAX-GFP-*omp*(211-382) and pVAX-GFP-*omp*(703-999) sequence with their respective optimized sequences [pVAX-GFP-*omp*(211-382)opt and pVAX-GFP-*omp*(703-999)opt showing the nucleotide differences.



Both the 2 designed sequences were crosschecked for restriction sites after inserting into pVAX-GFP plasmid sequence map. All above bioinformatics work was carried with the help of ApE (A Plasmid Editor software). All four designed sequences were synthesized (NZYTech, Portugal).

### 6.3.2. Cloning

In order to construct the corrected vectors pVAX-GFP and *Omp* insert were double digested with KpnI and EcoRI in order to create compatible cohesive ends in both structures. Due to the difference of activity of restriction enzymes, digestion conditions had to be optimized throughout a series of cloning experiments. Finally, the digestion procedures were accomplished by sequential digestion with KpnI at 37°C for 2hr followed by EcoRI at 37°C for 2hr.

Following restriction digestions, the base vectors were purified by 1% agarose gel. The agarose extracts containing the linearized vectors were subsequently purified with the Qiagen Gel Extraction Kit (Qiagen). The successful ligation of gel-purified pVAX-GFP vector to desired antigenic insert was done by using T4 DNA ligase (Promega), at 3:1 molar ratios (Insert:Vector) for 3h at room temperature followed by an overnight period at 4°C. On the other hand, lower temperatures are responsible for bringing the DNA molecules together (due to lower mobility of molecules). The two temp methods used are therefore a balance between contradicting ideal temperatures. Too low temperatures would affect DNA ligase activity while too high temperatures would affect the cloning efficiency by melting the annealed DNA ends and by increasing molecular movement in the reaction [356], so room temperature incubation (25°C) followed by an overnight incubation at 4°C would favor the reaction. Both ligation mixtures and negative controls were transformed by heat shock into *E. coli* DH5  $\alpha$  competent cells and plated in kanamycin-supplemented LB agar plates. The selected plasmids were isolated using High Pure Plasmid Isolation Kit (Roche) and screened for the positive clones by restriction digestion with EcoRI and KpnI by comparing compare the fragment sizes in 1% agarose gel (Figure 6.2).

### 6.3.3. Sequence analysis

All the positive clones (confirmed from gel photographs) were processed for sequencing. The obtained sequences were aligned with original sequences to observe the sequence similarity. From the sequence analysis, the successful cloning of *omp*(211-382), *omp*(211-382) opt, *omp*(703-999) and *omp*(703-999)opt sequences were confirmed.

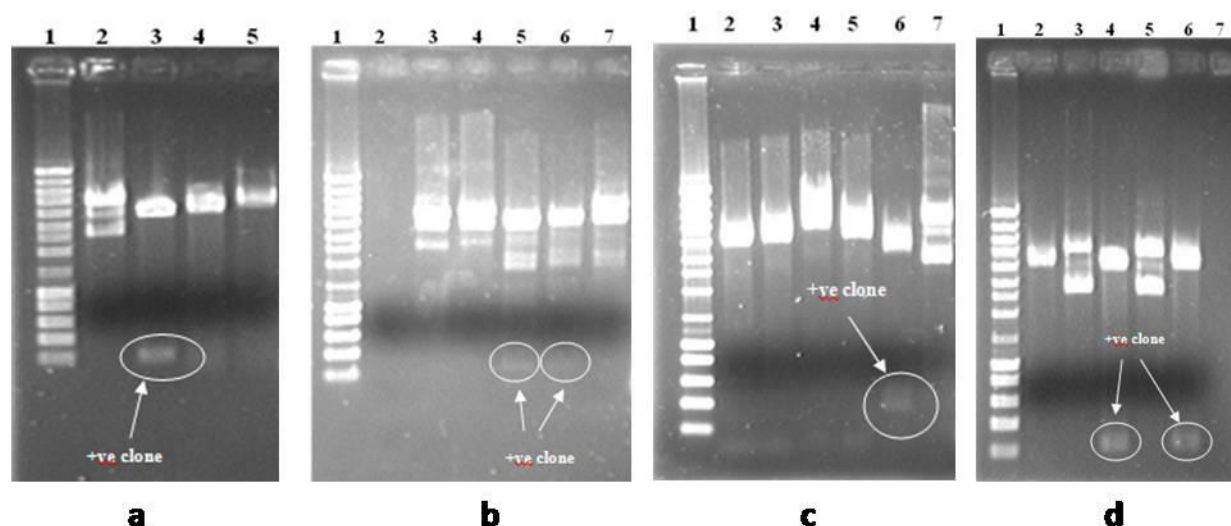
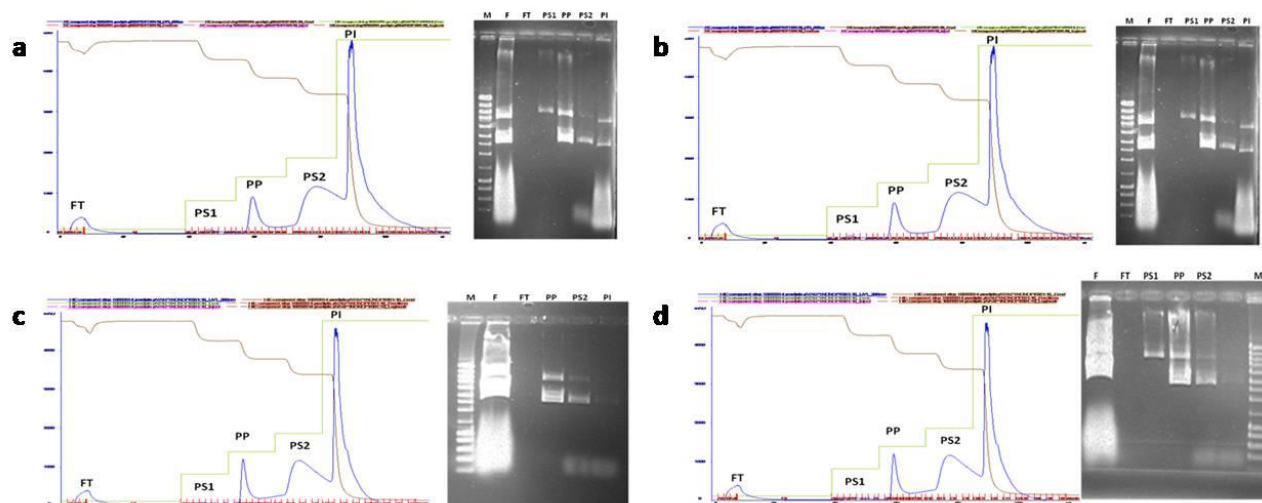


Figure 6.2. Screening of positive clones based on pVAX-GFP for pVAX-GFP-omp(211-382) (a), pVAX-GFP-omp(211-382)opt (b), pVAX-GFP-omp(703-999) (c), pVAX-GFP-omp(703-999)opt (d). Lanes 1: DNA ladder (200 bp-10,000bp) and other lanes; 2-5 (a), 2-7 (b), 2-7 (c), 2-7 (d): RE digestion (Eco R1 and Kpn 1) of corresponding cloned plasmids.

#### 6.3.4. Plasmid DNA production and its up-scaled purification by hydrophobic interaction chromatography (HIC)

The up-scaled production of plasmids was performed by culturing the four strains in larger culture volumes (250 mL in 2 ltr flask) for 8 h ( $OD_{600} \sim 3.2$ ), harvesting the cells in late exponential growth phase. For the *in vitro* assays, the chosen pDNA purification approach was the hydrophobic interaction chromatography that correlated with more stable lipoplexes, higher plasmid transfection and GFP expression [353], [354]. Separation was accomplished in bind and elute mode using an optimized stepwise elution profile [354]. Plasmid-containing samples pre-conditioned with 1.8 M ammonium sulfate were injected at 1 mL/min in a 3 mL bed volume pre-equilibrated with 1.8 M ammonium sulfate in 10 mM Tris-HCl pH 8.0. The weakly retained molecules were washed with the equilibration buffer and the ionic strength was decreased stepwise by changing gradually to 10 mM Tris-HCl pH 8.0 in order to elute the bound impurities. Chromatography is performed using 1.8 M ammonium sulfate in 10 mM Tris at pH 8 as running buffer (conductivity  $\approx 205$  mS/cm) that promotes the hydrophobic interaction of the solutes present (pDNA, RNA, gDNA, and endotoxins) with the phenyl matrix. Relevant chromatographic fractions, for both flow through and eluted peaks, were analyzed by horizontal gel electrophoresis using 15 cm, 1% agarose gels run at 90 V for 2 h with TAE buffer (Figure 6.3).



**Figure 6.3. Chromatogram and Gel photograph of sample pulls at the different peak in the chromatogram (a. pVAX-GFP-omp(211-382), b. pVAX-GFP-omp(211-382)opt, c. pVAX-GFP-omp(703-999), d. pVAX-GFP-omp(703-999)opt. M-Molecular weight marker, F- feed, FT- (A3-A4), PS1- (A9-A12), PP- (B3-B7), PS2- (B12-C6), PI- (C7-C10).**

The pure pDNA fractions collected from the eluted peaks were concentrated. The diafiltration step was performed by adding 10mM Tris-HCl pH 8.0 in 5 times the volume present in the Amicon ( $V \approx 1.5\text{mL}$ ) followed by a centrifugation step using the same settings as before [354]. After purification, the final plasmid DNA concentration was measured on nanodrop (Thermo Fisher) and analyzed for purity by agarose electrophoresis. The quality parameters of the pDNA pool obtained (at 1 mL/min flow rate) are comparable with those reported by Pereira et al., 2014 for an identical system[354]. The final concentrated pDNA content were 407 ng/ $\mu\text{L}$ , 574 ng/ $\mu\text{L}$ , 417.5 ng/ $\mu\text{L}$  and 375 ng/ $\mu\text{L}$  for *omp*(211-382), *omp*(211-382)opt, *omp*(703-999) and *omp*(703-999)opt respectively.

### 6.3.5. In vitro Assays

#### Transfection Efficiency

The biological activity of purified plasmid fractions was evaluated by preparing lipoplexes by complexation with the cationic liposome-based reagent (Lipofectamine) and used to transfect CHO cells cultured in vitro. Higher percentages of transfected CHO cells were from the enhanced expression of GFP in the cell nucleus [355].

Positively charged liposome/DNA complexes (lipoplexes), formulated with the reagent Lipofectamine 2000TM, have been widely used as a safe transfection methodology. In vitro transfection assays have demonstrated to be improved by the use of cationic liposomes, due to its protective role of pDNA [357], [358] against nuclease attack, also enhancing cellular

uptake via endocytosis [355]. The outcome of the transfection was evaluated on the basis of two parameters: (i) the percentage of cells transfected and (ii) the mean intensity of individual cell fluorescence. After flow cytometry analysis, the mean value for % gated CHO cells (% Transfection) and fluorescence MI (Mean Intensity) of positive control (pVAX-GFP), pVAX-GFP-omp(211-382), pVAX-GFP-omp(211-382)opt, pVAX-GFP-omp(703-999) and pVAX-GFP-omp(703-999)opt were calculated, after subtraction of respective negative control (only non-transfected CHO cells) values (Table 6.1).

**Table 6.1. Transfection study results (% Transfection, Mean Intensity and %T × MI values of positive control (pVAX-GFP), pVAX-GFP-omp(211-382), pVAX-GFP-omp(211-382)opt, pVAX-GFP-omp(703-999) and pVAX-GFP-omp(703-999)opt transfected CHO cells) after 24 h and 48 h incubation**

Sample	Incubation Time	% Gated (% T)	MI (Mean Intensity)	%T × MI
Positive control	24 hr	11.39±.092	101.855 ± 5.190	1160.128 ± 49.753
	48 hr	11.17 ± 0.827	70.9 ± 11.816	791.953 ± 73.325
Omp1 nonopt-pVAX-GFP	24 hr	17.655±2.022	184.595 ± 25.088	3259.025 ± 816.242
	48 hr	44.46 ± 0.290	433.94 ± 21.871	19292.97 ± 1098.182
Omp1 opt-pVAX-GFP	24 hr	12.09±0.290	93.695 ± 19.322	1132.773 ± 260.891
	48 hr	15.03 ± 4.363	59.91 ± 3.415	900.447 ± 312.182
Omp2 nonopt-pVAX-GFP	24 hr	10.357± 1.213	82.11± 28.235	850.413 ±392.059
	48 hr	15.04 ± 1.365	33.43 ± 3.076	502.787 ± 0.639
Omp2 opt-pVAX-GFP	24 hr	20.125± 0.410	131.47 ± 23.568	2645.834 ± 528.222
	48 hr	7.945 ± 0.792	31.27 ± 7.347	248.440 ± 33.606

After 24 h incubation, transfection efficiency was highest for pVAX-GFP-omp(211-382) (%T × MI: 3259.025 ± 816.242) among all the designed plasmids. After 48 h incubation, the transfection efficiency was increased only for pVAX-GFP-omp(211-382) (%T × MI: 19292.97 ± 1098.182) (Figure 4). In other cases, overall transfection efficiency decreased due to a decrease in mean intensity (although there is a slight increase in %T), meaning that there was less amount of expressed green fluorescent protein in the cells at 48 h post-transfection, although there was a higher percentage of the cell with expressed protein. Cells lose faster the ability to express the protein coded by the plasmid, except for pVAX-GFP-omp(211-382).

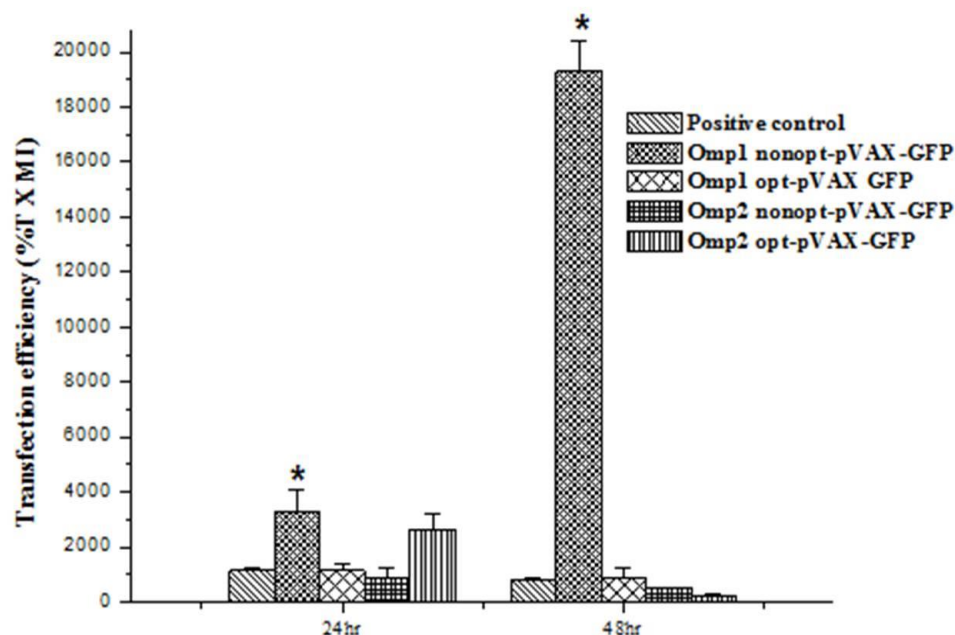


**Figure 6.4.** Transfection efficiency (%T×MI) of positive control (pVAX-GFP), pVAX-GFP-*omp*(211-382), pVAX-GFP-*omp*(211-382)opt, pVAX-GFP-*omp*(703-999) and pVAX-GFP-*omp*(703-999)opt transfected CHO cells after 24 hr and 48 hr of incubation.

The results obtained for pVAX-GFP-*omp*(211-382) was again verified by a separate experiment, where *in vitro* transfection was carried out with pVAX-GFP-*omp*(211-382), pVAX-GFP-*omp*(211-382)opt and pVAX-GFP (as control) and transfected cells were incubated for 24 hr, 48 hr, 3day, 6 day, 8 days (table 2). In both the case [(pVAX-GFP-*omp*(211-382), pVAX-GFP-*omp*(211-382)opt], the transfection efficiency was increased up to 24h incubation. Subsequently, the transfection efficiency was decreased from 1 day to 8<sup>th</sup> day incubation. From the current experiment, it can be concluded that optimum incubation time for transfection is 24 hr (1 day). Therefore, the behavior of transfect pDNA constructs harboring all four gene constructs were tested for GFP expression, in order to achieve a quantitative understanding of the effect of such sequences in intracellular trafficking and protein expression. The difference in the transfection relies upon the gene expression and the efficient gene expression dependent on several factors, such as plasmid uptake, degradation rate of plasmid copies inside the cell, efficient delivery to the nucleus through successful intracellular trafficking and, finally, transcription and translation efficiencies. The ultimate goal of transfection is gene expression. Efficient gene expression, one of the setbacks of non-viral vectors, is dependent on several factors, such as plasmid uptake, the degradation rate of plasmid copies inside the cell, plasmid access to the nucleus through successful intracellular trafficking and, finally, transcription and translation efficiencies. In the context of DNA

vaccination, one of the principal setbacks is the efficient delivery of pDNA to cell nucleus [359]. The analysis of GFP-positive cells, compared with control non-transfected cells exposed to the same amount of lipofectamine, confirmed the expected results regarding the most efficient plasmid uptake. Plasmid size is an important role in transfection, as in the number of cells presenting fluorescence, and plasmid copy number [357]. Significant smaller sizes are correlated with higher transfection efficiencies [357], [360]. The significant higher ( $p \leq 0.05$ ) expression in pVAX-GFP-omp(211-382) might be due to the smaller antigenic insert. Regarding the percentage of transfection, the value was low for the positive control where pDNA is complexed with the transfection reagent Lipofectamine 2000. This is an established complex with transfection normally higher than 30% when GFP is used as a reporter gene [361]. The results obtained are probably related with the 100% cell confluency used for control assay. Too many cells might result in contact inhibition, making cells resistant to the uptake of foreign DNA or due to pH variation as the ideal pH for CHO cell culture varies between 6.8 and 7.4 [362].

**Table 6.2.** Transfection study results (% Transfection, Mean Intensity & %T  $\times$  MI values of pVAX-GFP-omp(211-382), pVAX-GFP-omp(211-382)opt transfected CHO cells) after 1day, 2day, 3 day, 6 day, 8 day incubation.

	pVAX-GFP-omp(211-382)			pVAX-GFP-omp(211-382)opt		
	%Transfection (%T)	Mean Intensity (MI)	%T $\times$ MI	%Transfection (%T)	Mean Intensity (MI)	%T $\times$ MI
1 day	21.275 $\pm$ 0.417	251.725 $\pm$ 40.432	5363.88 $\pm$ 965.216	13.465 $\pm$ 1.675	96.462 $\pm$ 5.957	1293.876 $\pm$ 81.439
2 day	22.78 $\pm$ 0.226	184.205 $\pm$ 21.913	4193.711 $\pm$ 457.503	15.8 $\pm$ 0.735	74.325 $\pm$ 8.690	1171.14 $\pm$ 82.649
3 day	20.62 $\pm$ 4.652	113.915 $\pm$ 33.396	2271.234 $\pm$ 158.619	9.88 $\pm$ 1.824	77.095 $\pm$ 5.635	766.839 $\pm$ 196.327
6 day	17.082 $\pm$ 0.866	71.95 $\pm$ 12.077	1234.317 $\pm$ 268.635	4.56 $\pm$ 0.233	21.32 $\pm$ 6.590	97.988 $\pm$ 35.026
8 day	15.855 $\pm$ 5.451	45.23 $\pm$ 8.626	740.637 $\pm$ 383.361	3.025 $\pm$ 0.190	5.695 $\pm$ 1.774	17.057 $\pm$ 4.281

### 6.3.6. Physico-chemical properties of pDNA-NP complex

Size and charge (zeta potential) distribution pattern of pDNA-NP complex have been characterized by dynamic light scattering (DLS) method. The average size and zeta potential of pVAX-GFP-omp(211-382)-NP complex were 199.25  $\pm$  22.29nm and 23.25 $\pm$  33.59 mV respectively. Similarly, The average size and zeta potential of pVAX-GFP-omp(211-382)opt-NP complex were 205.25  $\pm$  3.59 nm and 26.35 $\pm$  2.38 mV respectively (Figure 6.5). Zeta potential otherwise known as the electrokinetic potential at the surface of the colloidal particles has a great significance in comparing the stability of colloidal dispersions [333]. The high positive charge of formulated nano complex confirmed the complete exposure of



chitosan towards the surface in the complex and higher stability. The polydispersity index (PDI) is a measurement of particle distribution and gave a distribution range from 0.000 to 0.500 [298]. The PDI value of pVAX-GFP-*omp*(211-382)-NP complex ( $0.152 \pm 0.06$ ) and pVAX-GFP-*omp*(211-382)opt-NP complex ( $0.216 \pm 0.05$ ) confirmed the monodispersity nature.

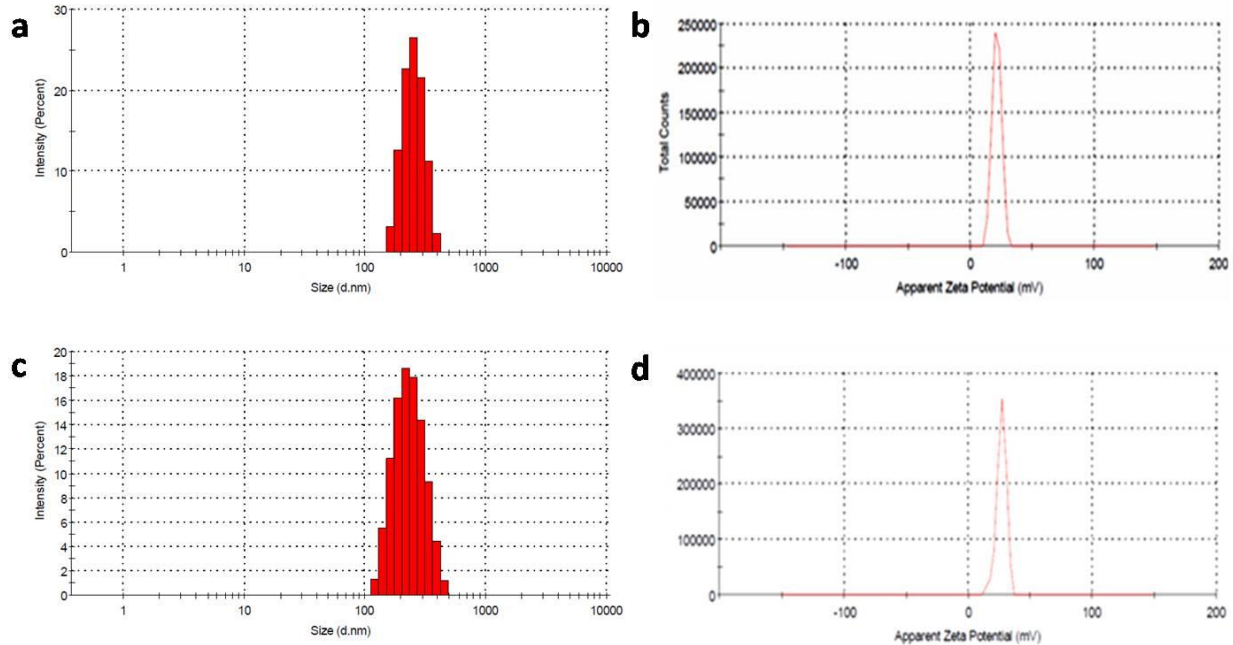


**Figure 6.5.** Size and charge (zeta potential) distribution pattern of pDNA loaded Chi/PLGA NPs by dynamic light scattering (DLS) method. The average size of pVAX-GFP-*omp*(211-382)-NP complex was  $199.25 \pm 22.29$  nm (a) and zeta potential was  $23.25 \pm 2.25$  mV. Similarly, The average size of the pVAX-GFP-*omp*(211-382)-NP complex was  $205.25 \pm 33.59$  nm (c) and zeta potential was  $26.35 \pm 2.38$  mV.

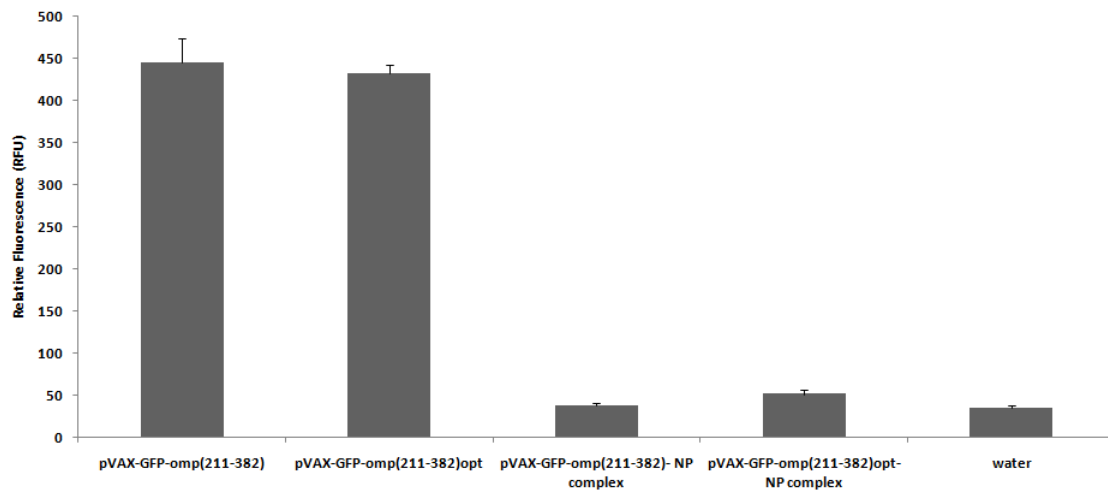


**Figure 6.6:** DNA entrapment assay: The relative fluorescence of pDNA and pDNA-NP complex ( $n = 5$ ; mean  $\pm$  standard error). Maximum fluorescence is exhibited by free pDNA [pVAX-GFP-*omp*(211-382) and pVAX-GFP-*omp*(211-382)opt]. Decreasing pDNA/NP ratios yield decreasing fluorescence intensities. The value corresponding to fluorescence of water (negative control) indicates complete complexation of all free pDNA with NPs.

### 6.3.7. DNA entrapment assay

The complex formation of pDNA and NPs was confirmed by fluorescence and gel electrophoresis. The relative fluorescence from the OliGreen nucleic acid stain is an indication of free, or incompletely complexed, DNA within the sample. Maximum fluorescence is exhibited by the sample that contained only free plasmid in water. As seen in Figure 6, a decrease in the fluorescence intensity was observed in pDNA-NP complex in comparison to the only pDNA. Such a decrease in fluorescence indicates that the pDNA is complexed to the point that DNA dye association and fluorescence are prevented. In the case of pVAX-GFP-omp(211-382)-NP complex (pDNA/NP:0.02), a 91% decrease in fluorescence intensity is observed compared to that of the free pDNA. Similarly, in the case of pVAX-GFP-omp(211-382)opt-NP complex, a 88% decrease in fluorescence intensity is observed compared to that of the free pDNA. The value corresponding to fluorescence of water (negative control) was same as complete complexation of all free pDNA with NPs. The complete uptake of all of the pDNA in pDNA-NP complex indicates the ideal ratio (1:50) for protection and delivery of the entire DNA load. Similar results regarding successful complexation of pDNA with Chi/PLGA NPs was confirmed by comparison of the relative fluorescence of samples containing pDNA-NP complexes (0.02 ratio) to a pure water sample that indicates the absence of free pDNA [363].

### 6.3.8. Enzymatic Degradation of pDNA and Complexes

The protection from enzymatic digestion that NP complexes afford to pDNA was confirmed by gel electrophoresis after treatment with DNase [363]. In the case of free pDNA, no bands were observed after incubation with DNase I except a faint band of high mobility at the bottom of the gel (Figure 6.7). The smeared pattern in lane 5 is an indication that some of the pDNA in the complex was available for digestion, as fragments of various sizes with higher mobility than those of undigested plasmid are visible. A lesser degree of digestion occurs for complexes, as the smeared band does not contain fragments as small as those in lane 4. In the pDNA-NP sample exposed to DNase, there is still a large amount of remaining complexes that exhibit no electrophoretic mobility and are thus seen as bands in the gel well, suggesting protection from endonuclease digestion. The complete protection of pDNA in pDNA-NP complex was also observed through enzymatic degradation study (DNase I) [363]. Complexes treated with the nuclease exhibit limited electrophoretic mobility, indicating that within the complex, some of the pDNA must be exposed to the introduced enzyme and the degraded DNA is located on the outside of the complex.



Such approaches could also prove useful in studying the delivery of the biological agents into cells via nanoparticle platforms and the release of the active therapeutics from polymeric nanosurfaces.

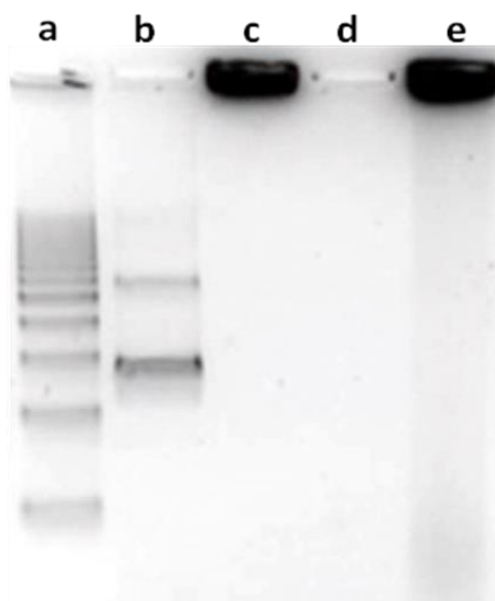


**Figure 6.7.** Plasmid and pDNA/NP complexes after nuclease digestion using DNase I: lane A: 1 kb Molecular weight marker; lane B: 100 ng plasmid [pVAX-GFP-*omp*(211-382)]; lane C: pVAX-GFP-*omp*(211-382)-NP complex; lane D: 100 ng pVAX-GFP-*omp*(211-382) with DNase I; lane E: pVAX-GFP-*omp*(211-382)-NP complex with DNase I.

### 6.3.9. SEM study

The morphology of pVAX-GFP-*omp*(211-382)-NP complex and pVAX-GFP-*omp*(211-382)opt-NP complex were analyzed by SEM analysis (Figure 6.8). The NPs were spherical in structures as confirmed by scanning electron microscope (SEM). The particles were found to be round, uniform and isolated in nature.

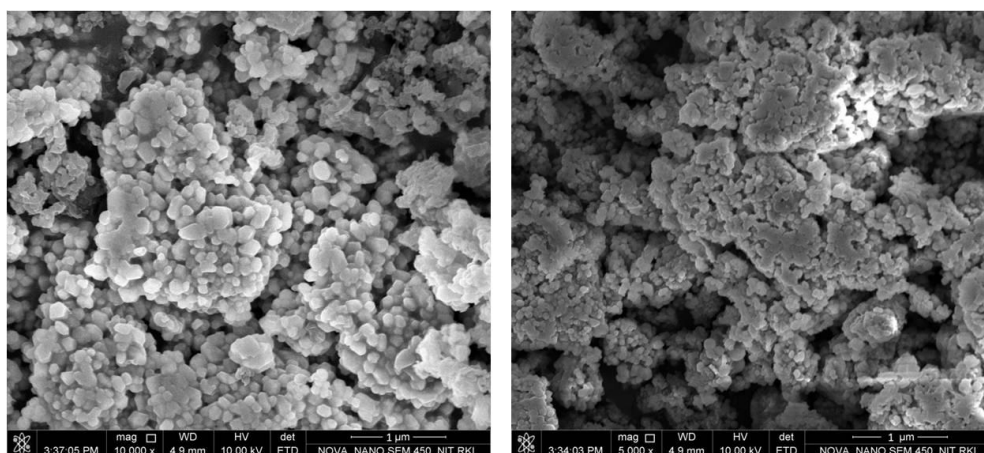


**Figure 6.8.** SEM photograph of (a) pVAX-GFP-*omp*(211-382)-NP complex (b) pVAX-GFP-*omp*(211-382)opt-NP complex

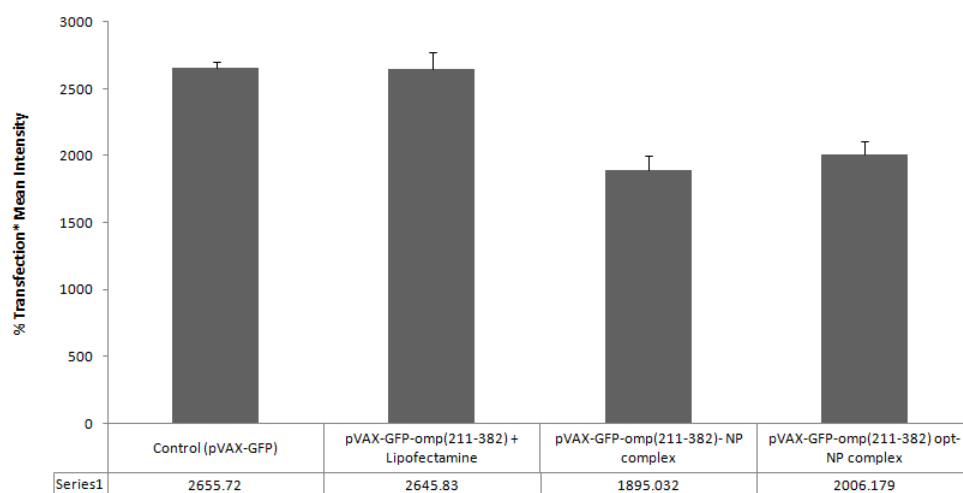


**Figure 6.9.** Transfection efficiency (%T×MI) patterns of control (pVAX-GFP), pVAX-GFP-omp(211-382)+ Lipofectamine 2000, pVAX-GFP-omp(211-382)-NP complex and pVAX-GFP-omp(211-382)opt-NP complex after 24 hr incubation.

### 6.3.10. In vitro transfection study with pDNA-NPs complex

The selection of those nanoparticles (Chi/PLGA), to be used in transfection assays, was made in order to obtain the maximum efficiency of this delivery process, i.e. high percentages of transfected CHO cells, resulting from the expression of GFP in the cell nucleus. The formulated nanocomplex pVAX-GFP-omp(211-382)-NP complex and pVAX-GFP-omp(211-382)opt-NP complex were transfected in the similar fashion in to CHO cells and transfection efficiency was evaluated and compared with transfection efficiency of Omp-pVAX-GFP plus transfection agent Lipofectamine 2000. The comparable transfection efficiency was observed in case of pVAX-GFP-omp(211-382)-NP complex and pVAX-GFP-omp(211-382)opt-NP complex with pVAX-GFP-omp(211-382)- Lipofectamine complex.

## 6.4. Discussion

The main goal of this study is to develop a DNA vaccine candidate, based on the outer membrane protein of *A. hydrophila*, for immunization along with characterization of self-assembled polymeric-pDNA nanoparticles for improved vaccine delivery. The two antigenic coding sequences (**KF938895**<sub>211-381</sub> and **KF938895**<sub>703-999</sub>) were successfully inserted in pVAX-GFP expression vector. Codon optimization was performed for fish (*D. rerio*) to generate two other optimized sequences. Thus, the four conserved protein sequences [*ahal*(211-381), *ahal*(211-381)opt, *ahal*(703-999) and *ahal*(703-999)opt] of antigenic outer membrane protein were cloned into pVAX-GFP expression vector and successfully transformed into *E. coli* DH5α. Then, larger productions of plasmids were performed (250 mL culture volumes) and pDNAs were purified by HIC membrane chromatography with high

purity and high concentration. The purified plasmids [pVAX-GFP-*ahal*(211-381), pVAX-GFP-*ahal*(211-381)opt, pVAX-GFP-*ahal*(703-999), pVAX-GFP-*ahal*(211-381)opt] were transfected with Lipofectamine into CHO (Chinese hamster ovary) cells.

Positively charged liposome/DNA complexes (lipoplexes) were obtained by complexation of purified pVAX-GFP (control) and of pVAX-GFP-*ahal* derivative plasmids with the cationic liposome-based reagent Lipofectamine 2000™. Lipofectamine cationic lipoplexes have been widely used as a safe transfection methodology with the in vitro transfection assays demonstrating improved efficiencies due to its ability to protect pDNA against nuclease attack [357], [358] and to enhance cellular uptake via endocytosis [355].

Transient transfection efficiency was evaluated by fluorescence intensity measurement corresponding to GFP reporter expression level at different time intervals. The transfection with designed *ahal*-pVAX-GFP showed transfection efficiencies higher than the obtained for the positive control (pVAX-GFP), but in the same order of magnitude. Values of  $850 \pm 392$  to  $3,259 \pm 816$  (Table 6.1) obtained with all of the four constructs points that these putative antigenic proteins can be easily expressed in eukaryotic cells.

An independent experiment of transfection of CHO cells with *ahal*(211-381)-pVAX-GFP (Table 2) confirmed the highest transfection efficiency after 24 h incubation with a regular decrease of expressed *Ahal*-GFP from the 1st to the 8th day post-transfection (to 1.3% of the 24 h expression level). However, the pVAX-GFP-*ahal*(211-381)opt clearly gives less fusion antigenic protein than the pVAX-GFP-*ahal*(211-381). There is a confirmed impact of the nucleotide composition on the transfection efficiency of the pVAX-GFP-*ahal*(703-999) and pVAX-GFP-*ahal*(703-999)opt. In this case, however, the plasmid containing the optimized sequence was the more expressed. As pVAX-GFP-*ahal*(211-381) and pVAX-GFP-*ahal*(211-381)opt have the same size, the lower expression of Aha1(211-381)-GFP protein is probably due to the different nucleotide composition that may increase the susceptibility of the plasmid to nucleases or decrease the levels of the transcripts due to a lower transcription and/or a higher degradation. Although significant smaller plasmid sizes are correlated with higher transfection efficiencies [357], [360] the size differences between pVAX-GFP-*ahal*(211-381) (3,850 bp) and pVAX-GFP-*ahal*(703-999) (3,976 bp) are not relevant in this system.

Based on the transfection efficiency, *ahal*(211-381) and *ahal*(211-381)opt were selected for nanoparticle-based pDNA vaccine delivery studies. PLGA-chitosan nanoparticle/plasmid DNA complexes were formulated and characterized in terms of size, size distribution and zeta potential by dynamic light scattering. The formulated nanocomplexes (pVAX-GFP-

*ahal*(211-381)-NP complex,  $d=171\pm73$  nm and pVAX-GFP-*ahal*(211-381)opt-NP complex,  $d=153\pm54$  nm) had overall positive charges, as confirmed from zeta potential measurements, which anticipates very stable nature. SEM analysis (Figure 6.8) revealed a spherical shape of the formulated nanocomplexes and sizes that correlate with DLS measurements (Figure 6.5). The ability of PLGA-chitosan nanoparticles to form complexes with pDNA was evaluated by using the fluorescent intercalating dye Oil Green to label free plasmid DNA. Fluorescence from the Oil Green nucleic acid staining is an indication of free, or incompletely complexed, DNA within a sample. Maximum fluorescence is exhibited by the sample that contained only free plasmid in water. As seen in Figure 6.6, a decrease in the fluorescence intensity was observed in pDNA-NP complexes in comparison to naked pDNA. Such decrease in fluorescence indicates that the pDNA is complexed to the point that DNA dye association and fluorescence are prevented. In case of pVAX-GFP-*ahal*(211-381)-NP complexes (pDNA/NP mass ratio of 1:50), a 91% decrease in fluorescence intensity is observed compared to that of the free pDNA. Similarly, pVAX-GFP-*ahal*(211-381)opt-NP complexes showed a 88% decrease in fluorescence intensity when compared to that of the free pDNA. The value corresponding to fluorescence of water (negative control) mimics the complete complexation of all pDNA within NPs. The complete uptake of all of the pDNA in pDNA-NP complexes is ideal for protection and delivery of the entire DNA load. Bordelon and coworkers (2011) also verified a 94% decrease in fluorescence intensity upon Chi/PLGA NP complexation of plasmid for the same pDNA/NP ratio of 1:50, by comparison of the fluorescence of samples towards that of pure water, proving that such successful complexation of plasmids is achievable [363].

The protection from enzymatic digestion that NP complexes confer to pDNA was confirmed by gel electrophoresis after treatment with DNase (Figure 6.7) [363]. In case of free pDNA, typical bands of open circular and supercoiled pDNA isoforms (lane B) were no longer observed after incubation with DNase I (lane D). Regarding the protection of plasmid pVAX-GFP-*ahal*(211-381) within NPs (lane C), the smeared pattern that could be seen when DNase digestion was implemented (lane E) is an indication that some of the pDNA in the complexes was still freely available, as fragments of various sizes with higher mobility than those of undigested plasmid are visible. A lesser degree of digestion occurs for complexes. In the pDNA-NP sample exposed to DNase (lane E), there is still a large amount of remaining complexes that exhibit no electrophoretic mobility and are thus seen as bands in the gel well, suggesting protection from endonuclease digestion. The density of the stained pDNA in the well is very strong and comparable to that of lane C. A higher level of protection of pDNA in

pDNA-NP complex was observed through the same enzymatic degradation study by [363] who suggested that within a NP complex, some of the pDNA must be exposed to the introduced enzyme and the consequent degraded DNA is located on the outside of the complex.

## 6.5. Conclusion

The selection of those nanoparticles (Chi/PLGA), to be used in transfection assays, was made in order to obtain the maximum efficiency of this delivery process, *i.e.* high percentages of transfected CHO cells, resulting from the expression of GFP in cell nucleus. In CHO cells, the formulated nanocomplexes (pVAX-GFP-*aha1*(211-381)-NP complex and pVAX-GFP-*aha1*(211-381)opt-NP complex) showed transfection efficiencies comparable with those found when using same plasmid with lipofection. This study will aid in designing and optimizing formulations of DNA therapeutics with major transfection efficiency and minimal degradation.

# Chapter 7

## **In silico identification of outer membrane protein (Omp) and subunit vaccine design against pathogenic *Vibrio cholerae***

### **7.1. Introduction**

Vaccines have been demonstrated to be successful and effective medical strategies for preventing infectious diseases, reducing the incidence of diseases and mortality significantly. In recent years vaccine development exploration accelerates the new strategies based on genomics, proteomics, functional genomics and synthetic chemistry. With the advancement of vaccine technology, Reverse Vaccinology (RV) has provided a change in the perspective of vaccine design by targeting proteins either exposed on the surface of the pathogen or secreted into the extracellular milieu [364]. This approach has been termed as “reverse vaccinology”, since the process of vaccine discovery starts *in silico* using genetic information rather than the pathogen itself to visualize all possible molecular interactions based on the pathogen genome, and any promising molecules/processes then selected for *in vitro/in vivo* studies. It reduces the time and cost required for the identification of vaccine candidates and provides new solutions for those diseases for which vaccines are not available. The demand and role of proteins and peptide specially designed for pharmacotherapeutics purpose are increasing in clinical practice to solve many of the currently untreatable diseases. Proteins are large molecular weight polypeptides which are susceptible to proteolysis, chemical modification, and denaturation during storage and administration. Nowadays, peptide-based vaccine are getting more importance due their many desirable properties. Peptide-mediated molecular therapeutic delivery systems have recently emerged as an alternative means to address effectively to current vaccine forms. Owing to their excellent specificity, low toxicity, rich chemical diversity and availability from natural sources, FDA has successfully approved a number of peptide-based drugs and several are in various stages of drug development [365]. The relative ease of construction and production, chemical stability, and lack of oncogenic or infectious potential has made the peptides attractive vaccine candidates [366]. Subunit peptide vaccines can be designed to contain the minimal microbial

component necessary to stimulate an appropriate immune response. This has the advantage of removing unnecessary components, thus decreasing the risk of stimulating an autoimmune response or other adverse effects. Synthetic vaccines can also be tailored to stimulate a targeted immune response. Likewise, peptide-based vaccines can also be used as safer ways of inducing allergen-specific tolerance [367].

Vaccines work by inducing profound changes in the cellular components of adaptive immunity, comprising T- and B-cells. The concept of peptide vaccines is based on identification and chemical synthesis of B-cell and T-cell epitopes which are immunodominant and can induce specific immune responses [368]. Our increased understanding of antigen recognition at the molecular level has resulted in the development of rationally designed peptide vaccines.

Consequently, focuses on vaccine design shifted to explore surface-exposed antigens susceptible to antibody recognition and T-cell induction through comparative pan-genome reverse vaccinology [369]. Peptides complexed with major histocompatibility complex class I molecules in the endoplasmic reticulum are then transported to the cell surface for recognition by cytotoxic T lymphocytes (CTLs) [370]. Since activation of CD4<sup>+</sup> helper T-cells is essential for the development of adaptive immunity against pathogens [371], T-cell promiscuous peptides became a prime target for vaccine and immunotherapy [372].

*Vibrio cholerae* is a "comma" shaped Gram-negative pathogenic bacteria mostly associated with humans that infect the intestine and increases mucous production causing diarrhea and vomiting which result in extreme dehydration and if not treated may lead to death. Cholera affects an estimated 3-5 million people worldwide and causes 100,000-130,000 deaths a year as of 2010 [33]. Cholera remains both epidemic and endemic in many areas of the world. High levels of transcripts for OmpU and multiple OM structures (OmpV, OmpS, OmpC, OmpA, OmpK and OmpW) were present in *V. cholerae*. ToxR activates the transcription of OmpU and represses the transcription of OmpT, outer membrane porins important for *V. cholerae* virulence [272].

Thus, identification of T-cell epitopes would significantly add to the development of novel subunit vaccines for *V. cholerae*. In the present study, computational analysis was performed to predict novel vaccine candidates of HLADRB, most prevalent HLA, among all pathogenic strains of *V. cholerae* to avoid barriers of cross-protection against different serovars.

## **7.2. Materials and Methods**

### **7.2.1. In silico epitope vaccine design**

To identify epitopes, a classical strategy was taken where the identified epitopes should be antigenic and have the ability to induce both the T-cell and B-cell mediated immunity.

### **7.2.2. Sequence retrieval and B–cell antigenic site prediction**

Briefly, amino acid sequence of Outer Membrane Protein (*Vibrio cholerae*) was retrieved from Swiss-Prot protein database (<http://us.expasy.org/sprot>) and subsequently was analyzed for antigenicity using B-cell antigenic site prediction server “Antigenic” (<http://bio.dfci.harvard.edu/Tools/antigenic.pl>).

### **7.2.3. B-cell epitope prediction**

Using the default parameters of both the BCPred and AAP prediction modules of BCPreds [373], B-cell non-overlapping epitopes were identified from protein sequences. Primary selections of the predicted B-cell epitopes were done based on the scores. In the next step, overlapping epitope sequences from “Antigenic” and BCPreds were selected and sequences were aligned to get a continuous stretch of amino acid sequence that possess both antigenic sequences as-well-as the B-cell binding sites.

### **7.2.4. T-cell epitope prediction**

This continuous stretch of the antigenic B-cell epitope was then analyzed using ProPred-1 [374] and ProPred [375] with default parameters to identify MHC class I and MHC class II binding epitopes respectively. Selected numbers of MHC binding alleles were 47 and 51 respectively for MHC class I and II. Proteasomal cleavage sites of identified epitopes were analyzed. Epitopes that can bind both the MHC classes and maximum MHC alleles were selected.

### **7.2.5. Selection of epitopes**

The final selections of epitope sequences were done based on the criteria that the epitope sequence should have antigenic B-cell epitope binding sequences as-well-as both the MHC classes binding sequences. Therefore, the selected sequences, in this way, have the ability to generate both the B-cell and T-cell mediated immune responses. The strategy of the epitope prediction is represented in Figure 1.

To confirm the parameters of epitopes, each epitope was further analyzed with VaxiJen v2.0 antigen prediction server [376] for antigenicity. To verify MHC binding properties, less than



1000 nM IC50 scores for DRB1\*0101 based on MHCpred v.2 (<http://193.133.255.13/mhcpred/>) [377] was used. Exomembrane localization and fold level topology of epitopes were confirmed using TMHMM 2.0 (<http://www.cbs.dtu.dk/services/TMHMM-2.0/>) [378]. The finally selected epitopes were used for structural characterization.

### **7.2.6. Homology modeling and model validation**

To carry out homology modeling, automated Alignment, and Project modes of Swiss model server [379] was used. The resultant models were optimized using Swiss-PdbViewer [380] and Accelrys Discovery Studio (<http://accelrys.com/>). Best model were selected based on reliability assessment that was carried out using Procheck [381] tools at SAVS server (<http://nihserver.mbi.ucla.edu/SAVS/>). ProFunc [382] was used to predict domains, motifs, ligand binding clefts, and various other functional parameters of 3D structures.

### **7.2.7. Characterization of epitopes**

Due to the short sequence (9-20 mers) of epitopes, it was difficult to find the template from PDB database and to make a homology model using Swiss-model server. Therefore, initially drug discovery studio was used to identify and determine the native site and the structure of epitopes within the protein. In another effort, the DISTILL server [383] that can predict the 3-D structure of small fragments of proteins based on the similarity with PDB template was also be used for epitope modeling. Resultant epitopes were then validated with ProSA-web and PROCHECK. ProFunc, Motif Scan ([http://myhits.isb-sib.ch/cgi-bin/motif\\_scan](http://myhits.isb-sib.ch/cgi-bin/motif_scan)), and Inter ProScan [384] was used for domain, motif, and functionality assignment of epitopes. Protein Digest ([http://db.systemsbio.org.net:8080/proteomics Toolkit/proteinDigest.html](http://db.systemsbio.org.net:8080/proteomicsToolkit/proteinDigest.html)) will be used to determine molecular weight, pI, and enzymatic degradation site (s) of epitopes.

## **7.3. Results**

### **7.3.1. Antigen Selection**

One outer membrane protein (Genebank ID: H8JSM7) was retrieved from Genebank database and confirmed as antigenic (VaxiJen score = 0.528).TMHMM 2.0 based exo-membrane

localization and topology of OMP shows that it is fully exposed to outside the cell

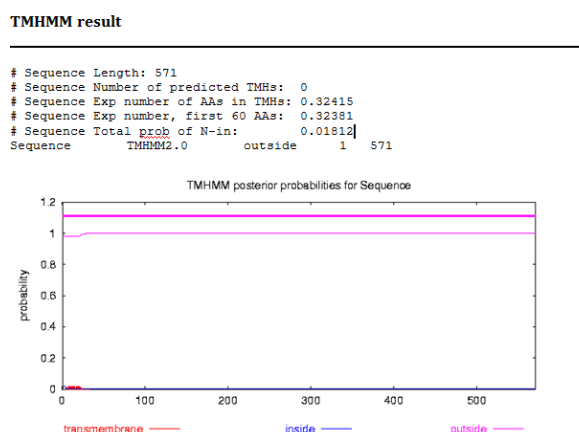


(Figure7.1).

Figure 7.1. TMHMM 2.0 based exo-membrane localization and topology of OMP

### 7.3.2. Identified antigenic B-cell epitopes

The common antigenic B-cell epitopes for each transporter were identified using “Antigenic” and BCPreds. It was found that the predicted B-cell epitope sequences by BCPred and AAP prediction modules of BCPreds highly varied. Therefore, the common sequences predicted by these two algorithms of BCPreds were considered to select B-cell epitopes. The variable lengths of antigenic sequences generated by “Antigenic” and the 20 mers length B-cell epitope sequences predicted by BCPreds were then analyzed to find common B-cell antigenic epitope sequences those are listed in Table 1. The common B-cell epitopes were identified using AAP and BCPreds method of BCPREDS Server 1.0. This method generates a stretch of 26 mers sequence (RTRSNSGLLTWGDQKQTITLEYGDPAL) (amino acid position 391-416) and 31 mer sequence (FFAGGDNNLRGYGYKSISPQDASGALTGAKY) (amino acid position 464-494) that meets all selection criteria for the antigenic B-cell epitope.

Table 7.1: Antigenic B-cell epitopes of *V. cholerae* OMP Epitopes are identified by B-cell epitope prediction with BCPreds (BCPred algorithm and AAP Prediction algorithm)

Sequence	Amino acid position	Length (mers)
<b>B-cell epitope prediction with BCPreds</b>		
<b>BCPred algorithm</b>		
DVGDAFNDNPEWKKGVGTGI	517	20
LKWKKPWVNSQGHFSFSSFS	280	20
IRGEAEGDRDFQRLIRRSGL	108	20
<b>GLLTWGDQKQTITLEYGDPAL</b>	<b>397</b>	<b>20</b>
<b>FFAGGDNNLRGYGYKSISPQ</b>	<b>464</b>	<b>20</b>
ISPVGPIRLDFAWGLDAAPG	539	20
QTITAGYKIPLDALNEYR	305	20
RPFKQGEPLYLSQVGEFNQN	206	20
DNSQFLLPGMTYTRTRRSN	376	20

ATSSIEYQYRLTGNWWAAMF	496	20
<b>AAP Prediction algorithm</b>		
SPVGPIRLDFAWGLDAAPGD	540	20
<b>RTRSNSGLLTWGDQKQTITLE</b>	<b>391</b>	<b>20</b>
VTRLSEVDIVIRGEAEGDRD	98	20
GSLKWKKPWVNSQGHSDSS	278	20
ATSSIEYQYRLTGNWWAAMF	496	20
GDPALLSETRVRLQTGSSW	412	20
EQTITAGYKIPLEDALNEYY	304	20
RQGLQDDNSQFLPGMTYTR	370	20
VGDAFNDNPEWKKGVGTGIR	518	20
<b>YGYKSISPQDASGALTGAKY</b>	<b>475</b>	<b>20</b>
QRLIRRSGLRVDAPLNHSLY	119	20
<b>Common antigenic B-cell epitope (s)</b>		
<b>RTRSNSGLLTWGDQKQTITLEYGDPA</b>	<b>391-416</b>	<b>26</b>
<b>FFAGGDNNLRGYGYKSISPQDASGALTGAKY</b>	<b>464-494</b>	<b>31</b>

### 7.3.3. Identified candidate peptide vaccines

Selected antigenic B-cell epitope sequences were analyzed with ProPred 1 and ProPred to identify respectively MHC I and MHC II binding T-cell epitopes. The common T-cell epitope sequences those bind to both the MHC molecules were selected. Predicted peptides that would be considered for vaccine development based on MHC allele binding ability are listed in Table 2. MHC binding T-cell epitopes were identified using ProPred 1 (for MHC I) and ProPred (for MHC II) with default parameters. The two B-cell epitope sequences (26 mer and 31-mer) were analyzed and the common epitope (s) that can bind both the MHC classes and covers maximum MHC alleles were selected. In this way only one 9-mer sequence (YKSISPQDA) spanning at amino acid position 477 to 485 of the OMP protein was selected. YKSISPQDA was found to bind 5 MHC I and 41 MHCII alleles. VaxiJen and MHCPre v.2 analysis of the epitope (YKSISPQDA) further confirm that the epitope is antigenic (VaxiJen score = 0.528) and can bind to DRB1\*0101 allele (MHCPre nM IC50 score = 104.23) (Table 3). Another peptide LRGYGYKSI was able to bind 9 MHC I and 28 MHCII alleles. But it was not antigenic as predicted by VaxiJen v2.0 antigen prediction server (VaxiJen score = 0.232).

**Table 7.2.** T-cell epitopes of OMP (*V. cholerae*). The common antigenic B-cell epitope “FFAGDNNLRGYGYKSISPQDASGALTGAKY” was analyzed for its ability to bind MHC I and MHC II molecules using Propred I and Propred. A common epitope “YKSISPQDA” (9 mers) that generates both TCL and HCL mediated immune response was selected.

<b>ProPred 1 (MHC I)</b>		
<b>TCL epitope sequences</b>	<b>Amino acid position</b>	<b>No of MHC-I binding alleles</b>
GGDNNLRGY	467	5
ASGALTGAK	485	6
<b>YKSISPQDA</b>	<b>477</b>	<b>5</b>
FFAGDNNL	464	10
ISPQDASGA	480	6
SPQDASGAL	481	23
NNLRGYGYK	470	4
FAGGDNNLR	465	6
NLRGYGYKS	471	4
<b>LRGYGYKSI</b>	<b>472</b>	<b>9</b>
SGALTGAKY	486	5
KSISPQDAS	478	3
DASGALTGA	484	4
RGYGYKSYS	473	3
<b>ProPred (MHC II)</b>		
<b>HCL epitope sequences</b>	<b>Amino acid position</b>	<b>No of MHC II binding alleles</b>
<b>YKSISPQDA</b>		<b>41</b>
ISPQDASGA	480	7
YGYKSISPQ	475	33
FAGGDNNLR	465	4
FFAGDNNL	464	5
<b>LRGYGYKSI</b>	<b>472</b>	<b>28</b>

**Table 7.3.** MHC Pred Result of sequence YKSISPQDA

<b>The HLA allele used in the test is: DRB0101</b>			
<b>The query sequence</b>			
<b>YKSISPQDA</b>			
<b>Amino acid groups</b>	<b>Predicted - logIC<sub>50</sub> (M)</b>	<b>Predicted IC<sub>50</sub> Value (nM)</b>	<b>Confidence of prediction (Max = 1)</b>
YKSISPQDA	6.982	104.23	0.89

### 7.3.4. 3-D modeling of *V. cholerae* OMP

The 3D structure of *V. cholerae* OMP is not available and in this study, we have focused 3D modeling of OMP using homology modeling. Based on blast parameters, with highest similarity (PDB id: 2HUE) having 35% sequence identity with an E- value of 2e-69 was selected as the template. The X-Ray diffraction structure has 1.70 Å resolutions. The optimized 3D model of *V. cholerae* OMP consists of 9 helices, 15 strands and 23 turns (Figure 7.2). The molecular weight and PI of the model were estimated to be 26.74kDa and 4.95 respectively.

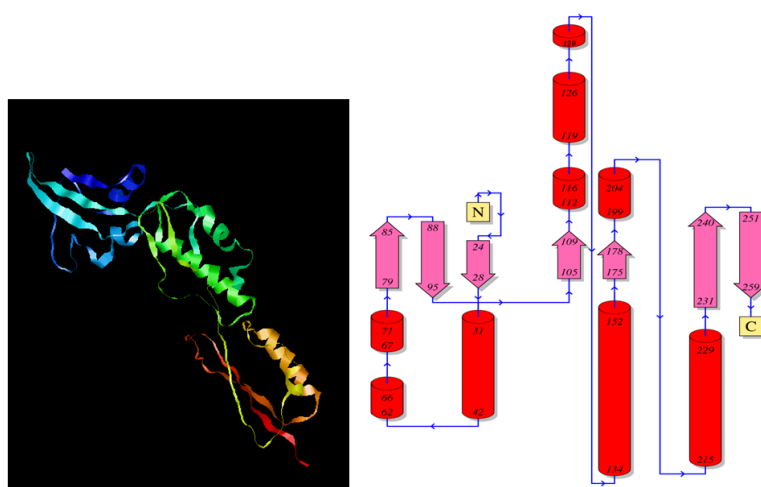
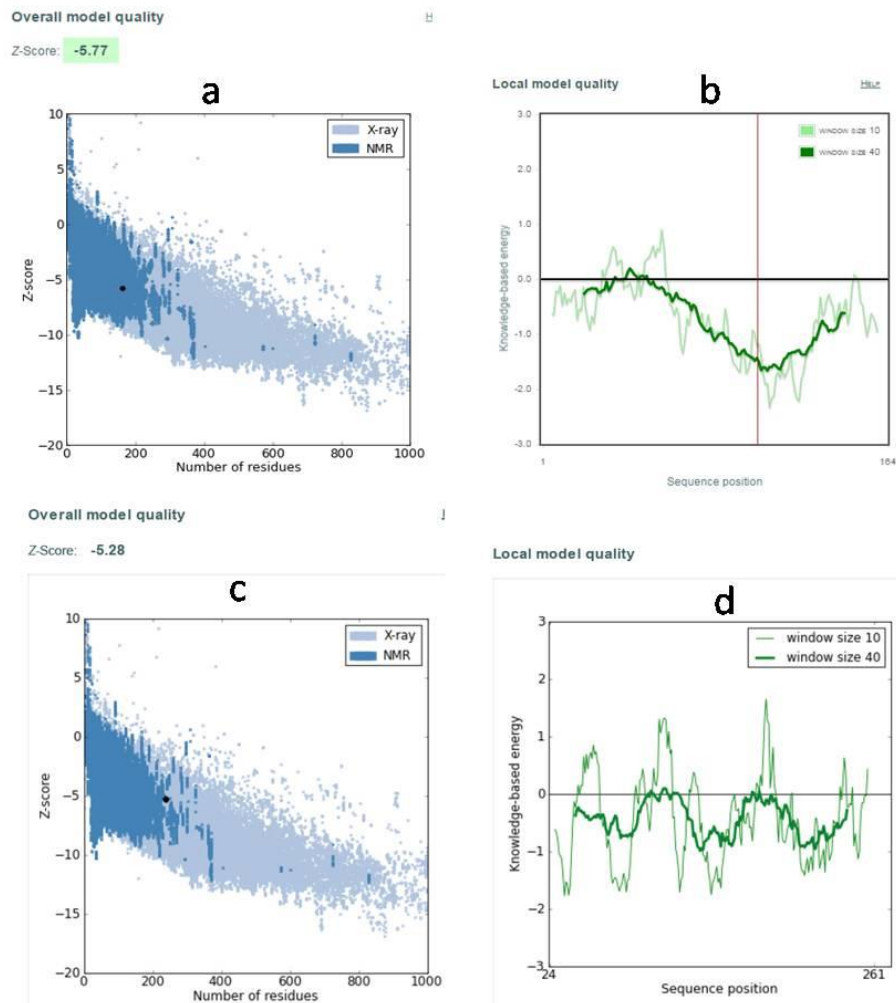


Figure 7.2. The 3D model *V. Cholerae* OMP from various angles.

### 7.3.5. Validation of the model

To validate the model, initially ProSA-web was used that compares and analyzes the energy distribution in protein structure as a function of sequence position to determine a structure as native-like or fault. As shown in Figure 3 and the Z-scores, the model is of good quality of structure (Figure 7.3). The Procheck of SAVAs master server was used for assessment of the stereochemical quality of the model. According to the Ramachandran plot, residues in most favored regions, residues in additional allowed regions residues in generously allowed regions, and residues in disallowed regions were respectively, 79.2%, 14.6%, 4.2%, and 1.9% that ensures the geometrically acceptable quality of the model (Figure 7.4).



**Figure 7.3. Validation of the 3-D model of *V. cholerae* OMP with ProSa-web. The upper panel is template (PDB id: 2HUE) and lower is OMP. (a) Overall model quality of 2HUE (Z=-5.77). (b) Local model quality of 2HUE. (c) Overall model quality of OMP (Z=-5.28). (d) Local model quality of OMP.**

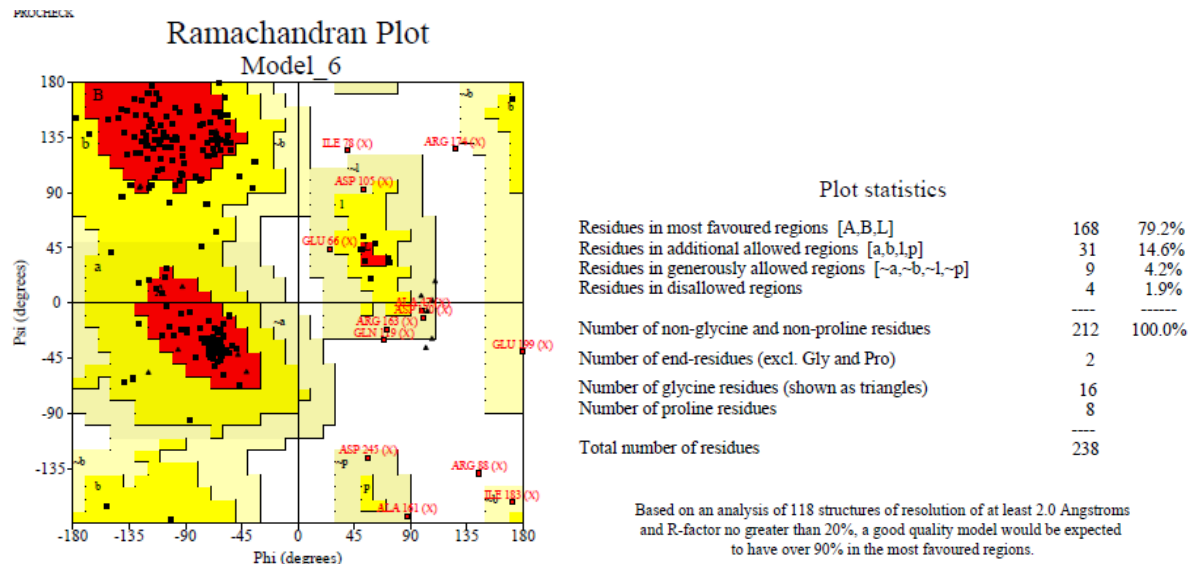


**Figure 7.4.** The Ramachandran plot for *V. cholerae* OMP. The plot shows the acceptability of the model

### 7.3.6. Characterization of the epitope

The epitope position within the *V. cholerae* OMP protein was determined using Accelrys Discovery Studio Visualizer (v1.7). Combining the results of the 3D model and TMHMM 2.0 based topology analysis, it is evident that the epitope is exposed to the surface of the protein and therefore it also supports that the predicted sequence is a potential candidate peptide vaccine. Due to the very short length (9 mers) of the epitope, instead of Swiss model server, the DISTILL server was used to generate 3-D structure (Figure 7.5). Calculated molecular weight and pI of the 9 mers epitope are respectively, 1008.10 and 5.83. As the focus of this study is on *V.cholerae* OMP, we have excluded 3D characterization of epitopes from other pathogens. But based on sequence homology and topology analysis, it is found that, epitopes identified from other pathogens are also antigenic, MHC II (DRB1\*0101) binding, located at nearly same accessible region, and exposed to cell surface similar to the *V. cholerae* OMP. Therefore, they are also potential vaccine candidates.

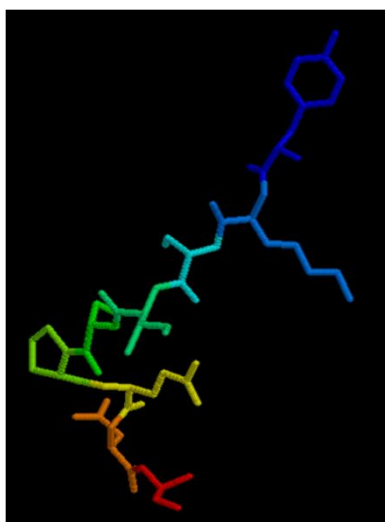


Figure 7.5. 3-D structures of 9 mers (YKSISPQDA) epitopes created by DISTILL.

## 7.4. Discussion

Virulence-related outer membrane proteins (Omps) are expressed in Gram-negative bacteria such as *V. cholerae* and are essential to bacterial survival within macrophages and for eukaryotic cell invasion. The kW-C cholera vaccine stimulates good immunity in people living in endemic cholera areas, proving protective Vc OM immunogens exist [37]. OmpU is more protective (compared to OmpT) against the bactericidal effects of bile salts and other anionic detergents [273]. An OmpU (a general porin) prologue, vca1008, identified by IVET is required for mouse colonization [274]. Omps are also conserved in nature so that Omp based vaccine therapeutics would be beneficial for different serovars of *V. cholerae*. In this study, we developed and characterized 3D model of *V. cholerae* Omp for in order to understand structural identity which can be employed for the design of therapeutic molecules [385].

In general, earlier studies have reported either T-cell or B-cell based epitope designing for a pathogen [386]–[388]. Similarly, some vaccines can only activate helper T lymphocytes (HTL)/CD4+ / MHC II. But activation of CD8+ cytotoxic T- lymphocytes (CTLs)/ MHC I is also required in many cases [389]. Therefore, an epitope that can produce both the B-cell and T-cell (MHC I and MHC II) mediated immunity is highly useful in developing peptide-based vaccines.

In the current experiment, VaxiJen and MHCPred were used to support the efficacy of epitopes. Similarly, using subtractive genomics and homology analysis, a single epitope was designed within a nearly same accessible region of corresponding Omp proteins in various *V. cholerae* serovars. So, the identified epitope may be useful against a wide range *V. cholerae* strains. The identified peptide (YKSISPQDA) from *V. cholerae* Omp may induce B-cell and both CD4+ and CD8+ T-cell mediated immunity. The sequence homology analysis



demonstrates that this epitope sequence is conserved in Omcs of *V. cholerae* at the nearly same accessible region. Therefore, this peptide might be useful in designing a vaccine against all cholera pathogens by developing broad-spectrum peptide vaccine.

## 7.5. Conclusion

Immunoinformatics study of Omp from *V. cholerae* confirmed its antigenicity, hence plays a measure role in virulence. So it could be targeted as a vaccine. The successful design of 3D model of Omp leads to give more information about the structural interaction that can be employed for drug design. Similarly, the identified epitope (YKSISPQDA) require proper design and subsequent validation for their uses as broad-spectrum peptide vaccine against *V. cholerae*.

# Chapter 8

## Summary & Conclusion

### 8.1. Summary

In the present study, various NPs formulations of PLA and PLGA loaded with model protein (BSA) or drug (clindamycin hydrochloride) were prepared by solvent evaporation method varying drug/protein: polymer concentration and optimized for size, encapsulation efficiency, drug loading, morphology, etc. Then, PLA/PLGA NPs encapsulating Omp antigen from *A. hydrophila* were formulated and their efficacy were compared with adjuvant formulations to develop a better antigenic carrier model in fish. Similarly, the efficacy is also compared between PLA encapsulated and PLGA encapsulated OmpNP-immunized groups and a correlation is established evaluating the results of innate and adaptive immune response studies in *L. rohita*. In another attempt, PLA/PLGA-Omp (Omp from *V. cholerae*) nanoparticles were formulated with desired physicochemical properties and evaluation of type and strength of immune responses (Humoral and cellular) elicited by formulated NPs was elucidated by comparing all possible combinations in mice.

Thus, the specific objectives of the current study are

1. Preparation and characterization of PLA and PLGA loaded with model protein (BSA) or drug (Clindamycin hydrochloride) NPs varying drug/protein:polymer concentration
2. Preparation, Characterization and *In vitro* study of biodegradable and biocompatible based PLA and PLGA nanoparticles with encapsulation of OMP antigens.
3. Parenteral immunization of PLA/PLGA nanoparticle encapsulating outer membrane protein (Omp) from *A. hydrophila*; Evaluation of immunostimulatory action in lower vertebrate (fish).
4. Evaluation of the immune responses (specific) in mice model after intraperitoneal immunization of Omp antigen (*V. cholerae*) encapsulated PLA/PLGA nanoparticles
5. Development of DNA vaccines to boost antigenic OMP (outer membrane protein) antigenicity
6. In silico identification of outer membrane protein (Omp) and subunit vaccine design against pathogenic *V. cholerae*

The salient results have been presented below:

### **Formulation and characterization of PLA and PLGA loaded with model protein (BSA) or drug (Clindamycin hydrochloride) nanoparticles**

CLH-PLA and CLH-PLGANPs of various sized particles were formulated by varying the drug to polymer ratio from 1:5 to 1:20. The size, zeta potential and polydispersity index values of CLH-PLA NPs and CLH-PLGA NPs confirmed that the drug: polymer concentration is important for the stability of drug loaded NPs. The drug to polymer ratio 1:10 were found to be optimal ratio for the formulation to be stable and monodispersed CLH loaded PLA and PLGA NPs. NPs formulation (both CLH-PLA 2 and CLH-PLGA 2) showed a significantly higher drug loading efficiency and a controlled release profile extended up to 144 h. Higher drug loading and an extended CLH release profile were observed in the case of CLH-PLGA NPs which might be due to higher hydrophilic nature of PLGA that causes enhanced molecular interaction. The spherical and isolated structures of both CLH-PLA2 and CLH-PLGA2 NPs were confirmed by scanning electron microscope (SEM) study. The smooth surface and isolated nature of NPs can also be correlated to the presence of lactide that adds hydrophobicity to the polymer ultimately prevents agglomeration. The thermal behavior (DSC) studies of CLH-PLGANPs confirmed the disappearance of CLH endothermic peak (150<sup>0</sup>C) that indicated the uniform dispersion of drug at a molecular level within the system. From FTIR studies, it was found that there was not much alteration in the general structure of CLH drug (due to conserved OH, CH and C-O group etc.) after loading in PLA and PLGA NPs. The antimicrobial activities were enhanced in CLH-PLA NPs and CLH-PLGA NPs than the standard free drug evidenced from a decrease in MIC values tested against *Streptococcus faecalis* and *Bacillus cereus*.

### **Evaluation of immunostimulatory action in *L. rohita* (rohu) upon parenteral immunization of PLA/PLGA nanoparticle encapsulating outer membrane protein (Omp) from *A. hydrophila***

PLA/PLGA NPs were evaluated for their ability to serve as an excellent carrier for site specific delivery of macromolecules such as Omp through parenteral immunization in *L. rohita*. PLA-Omp NPs (size: 223.5± 13.19 nm) and PLGA-Omp NPs (size:166.4± 21.23 nm) were prepared using double emulsion method in which antigen was efficiently encapsulated reaching encapsulation efficiency 44 ± 4.58 % and 59.33± 5.13 % respectively. The physical properties like zeta potential values and polydispersity index (PDI) values confirmed the stability as well as monodisperse nature of the formulated NPs. The spherical and isolated

nature of Omp loaded PLA and PLGA NPs were revealed by SEM analysis. Upon immunization in *L. rohita*, PLA/PLGA-Omp NPs showed encouraging results by activating both innate and specific immune response against *A. hydrophila* in fish without any side effects. Significant higher bacterial agglutination titre, haemolytic activity and specific antibody titre confirmed the combined immune activation. Considering the adverse side effects of oil adjuvant (FIA), the current study also proved the comparable antibody response of PLA-Omp NPs and PLGA-Omp NPs with that of FIA-Omp treated groups. Again, the better efficacy of PLA/PLGA-Omp NPs system was confirmed by increased protection against *A. hydrophila* by activating immune responses by challenge study. In comparison to PLGA-Omp NPs, PLA-Omp NPs offered a better immune response in terms of higher bacterial agglutination titre, haemolytic activity, specific antibody titre, higher percent survival upon *A. hydrophila* challenge in *L. rohita*. It can be concluded that PLA/PLGA NPs based delivery system would be a novel antigen carrier for parenteral immunization in fish. This is probably the first report on the delivery of PLA-Omp and PLGA-Omp NPs against *A. hydrophila* in *L. rohita*. Hence, more focused research on designing and formulation would be attributed to PLA/PLGA NPs based on vaccine delivery system in fish model.

### **Evaluation of the immune responses (specific) in mice after intraperitoneal immunization of Omp antigen (*V. cholerae*) encapsulated PLA/PLGA nano-particles**

This study was focused with an aim to elucidate the formulation of polymeric (PLA/PLGA)-Omp NPs and to evaluate the immune response (humoral and cellular) in terms of antigen processing and generation of a response. The formulated PLA-Omp NPs and PLGA-Omp NPs were < 500 nm size range; these particles could be successfully endocytosed in the body. The lower size was observed in the case of fabricated PLGA-Omp NPs than PLA-Omp nanoparticles. PLA and PLGA being negatively charged polymers impacts anionic nature to formulated NPs (PLA, PLA-Omp, PLGA, and PLGA-Omp). Also, zeta potential values were more negative after successful encapsulation of Omp in both PLA and PLGA (PLA-Omp NPs:  $-25.2 \pm 5.45$  mV; PLGA-Omp NPs:  $-32.5 \pm 6.15$  mV), that proves more stability. Significantly higher encapsulation of Omp protein ( $p < 0.05$ ) was achieved in the case of PLGA-Omp NPs ( $69.18 \pm 1.68$  %) than PLA-Omp NPs ( $57.85 \pm 4.15$  %). However, the Omp protein release profile in PLA-Omp NPs is comparatively slower than PLGA-Omp that could also be attributed to hydrophilic nature of PLGA and higher antigen loading. Higher lactide content in PLA might be an another cause in delaying the rapid burst effect as we observed in

the case of PLA-Omp NPs (50% antigen release  $\approx$  24 hr). Surface morphology of the PLA and PLGA nanoparticles loaded with Omp were studied using a scanning electron microscope (SEM). From the FTIR spectrum, it was also observed that upon encapsulation of Omp to PLA and PLGA the characteristic peaks associated with Omp, PLA and PLGA remained intact, so there was no loss of any functional peaks between the absorbance spectra of Omp and Omp encapsulated nanoparticles.

The serum antibody level (IgG1, IgG2a) in different antigen-NP treated sera was measured by ELISA. Antigen-specific IgG1, IgG2a titers were above control levels for intraperitoneally immunized mice for all groups (7-56 days). Both IgG1 and IgG2 titers in vaccinated mice followed the similar pattern, but the IgG1 response is higher than IgG2 response. Both PLA-Omp and PLGA-Omp NPs causes more efficient splenocyte proliferation in comparison to Omp antigen alone ( $p < 0.05$ ), which confirmed more potent induction of antigen-specific immune responses. Again, a significant higher cellular activation was observed in the case of PLA-Omp and PLGA-Omp NPs in comparison to Omp antigen alone. PLA-Omp NPs and PLGA-Omp NPs induced significantly higher ( $p < 0.05$ ) CD4<sup>+</sup>CXCR5<sup>hi</sup>PD-1<sup>hi</sup> cells than respective PLA and PLGA NPs. Also, the percentage of follicular CD4<sup>+</sup> T helper cells was significantly higher in the case of PLA-Omp and PLGA-Omp NPs in comparison to Omp.

### **Development of DNA vaccines to boost antigenic outer membrane protein antigenicity**

The current investigation aimed at developing a DNA vaccine as well as a delivery system to boost antigenic outer membrane protein (Omp) that would act as a potential vaccine candidate. The conserved protein sequences [*omp*(211-382), *omp*(211-382)opt, *omp*(703-999) and *omp*(703-999)opt] of antigenic outer membrane protein was cloned into pVAX-GFP expression vector and successfully transformed into *E. coli* (DH5 $\alpha$ ). The large scale pDNA production was achieved with shake flask cultures and the pDNA was purified by hydrophobic interaction chromatography (HIC). The purified pDNA was transfected (with or without Lipofectamine 2000<sup>TM</sup>) into CHO (Chinese hamster ovary) cells and transient transfection efficiency was evaluated by fluorescence intensity measurement corresponding to GFP expression level at different time interval. The transfection of CHO cells with Omp-pVAX-GFP confirmed the highest transfection efficiency after 24 h incubation. PLGA-chitosan nanoparticle/plasmid DNA complex were formulated and characterized in terms of size, size distribution and zeta potential by dynamic light scattering (DLS) method. The formulated nano complex of  $\sim$ 200 nm ( $199.25 \pm 22.29$  nm and  $205.25 \pm 33.59$ ) was transfected in the similar fashion into CHO cells that confirmed improved transfection

efficiency at a lower dose. The DNA entrapment assay demonstrated the possible protection of pDNA inside the pDNA-nanoparticle complex. The protection from enzymatic digestion that NP complexes afford to pDNA was evaluated by gel electrophoresis after treatment with DNase. However, more physicochemical characterization of formulated nano complex and extensive transfection studies are to be focused on observing the expression pattern of antigen that will facilitate future investigations into the functionality of the system *in vitro* and *in vivo*.

### **In Silico identification of outer membrane protein (Omp) and subunit vaccine design**

Using *in silico* approaches, the 3-D model of the Omp was developed using Swiss model server and validated by ProSA and Procheck web server. B cell epitopes were identified by BCPred and AAP prediction modules of BCPreds and sequences were aligned to get a continuous stretch of amino acid sequence (26 mer: RTRSNSGLLTWGDQKQTITLEYGDPAL and 31 mer: FFAGGDNNLRGYGYKSISPQDASGALTGAKY) that are B-cell binding sites. Further, Selected antigenic B-cell epitope sequences were analyzed with ProPred 1 and ProPred to identify MHC I and MHC II binding T-cell epitopes respectively and the common epitope (9 mer: YKSISPQDA) that can bind both the MHC classes (MHC I and MHC II) and covers maximum MHC alleles were identified. The identified epitopes can be useful in designing broad-spectrum peptide vaccine development against *V. cholerae* by inducing an optimal immune response (both B cell and T cell-mediated immune response).

## **8.2. Future investigation**

The successful formulations of NP-based antigen delivery system with all suitable physicochemical characteristics were achieved with highly controlled conditions and reproducibility. The immunological evaluation studies suggest that PLA/PLGA NPs based delivery system could be a novel antigen carrier for fish and mice ensuring its application for commercial value and vaccine development. Further work based on present optimized results can be taken forward for next level vaccine design and approval. However, more physicochemical characterization of formulated nano-DNA complex and extensive transfection studies are to be focused on observing the expression pattern of antigen that will facilitate future investigations into the functionality of the system *in vitro* and *in vivo*. In Silico identification of outer membrane protein (Omp) and subunit vaccine design against

pathogenic *Vibrio cholerae* require proper design and subsequent validation for their uses as broad-spectrum peptide vaccine against *V. cholerae*.

# References

- [1] Z. Zhao and K. W. Leong, “Controlled delivery of antigens and adjuvants in vaccine development,” *J. Pharm. Sci.*, vol. 85, no. 12, pp. 1261–1270, 1996.
- [2] M. Singh and D. T. O’Hagan, “Recent advances in vaccine adjuvants,” *Pharm. Res.*, vol. 19, no. 6, pp. 715–28, 2002.
- [3] T. Mohan, P. Verma, and D. N. Rao, “Novel adjuvants & delivery vehicles for vaccines development: A road ahead,” *Indian J. Med. Res.*, vol. 138, no. 5, pp. 779–795, 2013.
- [4] I. Delany, R. Rappuoli, and E. De Gregorio, “Vaccines for the 21st century,” *EMBO Mol. Med.*, vol. 6, no. 6, pp. 708–720, 2014.
- [5] T. Akagi, M. Baba, and M. Akashi, “Biodegradable nanoparticles as vaccine adjuvants and delivery systems: Regulation of immune responses by nanoparticle-based vaccine,” *Advances in Polymer Science*, vol. 247, no. 1, pp. 31–64, 2012.
- [6] L. Li, F. Saade, and N. Petrovsky, “The future of human DNA vaccines,” *J. Biotechnol.*, vol. 162, no. 2–3, pp. 171–182, 2012.
- [7] E. Lawrence, *Henderson’s Dictionary of Biological Terms*, 12th ed. Prentice Hall, 1999.
- [8] C. Janeway, P. Travers, M. Walport, and M. Shlomchik, *Immunobiology: The Immune system in health and disease*, 6th ed. Taylor & Francis Group, 2005.
- [9] N. Petrovsky and J. C. Aguilar, “Vaccine adjuvants: Current state and future trends,” *Immunol. Cell Biol.*, vol. 82, no. 5, pp. 488–496, 2004.
- [10] J. Freund and E. L. Opie, “Sensitization and antibody formation with increased resistance to tuberculous infection induced by heat killed tubercle bacilli,” *J. Exp. Med.*, vol. 68, no. 2, pp. 273–298, Jul. 1938.
- [11] J. Aucouturier, L. Dupuis, S. Deville, S. Ascarateil, and V. Ganne, “Montanide ISA 720 and 51: a new generation of water in oil emulsions as adjuvants for human vaccines,” *Expert Rev. Vaccines*, vol. 1, no. 1, pp. 111–118, 2002.
- [12] H. HogenEsch, “Mechanisms of stimulation of the immune response by aluminum adjuvants,” *Vaccine*, vol. 20, no. SUPPL. 3, pp. 34–39, 2002.
- [13] G. Ciofani, V. Raffa, A. Menciacsi, and P. Dario, “Alginate and chitosan particles as drug delivery system for cell therapy,” *Biomed. Microdevices*, vol. 10, no. 2, pp. 131–



- 140, 2008.
- [14] J. P. Y. Scheerlinck and D. L. V Greenwood, "Virus-sized vaccine delivery systems," *Drug Discov. Today*, vol. 13, no. 19–20, pp. 882–887, 2008.
  - [15] Y. Shi and G. Huang, "Recent developments of biodegradable and biocompatible materials based micro/nanoparticles for delivering macromolecular therapeutics.," *Crit. Rev. Ther. Drug Carrier Syst.*, vol. 26, no. 1, pp. 29–84, 2009.
  - [16] J. C. Cox and A. R. Coulter, "Adjuvants - A classification and review of their modes of action," *Vaccine*, vol. 15, no. 3, pp. 248–256, 1997.
  - [17] J. C. Aguilar and E. G. Rodríguez, "Vaccine adjuvants revisited.," *Vaccine*, vol. 25, no. 19, pp. 3752–3762, 2007.
  - [18] A. Salvador, M. Igartua, R. M. Hernández, and J. L. Pedraz, "An overview on the field of micro- and nanotechnologies for synthetic Peptide-based vaccines.," *J. Drug Deliv.*, p. ID 181646, 2011.
  - [19] O. Harush-Frenkel, N. Debotton, S. Benita, and Y. Altschuler, "Targeting of nanoparticles to the clathrin-mediated endocytic pathway.," *Biochem. Biophys. Res. Commun.*, vol. 353, no. 1, pp. 26–32, 2007.
  - [20] B. Semete, L. Booyesen, Y. Lemmer, L. Kalombo, L. Katata, J. Verschoor, and H. S. Swai, "In vivo evaluation of the biodistribution and safety of PLGA nanoparticles as drug delivery systems.," *Nanomedicine*, vol. 6, no. 5, pp. 662–671, 2010.
  - [21] S. Salmaso, S. Bersani, A. Semenzato, and P. Caliceti, "Nanotechnologies in protein delivery," *J. Nanosci. Nanotechnol.*, vol. 6, no. 9–10, pp. 2736–2753, 2006.
  - [22] B. N. Violand and N. . Siegel, "Peptide and protein drug analysis. In protein and peptide chemical and physical stability," in *Peptide and Protein Drug Analysis*, R. E. Reid, Ed. Marcel Dekker: New York, NY, USA, 2000, pp. 257–284.
  - [23] Y. Lu, J. Yang, and E. Sega, "Issues related to targeted delivery of proteins and peptides," *AAPS J.*, vol. 8, no. 3, pp. E466–E478, 2006.
  - [24] M. a Liu, "DNA vaccines: an historical perspective and view to the future.," *Immunol. Rev.*, vol. 239, no. 1, pp. 62–84, 2011.
  - [25] M. A. Kutzler and D. B. Weiner, "DNA vaccines: ready for prime time?," *Nat. Rev. Genet.*, vol. 9, no. 10, pp. 776–788, 2008.
  - [26] S. Manoj, L. a Babiuk, and S. van Drunen Littel-van den Hurk, "Approaches to enhance the efficacy of DNA vaccines.," *Crit. Rev. Clin. Lab. Sci.*, vol. 41, no. 1, pp. 1–39, 2004.
  - [27] D. N. Nguyen, J. J. Green, J. M. Chan, R. Langer, and D. G. Anderson, "Polymeric

- materials for gene delivery and DNA vaccination,” *Adv. Mater.*, vol. 21, no. 8, pp. 847–867, 2009.
- [28] B. Austin, D. A. Austin, I. Dalsgaard, B. K. Gudmundsdottir, S. Høie, J. M. Thornton, J. L. Larsen, B. O’Hici, R. Powell, and S. Hoie, “Characterization of atypical *Aeromonas salmonicida* by different methods,” *Syst. Appl. Microbiol.*, vol. 21, no. 1, pp. 50–64, 1998.
- [29] R. Harikrishnan and C. Balasundaram, “Modern trends in *Aeromonas hydrophila* disease management with fish,” *Rev. Fish. Sci.*, vol. 13, no. 4, pp. 281–320, 2005.
- [30] H. Chen and C. Lu, “Study on pathogen of bacterial hemorrhagic septicemia of rice eel (*Monopterus albus*),” *Chinese J. Zoonoses*, vol. 7, pp. 21–23, 1991.
- [31] J. F. Heidelberg, J. A. Eisen, W. C. Nelson, R. A. Clayton, M. L. Gwinn, R. J. Dodson, D. H. Haft, E. K. Hickey, J. D. Peterson, L. Umayam, S. R. Gill, K. E. Nelson, T. D. Read, H. Tettelin, D. Richardson, M. D. Ermolaeva, J. Vamathevan, S. Bass, H. Qin, I. Dragoi, P. Sellers, L. McDonald, T. Utterback, R. D. Fleishmann, W. C. Nierman, O. White, S. L. Salzberg, H. O. Smith, R. R. Colwell, J. J. Mekalanos, J. C. Venter, and C. M. Fraser, “DNA sequence of both chromosomes of the cholera pathogen *Vibrio cholerae*,” *Nature*, vol. 406, no. 6795, pp. 477–483, 2000.
- [32] N. Howard-Jones, “Robert Koch and the cholera vibrio: a centenary,” *Br. Med. J.*, vol. 288, no. 6414, pp. 379–381, Feb. 1984.
- [33] World Health Organization, “Cholera vaccines: WHO position paper,” *Wkly. Epidemiol. Rec.*, no. 13, pp. 117–128, 2010.
- [34] D. A. Sack, R. B. Sack, G. B. Nair, and A. K. Siddique, “Cholera,” *Lancet (London, England)*, vol. 363, no. 9404, pp. 223–233, Jan. 2004.
- [35] G. Seltman and O. Holst, *The Bacterial Cell Wall*. Springer-Verlag Berlin Heidelberg, 2002.
- [36] R. Khushiramani, S. K. Girisha, P. P. Bhowmick, I. Karunasagar, and I. Karunasagar, “Prevalence of different outer membrane proteins in isolates of *Aeromonas* species,” *World J. Microbiol. Biotechnol.*, vol. 24, no. 10, pp. 2263–2268, 2008.
- [37] W. F. Wade, “Is A Universal, One Dose Cholera Vaccine Possible?,” *Open Vaccine J.*, vol. 4, pp. 18–30, 2011.
- [38] S. Morales, Carolina, “Recent developments in multifunctional hybrid nanoparticles: Opportunities and challenges in cancer therapy,” *Front. Biosci.*, vol. E4, no. 1, p. 529, 2012.
- [39] A. del Pozo-Rodríguez, D. Delgado, A. R. Gascón, and M. Á. Solinís, “Lipid

- nanoparticles as drug/gene delivery systems to the retina.,” *J. Ocul. Pharmacol. Ther.*, vol. 29, no. 2, pp. 173–188, 2013.
- [40] T. Mamo and G. A. Poland, “Nanovaccinology: the next generation of vaccines meets 21st century materials science and engineering.,” *Vaccine*, vol. 30, no. 47. Netherlands, pp. 6609–6611, Oct-2012.
- [41] P. Couvreur and C. Vauthier, *Nanotechnology: Intelligent design to treat complex disease*, vol. 23, no. 7. 2006.
- [42] P. Maurer, G. T. Jennings, J. Willers, F. Rohner, Y. Lindman, K. Roubicek, W. A. Renner, P. Müller, and M. F. Bachmann, “A therapeutic vaccine for nicotine dependence: Preclinical efficacy, and phase I safety and immunogenicity,” *Eur. J. Immunol.*, vol. 35, no. 7, pp. 2031–2040, 2005.
- [43] M. A. Dobrovolskaia and S. E. McNeil, “Immunological properties of engineered nanomaterials.,” *Nat. Nanotechnol.*, vol. 2, no. 8, pp. 469–478, 2007.
- [44] A. Roldão, M. C. M. Mellado, L. R. Castilho, M. J. T. Carrondo, and P. M. Alves, “Virus-like particles in vaccine development.,” *Expert Rev. Vaccines*, vol. 9, no. 10, pp. 1149–1176, 2010.
- [45] S. M. Douglas, I. Bachelet, and G. M. Church, “A Logic-gated nanorobot for targeted transport of molecular payloads,” *Science (80-. )*, vol. 335, no. 6070, pp. 831–834, 2012.
- [46] C. He, L. Yin, C. Tang, and C. Yin, “Multifunctional polymeric nanoparticles for oral delivery of TNF- $\alpha$  siRNA to macrophages,” *Biomaterials*, vol. 34, no. 11, pp. 2843–2854, 2013.
- [47] D. Pissuwan, T. Niidome, and M. B. Cortie, “The forthcoming applications of gold nanoparticles in drug and gene delivery systems,” *J. Control. Release*, vol. 149, no. 1, pp. 65–71, 2011.
- [48] A. Bolhassani, S. Safaiyan, and S. Rafati, “Improvement of different vaccine delivery systems for cancer therapy.,” *Mol. Cancer*, vol. 10, no. 1, p. 3, 2011.
- [49] Y. Krishnamachari, S. M. Geary, C. D. Lemke, and A. K. Salem, “Nanoparticle delivery systems in cancer vaccines,” *Pharm. Res.*, vol. 28, pp. 215–236, 2011.
- [50] S. Hamdy, A. Haddadi, R. W. Hung, and A. Lavasanifar, “Targeting dendritic cells with nano-particulate PLGA cancer vaccine formulations,” *Adv. Drug Deliv. Rev.*, vol. 63, no. 10–11, pp. 943–955, 2011.
- [51] B. Chackerian, “Virus-like particle based vaccines for Alzheimer disease.,” *Hum. Vaccine*, vol. 6, no. 11, pp. 926–930, 2010.

- [52] A. C. Tissot, P. Maurer, J. Nussberger, R. Sabat, T. Pfister, S. Ignatenko, H. D. Volk, H. Stocker, P. Müller, G. T. Jennings, F. Wagner, and M. F. Bachmann, "Effect of immunisation against angiotensin II with CYT006-AngQb on ambulatory blood pressure: a double-blind, randomised, placebo-controlled phase IIa study," *Lancet*, vol. 371, no. 9615, pp. 821–827, 2008.
- [53] J. F. Correia-Pinto, N. Csaba, and M. J. Alonso, "Vaccine delivery carriers: Insights and future perspectives," *Int. J. Pharm.*, vol. 440, no. 1, pp. 27–38, 2013.
- [54] E. M. Plummer and M. Manchester, "Viral nanoparticles and virus-like particles: Platforms for contemporary vaccine design," *Wiley Interdiscip. Rev. Nanomedicine Nanobiotechnology*, vol. 3, no. 2, pp. 174–196, 2011.
- [55] S. D. Caruthers, S. a. Wickline, and G. M. Lanza, "Nanotechnological applications in medicine," *Curr. Opin. Biotechnol.*, vol. 18, no. 1, pp. 26–30, 2007.
- [56] J. M. Knipe, J. T. Peters, and N. A. Peppas, "Theranostic agents for intracellular gene delivery with spatiotemporal imaging," *Nano Today*, vol. 8, no. 1, pp. 21–38, 2013.
- [57] W. H. De Jong and P. J. a Borm, "Drug delivery and nanoparticles: applications and hazards," *Int. J. Nanomedicine*, vol. 3, no. 2, pp. 133–149, 2008.
- [58] K. Sowjanya, "A review on current advancements in Nanotechnology," *Res. Rev. J. Med. Heal. Sci.*, vol. 4, no. 3, pp. 1–11, 2015.
- [59] S. M. Moghimi, A. C. Hunter, and J. C. Murray, "Nanomedicine: Current status and future prospects," *FASEB J.*, vol. 19, no. 3, pp. 311–330, 2005.
- [60] L. Treuel, X. Jiang, and G. U. Nienhaus, "New views on cellular uptake and trafficking of manufactured nanoparticles," *J. R. Soc.*, vol. 10, no. 82, p. 20120939, 2013.
- [61] A. E. Gregory, R. Titball, and D. Williamson, "Vaccine delivery using nanoparticles," *Front. Cell. Infect. Microbiol.*, vol. 3, p. 13, 2013.
- [62] S. Y. Kim, H. J. Doh, M. H. Jang, Y. J. Ha, S. I. Chung, and H. J. Park, "Oral immunization with *Helicobacter pylori*-loaded poly(D,L-lactide-co-glycolide) nanoparticles," *Helicobacter*, vol. 4, pp. 33–39, 1999.
- [63] A. Vila, A. Sanchez, C. Evora, I. Soriano, J. L. Vila Jato, and M. J. Alonso, "PEG-PLA nanoparticles as carriers for nasal vaccine delivery," *J. aerosol Med.*, vol. 17, no. 2, pp. 174–185, 2004.
- [64] C. Thomas, A. Rawat, L. Hope-Weeks, and F. Ahsan, "Aerosolized PLA and PLGA nanoparticles enhance humoral, mucosal and cytokine responses to hepatitis B vaccine," *Mol. Pharm.*, vol. 8, pp. 405–415, 2011.

- [65] B. D. Ulery, L. S. Nair, and C. T. Laurencin, "Biomedical applications of biodegradable polymers," *J. Polym. Sci. Part B Polym. Phys.*, vol. 49, no. 12, pp. 832–864, 2011.
- [66] T. Akagi, T. Kaneko, T. Kida, and M. Akashi, *Preparation and characterization of biodegradable nanoparticles based on poly(gamma-glutamic acid) with l-phenylalanine as a protein carrier.*, vol. 108, no. 2–3. 2005.
- [67] S. L. Demento, W. Cui, J. M. Criscione, E. Stern, J. Tulipan, S. M. Kaech, and T. M. Fahmy, "Role of sustained antigen release from nanoparticle vaccines in shaping the T cell memory phenotype," *Biomaterials*, vol. 33, no. 19, pp. 4957–4964, 2012.
- [68] M. Manish, A. Rahi, M. Kaur, R. Bhatnagar, and S. Singh, "A single-dose PLGA encapsulated protective antigen domain 4 nanoformulation protects mice against *Bacillus anthracis* spore challenge.," *PLoS One*, vol. 8, no. 4, p. e61885, 2013.
- [69] A. L. Silva, R. A. Rosalia, A. Sazak, M. G. Carstens, F. Ossendorp, J. Oostendorp, and W. Jiskoot, "Optimization of encapsulation of a synthetic long peptide in PLGA nanoparticles: Low-burst release is crucial for efficient CD8<sup>+</sup> T cell activation," *Eur. J. Pharm. Biopharm.*, vol. 83, pp. 338–345, 2013.
- [70] M. Kalkanidis, G. A. Pietersz, S. D. Xiang, P. L. Mottram, B. Crimeen-Irwin, K. Ardipradja, and M. Plebanski, "Methods for nano-particle based vaccine formulation and evaluation of their immunogenicity," *Methods*, vol. 40, no. 1, pp. 20–29, 2006.
- [71] G. Minigo, A. Scholzen, C. K. Tang, J. C. Hanley, M. Kalkanidis, G. A. Pietersz, V. Apostolopoulos, and M. Plebanski, "Poly-l-lysine-coated nanoparticles: A potent delivery system to enhance DNA vaccine efficacy," *Vaccine*, vol. 25, no. 7, pp. 1316–1327, 2007.
- [72] F. Danhier, E. Ansorena, J. M. Silva, R. Coco, A. Le Breton, and V. Préat, "PLGA-based nanoparticles: An overview of biomedical applications," *J. Control. Release*, vol. 161, no. 2, pp. 505–522, 2012.
- [73] H. Pinto-Alphandary, A. Andremont, and P. Couvreur, "Targeted delivery of antibiotics using liposomes and nanoparticles: Research and applications," *Int. J. Antimicrob. Agents*, vol. 13, no. 3, pp. 155–168, 2000.
- [74] S. M. Abdelghany, D. J. Quinn, R. J. Ingram, B. F. Gilmore, R. F. Donnelly, C. C. Taggart, and C. J. Scott, "Gentamicin-loaded nanoparticles show improved antimicrobial effects towards *Pseudomonas aeruginosa* infection," *Int. J. Nanomedicine*, vol. 7, pp. 4053–4063, 2012.
- [75] M. N. Seleem, P. Munusamy, A. Ranjan, H. Alqublan, G. Pickrell, and N.

- Sriranganathan, “Silica-antibiotic hybrid nanoparticles for targeting intracellular pathogens,” *Antimicrob. Agents Chemother.*, vol. 53, no. 10, pp. 4270–4274, 2009.
- [76] P. Gao, X. Nie, M. Zou, Y. Shi, and G. Cheng, “Recent advances in materials for extended-release antibiotic delivery system,” *J. Antibiot. (Tokyo)*, vol. 64, no. 9, pp. 625–634, 2011.
- [77] O. Borges, A. Cordeiro-da-Silva, J. Tavares, N. Santarem, A. de Sousa, G. Borchard, and H. E. Junginger, “Immune response by nasal delivery of hepatitis B surface antigen and codelivery of a CpG ODN in alginate coated chitosan nanoparticles,” *Eur. J. Pharm. Biopharm.*, vol. 69, no. 2, pp. 405–416, Jun. 2008.
- [78] G. Feng, Q. Jiang, M. Xia, Y. Lu, W. Qiu, D. Zhao, L. Lu, G. Peng, and Y. Wang, “Enhanced immune response and protective effects of Nano-chitosan-based DNA vaccine encoding T cell epitopes of Esat-6 and FL against *Mycobacterium Tuberculosis* infection,” *PLoS One*, vol. 8, no. 4, p. e61135, Apr. 2013.
- [79] F. Zhao, X. Zhang, S. Liu, T. Zeng, J. Yu, W. Gu, Y. Zhang, X. Chen, and Y. Wu, “Assessment of the immune responses to *Treponema pallidum* Gpd DNA vaccine adjuvanted with IL-2 and chitosan nanoparticles before and after *Treponema pallidum* challenge in rabbits,” *Sci. China. Life Sci.*, vol. 56, no. 2, pp. 174–180, 2013.
- [80] P. Li, Z. Luo, P. Liu, N. Gao, Y. Zhang, H. Pan, L. Liu, C. Wang, L. Cai, and Y. Ma, “Bio-reducible alginate-poly(ethylenimine) nanogels as an antigen-delivery system robustly enhance vaccine-elicited humoral and cellular immune responses,” *J. Control. Release*, vol. 168, no. 3, pp. 271–279, 2013.
- [81] K. Hasegawa, Y. Noguchi, F. Koizumi, A. Uenaka, M. Tanaka, M. Shimono, H. Nakamura, H. Shiku, S. Gnjjatic, R. Murphy, Y. Hiramatsu, L. J. Old, and E. Nakayama, “In vitro Stimulation of CD8 and CD4 T Cells by Dendritic Cells Loaded with a Complex of Cholesterol-Bearing Hydrophobized Pullulan and NY-ESO-1 Protein: Identification of a New HLA-DR15–Binding CD4 T-Cell Epitope,” *Clin. Cancer Res.*, vol. 12, no. 6, pp. 1921–1927, Mar. 2006.
- [82] A. Uenaka, H. Wada, M. Isobe, T. Saika, K. Tsuji, E. Sato, S. Sato, Y. Noguchi, R. Kawabata, T. Yasuda, Y. Doki, H. Kumon, K. Iwatsuki, H. Shiku, M. Monden, A. A. Jungbluth, G. Ritter, R. Murphy, E. Hoffman, L. J. Old, and E. Nakayama, “T cell immunomonitoring and tumor responses in patients immunized with a complex of cholesterol-bearing hydrophobized pullulan (CHP) and NY-ESO-1 protein,” *Cancer Immun.*, vol. 7, no. 9, pp. 1–11, 2007.
- [83] Y. Honda-Okubo, F. Saade, and N. Petrovsky, “Advax, a polysaccharide adjuvant

- derived from delta inulin, provides improved influenza vaccine protection through broad-based enhancement of adaptive immune responses,” *Vaccine*, vol. 30, no. 36, pp. 5373–5381, 2012.
- [84] F. Saade, Y. Honda-Okubo, S. Trec, and N. Petrovsky, “A novel hepatitis B vaccine containing Advax™, a polysaccharide adjuvant derived from delta inulin, induces robust humoral and cellular immunity with minimal reactogenicity in preclinical testing,” *Vaccine*, vol. 31, no. 15, pp. 1999–2007, 2013.
- [85] H. C. Arca, M. Gunbeyaz, and S. Senel, “Chitosan-based systems for the delivery of vaccine antigens,” *Expert Rev. Vaccines*, vol. 8, no. 7, pp. 937–953, Jul. 2009.
- [86] B. Y. Chua, M. Al Kobaisi, W. Zeng, D. Mainwaring, and D. C. Jackson, “Chitosan microparticles and nanoparticles as biocompatible delivery vehicles for peptide and protein-based immunocontraceptive vaccines,” *Mol. Pharm.*, vol. 9, no. 1, pp. 81–90, 2012.
- [87] O. Kayser, a Lemke, and N. Hernández-Trejo, “The impact of nanobiotechnology on the development of new drug delivery systems,” *Curr. Pharm. Biotechnol.*, vol. 6, pp. 3–5, 2005.
- [88] R. Ladj, A. Bitar, M. Eissa, Y. Mugnier, R. Le Dantec, H. Fessi, and A. Elaissari, “Individual inorganic nanoparticles: preparation, functionalization and in vitro biomedical diagnostic applications,” *J. Mater. Chem. B*, vol. 1, no. 10, pp. 1381–1396, 2013.
- [89] K. Kobayashi, J. Wei, R. Iida, K. Ijiro, and K. Niikura, “Surface engineering of nanoparticles for therapeutic applications,” *Polym. J.*, vol. 46, no. 8, pp. 460–468, Aug. 2014.
- [90] J. Zhang, L. Chen, W. H. Tse, R. Bi, and L. Chen, “Inorganic Nanoparticles: Engineering for Biomedical Applications,” *Nanotechnology Magazine, IEEE*, vol. 8, no. 4, pp. 21–28, 2014.
- [91] L. J. Peek, C. R. Middaugh, and C. Berkland, “Nanotechnology in vaccine delivery,” *Adv. Drug Deliv. Rev.*, vol. 60, no. 8, pp. 915–928, 2008.
- [92] K. Niikura, T. Matsunaga, T. Suzuki, S. Kobayashi, H. Yamaguchi, Y. Orba, A. Kawaguchi, H. Hasegawa, K. Kajino, T. Ninomiya, K. Ijiro, and H. Sawa, “Gold nanoparticles as a vaccine platform: influence of size and shape on immunological responses in vitro and in vivo,” *ACS Nano*, vol. 7, no. 5, pp. 3926–3938, May 2013.
- [93] M. Marradi, F. Chiodo, I. García, and S. Penadés, “Glyconanoparticles as multifunctional and multimodal carbohydrate systems,” *Chem. Soc. Rev.*, vol. 42, no.

- 11, pp. 4728–4745, 2013.
- [94] W. Tao, K. S. Ziemer, and H. S. Gill, “Gold nanoparticle-M2e conjugate coformulated with CpG induces protective immunity against influenza A virus,” *Nanomedicine*, vol. 9, no. 2, pp. 237–251, 2014.
- [95] Y.-S. Chen, Y.-C. Hung, W.-H. Lin, and G. S. Huang, “Assessment of gold nanoparticles as a size-dependent vaccine carrier for enhancing the antibody response against synthetic foot-and-mouth disease virus peptide,” *Nanotechnology*, vol. 21, no. 19, p. 195101, May 2010.
- [96] L. Xu, Y. Liu, Z. Chen, W. Li, Y. Liu, L. Wang, Y. Liu, X. Wu, Y. Ji, Y. Zhao, L. Ma, Y. Shao, and C. Chen, “Surface-engineered gold nanorods: promising DNA vaccine adjuvant for HIV-1 treatment,” *Nano Lett.*, vol. 12, no. 4, pp. 2003–2012, Apr. 2012.
- [97] D. Pantarotto, C. D. Partidos, J. Hoebeke, F. Brown, E. Kramer, J. P. Briand, S. Muller, M. Prato, and A. Bianco, “Immunization with Peptide-functionalized Carbon nanotubes enhances virus-specific neutralizing antibody responses,” *Chem. Biol.*, vol. 10, pp. 961–966, 2003.
- [98] T. Wang, M. Zou, H. Jiang, Z. Ji, P. Gao, and G. Cheng, “Synthesis of a novel kind of carbon nanoparticle with large mesopores and macropores and its application as an oral vaccine adjuvant,” *Eur. J. Pharm. Sci.*, vol. 44, no. 5, pp. 653–659, 2011.
- [99] C. H. Villa, T. Dao, I. Ahearn, N. Fehrenbacher, E. Casey, D. A. Rey, T. Korontsvit, V. Zakhaleva, C. A. Batt, M. R. Philips, and D. A. Scheinberg, “Single-walled carbon nanotubes deliver peptide antigen into dendritic cells and enhance IgG responses to tumor-associated antigens,” *ACS Nano*, vol. 5, no. 7, pp. 5300–5311, 2011.
- [100] J. Parra, A. Abad-Somovilla, J. V. Mercader, T. A. Taton, and A. Abad-Fuentes, “Carbon nanotube-protein carriers enhance size-dependent self-adjuvant antibody response to haptens,” *J. Control. Release*, vol. 170, no. 2, pp. 242–251, 2013.
- [101] H. Ow, D. R. Larson, M. Srivastava, B. A. Baird, W. W. Webb, and U. Wiesnert, “Bright and stable core-shell fluorescent silica nanoparticles,” *Nano Lett.*, vol. 5, no. 1, pp. 113–117, 2005.
- [102] M. Benezra, O. Penate-Medina, P. B. Zanzonico, D. Schaer, H. Ow, A. Burns, E. DeStanchina, V. Longo, E. Herz, S. Iyer, J. Wolchok, S. M. Larson, U. Wiesner, and M. S. Bradbury, “Multimodal silica nanoparticles are effective cancer-targeted probes in a model of human melanoma,” *J. Clin. Invest.*, vol. 121, no. 7, pp. 2768–2780, 2011.
- [103] D. H. Joyappa, C. Ashok Kumar, N. Banumathi, G. R. Reddy, and V. V. S.



- Suryanarayana, "Calcium phosphate nanoparticle prepared with foot and mouth disease virus P1-3CD gene construct protects mice and guinea pigs against the challenge virus," *Vet. Microbiol.*, vol. 139, no. 1–2, pp. 58–66, 2009.
- [104] Q. He, A. Mitchell, T. Morcol, and S. J. Bell, "Calcium phosphate nanoparticles induce mucosal immunity and protection against Herpes Simplex virus Type 2," *Clin. Diagn. Lab. Immunol.*, vol. 9, no. 5, pp. 1021–1024, 2002.
- [105] R. J. Lee, "Liposomal delivery as a mechanism to enhance synergism between anticancer drugs.," *Mol. Cancer Ther.*, vol. 5, no. 7, pp. 1639–1640, Jul. 2006.
- [106] L. Zhang, F. Gu, J. Chan, A. Wang, R. Langer, and O. Farokhzad, "Nanoparticles in Medicine: Therapeutic Applications and Developments," *Clin. Pharmacol. Ther.*, vol. 83, no. 5, pp. 761–769, 2007.
- [107] A. Akbarzadeh, R. Rezaei-Sadabady, S. Davaran, S. W. Joo, N. Zarghami, Y. Hanifepour, M. Samiei, M. Kouhi, and K. Nejati-Koshki, "Liposome: classification, preparation, and applications.," *Nanoscale Res. Lett.*, vol. 8, no. 1, p. 102, 2013.
- [108] A. K. Giddam, A. K. Giddam, M. Zaman, M. Skwarczynski, and I. Toth, "Liposome-based delivery system for vaccine candidates: constructing an effective formulation.," *Nanomedicine*, vol. 7, no. 12, pp. 1877–1893, 2012.
- [109] D. S. Watson, A. N. Endsley, and L. Huang, "Design considerations for liposomal vaccines: Influence of formulation parameters on antibody and cell-mediated immune responses to liposome associated antigens," *Vaccine*, vol. 30, no. 13, pp. 2256–2272, 2012.
- [110] B. Morein, B. Sundquist, S. Höglund, K. Dalsgaard, and A. Osterhaus, "Iscom, a novel structure for antigenic presentation of membrane proteins from enveloped viruses," *Nature*, vol. 308, no. 5958, pp. 457–460, 1984.
- [111] A. Homhuan, S. Prakongpan, P. Poomvises, R. A. Maas, D. J. A. Crommelin, G. F. A. Kersten, and W. Jiskoot, "Virosome and ISCOM vaccines against Newcastle disease: preparation, characterization and immunogenicity.," *Eur. J. Pharm. Sci.*, vol. 22, no. 5, pp. 459–468, 2004.
- [112] M. J. Pearse and D. Drane, "ISCOMATRIX adjuvant for antigen delivery.," *Adv. Drug Deliv. Rev.*, vol. 57, no. 3, pp. 465–474, 2005.
- [113] A. Aguila, A. M. Donachie, M. Peyre, C. P. McSharry, D. Sesardic, and A. M. Mowat, "Induction of protective and mucosal immunity against diphtheria by a immune stimulating complex (ISCOMS) based vaccine.," *Vaccine*, vol. 24, no. 24, pp. 5201–5210, 2006.

- [114] H. X. Sun, Y. Xie, and Y. P. Ye, “ISCOMs and ISCOMATRIX™,” *Vaccine*, vol. 27, pp. 4388–4401, 2009.
- [115] R. Noad and P. Roy, “Virus-like particles as immunogens,” *Trends Microbiol.*, vol. 11, no. 9, pp. 438–444, 2003.
- [116] E. V. L. Grgacic and D. A. Anderson, “Virus-like particles: passport to immune recognition,” *Methods*, vol. 40, no. 1, pp. 60–65, 2006.
- [117] L. Zhang, “HPV6b virus like particles are potent immunogens without adjuvant in man,” *Vaccine*, vol. 18, no. 11–12, pp. 1051–1058, 2000.
- [118] A. C. Tissot, R. Renhofa, N. Schmitz, I. Cielens, E. Meijerink, V. Ose, G. T. Jennings, P. Saudan, P. Pumpens, and M. F. Bachmann, “Versatile virus-like particle carrier for epitope based vaccines,” *PLoS One*, vol. 5, no. 3, pp. 3–10, 2010.
- [119] M. Kanekiyo, C.-J. Wei, H. M. Yassine, P. M. McTamney, J. C. Boyington, J. R. R. Whittle, S. S. Rao, W.-P. Kong, L. Wang, and G. J. Nabel, “Self-assembling influenza nanoparticle vaccines elicit broadly neutralizing H1N1 antibodies,” *Nature*, vol. 499, no. 7456, pp. 102–106, 2013.
- [120] J. Aucouturier, L. Dupuis, and V. Ganne, “Adjuvants designed for veterinary and human vaccines,” *Vaccine*, vol. 19, no. 17–19, pp. 2666–2672, 2001.
- [121] P. Shah, D. Bhalodia, and P. Shelat, “Nanoemulsion: A pharmaceutical review,” *Syst. Rev. Pharm.*, vol. 1, no. 1, p. 24, 2010.
- [122] D. T. O’Hagan, “MF59 is a safe and potent vaccine adjuvant that enhances protection against influenza virus infection,” *Expert Rev. Vaccines*, vol. 6, no. 5, pp. 699–710, 2007.
- [123] Y. P. Chuan, B. Y. Zeng, B. O’Sullivan, R. Thomas, and A. P. J. Middelberg, “Co-delivery of antigen and a lipophilic anti-inflammatory drug to cells via a tailorable nanocarrier emulsion,” *J. Colloid Interface Sci.*, vol. 368, no. 1, pp. 616–624, Feb. 2012.
- [124] B. J. Zeng, Y. P. Chuan, B. O’Sullivan, I. Caminschi, M. H. Lahoud, R. Thomas, and A. P. J. Middelberg, “Receptor-specific delivery of protein antigen to dendritic cells by a nanoemulsion formed using top-down non-covalent click self-assembly,” *Small*, vol. 9, no. 22, pp. 3736–3742, 2013.
- [125] R. Veerasamy, T. Z. Xin, S. Gunasagaran, T. F. W. Xiang, E. F. C. Yang, N. Jeyakumar, and S. A. Dhanaraj, “Biosynthesis of silver nanoparticles using mangosteen leaf extract and evaluation of their antimicrobial activities,” *J. Saudi Chem. Soc.*, vol. 15, no. 2, pp. 113–120, 2011.

- [126] S. R. Bhuvanasree, D. Harini, A. Rajaram, and R. Rajaram, "Rapid synthesis of gold nanoparticles with *Cissus quadrangularis* extract using microwave irradiation," *Spectrochim. Acta - Part A Mol. Biomol. Spectrosc.*, vol. 106, no. 2013, pp. 190–196, 2013.
- [127] K. Raja, A. Saravanakumar, and R. Vijayakumar, "Efficient synthesis of silver nanoparticles from *Prosopis juliflora* leaf extract and its antimicrobial activity using sewage," *Spectrochim. Acta - Part A Mol. Biomol. Spectrosc.*, vol. 97, pp. 490–494, 2012.
- [128] A. Syed and A. Ahmad, "Extracellular biosynthesis of CdTe quantum dots by the fungus *Fusarium oxysporum* and their anti-bacterial activity," *Spectrochim. Acta - Part A Mol. Biomol. Spectrosc.*, vol. 106, pp. 41–47, 2013.
- [129] V. Gopinath and P. Velusamy, "Extracellular biosynthesis of silver nanoparticles using *Bacillus* sp. GP-23 and evaluation of their antifungal activity towards *Fusarium oxysporum*," *Spectrochim. Acta - Part A Mol. Biomol. Spectrosc.*, vol. 106, pp. 170–174, 2013.
- [130] X. Li, X. Deng, M. Yuan, C. Xiong, Z. Huang, Y. Zhang, and W. Jia, "In vitro degradation and release profiles of poly-DL-lactide-poly(ethylene glycol) microspheres with entrapped proteins," *J. Appl. Polym. Sci.*, vol. 78, no. 1, pp. 140–148, 2000.
- [131] S. K. Sahoo, J. Panyam, S. Prabha, and V. Labhasetwar, "Residual polyvinyl alcohol associated with poly (D,L-lactide-co-glycolide) nanoparticles affects their physical properties and cellular uptake," *J. Control. Release*, vol. 82, no. 1, pp. 105–114, 2002.
- [132] J.-M. Lü, X. Wang, C. Marin-Muller, H. Wang, P. H. Lin, Q. Yao, and C. Chen, "Current advances in research and clinical applications of PLGA-based nanotechnology.," *Expert Rev. Mol. Diagn.*, vol. 9, no. 4, pp. 325–341, 2009.
- [133] L. Feng, X. R. Qi, X. J. Zhou, Y. Maitani, S. Cong Wang, Y. Jiang, and T. Nagai, "Pharmaceutical and immunological evaluation of a single-dose hepatitis B vaccine using PLGA microspheres," *J. Control. Release*, vol. 112, no. 1, pp. 35–42, 2006.
- [134] H. F. Florindo, S. Pandit, L. M. D. Gonçalves, M. Videira, O. Alpar, and A. J. Almeida, "Antibody and cytokine-associated immune responses to *S. equi* antigens entrapped in PLA nanospheres," *Biomaterials*, vol. 30, no. 28, pp. 5161–5169, 2009.
- [135] R. Harikrishnan, C. Balasundaram, and M.-S. Heo, "Poly D,L-lactide-co-glycolic acid (PLGA)-encapsulated vaccine on immune system in *Epinephelus bruneus* against *Uronema marinum*," *Exp. Parasitol.*, vol. 131, no. 3, pp. 325–332, 2012.

- [136] H. Sah, "Stabilization of proteins against methylene chloride/water interface-induced denaturation and aggregation," *J. Control. Release*, vol. 58, no. 2, pp. 143–151, 1999.
- [137] E. S. Lee, H. J. Shin, K. Na, and Y. H. Bae, "Poly(L-histidine)-PEG block copolymer micelles and pH-induced destabilization," *J. Control. Release*, vol. 90, no. 3, pp. 363–374, Jul. 2003.
- [138] M. Matsusaki, T. Fuchida, T. Kaneko, and M. Akashi, "Self-assembling bionanoparticles of poly(epsilon-lysine) bearing cholesterol as a biomesogen," *Biomacromolecules*, vol. 6, no. 4, pp. 2374–2379, 2005.
- [139] E. P. Holowka, V. Z. Sun, D. T. Kamei, and T. J. Deming, "Polyarginine segments in block copolypeptides drive both vesicular assembly and intracellular delivery," *Nat. Mater.*, vol. 6, no. 1, pp. 52–57, 2007.
- [140] K. Letchford and H. Burt, "A review of the formation and classification of amphiphilic block copolymer nanoparticulate structures: micelles, nanospheres, nanocapsules and polymersomes," *Eur. J. Pharm. Biopharm.*, vol. 65, no. 3, pp. 259–269, 2007.
- [141] M. Obst and A. Steinbüchel, "Microbial degradation of poly(amino acid)s," *Biomacromolecules*, vol. 5, pp. 1166–1176, 2004.
- [142] H. Kim, T. Akagi, and M. Akashi, "Preparation of size tunable amphiphilic poly(amino acid) nanoparticles," *Macromol. Biosci.*, vol. 9, no. 9, pp. 842–848, 2009.
- [143] T. Akagi, F. Shima, and M. Akashi, "Intracellular degradation and distribution of protein-encapsulated amphiphilic poly(amino acid) nanoparticles," *Biomaterials*, vol. 32, no. 21, pp. 4959–4967, 2011.
- [144] K. Sonaje, E. Y. Chuang, K. J. Lin, T. C. Yen, F. Y. Su, M. T. Tseng, and H. W. Sung, "Opening of epithelial tight junctions and enhancement of paracellular permeation by chitosan: Microscopic, ultrastructural, and computed-tomographic observations," *Mol. Pharm.*, vol. 9, no. 5, pp. 1271–1279, 2012.
- [145] K. Y. Lee, I. C. Kwon, Y. H. Kim, W. H. Jo, and S. Y. Jeong, "Preparation of chitosan self-aggregates as a gene delivery system," *J. Control. Release*, vol. 51, no. 2–3, pp. 213–220, 1998.
- [146] H. Q. Mao, K. Roy, V. L. Troung-Le, K. A. Janes, K. Y. Lin, Y. Wang, J. T. August, and K. W. Leong, "Chitosan-DNA nanoparticles as gene carriers: Synthesis, characterization and transfection efficiency," *J. Control. Release*, vol. 70, no. 3, pp. 399–421, 2001.
- [147] Y. Xu and Y. Du, "Effect of molecular structure of chitosan on protein delivery properties of chitosan nanoparticles," *Int. J. Pharm.*, vol. 250, no. 1, pp. 215–226,

- 2003.
- [148] A. Rivas-Aravena, A. M. Sandino, and E. Spencer, “Nanoparticles and microparticles of polymers and polysaccharides to administer fish vaccines,” *Biol Res*, vol. 46, no. 4, pp. 407–419, 2013.
  - [149] J. Panyam and V. Labhasetwar, “Biodegradable nanoparticles for drug and gene delivery to cells and tissue,” *Adv. Drug Deliv. Rev.*, vol. 55, no. 3, pp. 329–347, 2003.
  - [150] H. M. Redhead, S. S. Davis, and L. Illum, “Drug delivery in poly(lactide-co-glycolide) nanoparticles surface modified with poloxamer 407 and poloxamine 908: In vitro characterisation and in vivo evaluation,” *J. Control. Release*, vol. 70, no. 3, pp. 353–363, 2001.
  - [151] M. Dunne, O. I. Corrigan, and Z. Ramtoola, “Influence of particle size and dissolution conditions on the degradation properties of polylactide-co-glycolide particles,” *Biomaterials*, vol. 21, no. 16, pp. 1659–1668, 2000.
  - [152] R. H. Muller and K. H. Wallis, “Surface modification of i.v. injectable biodegradable nanoparticles with poloxamer polymers and poloxamine 908,” *Int. J. Pharm.*, vol. 89, no. 1, pp. 25–31, 1993.
  - [153] I. Brigger, C. Dubernet, and P. Couvreur, “Nanoparticles in cancer therapy and diagnosis,” *Adv. Drug Deliv. Rev.*, vol. 54, no. 5, pp. 631–651, 2002.
  - [154] L. Grislain, P. Couvreur, V. Lenaerts, M. Roland, D. Deprez-Decampeneere, and P. Speiser, “Pharmacokinetics and distribution of a biodegradable drug-carrier,” *Int. J. Pharm.*, vol. 15, pp. 335–345, 1983.
  - [155] P. Couvreur, G. Barratt, E. Fattal, P. Legrand, and C. Vauthier, “Nanocapsule technology: a review,” *Crit. Rev. Ther. Drug Carrier Syst.*, vol. 19, no. 2, pp. 99–134, 2002.
  - [156] A. McNaught and A. Wilkinson, *IUPAC. Compendium of chemical terminology*, 2nd ed. (t. Blackwell Scientific Publications, Oxford, 1997).
  - [157] A. Garcia, A. Cuesta, M. Montes-Moran, A. Martinez-Alonso, and J. Tascon, “Zeta potential as a tool to characterize plasma oxidation of carbon fibers,” *J. Colloid Interface Sci.*, vol. 192, no. 2, pp. 363–367, Aug. 1997.
  - [158] V. Mohanraj and Y. Chen, “Nanoparticles – A Review,” *Trop. J. Pharm. Res.*, vol. 5, no. 51, pp. 561–573, 2006.
  - [159] D. B. Shenoy and M. M. Amiji, “Poly(ethylene oxide)-modified poly(epsilon-caprolactone) nanoparticles for targeted delivery of tamoxifen in breast cancer,” *Int. J. Pharm.*, vol. 293, no. 1–2, pp. 261–270, Apr. 2005.

- [160] S. Prior, C. Gamazo, J. M. Irache, H. P. Merkle, and B. Gander, "Gentamicin encapsulation in PLA/PLGA microspheres in view of treating Brucella infections.," *Int. J. Pharm.*, vol. 196, no. 1, pp. 115–125, Feb. 2000.
- [161] T. Govender, S. Stolnik, M. C. Garnett, L. Illum, and S. S. Davis, "PLGA nanoparticles prepared by nanoprecipitation: drug loading and release studies of a water soluble drug.," *J. Control. Release*, vol. 57, no. 2, pp. 171–185, Feb. 1999.
- [162] T. Govender, T. Riley, T. Ehtezazi, M. C. Garnett, S. Stolnik, L. Illum, and S. S. Davis, "Defining the drug incorporation properties of PLA-PEG nanoparticles," *Int. J. Pharm.*, vol. 199, no. 1, pp. 95–110, 2000.
- [163] J. Panyam, D. Williams, A. Dash, D. Leslie-Pelecky, and V. Labhasetwar, "Solid-state solubility influences encapsulation and release of hydrophobic drugs from PLGA/PLA nanoparticles," *J. Pharm. Sci.*, vol. 93, pp. 1804–1814, 2004.
- [164] P. Calvo and C. Remunan-Lopez, "Novel hydrophilic chitosan-polyethylene oxide nanoparticles as protein carriers," *J. Appl. Polym. Sci.*, pp. 125–132, 1997.
- [165] Y. Chen, V. J. Mohanraj, and J. E. Parkin, "Chitosan-dextran sulfate nanoparticles for delivery of an anti-angiogenesis peptide," *Lett. Pept. Sci.*, vol. 10, pp. 621–629, 2003.
- [166] B. Magenheimer, M. Y. Levy, and S. Benita, "A new in vitro technique for the evaluation of drug release profile from colloidal carriers - ultrafiltration technique at low pressure," *Int. J. Pharm.*, vol. 94, no. 1–3, pp. 115–123, 1993.
- [167] M. Fresta, G. Puglisi, G. Giammona, G. Cavallaro, N. Micali, and P. M. Furneri, "Pefloxacin mesilate- and ofloxacin-loaded polyethylcyanoacrylate nanoparticles: Characterization of the colloidal drug carrier formulation," *J. Pharm. Sci.*, vol. 84, no. 7, pp. 895–902, 1995.
- [168] B. Pulendran, "Learning immunology from the yellow fever vaccine: innate immunity to systems vaccinology," *Nat Rev Immunol*, vol. 9, no. 10, pp. 741–747, 2009.
- [169] M. F. Bachmann and G. T. Jennings, "Vaccine delivery: a matter of size, geometry, kinetics and molecular patterns.," *Nat. Rev. Immunol.*, vol. 10, no. 11, pp. 787–796, 2010.
- [170] T. Storni, T. M. Kündig, G. Senti, and P. Johansen, "Immunity in response to particulate antigen-delivery systems.," *Adv. Drug Deliv. Rev.*, vol. 57, no. 3, pp. 333–355, 2005.
- [171] J. S. Blum, P. A. Wearsch, and P. Cresswell, "Pathways of Antigen Processing," *Annu. Rev. Immunol.*, vol. 31, pp. 443–473, Jan. 2013.
- [172] H. Shen, A. L. Ackerman, V. Cody, A. Giodini, E. R. Hinson, P. Cresswell, R. L.

- Edelson, W. M. Saltzman, and D. J. Hanlon, "Enhanced and prolonged cross-presentation following endosomal escape of exogenous antigens encapsulated in biodegradable nanoparticles," *Immunology*, vol. 117, no. 1, pp. 78–88, 2006.
- [173] A. Bot, K. A. Smith, and M. von Herrath, "Molecular and cellular control of T1/T2 immunity at the interface between antimicrobial defense and immune pathology.," *DNA Cell Biol.*, vol. 23, no. 6, pp. 341–350, 2004.
- [174] M. E. C. Lutsiak, D. R. Robinson, C. Coester, G. S. Kwon, and J. Samuel, "Analysis of poly(D,L-lactic-co-glycolic acid) nanosphere uptake by human dendritic cells and macrophages in vitro.," *Pharm. Res.*, vol. 19, no. 10, pp. 1480–1487, 2002.
- [175] P. Elamanchili, M. Diwan, M. Cao, and J. Samuel, "Characterization of poly(D,L-lactic-co-glycolic acid) based nanoparticulate system for enhanced delivery of antigens to dendritic cells.," *Vaccine*, vol. 22, no. 19, pp. 2406–2412, 2004.
- [176] S. T. Reddy, M. A. Swartz, and J. A. Hubbell, "Targeting dendritic cells with biomaterials: Developing the next generation of vaccines," *Trends Immunol.*, vol. 27, no. 12, pp. 573–579, 2006.
- [177] J. E. Babensee, "Interaction of dendritic cells with biomaterials.," *Semin. Immunol.*, vol. 20, no. 2, pp. 101–108, 2008.
- [178] S. P. Kasturi, I. Skountzou, R. A. Albrecht, D. Koutsoukos, T. Hua, H. I. Nakaya, R. Ravindran, S. Stewart, M. Alam, M. Kwissa, F. Villinger, N. Murthy, J. Steel, J. Jacob, R. J. Hogan, A. García-Sastre, R. Compans, and B. Pulendran, "Programming the magnitude and persistence of antibody responses with innate immunity.," *Nature*, vol. 470, no. 7335, pp. 543–547, 2011.
- [179] M. Black, A. Trent, M. Tirrell, and C. Olive, "Advances in the design and delivery of peptide subunit vaccines with a focus on toll-like receptor agonists.," *Expert Rev. Vaccines*, vol. 9, pp. 157–173, 2010.
- [180] T. Uto, T. Akagi, T. Hamasaki, M. Akashi, and M. Baba, "Modulation of innate and adaptive immunity by biodegradable nanoparticles.," *Immunol. Lett.*, vol. 125, no. 1, pp. 46–52, 2009.
- [181] H. Kim, T. Uto, T. Akagi, M. Baba, and M. Akashi, "Amphiphilic Poly(Amino Acid) nanoparticles induce size-dependent dendritic cell maturation," *Adv. Funct. Mater.*, vol. 20, no. 22, pp. 3925–3931, Nov. 2010.
- [182] T. Musumeci, C. A. Ventura, I. Giannone, B. Ruozi, L. Montenegro, R. Pignatello, and G. Puglisi, "PLA/PLGA nanoparticles for sustained release of docetaxel," *Int. J. Pharm.*, vol. 325, no. 1–2, pp. 172–179, 2006.

- [183] S. Dhar, W. L. Daniel, D. A. Giljohann, C. A. Mirkin, and S. J. Lippard, “Polyvalent oligonucleotide gold nanoparticle conjugates as delivery vehicles for platinum(IV) warheads,” *J. Am. Chem. Soc.*, vol. 131, no. 41, pp. 14652–14653, 2009.
- [184] A. Taki and P. Smooker, “Small wonders—The use of nanoparticles for delivering antigen,” *Vaccines*, vol. 3, pp. 638–661, 2015.
- [185] D. R. Bhumkar, H. M. Joshi, M. Sastry, and V. B. Pokharkar, “Chitosan reduced gold nanoparticles as novel carriers for transmucosal delivery of insulin,” *Pharm. Res.*, vol. 24, no. 8, pp. 1415–1426, 2007.
- [186] D. J. Bharali, V. Pradhan, G. Elkin, W. Qi, A. Hutson, S. a. Mousa, and Y. Thanavala, “Novel nanoparticles for the delivery of recombinant hepatitis B vaccine,” *Nanomedicine Nanotechnology, Biol. Med.*, vol. 4, no. 4, pp. 311–317, 2008.
- [187] A. Caputo, A. Castaldello, E. Brocca-Cofano, R. Voltan, F. Bortolazzi, G. Altavilla, K. Sparnacci, M. Laus, L. Tondelli, R. Gavioli, and B. Ensoli, “Induction of humoral and enhanced cellular immune responses by novel core-shell nanosphere- and microsphere-based vaccine formulations following systemic and mucosal administration,” *Vaccine*, vol. 27, no. 27, pp. 3605–3615, 2009.
- [188] M. E. Baca-Estrada, M. Foldvari, M. Snider, K. Harding, B. Kournikakis, L. A. Babiuk, and P. Griebel, “Intranasal immunization with liposome-formulated *Yersinia pestis* vaccine enhances mucosal immune responses,” *Vaccine*, vol. 18, no. 21, pp. 2203–2211, 2000.
- [189] W. Zhao, W. Wu, and X. Xu, “Oral vaccination with liposome-encapsulated recombinant fusion peptide of urease B epitope and cholera toxin B subunit affords prophylactic and therapeutic effects against *H. pylori* infection in BALB/c mice,” *Vaccine*, vol. 25, no. 44, pp. 7664–7673, 2007.
- [190] M. Karkada, G. M. Weir, T. Quinton, A. Fuentes-Ortega, and M. Mansour, “A liposome-based platform, VacciMax, and its modified water-free platform DepoVax enhance efficacy of in vivo nucleic acid delivery,” *Vaccine*, vol. 28, no. 38, pp. 6176–6182, 2010.
- [191] S. L. Giannini, E. Hanon, P. Moris, M. Van Mechelen, S. Morel, F. Dessy, M. a Fourneau, B. Colau, J. Suzich, G. Losonksy, M.-T. Martin, G. Dubin, and M. A. Wettendorff, “Enhanced humoral and memory B cellular immunity using HPV16/18 L1 VLP vaccine formulated with the MPL/aluminium salt combination (AS04) compared to aluminium salt only,” *Vaccine*, vol. 24, no. 33–34, pp. 5937–5949, 2006.
- [192] G. Sailaja, I. Skountzou, F.-S. Quan, R. W. Compans, and S.-M. Kang, “Human



- immunodeficiency virus-like particles activate multiple types of immune cells.,” *Virology*, vol. 362, no. 2, pp. 331–341, 2007.
- [193] K. Slupetzky, R. Gambhira, T. Culp, S. Shafti-Keramat, C. Schellenbacher, N. Christensen, R. Roden, and R. Kirnbauer, “A papillomavirus-like particle (VLP) vaccine displaying HPV16 L2 epitopes induces cross-neutralizing antibodies to HPV11.,” *Vaccine*, vol. 25, no. 11, pp. 2001–2010, 2007.
- [194] M. Tyler, E. Tumban, D. S. Peabody, and B. Chackerian, “The use of hybrid virus-like particles to enhance the immunogenicity of a broadly protective HPV vaccine.,” *Biotechnol. Bioeng.*, vol. 111, no. 12, pp. 2398–2406, 2014.
- [195] M. Kazanji, F. Laurent, and P. Pery, “Immune responses and protective effect in mice vaccinated orally with surface sporozoite protein of *Eimeria falciformis* in ISCOMs.,” *Vaccine*, vol. 12, no. 9, pp. 798–804, Jul. 1994.
- [196] G. F. Rimmelzwaan, K. H. Siebelink, R. C. Huisman, B. Moss, M. J. Francis, and A. D. Osterhaus, “Removal of the cleavage site of recombinant feline immunodeficiency virus envelope protein facilitates incorporation of the surface glycoprotein in immune-stimulating complexes.,” *J. Gen. Virol.*, vol. 75 ( Pt 8), pp. 2097–2102, Aug. 1994.
- [197] M. T. Sanders, L. E. Brown, G. Deliyannis, and M. J. Pearse, “ISCOM-based vaccines: the second decade.,” *Immunol. Cell Biol.*, vol. 83, no. 2, pp. 119–128, Apr. 2005.
- [198] S.-D. Li and L. Huang, “Gene therapy progress and prospects: non-viral gene therapy by systemic delivery.,” *Gene Ther.*, vol. 13, no. 18, pp. 1313–1319, 2006.
- [199] M. A. Kotterman, T. W. Chalberg, and D. V. Schaffer, “Viral Vectors for Gene Therapy: Translational and Clinical Outlook,” *Annu. Rev. Biomed. Eng.*, vol. 17, pp. 63–89, Aug. 2015.
- [200] A. Ghaemi, H. Soleimanjahi, T. Bamdad, S. Soudi, E. Arefeian, S. M. Hashemi, and M. Ebtekar, “Induction of humoral and cellular immunity against latent HSV-1 infections by DNA immunization in BALB/c mice.,” *Comp. Immunol. Microbiol. Infect. Dis.*, vol. 30, no. 4, pp. 197–210, 2007.
- [201] A. Ghaemi, H. Soleimanjahi, P. Gill, Z. M. Hassan, S. Razeghi, M. Fazeli, and S. M. Razavinikoo, “Protection of mice by a lambda-based therapeutic vaccine against cancer associated with human papillomavirus type 16,” *Intervirology*, vol. 54, no. 3, pp. 105–112, 2011.
- [202] M. Ingolotti, O. Kawalekar, D. J. Shedlock, K. Muthumani, and D. B. Weiner, “DNA vaccines for targeting bacterial infections.,” *Expert Rev. Vaccines*, vol. 9, no. 7, pp.

- 747–763, 2010.
- [203] B. Ferraro, M. P. Morrow, N. A. Hutnick, T. H. Shin, C. E. Lucke, and D. B. Weiner, “Clinical applications of DNA vaccines: current progress.,” *Clin. Infect. Dis.*, vol. 53, no. 3, pp. 296–302, 2011.
- [204] K. Okuda, Y. Wada, and M. Shimada, “Recent developments in preclinical DNA vaccination,” *Vaccines*, vol. 2, no. 1, pp. 89–106, 2014.
- [205] C. Saroja, P. Lakshmi, and S. Bhaskaran, “Recent trends in vaccine delivery systems: A review,” *Int. J. Pharm. Investig.*, vol. 1, no. 2, pp. 64–74, 2011.
- [206] A. Mann, R. Richa, and M. Ganguli, “DNA condensation by poly-l-lysine at the single molecule level: Role of DNA concentration and polymer length,” *J. Control. Release*, vol. 125, no. 3, pp. 252–262, 2008.
- [207] A. Tahamtan, A. Ghaemi, A. Gorji, H. R. Kalhor, A. Sajadian, A. Tabarraei, A. Moradi, F. Atyabi, and M. Kelishadi, “Antitumor effect of therapeutic HPV DNA vaccines with chitosan-based nanodelivery systems.,” *J. Biomed. Sci.*, vol. 21, no. 69, pp. 1–10, 2014.
- [208] L. Zhao, A. Seth, N. Wibowo, C. X. Zhao, N. Mitter, C. Yu, and A. P. J. Middelberg, “Nanoparticle vaccines,” *Vaccine*, vol. 32, no. 3, pp. 327–337, 2014.
- [209] L. Illum, M. Hinchcliffe, A. N. Fisher, S. S. Davis, and I. Jabbal-Gill, “Chitosan as a novel nasal delivery system for vaccines.,” *Adv. Drug Deliv. Rev.*, vol. 51, no. 1–3, pp. 81–96, 2001.
- [210] H. O. Alpar, I. Papanicolaou, and V. W. Bramwell, “Strategies for DNA vaccine delivery,” *Expert Opin. Drug Deliv.*, vol. 2, no. 5, pp. 829–842, 2005.
- [211] S. A. Galindo-Rodriguez, E. Allemann, H. Fessi, and E. Doelker, “Polymeric nanoparticles for oral delivery of drugs and vaccines: a critical evaluation of in vivo studies.,” *Crit. Rev. Ther. Drug Carrier Syst.*, vol. 22, pp. 419–464, 2005.
- [212] T. Kurosaki, T. Kitahara, S. Fumoto, K. Nishida, J. Nakamura, T. Niidome, Y. Kodama, H. Nakagawa, H. To, and H. Sasaki, “Ternary complexes of pDNA, polyethylenimine, and gamma-polyglutamic acid for gene delivery systems.,” *Biomaterials*, vol. 30, no. 14, pp. 2846–2853, 2009.
- [213] K. T. Mody, A. Popat, D. Mahony, A. S. Cavallaro, C. Yu, and N. Mitter, “Mesoporous silica nanoparticles as antigen carriers and adjuvants for vaccine delivery.,” *Nanoscale*, vol. 5, no. 12, pp. 5167–5179, 2013.
- [214] J. Wendorf, M. Singh, J. Chesko, J. Kazzaz, E. Soewanan, M. Ugozzoli, and D. O’Hagan, “A practical approach to the use of nanoparticles for vaccine

- delivery,” *J. Pharm. Sci.*, vol. 95, pp. 2738–2750, 2006.
- [215] B. Slütter, P. C. Soema, Z. Ding, R. Verheul, W. Hennink, and W. Jiskoot, “Conjugation of ovalbumin to trimethyl chitosan improves immunogenicity of the antigen,” *J. Control. Release*, vol. 143, no. 2, pp. 207–214, 2010.
- [216] K. S. Jones, “Biomaterials as vaccine adjuvants,” *Biotechnol. Prog.*, vol. 24, pp. 807–814, 2008.
- [217] M. A. Dobrovolskaia, P. Aggarwal, J. B. Hall, and S. E. McNeil, “Preclinical studies to understand nanoparticle interaction with the immune system and its potential effects on nanoparticle biodistribution,” *Mol. Pharm.*, vol. 5, no. 4, pp. 487–495, 2008.
- [218] A. Kumari and S. K. Yadav, “Cellular interactions of therapeutically delivered nanoparticles,” *Expert Opin. Drug Deliv.*, vol. 8, no. 2, pp. 141–151, 2011.
- [219] S. D. Xiang, A. Scholzen, G. Minigo, C. David, V. Apostolopoulos, P. L. Mottram, and M. Plebanski, “Pathogen recognition and development of particulate vaccines: does size matter?,” *Methods*, vol. 40, no. 1, pp. 1–9, 2006.
- [220] C. Foged, B. Brodin, S. Frokjaer, and A. Sundblad, “Particle size and surface charge affect particle uptake by human dendritic cells in an in vitro model,” *Int. J. Pharm.*, vol. 298, no. 2, pp. 315–322, 2005.
- [221] V. Kanchan and A. K. Panda, “Interactions of antigen-loaded polylactide particles with macrophages and their correlation with the immune response,” *Biomaterials*, vol. 28, no. 35, pp. 5344–5357, 2007.
- [222] J. A. Champion and S. Mitragotri, “Shape induced inhibition of phagocytosis of polymer particles,” *Pharm. Res.*, vol. 26, no. 1, pp. 244–249, 2009.
- [223] R. S. Raghuvanshi, Y. K. Katare, K. Lalwani, M. M. Ali, O. Singh, and A. K. Panda, “Improved immune response from biodegradable polymer particles entrapping tetanus toxoid by use of different immunization protocol and adjuvants,” *Int. J. Pharm.*, vol. 245, no. 1–2, pp. 109–121, 2002.
- [224] H. Hillaireau and P. Couvreur, “Nanocarriers’ entry into the cell: Relevance to drug delivery,” *Cell. Mol. Life Sci.*, vol. 66, no. 17, pp. 2873–2896, 2009.
- [225] L. J. Thomann-Harwood, P. Kaeuper, N. Rossi, P. Milona, B. Herrmann, and K. C. McCullough, “Nanogel vaccines targeting dendritic cells: contributions of the surface decoration and vaccine cargo on cell targeting and activation,” *J. Control. Release*, vol. 166, no. 2, pp. 95–105, 2013.
- [226] P. Aggarwal, J. B. Hall, C. B. McLeland, M. a. Dobrovolskaia, and S. E. McNeil, “Nanoparticle interaction with plasma proteins as it relates to particle biodistribution,

- biocompatibility and therapeutic efficacy,” *Adv. Drug Deliv. Rev.*, vol. 61, no. 6, pp. 428–437, 2009.
- [227] A. E. Nel, L. Mädler, D. Velegol, T. Xia, E. M. V Hoek, P. Somasundaran, F. Klaessig, V. Castranova, and M. Thompson, “Understanding biophysicochemical interactions at the nano-bio interface,” *Nat. Mater.*, vol. 8, no. 7, pp. 543–557, 2009.
- [228] S. T. Reddy, A. J. van der Vlies, E. Simeoni, V. Angeli, G. J. Randolph, C. P. O’Neil, L. K. Lee, M. A. Swartz, and J. A. Hubbell, “Exploiting lymphatic transport and complement activation in nanoparticle vaccines,” *Nat. Biotechnol.*, vol. 25, no. 10, pp. 1159–1164, 2007.
- [229] J. J. Moon, H. Suh, A. V. Li, C. F. Ockenhouse, A. Yadava, and D. J. Irvine, “From the cover: Enhancing humoral responses to a malaria antigen with nanoparticle vaccines that expand Tfh cells and promote germinal center induction,” *Proc. Natl. Acad. Sci.*, vol. 109, no. 4, pp. 1080–1085, 2012.
- [230] A. Seubert, E. Monaci, M. Pizza, D. T. O’Hagan, and A. Wack, “The adjuvants aluminum hydroxide and MF59 induce monocyte and granulocyte chemoattractants and enhance monocyte differentiation toward dendritic cells,” *J. Immunol.*, vol. 180, pp. 5402–5412, 2008.
- [231] T. M. Allen, C. B. Hansen, and L. S. Guo, “Subcutaneous administration of liposomes: a comparison with the intravenous and intraperitoneal routes of injection,” *Biochim. Biophys. Acta*, vol. 1150, no. 1, pp. 9–16, 1993.
- [232] M. Longmire, P. L. Choyke, and H. Kobayashi, “Clearance properties of nano-sized particles and molecules as imaging agents: considerations and caveats,” *Nanomedicine*, vol. 3, no. 5, pp. 703–717, 2008.
- [233] V. B. Patravale, A. A. Date, and R. M. Kulkarni, “Nanosuspensions: a promising drug delivery strategy,” *J. Pharm. Pharmacol.*, vol. 56, no. 7, pp. 827–840, 2004.
- [234] C. Damgé, C. Michel, M. Aprahamian, P. Couvreur, and J. P. Devissaguet, “Nanocapsules as carriers for oral peptide delivery,” *Journal of Controlled Release*, vol. 13, pp. 233–239, 1990.
- [235] B. Slütter, N. Hageraars, and W. Jiskoot, “Rational design of nasal vaccines,” *J. Drug Target.*, vol. 16, no. January, pp. 1–17, 2008.
- [236] J. S. Patton and P. R. Byron, “Inhaling medicines: delivering drugs to the body through the lungs,” *Nat. Rev. Drug Discov.*, vol. 6, no. 1, pp. 67–74, 2007.
- [237] B. L. Laube, “The expanding role of aerosols in systemic drug delivery, gene therapy and vaccination: an update,” *Transl. Respir. Med.*, vol. 2, p. 3, 2014.

- [238] R. H. Müller and C. Jacobs, “Buparvaquone mucoadhesive nanosuspension: Preparation, optimisation and long-term stability,” *Int. J. Pharm.*, vol. 237, no. 1–2, pp. 151–161, 2002.
- [239] J. Leleux and K. Roy, “Micro and nanoparticle-based delivery systems for vaccine immunotherapy: an immunological and materials perspective,” *Adv. Healthc. Mater.*, vol. 2, no. 1, pp. 72–94, 2013.
- [240] B. Combadière and B. Mahé, “Particle-based vaccines for transcutaneous vaccination,” *Comp. Immunol. Microbiol. Infect. Dis.*, vol. 31, no. 2–3, pp. 293–315, 2008.
- [241] P. Prabhu and V. Patravale, “Potential of Nanocarriers in antigen delivery: The path to successful vaccine delivery,” *Nanocarriers*, vol. 1, no. 1, pp. 10–45, 2014.
- [242] Z. Cui and R. J. Mumper, “Microparticles and nanoparticles as delivery systems for DNA vaccines,” *Crit. Rev. Ther. Drug Carrier Syst.*, vol. 20, no. 2–3, pp. 103–137, 2003.
- [243] M. Singh, A. Chakrapani, and D. O’Hagan, “Nanoparticles and microparticles as vaccine-delivery systems,” *Expert Rev. Vaccines*, vol. 6, no. 5, pp. 797–808, 2007.
- [244] H. Mishra, D. Mishra, P. K. Mishra, M. Nahar, V. Dubey, and N. K. Jain, “Evaluation of solid lipid nanoparticles as carriers for delivery of hepatitis b surface antigen for vaccination using subcutaneous route,” *J. Pharm. Pharm. Sci.*, vol. 13, no. 4, pp. 495–509, 2010.
- [245] S. M. Bal, B. Slütter, E. van Riet, A. C. Kruithof, Z. Ding, G. F. A. Kersten, W. Jiskoot, and J. A. Bouwstra, “Efficient induction of immune responses through intradermal vaccination with N-trimethyl chitosan containing antigen formulations,” *J. Control. Release*, vol. 142, no. 3, pp. 374–383, 2010.
- [246] I. Badea, S. Babiuk, L. Babiuk, and M. Foldvari, “Gemini nanoparticles as a co-delivery system for antigen – CpG oligodeoxynucleotide adjuvant combination,” *Int. J. Biomed. Nanosci. Nanotechnol.*, vol. 1, no. 2–4, pp. 290–307, Jan. 2010.
- [247] R. J. Verheul, B. Slütter, S. M. Bal, J. A. Bouwstra, W. Jiskoot, and W. E. Hennink, “Covalently stabilized trimethyl chitosan-hyaluronic acid nanoparticles for nasal and intradermal vaccination,” *J. Control. Release*, vol. 156, no. 1, pp. 46–52, 2011.
- [248] J. M. Janda and S. L. Abbott, “Evolving concepts regarding the genus *Aeromonas*: an expanding Panorama of species, disease presentations, and unanswered questions,” *Clin. Infect. Dis.*, vol. 27, no. 2, pp. 332–344, 1998.
- [249] T. C. Hazen, C. B. Fliermans, R. P. Hirsch, and G. W. Esch, “Prevalence and

- distribution of *Aeromonas hydrophila* in the United States.,” *Appl. Environ. Microbiol.*, vol. 36, no. 5, pp. 731–738, 1978.
- [250] J. J. Mathewson and H. L. Dupont, “*Aeromonas* species: role as human pathogens.,” *Curr. Clin. Top. Infect. Dis.*, vol. 12, pp. 26–36, 1992.
- [251] T. Miyazaki and N. Kaige, “A histopathological study on motile *Aeromonad* disease of crucian carp,” *Fish Pathol.*, vol. 21, no. 3, pp. 181–185, 1985.
- [252] J. M. Pemberton, S. P. Kidd, and R. Schmidt, “Secreted enzymes of *Aeromonas*,” *FEMS Microbiol. Lett.*, vol. 152, no. 1, pp. 1–10, 1997.
- [253] A. Aberoum and H. Jooyandeh, “A review on occurrence and characterization of the *Aeromonas* species from marine fishes,” *World J. Fish Mar. Sci.*, vol. 2, no. 6, pp. 519–523, 2010.
- [254] E. Valério, S. Chaves, and R. Tenreiro, “Diversity and impact of prokaryotic toxins on aquatic environments: A review,” *Toxins (Basel)*, vol. 2, no. 10, pp. 2359–2410, 2010.
- [255] A. Rey, N. Verján, H. W. Ferguson, and C. Iregui, “Pathogenesis of *Aeromonas hydrophila* strain KJ99 infection and its extracellular products in two species of fish.,” *Vet. Rec.*, vol. 164, no. 16, pp. 493–499, 2009.
- [256] H. Fukui, Y. Fujihara, and T. Kano, “In-Vitro and in-Vivo antibacterial activities of Florfenicol a new fluorinated analog of Thiamphenicol against fish pathogens,” *Fish Pathol.*, vol. 22, no. 4, pp. 201–208, 1987.
- [257] S. Sekkin and C. Kum, “Antibacterial drugs in fish farms: Application and its effects,” *Chapter*, 2011.
- [258] P. K. Sahoo, K. Das Mahapatra, J. N. Saha, A. Barat, M. Sahoo, B. R. Mohanty, B. Gjerde, J. Odegård, M. Rye, and R. Salte, “Family association between immune parameters and resistance to *Aeromonas hydrophila* infection in the Indian major carp, *Labeo rohita*.,” *Fish Shellfish Immunol.*, vol. 25, no. 1–2, pp. 163–169, 2008.
- [259] C. Lutz, M. Erken, P. Noorian, S. Sun, and D. McDougald, “Environmental reservoirs and mechanisms of persistence of *Vibrio cholerae*,” *Front. Microbiol.*, vol. 4, pp. 1–15, 2013.
- [260] S. M. Faruque, M. J. Albert, and J. J. Mekalanos, “Epidemiology, genetics, and ecology of toxigenic *Vibrio cholerae*.,” *Microbiol. Mol. Biol. Rev.*, vol. 62, no. 4, pp. 1301–1314, 1998.
- [261] A. K. Siddique, A. H. Baqui, A. Eusof, K. Haider, M. A. Hossain, I. Bashir, and K. Zaman, “Survival of classic cholera in Bangladesh.,” *Lancet*, vol. 337, no. 8750, pp. 1125–1127, 1991.

- [262] R. G. Zhang, D. L. Scott, M. L. Westbrook, S. Nance, B. D. Spangler, G. G. Shipley, and E. M. Westbrook, "The three-dimensional crystal structure of cholera toxin.," *J. Mol. Biol.*, vol. 251, no. 4, pp. 563–573, 1995.
- [263] B. M. Davis and M. K. Waldor, "Filamentous phages linked to virulence of *Vibrio cholerae*," *Curr. Opin. Microbiol.*, vol. 6, no. 1, pp. 35–42, 2003.
- [264] E. F. Boyd and M. K. Waldor, "Evolutionary and functional analyses of variants of the toxin-coregulated pilus protein TcpA from toxigenic *Vibrio cholerae* non-O1/non-O139 serogroup isolates.," *Microbiology*, vol. 148, no. Pt 6, pp. 1655–1666, 2002.
- [265] M. B. Miller, K. Skorupski, D. H. Lenz, R. K. Taylor, and B. L. Bassler, "Parallel quorum sensing systems converge to regulate virulence in *Vibrio cholerae*," *Cell*, vol. 110, no. 3, pp. 303–314, 2002.
- [266] A. T. Nielsen, N. A. Dolganov, G. Otto, M. C. Miller, C. Y. Wu, and G. K. Schoolnik, "RpoS controls the *Vibrio cholerae* mucosal escape response.," *PLoS Pathog.*, vol. 2, no. 10, p. e109, 2006.
- [267] D. Sinclair, K. Abba, K. Zaman, F. Qadri, and P. M. Graves, "Oral vaccines for preventing cholera.," *Cochrane database Syst. Rev.*, no. 3, p. CD008603, 2011.
- [268] T. Jelinek and H. Kollaritsch, "Vaccination with Dukoral against travelers' diarrhea (ETEC) and cholera.," *Expert Rev. Vaccines*, vol. 7, no. 5, pp. 561–567, 2008.
- [269] J. S. Matson, J. H. Withey, and V. J. DiRita, "Regulatory networks controlling *Vibrio cholerae* virulence gene expression," *Infect. Immun.*, vol. 75, no. 12, pp. 5542–5549, 2007.
- [270] S. Schild, E. J. Nelson, and A. Camilli, "Immunization with *Vibrio cholerae* outer membrane vesicles induces protective immunity in mice.," *Infect. Immun.*, vol. 76, no. 10, pp. 4554–4563, 2008.
- [271] V. Sperandio, C. Bailey, J. A. Girón, V. J. DiRita, W. D. Silveira, A. L. Vettore, and J. B. Kaper, "Cloning and characterization of the gene encoding the OmpU outer membrane protein of *Vibrio cholerae*," *Infect. Immun.*, vol. 64, no. 12, pp. 5406–5409, 1996.
- [272] C. C. Li, J. A. Crawford, V. J. DiRita, and J. B. Kaper, "Molecular cloning and transcriptional regulation of ompT, a ToxR-repressed gene in *Vibrio cholerae*," *Mol. Microbiol.*, vol. 35, no. 1, pp. 189–203, 2000.
- [273] D. Provenzano, C. M. Lauriano, and K. E. Klose, "Characterization of the role of the ToxR-modulated outer membrane porins OmpU and OmpT in *Vibrio cholerae* virulence.," *J. Bacteriol.*, vol. 183, no. 12, pp. 3652–3662, 2001.

- [274] C. G. Osorio, H. Martinez-Wilson, and A. Camilli, "The ompU paralogue vca1008 is required for virulence of *Vibrio cholerae*," *J. Bacteriol.*, vol. 186, no. 15, pp. 5167–5171, 2004.
- [275] E. Altindis, Y. Fu, and J. J. Mekalanos, "Proteomic analysis of *Vibrio cholerae* outer membrane vesicles," *Proc. Natl. Acad. Sci.*, vol. 111, no. 15, pp. E1548-1556, 2014.
- [276] D. Chatterjee and K. Chaudhuri, "Vibrio cholerae O395 outer membrane vesicles modulate intestinal epithelial cells in a NOD1 protein-dependent manner and induce dendritic cell-mediated Th2/Th17 cell responses.," *J. Biol. Chem.*, vol. 288, no. 6, pp. 4299–309, 2013.
- [277] J. Kreuter, "Evaluation of nanoparticles as drug-delivery systems. II: Comparison of the body distribution of nanoparticles with the body distribution of microspheres (diameter greater than 1 micron), liposomes, and emulsions.," *Pharm. Acta Helv.*, vol. 58, no. 8, pp. 217–226, 1983.
- [278] E. Lu, S. Franzblau, H. Onyuksel, and C. Popescu, "Preparation of aminoglycoside-loaded chitosan nanoparticles using dextran sulphate as a counterion.," *J. Microencapsul.*, vol. 26, no. 4, pp. 346–354, 2009.
- [279] C. Wang and P.-T. Pham, "Polymers for viral gene delivery.," *Expert Opin. Drug Deliv.*, vol. 5, no. 4, pp. 385–401, 2008.
- [280] R. S. Daum, "Clinical practice. Skin and soft-tissue infections caused by methicillin-resistant *Staphylococcus aureus*," *N. Engl. J. Med.*, vol. 357, pp. 380–390, 2007.
- [281] I. Brook, M. a O. Lewis, G. K. B. Sándor, M. Jeffcoat, L. P. Samaranayake, and J. Vera Rojas, "Clindamycin in dentistry: more than just effective prophylaxis for endocarditis?," *Oral Surg. Oral Med. Oral Pathol. Oral Radiol. Endod.*, vol. 100, no. 5, pp. 550–558, 2005.
- [282] E. S. R. Darley and A. P. MacGowan, "Antibiotic treatment of gram-positive bone and joint infections.," *J. Antimicrob. Chemother.*, vol. 53, no. 6, pp. 928–35, 2004.
- [283] D. Annane, B. Clair, and J. Salomon, "Managing toxic shock syndrome with antibiotics.," *Expert Opin. Pharmacother.*, vol. 5, no. 8, pp. 1701–1710, 2004.
- [284] B. et al. Lell, "MINIREVIEW Clindamycin as an Antimalarial Drug : Review of Clinical Trials," *Antimicrob. Agents Chemother.*, vol. 46, no. 8, pp. 2315–2320, 2002.
- [285] E. A. Coyle, "Targeting bacterial virulence: the role of protein synthesis inhibitors in severe infections. Insights from the Society of Infectious Diseases Pharmacists.," *Pharmacotherapy*, vol. 23, no. 5, pp. 638–642, May 2003.
- [286] M. N. Ravi Kumar, "Nano and microparticles as controlled drug delivery devices.," *J.*



- Pharm. Pharm. Sci. a Publ. Can. Soc. Pharm. Sci.*, vol. 3, no. 2, pp. 234–258, 2000.
- [287] S. R. . Machado and R. C. Evangelista, “Development and characterization of Cefoxitin loaded D, L-PLA nanoparticles,” *J. Basic Appl. Pharm. Sci.*, vol. 31, no. 3, pp. 193–202, 2010.
- [288] F. A. El-Yazbi and S. M. Blaih, “Spectrophotometric and titrimetric determination of clindamycin hydrochloride in pharmaceutical preparations,” *Analyst*, vol. 118, no. 5, pp. 577–579, 1993.
- [289] K. A. Janes and M. J. Alonso, “Depolymerized chitosan nanoparticles for protein delivery: Preparation and characterization,” *J. Appl. Polym. Sci.*, vol. 88, no. 12, pp. 2769–2776, Jun. 2003.
- [290] CLSI, “methods for dilution antimicrobial susceptibility tests for bacteria that grow aerobically. Approve Standard M7-A7, CLSI, , seventh ed., PA, USA,” 2006.
- [291] N. R. Ravikumara, B. Madhusudhan, T. S. Nagaraj, S. R. Hiremat, and G. Raina, “Preparation and evaluation of nimesulide-loaded ethylcellulose and methylcellulose nanoparticles and microparticles for oral delivery.,” *J. Biomater. Appl.*, vol. 24, no. 1, pp. 47–64, 2009.
- [292] C. Dubernet, “Thermoanalysis of microspheres,” *Thermochim. Acta*, vol. 248, pp. 259–269, 1995.
- [293] T. S. Renuga Devi and S. Gayathri, “FTIR And FT-Raman spectral analysis of Paclitaxel drugs,” *Int. J. Pharm. Sci. Rev. Res.*, vol. 2, no. 2, pp. 106–110, 2010.
- [294] C. Thomasin, G. Corradin, Y. Men, H. P. Merkle, and B. Gander, “Tetanus toxoid and synthetic malaria antigen containing poly(lactide)/poly(lactide-co-glycolide) microspheres: importance of polymer degradation and antigen release for immune response,” *J. Control. Release*, vol. 41, no. 1–2, pp. 131–145, Aug. 1996.
- [295] A. Rösler, G. W. Vandermeulen, and H. A. Klok, “Advanced drug delivery devices via self-assembly of amphiphilic block copolymers.,” *Adv. Drug Deliv. Rev.*, vol. 53, no. 1, pp. 95–108, 2001.
- [296] K. Santhi, D. N. Venkatesh, S. A. Dhanaraj, S. Sangeetha, and B. Suresh, “Development and in-vitro evaluation of a topical drug delivery system containing betamethazone loaded ethyl cellulose nanospheres,” *Trop. J. Pharm. Res.*, vol. 4, no. 2, pp. 495–500, 2005.
- [297] B. Nayak, A. K. Panda, P. Ray, and A. R. Ray, “Formulation, characterization and evaluation of rotavirus encapsulated PLA and PLGA particles for oral vaccination.,” *J. Microencapsul.*, vol. 26, no. 2, pp. 154–165, 2009.

- [298] A. Tripathi, R. Gupta, and S. A. Saraf, "PLGA nanoparticles of anti tubercular drug : Drug loading and release studies of a water in-soluble drug," *Int. J. PharmTech Res.*, vol. 2, no. 3, pp. 2116–2123, 2010.
- [299] B. Gander, P. Johansen, H. Nam-Trân, and H. P. Merkle, "Thermodynamic approach to protein microencapsulation into poly(D,L-lactide) by spray drying," *Int. J. Pharm.*, vol. 129, no. 95, pp. 51–61, 1996.
- [300] C. Yasemin, C. Robineau, and Y. Çapan, "Etodolac loaded Poly (Lactide Co-Glycolide) nanoparticles: formulation and in vitro characterization," *Hacettepe Univ. J. Fac. Pharm.*, vol. 29, no. 2, pp. 105–114, 2009.
- [301] T. S. J. Kashi, S. Eskandarion, M. Esfandyari-Manesh, S. M. A. Marashi, N. Samadi, S. M. Fatemi, F. Atyabi, S. Eshraghi, and R. Dinarvand, "Improved drug loading and antibacterial activity of minocycline-loaded PLGA nanoparticles prepared by solid/oil/water ion pairing method," *Int. J. Nanomedicine*, vol. 7, pp. 221–234, 2012.
- [302] A. Rawat, Q. H. Majumder, and F. Ahsan, "Inhalable large porous microspheres of low molecular weight heparin: In vitro and in vivo evaluation," *J. Control. Release*, vol. 128, no. 3, pp. 224–232, 2008.
- [303] J. L. Ford and P. Timmins, *Pharmaceutical thermal analysis*. Chichester, John Wiley & Sons, 1989.
- [304] A. Narladkar, E. Balnois, G. Vignaud, and Y. Grohens, "Difference in glass transition behavior between semi crystalline and amorphous poly(lactic acid) thin films," *Macromol. Symp.*, vol. 273, no. 1, pp. 146–152, 2008.
- [305] M. Hariharan and J. C. Price, "Solvent, emulsifier and drug concentration factors in poly(D,L-lactic acid) microspheres containing hexamethylmelamine," *J. Microencapsul.*, vol. 19, no. 1, pp. 95–109, 2002.
- [306] J. Jordan, K. I. Jacob, R. Tannenbaum, M. A. Sharaf, and I. Jasiuk, "Experimental trends in polymer nanocomposites - A review," *Mater. Sci. Eng. A*, vol. 393, no. 1–2, pp. 1–11, 2005.
- [307] M. Azhdarzadeh, F. Lotfipour, P. Zakeri-Milani, G. Mohammadi, and H. Valizadeh, "Anti-bacterial performance of azithromycin nanoparticles as colloidal drug delivery system against different gram-negative and gram-positive bacteria," *Adv. Pharm. Bull.*, vol. 2, no. 1, pp. 17–24, 2012.
- [308] R. C. Mundargi, V. R. Babu, V. Rangaswamy, P. Patel, and T. M. Aminabhavi, "Nano/micro technologies for delivering macromolecular therapeutics using poly(d,l-lactide-co-glycolide) and its derivatives," *J. Control. Release*, vol. 125, pp. 193–209,

- 2008.
- [309] V. Pavot, M. Berthet, J. Resseguier, S. Legaz, N. Handke, S. C. Gilbert, S. Paul, and B. Verrier, "Poly(lactic acid) and poly(lactic-co-glycolic acid) particles as versatile carrier platforms for vaccine delivery," *Nanomedicine (Lond)*, vol. 9, no. 17, pp. 2703–2718, 2014.
  - [310] T. Behera, P. K. Nanda, C. Mohanty, D. Mohapatra, P. Swain, B. K. Das, P. Routray, B. K. Mishra, and S. K. Sahoo, "Parenteral immunization of fish, *Labeo rohita* with Poly d, l-lactide-co-glycolic acid (PLGA) encapsulated antigen microparticles promotes innate and adaptive immune responses," *Fish Shellfish Immunol.*, vol. 28, no. 2, pp. 320–325, 2010.
  - [311] C. Uribe, H. Folch, R. Enriquez, and G. Moran, "Innate and adaptive immunity in teleost fish: a review.," *Vet. Med. (Praha)*, vol. 56, no. 10, pp. 486–503, 2011.
  - [312] M. Manning, *Fishes. In "Immunology: A comparative approach."* John Wiley Ltd.: Chichester, UK, 1994.
  - [313] C. Tafalla, J. Bøgwald, and R. A. Dalmo, "Adjuvants and immunostimulants in fish vaccines: current knowledge and future perspectives.," *Fish Shellfish Immunol.*, vol. 35, no. 6, pp. 1740–1750, 2013.
  - [314] N. Pirooznia, S. Hasannia, A. Lotfi, and M. Ghanei, "Encapsulation of Alpha-1 antitrypsin in PLGA nanoparticles: In Vitro characterization as an effective aerosol formulation in pulmonary diseases," *J. Nanobiotechnology*, vol. 10, no. 20, pp. 1–15, 2012.
  - [315] V. Lund, T. Joergensen, K. O. Holm, and G. Eggset, "Humoral immune response in Atlantic salmon, *Salmo salar* L., to cellular and extracellular antigens of *Aeromonas salmonicida*," *J. Fish Dis.*, vol. 14, pp. 443–452, 1991.
  - [316] J. A. Plumb and N. Areechon, "Effect of malathion on humoral immune response of channel catfish.," *Dev. Comp. Immunol.*, vol. 14, no. 3, pp. 355–358, 1990.
  - [317] J. Kumari and P. K. Sahoo, "Effects of cyclophosphamide on the immune system and disease resistance of Asian catfish *Clarias batrachus*," *Fish Shellfish Immunol.*, vol. 19, no. 4, pp. 307–16, 2005.
  - [318] P. K. Sahoo, P. R. Rauta, B. R. Mohanty, K. D. Mahapatra, J. N. Saha, M. Rye, and A. E. Eknath, "Selection for improved resistance to *Aeromonas hydrophila* in Indian major carp *Labeo rohita*: survival and innate immune responses in first generation of resistant and susceptible lines.," *Fish Shellfish Immunol.*, vol. 31, no. 3, pp. 432–438, 2011.

- [319] A. Mahapatro and D. K. Singh, “Biodegradable nanoparticles are excellent vehicle for site directed in-vivo delivery of drugs and vaccines,” *J. Nanobiotechnology*, vol. 9, no. 1, p. 55, 2011.
- [320] A. Kumari, S. K. Yadav, and S. C. Yadav, “Biodegradable polymeric nanoparticles based drug delivery systems,” *Colloids Surfaces B Biointerfaces*, vol. 75, no. 1, pp. 1–18, 2010.
- [321] J. A. Champion, Y. K. Katare, and S. Mitragotri, “Making polymeric micro- and nanoparticles of complex shapes,” *Proc. Natl. Acad. Sci. U. S. A.*, vol. 104, no. 29, pp. 11901–11904, 2007.
- [322] T. Behera and P. Swain, “Alginate-chitosan-PLGA composite microspheres induce both innate and adaptive immune response through parenteral immunization in fish,” *Fish Shellfish Immunol.*, vol. 35, no. 3, pp. 785–791, 2013.
- [323] T. Estey, J. Kang, S. P. Schwendeman, and J. F. Carpenter, “BSA Degradation under Acidic Conditions: A Model for Protein Instability during Release from PLGA delivery Systems,” *J. Pharm. Sci.*, vol. 95, no. 7, pp. 1626–1639, 2006.
- [324] Y. Yeo and K. Park, “Control of encapsulation efficiency and initial burst in polymeric microparticle systems,” *Arch. Pharm. Res.*, vol. 27, no. 1, pp. 1–12, 2004.
- [325] Y. Y. Yang, T. S. Chung, and N. Ping Ng, “Morphology, drug distribution, and in vitro release profiles of biodegradable polymeric microspheres containing protein fabricated by double-emulsion solvent extraction/evaporation method,” *Biomaterials*, vol. 22, no. 3, pp. 231–241, 2001.
- [326] B. N. Fredriksen and J. Grip, “PLGA/PLA micro- and nanoparticle formulations serve as antigen depots and induce elevated humoral responses after immunization of Atlantic salmon (*Salmo salar* L.),” *Vaccine*, vol. 30, no. 3, pp. 656–667, 2012.
- [327] S. Mutoloki, S. Alexandersen, and Ø. Evensen, “Sequential study of antigen persistence and concomitant inflammatory reactions relative to side-effects and growth of Atlantic Salmon (*Salmo salar* L.) following intraperitoneal injection with oil-adjuvanted vaccines,” *Fish Shellfish Immunol.*, vol. 16, no. 5, pp. 633–644, 2004.
- [328] J. Pedraz, M. Igartua, R. Hernandez, A. Esquisabel, G. AR, and B. Calvo, “Long term immune response in mice following subcutaneous administration of BSA-PLGA microspheres,” in *Proc Int Sym Control Release of Bioactive Materials*, 1997, pp. 879–880.
- [329] G. J. Nabel, “Designing Tomorrow’s Vaccines,” *N. Engl. J. Med.*, vol. 368, no. 6, pp. 551–560, Feb. 2013.

- [330] Y. Perrie, D. Kirby, V. W. Bramwell, and A. R. Mohammed, “Recent developments in particulate-based vaccines.,” *Recent Pat. Drug Deliv. Formul.*, vol. 1, no. 2, pp. 117–129, 2007.
- [331] M. O. Oyewumi, A. Kumar, and Z. Cui, “Nano-microparticles as immune adjuvants: Correlating particle sizes and the resultant immune responses.,” *Expert Rev. Vaccines*, vol. 9, no. 9, pp. 1095–1107, 2010.
- [332] M. L. De Temmerman, J. Rejman, J. Demeester, D. J. Irvine, B. Gander, and S. C. De Smedt, “Particulate vaccines: On the quest for optimal delivery and immune response,” *Drug Discov. Today*, vol. 16, no. 13–14, pp. 569–582, 2011.
- [333] P. R. Rauta and B. Nayak, “Parenteral immunization of PLA/PLGA nanoparticle encapsulating outer membrane protein (Omp) from *Aeromonas hydrophila*: Evaluation of immunostimulatory action in *Labeo rohita* (rohu),” *Fish Shellfish Immunol.*, vol. 44, no. 1, pp. 287–294, May 2015.
- [334] O. Gamucci, A. Bertero, M. Gagliardi, and G. Bardi, “Biomedical nanoparticles: Overview of their surface immune-compatibility,” *Coatings*, vol. 4, no. 1, pp. 139–159, 2014.
- [335] D. F. Moyano, M. Goldsmith, D. J. Solfiell, D. Landesman-Milo, O. R. Miranda, D. Peer, and V. M. Rotello, “Nanoparticle hydrophobicity dictates immune response,” *J. Am. Chem. Soc.*, vol. 134, no. 9, pp. 3965–3967, 2012.
- [336] D. Mohanan, B. Slütter, M. Henriksen-Lacey, W. Jiskoot, J. A. Bouwstra, Y. Perrie, T. M. Kündig, B. Gander, and P. Johansen, “Administration routes affect the quality of immune responses: A cross-sectional evaluation of particulate antigen-delivery systems.,” *J. Control. Release*, vol. 147, no. 3, pp. 342–349, 2010.
- [337] A. K. Salem, “Nanoparticles in Vaccine Delivery,” *AAPS J.*, vol. 17, no. 2, pp. 289–291, Mar. 2015.
- [338] V. Kanchan, Y. K. Katare, and A. K. Panda, “Memory antibody response from antigen loaded polymer particles and the effect of antigen release kinetics.,” *Biomaterials*, vol. 30, no. 27, pp. 4763–4776, 2009.
- [339] J. Banchemreau and R. M. Steinman, “Dendritic cells and the control of immunity.,” *Nature*, vol. 392, no. March, pp. 245–252, 1998.
- [340] W. Zhang, L. Wang, Y. Liu, X. Chen, Q. Liu, J. Jia, T. Yang, S. Qiu, and G. Ma, “Immune responses to vaccines involving a combined antigen-nanoparticle mixture and nanoparticle-encapsulated antigen formulation,” *Biomaterials*, vol. 35, no. 23, pp. 6086–6097, 2014.

- [341] R. Koch, "An Address on Cholera and its Bacillus," *Br. Med. J.*, vol. 2, no. 1235, pp. 403–407, Aug. 1884.
- [342] R. De Pascalis, A. Y. Chou, C. M. Bosio, C.-Y. Huang, D. A. Follmann, and K. L. Elkins, "Development of functional and molecular correlates of vaccine-induced protection for a model intracellular pathogen, *F. tularensis* LVS.," *PLoS Pathog.*, vol. 8, no. 1, p. e1002494, 2012.
- [343] P. O. Ilyinskii, C. J. Roy, C. P. O'Neil, E. A. Browning, L. a. Pittet, D. H. Altreuter, F. Alexis, E. Tonti, J. Shi, P. a. Basto, M. Iannacone, A. F. Radovic-Moreno, R. S. Langer, O. C. Farokhzad, U. H. von Andrian, L. P. M. Johnston, and T. K. Kishimoto, "Adjuvant-carrying synthetic vaccine particles augment the immune response to encapsulated antigen and exhibit strong local immune activation without inducing systemic cytokine release," *Vaccine*, vol. 32, no. 24, pp. 2882–2895, 2014.
- [344] D. Sharma, D. Maheshwari, G. Philip, R. Rana, S. Bhatia, M. Singh, R. Gabrani, S. K. Sharma, J. Ali, R. K. Sharma, and S. Dang, "Formulation and optimization of polymeric nanoparticles for intranasal delivery of lorazepam using Box-Behnken design: in vitro and in vivo evaluation.," *Biomed Res. Int.*, vol. 2014, p. 156010, 2014.
- [345] M. Stevanovic, A. Radulovic, B. Jordovic, and D. Uskokovic, "Poly(DL-lactide-co-glycolide) Nanospheres for the Sustained Release of Folic Acid," *J. Biomed. Nanotechnol.*, vol. 4, no. 3, pp. 349–358, 2008.
- [346] H. Keles, A. Naylor, F. Clegg, and C. Sammon, "Investigation of factors influencing the hydrolytic degradation of single PLGA microparticles," *Polym. Degrad. Stab.*, vol. 119, pp. 228–241, Sep. 2015.
- [347] H. Zhou, D. Liu, and C. Liang, "Challenges and strategies: the immune responses in gene therapy.," *Med. Res. Rev.*, vol. 24, no. 6, pp. 748–761, 2004.
- [348] R. Schirmbeck and J. Reimann, "Revealing the potential of DNA-based vaccination: lessons learned from the hepatitis B virus surface antigen," *Biol Chem*, vol. 382, no. 4, pp. 543–552, 2001.
- [349] C. J. Pachuk, D. E. McCallus, D. B. Weiner, and C. Satishchandran, "DNA vaccines--challenges in delivery.," *Curr. Opin. Mol. Ther.*, vol. 2, pp. 188–198, 2000.
- [350] F. Saade and N. Petrovsky, "Technologies for enhanced efficacy of DNA vaccines," *Expert Rev. Vaccines*, vol. 11, no. 2, pp. 189–209, 2012.
- [351] R. Khushiramani, S. K. Girisha, I. Karunasagar, and I. Karunasagar, "Cloning and expression of an outer membrane protein ompTS of *Aeromonas hydrophila* and study of immunogenicity in fish," *Protein Expression and Purification*, vol. 51, no. 2. pp.

- 303–307, 2007.
- [352] A. R. Azzoni, S. C. Ribeiro, G. A. Monteiro, and D. M. F. Prazeres, “The impact of polyadenylation signals on plasmid nuclease-resistance and transgene expression,” *J. Gene Med.*, vol. 9, no. 5, pp. 392–402, 2007.
- [353] L. R. Pereira, D. M. F. Prazeres, and M. Mateus, “Hydrophobic interaction membrane chromatography for plasmid DNA purification: Design and optimization,” *J. Sep. Sci.*, vol. 33, no. 9, pp. 1175–1184, 2010.
- [354] L. Raiado-Pereira, J. De La Vega, D. M. F. Prazeres, and M. Mateus, “Development of a phenyl membrane chromatography-based process yielding pharmaceutical grade plasmid deoxyribonucleic acid for mammalian cells transfection,” *J. Chromatogr. A*, vol. 1337, pp. 67–74, 2014.
- [355] J. De La Vega, B. Ter Braak, A. R. Azzoni, G. A. Monteiro, and D. M. F. Prazeres, “Impact of plasmid quality on lipoplex-mediated transfection,” *J. Pharm. Sci.*, vol. 102, no. 11, pp. 3932–3941, 2013.
- [356] A. H. Lund, M. Duch, and F. S. Pedersen, “Increased cloning efficiency by temperature-cycle ligation,” *Nucleic Acids Res.*, vol. 24, no. 4, pp. 800–801, Feb. 1996.
- [357] S. Ribeiro, J. Mairhofer, C. Madeira, M. M. Diogo, C. Lobato da Silva, G. Monteiro, R. Grabherr, and J. M. Cabral, “Plasmid DNA size does affect nonviral gene delivery efficiency in stem cells,” *Cell. Reprogram.*, vol. 14, no. 2, pp. 130–137, 2012.
- [358] K. Sun, X. Li, J. Jiang, A. Cheng, M. Wang, D. Zhu, R. Jia, S. Chen, Y. Zhou, X. Chen, and X. Wang, “Distribution characteristics of DNA vaccine encoded with glycoprotein C from Anatid herpesvirus 1 with chitosan and liposome as deliver carrier in ducks,” *Virol. J.*, vol. 10, p. 89, Mar. 2013.
- [359] E. Carapuça, A. R. Azzoni, D. M. F. Prazeres, G. A. Monteiro, and F. J. M. Mergulhão, “Time-course determination of plasmid content in eukaryotic and prokaryotic cells using real-time PCR,” *Mol. Biotechnol.*, vol. 37, no. 2, pp. 120–126, 2007.
- [360] H. Kamiya, J. Yamazaki, and H. Harashima, “Size and topology of exogenous DNA as determinant factors of transgene transcription in mammalian cells,” *Gene Ther.*, vol. 9, no. 22, pp. 1500–1507, 2002.
- [361] J. Klesing, S. Chernousova, and M. Eppe, “Freeze-dried cationic calcium phosphate nanorods as versatile carriers of nucleic acids (DNA, siRNA),” *J. Mater. Chem.*, vol. 22, p. 199, 2012.

- [362] H. Zhou, J. Purdie, T. Wang, and A. Ouyang, “pH measurement and a rational and practical pH control strategy for high throughput cell culture system,” *Biotechnol. Prog.*, vol. 26, no. 3, pp. 872–880, 2010.
- [363] H. Bordelon, A. S. Biris, C. M. Sabliov, and W. T. Monroe, “Characterization of plasmid DNA location within Chitosan/PLGA/pDNA nanoparticle complexes designed for gene delivery,” *J. Nanomater.*, pp. 1–9, 2011.
- [364] O. Finco and R. Rappuoli, “Designing Vaccines for the Twenty-First Century Society,” *Front. Immunol.*, vol. 5, p. 12, 2014.
- [365] A. Sharma, D. Singla, M. Rashid, and G. P. Raghava, “Designing of peptides with desired half-life in intestine-like environment,” *BMC Bioinformatics*, vol. 15, no. 1, p. 282, 2014.
- [366] R. K. Naz and P. Dabir, “Peptide vaccines against cancer, infectious diseases, and conception,” *Front. Biosci.*, vol. 12, pp. 1833–1844, 2007.
- [367] Y. Hailemichael and W. W. Overwijk, “Peptide-based anticancer vaccines: The making and unmaking of a T-cell graveyard,” *Oncoimmunology*, vol. 2, no. 7, p. e24743, 2013.
- [368] A. Patronov and I. Doytchinova, “T-cell epitope vaccine design by immunoinformatics,” *Open Biol.*, vol. 3, no. 1, p. 120139, 2013.
- [369] D. Serruto, L. Serino, V. Masignani, and M. Pizza, “Genome-based approaches to develop vaccines against bacterial pathogens,” *Vaccine*, vol. 27, no. 25–26, pp. 3245–3250, 2009.
- [370] P. J. Lehner and P. Cresswell, “Processing and delivery of peptides presented by MHC class I molecules,” *Curr. Opin. Immunol.*, vol. 8, no. 1, pp. 59–67, 1996.
- [371] M. K. Jenkins, A. Khoruts, E. Ingulli, D. L. Mueller, S. J. McSorley, R. L. Reinhardt, A. Itano, and K. A. Pape, “In vivo activation of antigen-specific CD4 T cells,” *Annu. Rev. Immunol.*, vol. 19, pp. 23–45, 2001.
- [372] A. Umamaheswari, D. Pradhan, and M. Hemanthkumar, “Computer aided subunit vaccine design against pathogenic *Leptospira* serovars,” *Interdiscip. Sci.*, vol. 4, no. 1, pp. 38–45, 2012.
- [373] Y. EL-Manzalawy, D. Dobbs, and V. Honavar, “Predicting linear B-cell epitopes using string kernels,” *J. Mol. Recognit.*, vol. 21, no. 4, pp. 243–255, 2008.
- [374] H. Singh and G. P. S. Raghava, “ProPred1: Prediction of promiscuous MHC class-I binding sites,” *Bioinformatics*, vol. 19, no. 8, pp. 1009–1014, 2003.
- [375] H. Singh and G. P. Raghava, “ProPred: prediction of HLA-DR binding sites,”



- Bioinformatics*, vol. 17, no. 12, pp. 1236–1237, 2001.
- [376] I. A. Doytchinova and D. R. Flower, “VaxiJen: a server for prediction of protective antigens, tumour antigens and subunit vaccines.,” *BMC Bioinformatics*, vol. 8, no. 1, p. 4, 2007.
- [377] P. Guan, I. A. Doytchinova, C. Zygouri, and D. R. Flower, “MHCpred: A server for quantitative prediction of peptide-MHC binding,” *Nucleic Acids Res.*, vol. 31, no. 13, pp. 3621–3624, 2003.
- [378] A. Krogh, B. Larsson, G. von Heijne, and E. L. Sonnhammer, “Predicting transmembrane protein topology with a hidden Markov model: application to complete genomes.,” *J. Mol. Biol.*, vol. 305, no. 3, pp. 567–580, 2001.
- [379] K. Arnold, L. Bordoli, J. Kopp, and T. Schwede, “The SWISS-MODEL workspace: a web-based environment for protein structure homology modelling,” *Bioinformatics*, vol. 22, no. 2, pp. 195–201, 2006.
- [380] N. Guex and M. C. Peitsch, “SWISS-MODEL and the Swiss-PdbViewer: an environment for comparative protein modeling.,” *Electrophoresis*, vol. 18, no. 15, pp. 2714–2723, 1997.
- [381] R. A. Laskowski, M. W. MacArthur, D. S. Moss, and J. M. Thornton, “PROCHECK: a program to check the stereochemical quality of protein structures,” *J. Appl. Crystallogr.*, vol. 26, pp. 283–291, 1993.
- [382] R. A. Laskowski, J. D. Watson, and J. M. Thornton, “ProFunc: A server for predicting protein function from 3D structure,” *Nucleic Acids Res.*, vol. 33, no. SUPPL. 2, pp. 89–93, 2005.
- [383] D. Baú, A. J. M. Martin, C. Mooney, A. Vullo, I. Walsh, and G. Pollastri, “Distill: a suite of web servers for the prediction of one-, two- and three-dimensional structural features of proteins.,” *BMC Bioinformatics*, vol. 7, p. 402, 2006.
- [384] E. Quevillon, V. Silventoinen, S. Pillai, N. Harte, N. Mulder, R. Apweiler, and R. Lopez, “InterProScan: Protein domains identifier,” *Nucleic Acids Res.*, vol. 33, no. SUPPL. 2, pp. 116–120, 2005.
- [385] Y. Gholizadeh, M. Prevost, F. Van Bambeke, B. Casadewall, P. M. Tulkens, and P. Courvalin, “Sequencing of the *ddl* gene and modeling of the mutated D-alanine:D-alanine ligase in glycopeptide-dependent strains of *Enterococcus faecium*.,” *Protein Sci.*, vol. 10, no. 4, pp. 836–844, 2001.
- [386] A. Arockiasamy and S. Krishnaswamy, “Prediction of B-cell epitopes for *Salmonella typhi* OmpC,” *J. Biosci.*, vol. 20, no. 2, pp. 235–243, 1995.

- [387] M. Arevalo-Herrera, A. Z. Valencia, J. Vergara, A. Bonelo, K. Fleischhauer, J. M. Gonzalez, J. C. Restrepo, J. A. Lopez, D. Valmori, G. Corradin, and S. Herrera, "Identification of HLA-A2 restricted CD8(+) T-lymphocyte responses to *Plasmodium vivax* circumsporozoite protein in individuals naturally exposed to malaria.," *Parasite Immunol.*, vol. 24, no. 3, pp. 161–169, Mar. 2002.
- [388] J. Sollner, R. Grohmann, R. Rapberger, P. Perco, A. Lukas, and B. Mayer, "Analysis and prediction of protective continuous B-cell epitopes on pathogen proteins," *Immunome Res.*, vol. 4, p. 1, 2008.
- [389] V. Pancre, H. Gras-Masse, A. Delanoye, J. Herno, A. Capron, and C. Auriault, "Induction of cytotoxic T-cell activity by the protective antigen of *Schistosoma mansoni* Sm28GST or its derived C-terminal lipopeptide," *Scand. J. Immunol.*, vol. 44, no. 5, pp. 485–492, 1996.

# Publications

## Journal Articles

1. **Rauta, P.R.**, Nayak, D., Ashe, S, Nayak, B. Immunological evaluation of PLA/PLGA nanoparticles encapsulating outer membrane protein (Omp) from *Vibrio cholerae* as a potential vaccine candidate. (Under review).
2. **Rauta PR**, Mateus M, Monteiro GA, Nayak B. Development of DNA vaccines to boost antigenic Omp (outer membrane protein) using nanoparticle based delivery. *Journal of Biotechnology*. (Accepted).
3. **Rauta PR**, Ashe S, Nayak D, Nayak B. In Silico identification of outer membrane protein (Omp) and subunit vaccine design against pathogenic *Vibrio cholerae*. *Computational Biology and Chemistry*, 65 (2016): 61-68.
4. **Rauta, P.R.**, Das, N.M., Nayak D., Ashe S., Nayak, B. Formulation and characterization of Clindamycin Hydrochloride loaded PLA and PLGA nanoparticles for effective oral delivery. *IET Nanobiotechnology* (Accepted, DOI: 10.1049/iet-nbt.2015.0021).
5. **Rauta, P.R.**, Nayak, B. Parenteral immunization of PLA/PLGA nanoparticle encapsulating outer membrane protein (Omp) from *Aeromonas hydrophila*: Evaluation of immunostimulatory action in *Labeo rohita* (rohu). *Fish & Shellfish Immunology*. 44 (2015) 1: 287-294.
6. **Rauta, P.R.**, Samanta, M., Dash, H.R., Nayak, B., Das, S. Toll-like receptors (TLRs) in aquatic animals: Signaling pathways, expressions and immune responses. *Immunology Letters* 158 (2014): 14–24.
7. **Rauta, P.R.**, Dhupal, M., Nayak, B. Screening and characterization of potential probiotic lactic acid bacteria isolated from vegetable waste and fish intestine. *Int. J. Curr. Microbiol. App.Sci* (2013) 2(8): 234-244.
8. **Rauta, P.R.**, Nayak, B., Das, S. Immune system and immune responses in fish and their role in comparative immunity study: A model for higher organisms. *Immunology Letters* 148 (2012): 23– 33.
9. Padhi, J.R., Nayak, D., Nanda, A., **Rauta, P.R.**, Ashe, S, Nayak, B. Development of highly biocompatible Gelatin & i-Carrageenan based composite hydrogels: In depth physiochemical analysis for biomedical applications. *Carbohydrate Polymers* (Accepted, 2016).
10. Chopra, P., Nayak, D., Nanda, A., Ashe, S, **Rauta, P.R.**, Nayak, B. Fabrication of poly(vinyl alcohol)-Carrageenan scaffolds for cryopreservation: Effect of composition on cell viability. *Carbohydrate Polymers* 147 (2016):509-516.
11. Nayak, D., Minz, A.P., Ashe, S, **Rauta, P.R.**, Kumari, M., Chopra, P., Nayak, B. Synergistic combination of antioxidants, silver nanoparticles and chitosan in a nanoparticle based formulation: Characterization and cytotoxic effect on MCF-7 breast cancer cell lines. *J Colloid Interface Sci*. 470 (2016):142-152.

12. Nayak D, Ashe S., **Rauta P.R.**, Kumari M, Nayak B. Bark extract mediated green synthesis of silver nanoparticles: Evaluation of antimicrobial activity and antiproliferative response against osteosarcoma. *Materials Science and Engineering C* 58 (2016) 44–52.
13. Nayak D, Pradhan S, Ashe S, **Rauta P.R.**, Nayak B. Biologically synthesised silver nanoparticles from three diverse family of plant extracts and their anticancer activity against epidermoid A431 carcinoma. *Journal of Colloid and Interface Science*. 457 (2015) 329-338.
14. Nayak, D., Ashe, S., **Rauta, P.R.**, Nayak, B. Biosynthesis, characterization and antimicrobial activity of Ag NPs using *Hibiscus rosa-sinensis* petals extracts *IET Nanobiotechnology* 9 (2015) 5: 288-293.
15. Ashe S., Nayak D., Tiwari G., **Rauta, P.R.**, Nayak, B. Development of liposome-encapsulated ketoconazole: formulation, characterisation and evaluation of pharmacological therapeutic efficacy. *Micro & Nano Letters*, 10 (2015) 2:126 - 129.

## Conference Proceedings and Poster Presentations

1. **Rauta PR**, Nayak B, Mateus M, Monteiro GA. “Developing a plasmid dna vaccine candidate against *Aeromonas hydrophila* fish infections.” poster presented at “Microbiotec’15” held at Évora, Portugal.
2. **Rauta PR**, Mateus M, Monteiro GA, Nayak B. “Development of DNA vaccines to boost antigenic Omp (outer membrane protein) using nanoparticle based delivery.” poster presented at “**International Conference on Frontiers in Biological Sciences [InCoFIBS-2]**” held at NIT Rourkela, Odisha India, 22<sup>nd</sup> - 24<sup>th</sup> January, 2015, page No-153.
3. Nayak B, **Rauta PR**, Ray AR, Ray P, Panda AK. Chitosan Coated PLA/PLGA Microparticles for Effective Mucosal Delivery of Therapeutic Proteins. **9<sup>th</sup> Biomaterials Congress. June 1-5, 2012.** , Chengdu, China.
4. **Rauta, P.R., Rohini N., Nayak B.** Bioleaching of slime metal ores collected from Joda mines of Orissa by the use of *Bacillus Sp.* National Seminar on “**Trends in microbial bioremediation of contaminated soil**” 24<sup>th</sup>-25<sup>th</sup> September, 2011.

# Curriculum Vitae

**Pradipta Ranjan Rauta**

C/O- Bijaya Kumar Rauta

AT/PO- Berboi

DIST- Puri

STATE- Orissa- 752016

E-mail: pradiptaranjan.s08@gmail.com

Tel: (+91)0661 2462682

Mob: 08895178107



## EDUCATIONAL QUALIFICATION:

---

Degree	Score	Institution	Period
PhD		National Institute of Technology Rourkela, Odisha	2011- 2015
Masters of Science (M.Sc.)	85.3%	Orissa University of Agriculture & Technology, Bhubaneswar, Orissa	2006-2008
Bachelors of Science (B.Sc.)	79.37%	B J B (auto) College, Bhubaneswar, Orissa	2003-2006
Higher Secondary Examination (10+2)	75.88%	B J B (Junior) College, Bhubaneswar, Orissa	2000 - 2002
Secondary Examination (10 <sup>th</sup> )	90.8%	Govt High School, Berboi, Puri, Orissa	2000

## OTHER EDUCATIONAL ACHIEVEMENTS:

---

- Qualified **CSIR-UGC NET** in **LIFE SCIENCES** under the “**Lectureship Category**” held on June 2010
- Qualified **GATE 2010** in **LIFE SCIENCES** held on February 2010
- Awarded **Erasmus Mundus Heritage Fellowship** (PhD mobility fellow at IST, Lisbon, Portugal, Sep, 2013- June, 2014)

## RESEARCH INTEREST:

---

Nanoparticle based drug delivery and their immunological evaluation

## PERSONAL DETAILS:

---

**Date of Birth:** 25th May 1985

**Nationality:** Indian

**Gender:** Male

**Marital Status:** Married

**Language Known:** English, Hindi, Oriya